Chapter 6

Microscopy study and geochemical results

6.1. Chapter overview

This chapter presents the geochemical results for both the modern and the mid-Holocene corals in the following order:

1) Section 6.2 examines the microanalytical studies on the modern and fossil corals to ensure that they are free of diagenesis and thus suitable for trace element and isotope analyses.
2) Section 6.3 explores the effect of the H_2O_2 chemical pre-treatment procedure on selected trace elements.
3) Section 6.4 presents the results of the coral SST proxies including Sr/Ca, Mg/Ca and U/Ca ratios as well as O isotopes.
4) Section 6.5 discusses the coral $\Delta^{18}O$ data to reconstruct seawater salinity.
5) Section 6.6 examines possible coral proxies of water quality including Ba/Ca ratio, Mn concentrations, rare earth elements (particularly Y, Pr, Sm and Ho) and Th concentrations.

6.2. Microscopic analyses of coral slices

6.2.1. Overview

Microanalyses were conducted on both the modern and mid-Holocene corals to examine if they were free of diagenetic alteration and, therefore, suitable for trace element and isotope analyses. This section presents the results from the scanning electron microscopy and the coral thin section analyses.

6.2.2. Scanning electron microscope (SEM) analyses

Scanning electron microscopy of the modern and mid-Holocene corals revealed there was no obvious addition of secondary aragonite in the coral pore spaces or on the

surface of the coral slices (Fig 6.1 a-p). In addition, there were no other signs that the corals had been diagenetically altered (e.g. calcite replacement). Therefore, it is considered that the modern and mid-Holocene corals are free of secondary aragonite and aragonite has not been replaced with calcite.

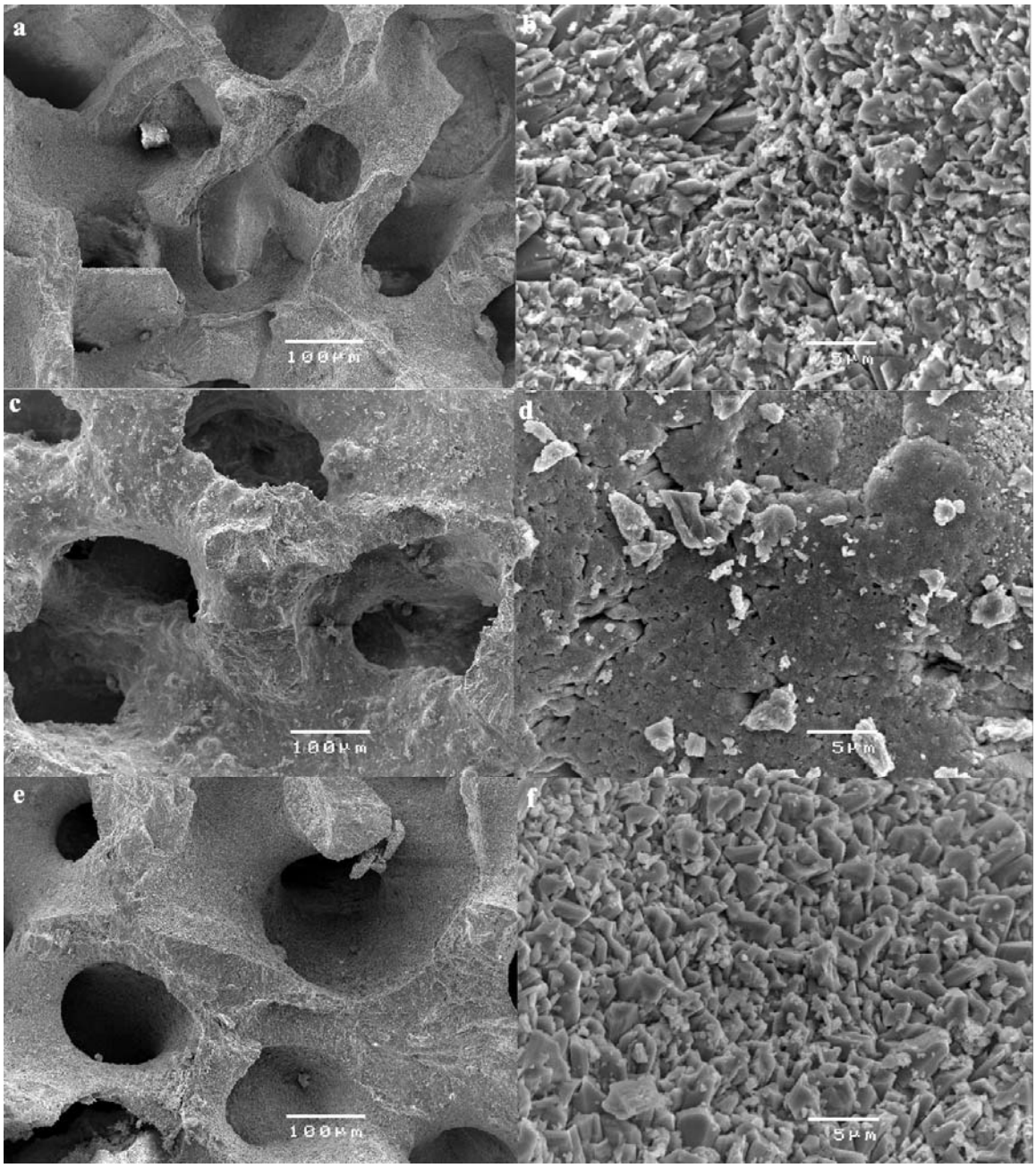

Figure 6.1 (a-f). Scanning electron microscope (SEM) images of the coral slices. (a-b) taken from the base of the modern coral record (MAG01D) at 100 × (a) and 2000 × (b) magnification. (c-d) taken from the top of MAG01D. (e-f) from the base of mid-Holocene coral slice NEL01D.

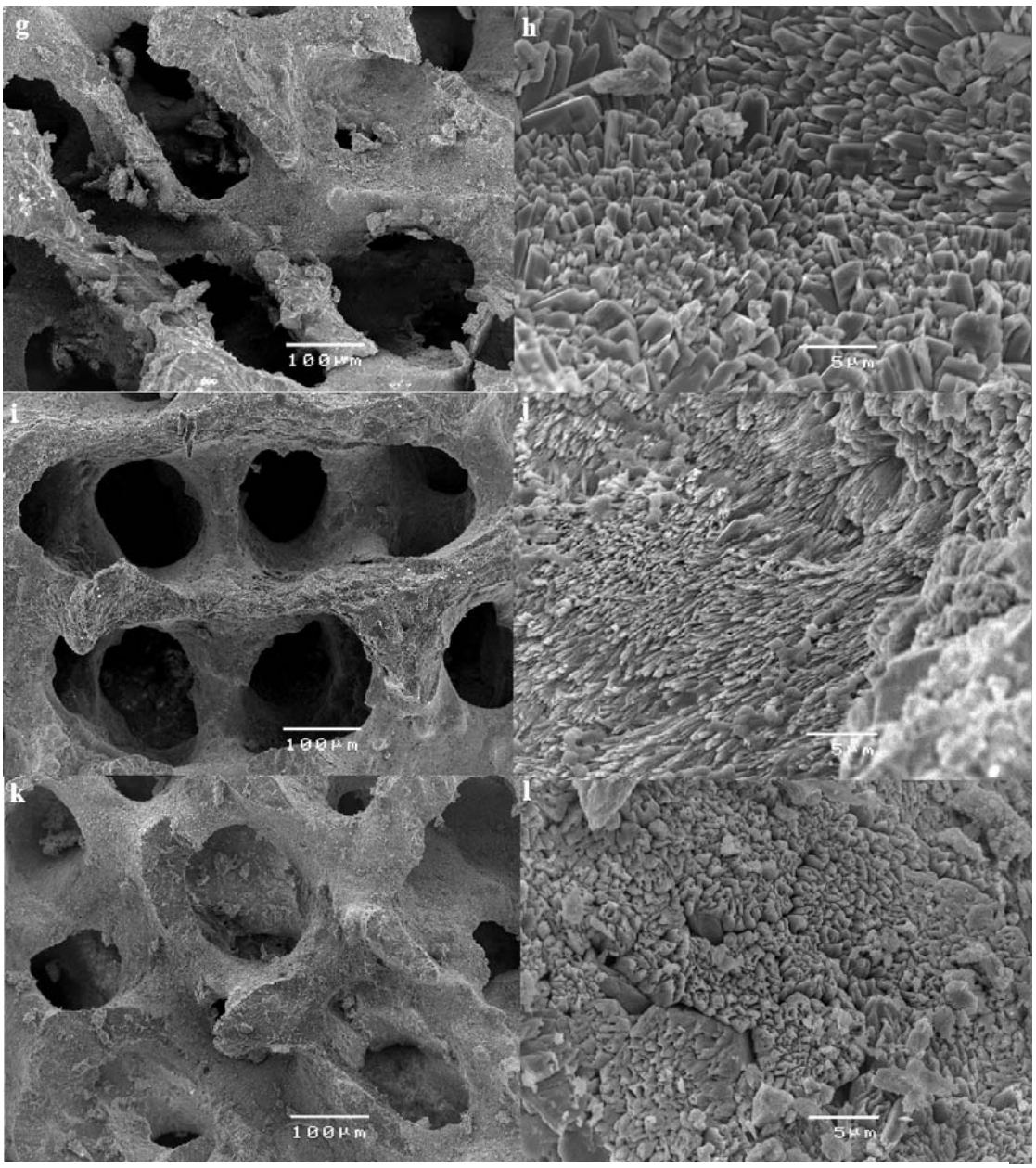

Figure 6.1 (g-l). SEM images (continued). (g-h) from top of NEL01D at 100 × (g) and 2000 × (h) magnification. (i-j) from the base of NEL03D. (k-l) from the top of NEL03D. There was no obvious difference between the modern and mid-Holocene corals and no apparent secondary aragonite infilling in the pore spaces. The 2000 × magnification images (on right) were thought to represent the crystal structure.

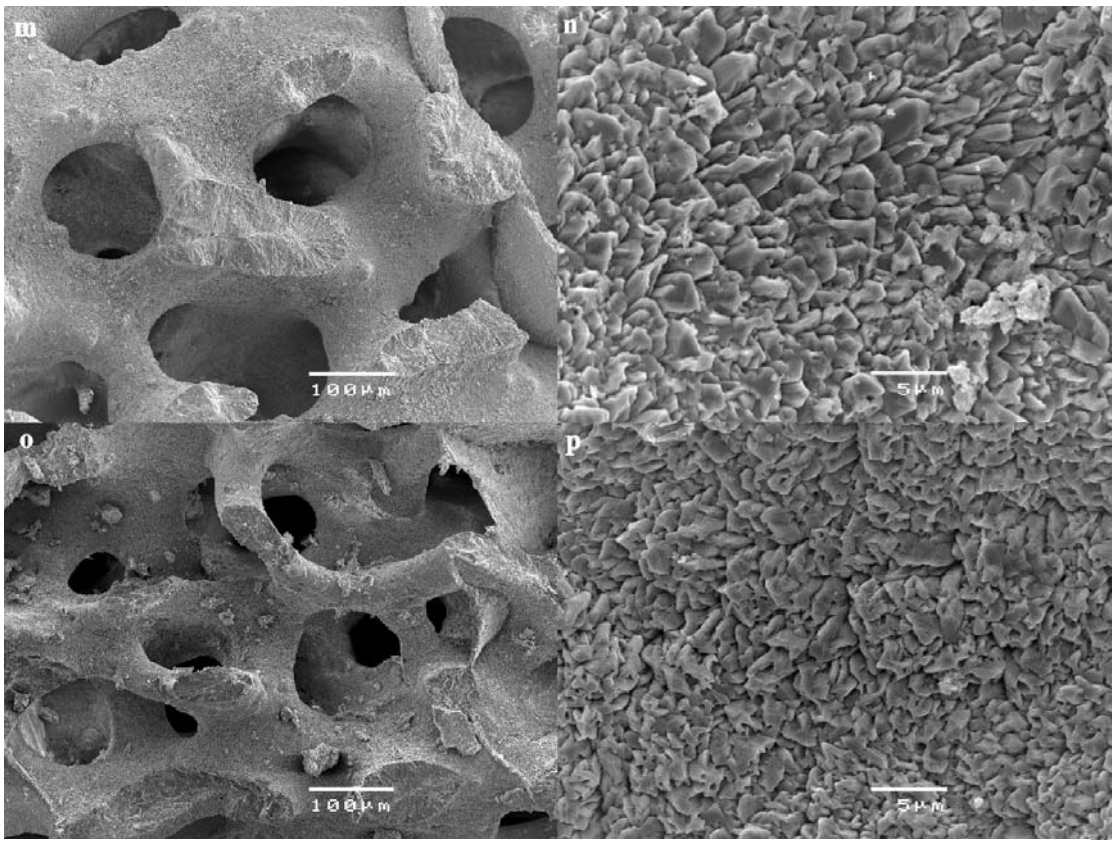

Figure 6.1 (m-p). SEM images (continued) for the mid-Holocene corals. (m-n) from the base of NEL06A. (o-p) from the base of NEL07C. Again, there was no apparent secondary aragonite infilling in the coral pore space.

6.2.3. Coral thin section analyses

The coral thin sections, ground to 60-100 µm thickness, displayed what appeared to be apparent cement surrounding some of the coral pores (Fig 6.2 a-ah). This feature was present throughout all the corals, including the top section of the modern coral from Geoffrey Bay; this section is unlikely to have been infilled with secondary aragonite or replaced with calcite. Therefore, this possible "cement" seems likely to be an artefact of the blue dye impregnation procedure.

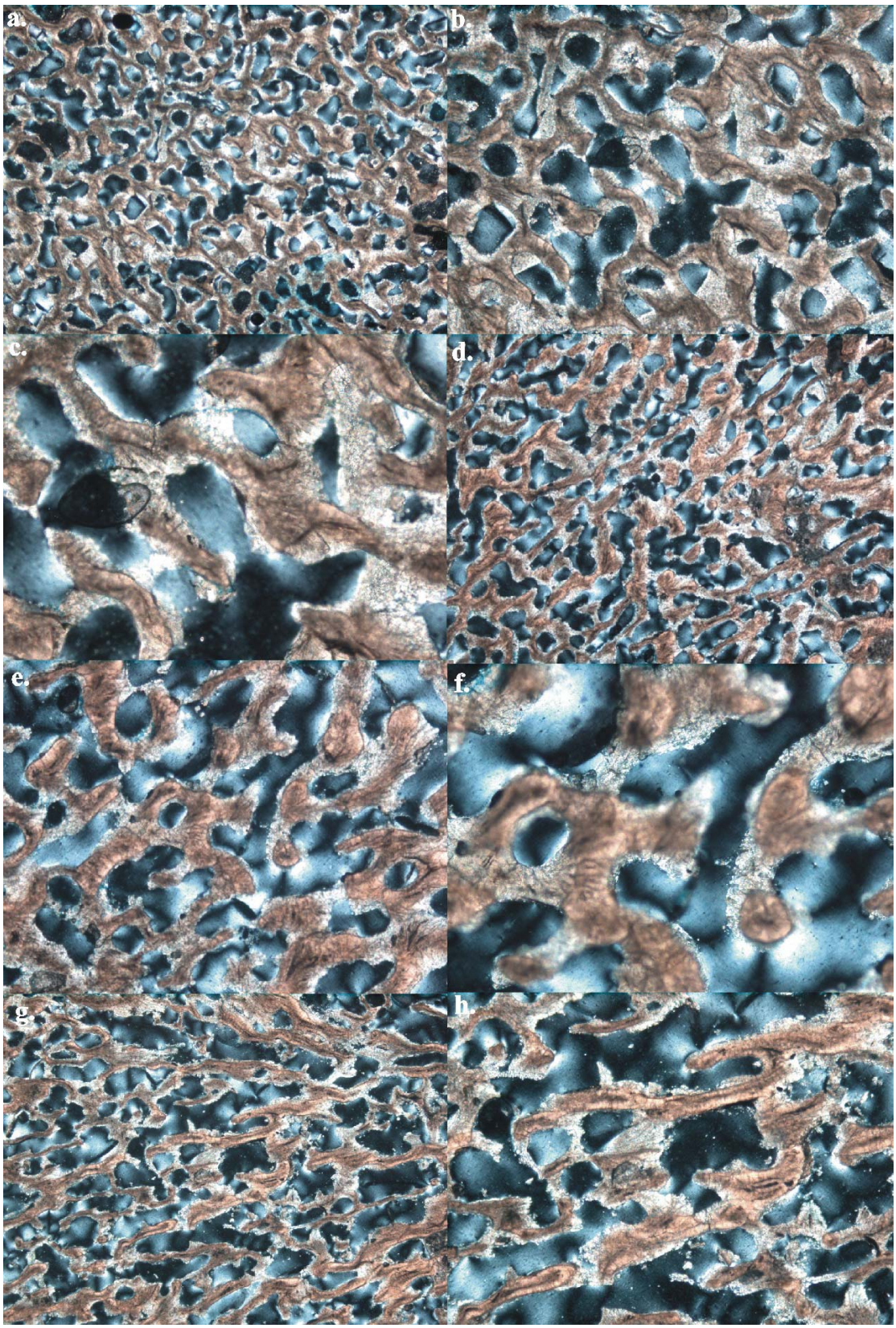

Figure 6.2 a-h. Coral thin sections of 60-100 µm in thickness. The corals were impregnated in a blue resin to fill in pore spaces and to recognise the difference between the pores and the coral aragonite. (a-c) from the base of the modern coral MAG01D at 2.5 ×, 5 × and 10 × magnifications. (d-f) 2.5 ×, 5 × and 10 × magnifications of the middle section of the MAG01D coral slice. (g-h) 2.5 × and 5 × magnifications of the top of MAG01D.

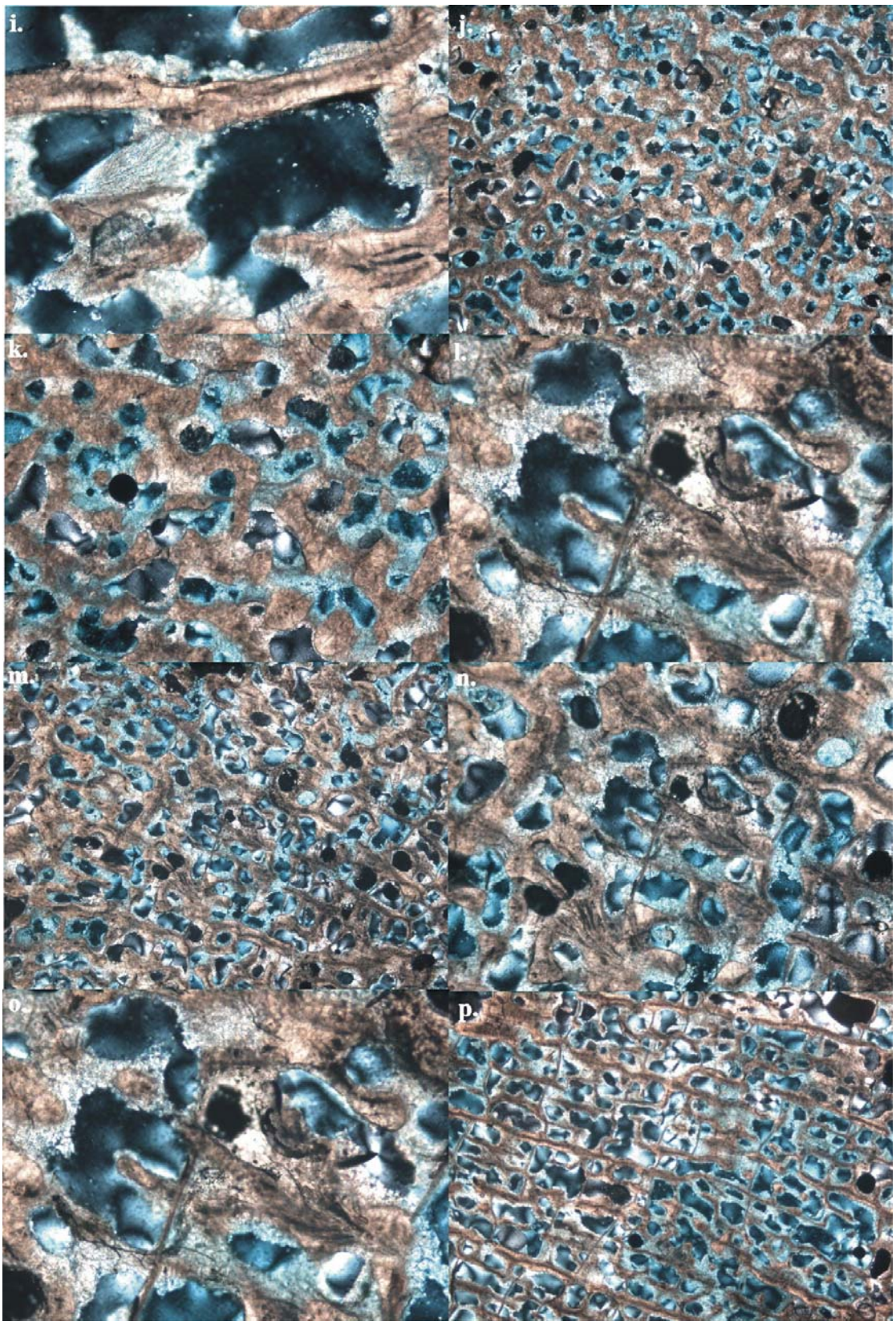

Figure 6.2 i-p. (i) 10 × magnification from top of MAG01D. (j-l) 2.5 ×, 5 × and 10 × magnifications of the base of mid-Holocene coral NEL01D. (m-o) 2.5 ×, 5 × and 10 × magnifications of the middle section of NEL01D coral slice. (p) 2.5 × magnification of the top of NEL01D.

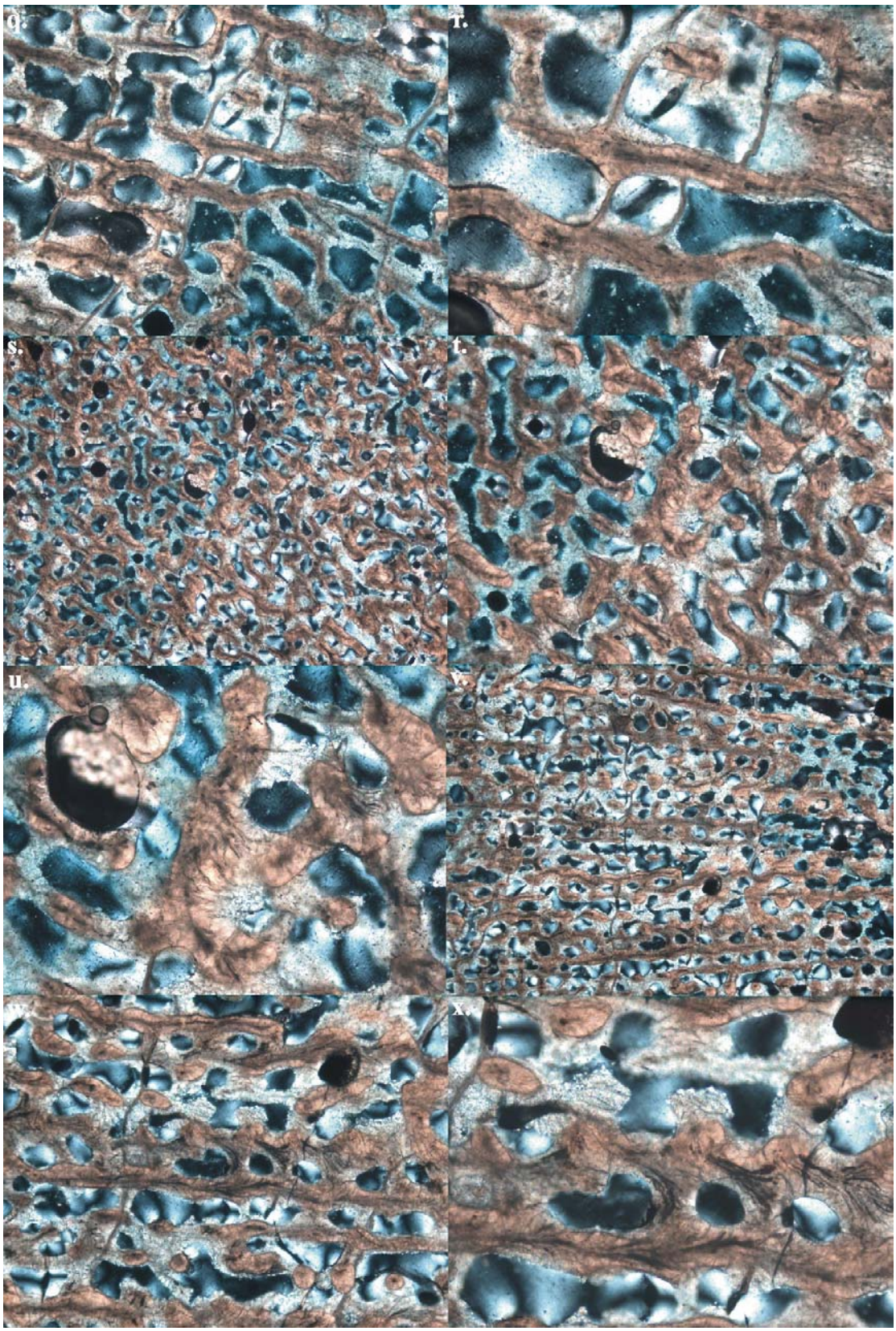

Figure 6.2 q-x. (q-r) 5 × and 10 × magnifications of the top of mid-Holocene coral NEL01D. (s-u) 2.5 ×, 5 × and 10 × magnifications of the base of mid-Holocene coral NEL03D. (v-x) 2.5 ×, 5 × and 10 × magnifications of the top of the NEL03D coral slice.

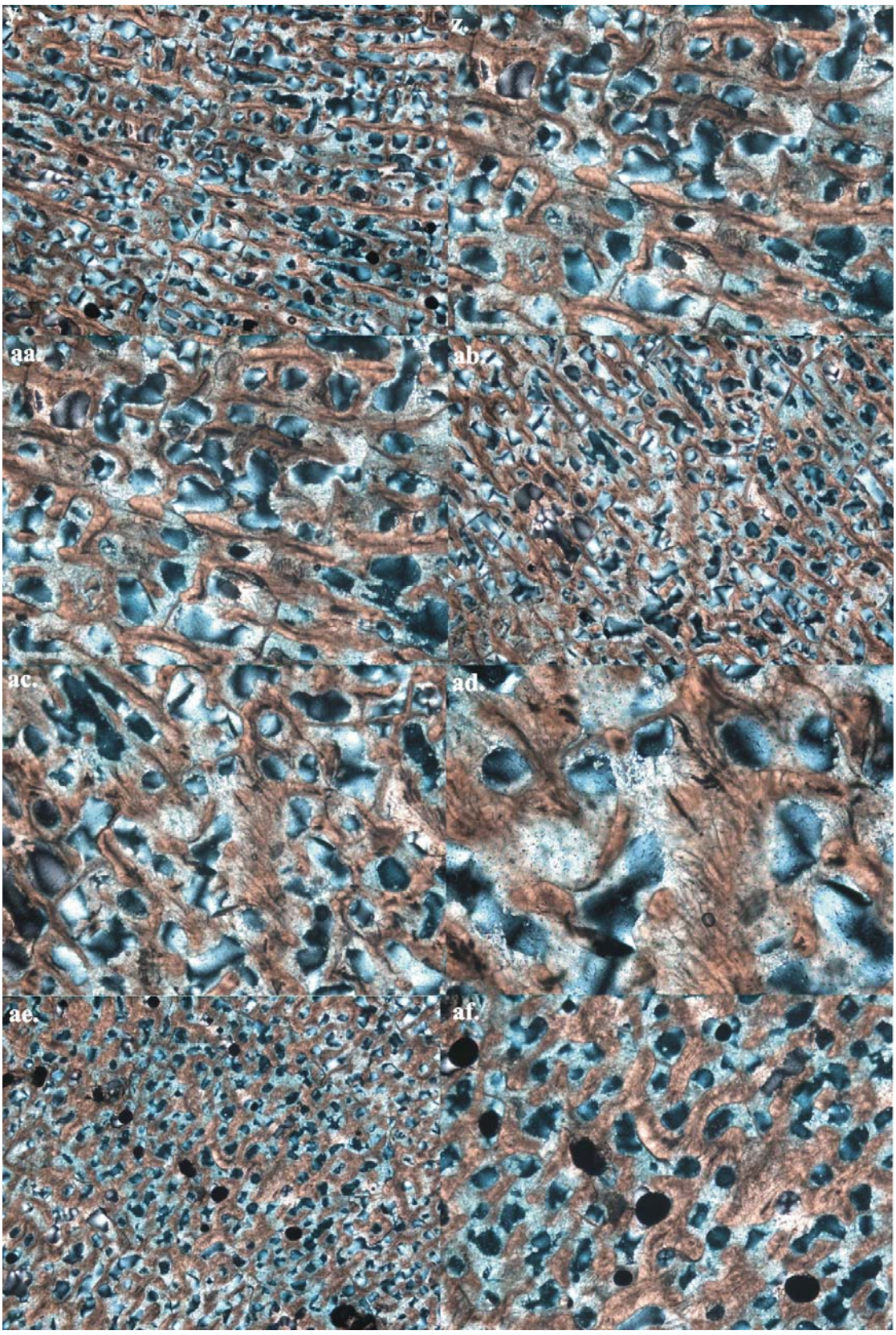

Figure 6.2 y-af. (y-aa) 2.5 ×, 5 × and 10 × magnifications of the base of mid-Holocene coral NEL06A. (ab-ad) 2.5 ×, 5 × and 10 × magnifications of the base of mid-Holocene coral NEL07C. (ae-af) 2.5 × and 5 × magnifications of the top of NEL07C.

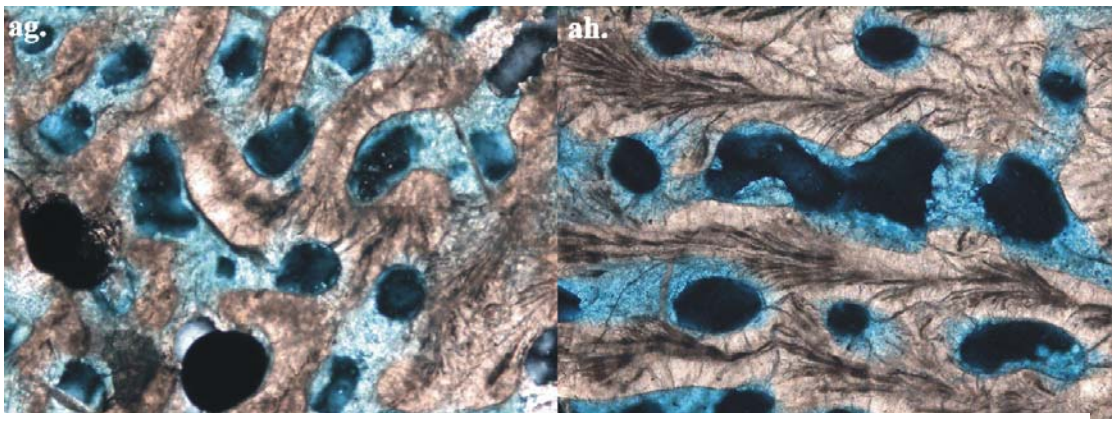

Figure 6.2 (ag-ah). (ag) 10 × magnification of the of the top of NEL07C. (ah) a 10 × magnification of a living coral taken from Pandora Reef. The Pandora coral was considered to be pristine and was used as a comparison with the other thin sections. There was a conspicuous "cement like" feature present in some of the coral pore spaces in both the modern (MAG01D) and mid-Holocene corals. However this "cement" is interpreted to be an artefact of the blue dye impregnation procedure.

6.2.4. Summary

Microanalytical analyses on both the modern and mid-Holocene corals suggest that the corals were free of diagenesis and thus were suitable for trace element and isotope geochemistry.

6.3. Effects of sample pretreatment

6.3.1. Overview

Some previous studies suggest that a chemical pre-treatment procedure is required to remove any detrital and organic components from the coral skeleton (e.g. Shen and Boyle, 1988; Watanabe et al., 2001). The treatment ensures that the analysed trace elements are genuinely substituted for Ca^{2+} or CO_3^{2-} in the coral aragonite skeleton. This section investigates the effects of the H_2O_2 treatment procedure on the trace element composition of the 2 yearly resolution samples from 1958-1960 to 1984-1986. These 15 pre-treated samples were compared to their corresponding untreated counterparts.

6.3.2. Sr/Ca ratios

The H_2O_2 treated coral Sr/Ca ratios (Fig 6.3a) were systematically lower than their untreated counterparts, but were within the analytical error (1σ) with one exception (1962-1964). The results suggest that the coral Sr/Ca ratio will produce reliable SST reconstructions independent of chemical pre-treatments; this finding is consistent with previous investigations (e.g. Watanabe et al., 2001; Mitsuguchi et al., 2001).

6.3.3. Mg/Ca ratios

The coral Mg/Ca ratios (Fig 6.3b) were all significantly lower in the pre-treated samples. This result suggests that some Mg was removed during the H_2O_2 treatment procedure. Mg can be associated with the organic fraction of the coral (Mitsuguchi et al., 2001; Watanabe et al., 2001). The Mg/Ca ratio of the anomalous "1962-1964" sample (previously reported in the Sr/Ca ratios) displayed a similar value to the corresponding untreated sample, which was inconsistent in comparison to the other H_2O_2 treated Mg/Ca ratios. From a thermometry perspective, the Mg/Ca ratios require two separate SST calibrations for the H_2O_2 treated QHSS samples and the untreated ACQUIRE samples. In addition, the SST reconstructions from the untreated coral Mg/Ca ratios, in the ACQUIRE dataset, could be compromised by organic material in the coral skeleton and this data needs to be approached with caution.

6.3.4. U/Ca ratios

The U/Ca ratios in the H_2O_2 treated samples plotted within or above the 1σ analytical error of the treated samples (Fig 6.3c). The results indicate that the untreated coral U/Ca ratios should provide reliable SST reconstructions.

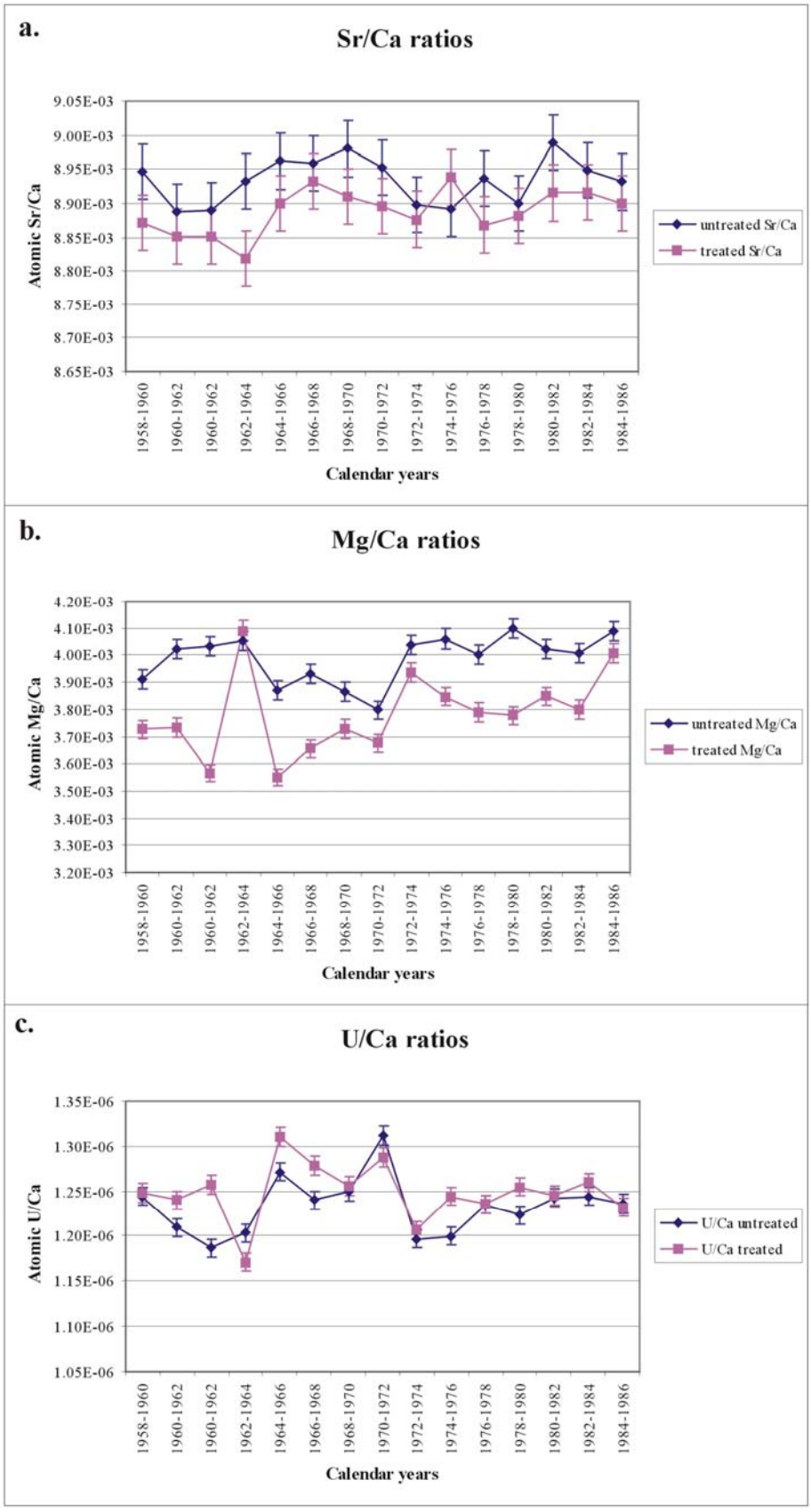

Figure 6.3 (a-c). The effect of the H_2O_2 treatment procedure on the coral SST proxies was evaluated. (a) The Sr/Ca ratios all fit within the error bars with one exception (see text) and were relatively unaffected by the H_2O_2 treatment. (b) Mg/Ca ratios were affected by the treatment procedure as some Mg may be associated with the organic fraction. (c) U/Ca ratios were largely unaffected by the H_2O_2 treatment but absolute values appear not to be reproducible.

6.3.5. Ba/Ca ratios

The coral Ba/Ca ratios (Fig 6.4a) displayed similar trends in the two datasets within analytical error, with one major (1962-1964) and two minor exceptions (1960-1962; 1966-1968). The coral Ba/Ca ratio has been measured previously without chemical pre-treatments (e.g. McCulloch et al., 2003) and appears to provide reliable reconstructions of the seawater Ba concentration irrespective of chemical pre-treatments.

6.3.6. Mn concentrations

The Mn concentrations (Fig 6.4b) in the pre-treated and untreated datasets were within the 1σ analytical error with a few minor exceptions. This result suggests that the majority of Mn is incorporated into the coral skeleton by substituting for Ca, and little Mn (if any) is held within organic phases. Therefore, coral Mn concentrations appear to be unaffected by the H_2O_2 treatment procedure.

6.3.7. Ni concentrations

The coral Ni concentrations were all significantly lower after the H_2O_2 treatment compared with the untreated data (Fig 6.4c). This finding suggests that Ni was strongly leached during the H_2O_2 treatment process and probably is held in the organic fraction.

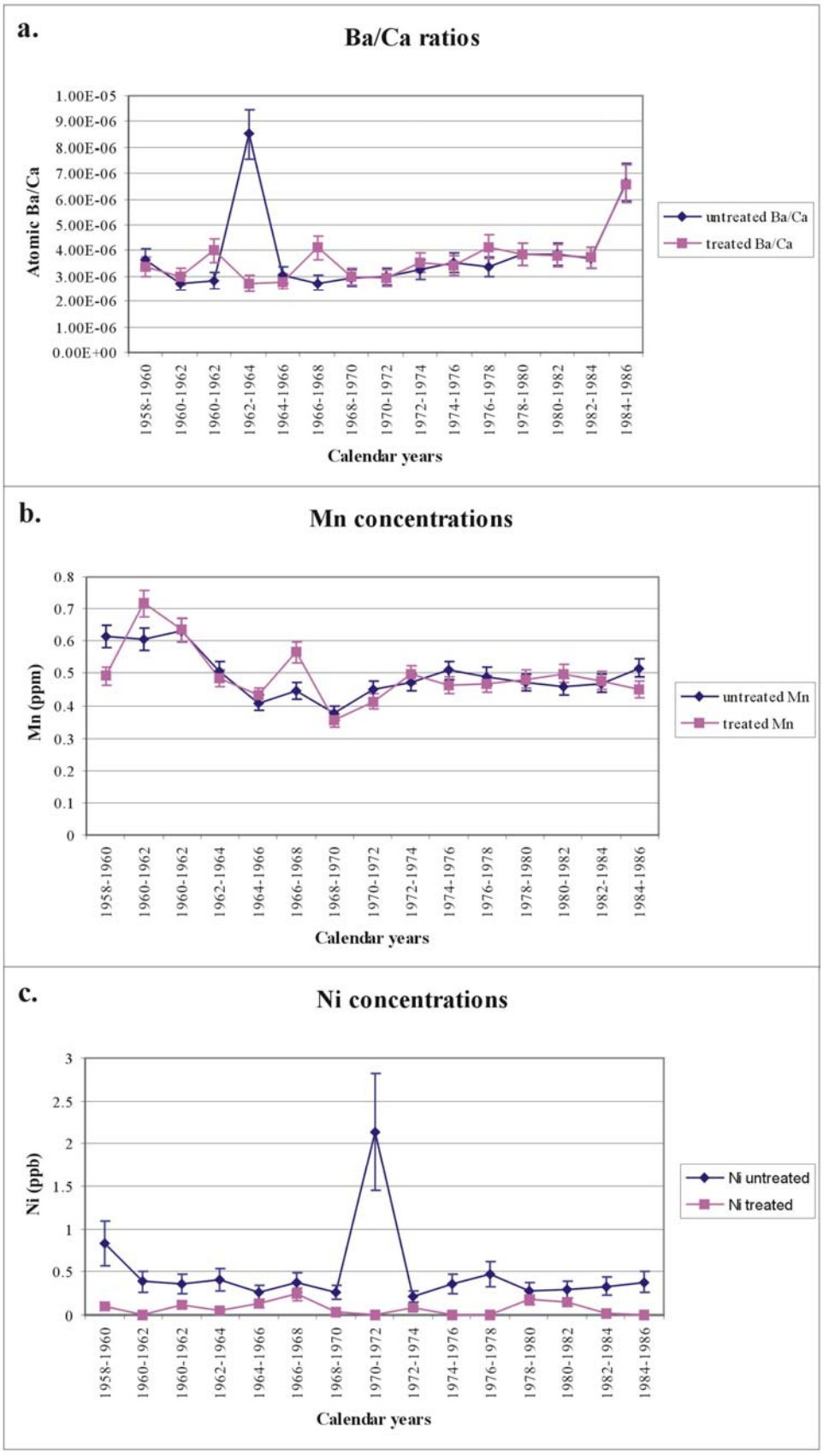

Figure 6.4 (a-c). The effects of the H_2O_2 treatment procedure were investigated on some of the possible water quality proxies. (a) The Ba/Ca ratios were mostly unaffected by the pre-treatment with a few exceptions (see text). (b) Mn concentrations were unaffected by the H_2O_2 treatment, which suggests it substitutes for Ca in the coral lattice. (c) Ni became strongly leached during the pre-treatment process and probably is within an organic phase.

6.3.8. Summary

The effect of a chemical pre-treatment procedure, designed to remove any organic material from the coral samples, on the Sr/Ca, Mg/Ca, U/Ca and Ba/Ca ratios as well as Mn and Ni concentrations were investigated. The coral Sr/Ca, U/Ca, Ba/Ca ratios and Mn concentrations were mostly unaffected by the chemical pre-treatment procedure. Therefore, these proxies would provide reliable data whether the coral samples analysed were either pre-treated or untreated. However, the coral Mg/Ca ratio and Ni concentrations were significantly affected by the pre-treatment procedure. This finding suggests that the untreated Mg/Ca analysis may not provide reliable SST estimations and that both Mg and Ni have some association with the organic component of the coral. Therefore, the coral Mg/Ca-SST reconstructions need to be approached with caution.

6.4. Sea surface temperature reconstructions

6.4.1. Overview

This section presents the results from the coral proxy SST reconstructions including the Sr/Ca, Mg/Ca and U/Ca ratios as well as the O isotope composition for the modern and mid-Holocene corals. This section will examine the reconstructed SST from these corals at sub-annual as well as at 2 and 5 yearly resolutions.

6.4.2. Sr/Ca ratios

The Sr/Ca-SST reconstructions for the 1980-1984 (ACQUIRE; Fig 6.5a) and 1992-1996 (QHSS; Fig 6.5b) datasets both displayed seasonal variations; however, the SST average and the range in the 1992-1996 sample (24.16 ± 1.14º C; 1σ standard deviation) was significantly lower than the 1980-1984 (26.50 ± 1.67º C) sample. The 1992-1996 coral contains a poor growth record and could not be sampled along the major growth axis (Fig 4.11). The failure to sample along the coral's major growth axis can underestimate SST by as much as 3º C (Alibert and McCulloch, 1997). The two-monthly resolution Sr/Ca-SST record of the mid-Holocene coral (NEL03D; Fig 6.5c)

has an average (26.78 ± 1.78º C), range and seasonality indistinguishable from the 1980-1984 Sr/Ca SST record (Table 6.1).

The average Sr/Ca-SST estimates for the MAG01D (1812-1986) coral slice at both 2 (ACQUIRE; 25.01 ± 3.12º C; Fig 6.6a) and 5 (QHSS; 25.08 ± 0.78º C; Fig 6.6b) yearly resolutions were identical despite the two sampling preparation procedures (untreated and H_2O_2 treated, respectively). Although a relatively poor analytical precision was achieved in the ACQUIRE (1812-1986) Sr/Ca record (± 0.65° C), the data still displays consistent trends that would be expected in the instrumental record. Interestingly, the first 4 samples in the ACQUIRE dataset and the first 2 in the QHSS data (representing 8 and 10 years of growth, respectively) show what appears to be cooler SSTs during the early 1800s. However, these data may need to be rejected as juvenile corals do not conform to the Sr/Ca-SST relationship compared to their mature counterparts (Marshall and McCulloch, 2002).

The mid-Holocene corals had similar average Sr/Ca-SST estimates compared to the modern corals (Fig 6.7a-d; Table 6.1). The NEL01D coral slice, sampled at 2 (ACQUIRE; 24.99 ± 0.82º C; Fig 6.7a) and 5 (QHSS; 24.44 ± 0.80º C; Fig 6.7b) yearly resolutions, displayed similar average SSTs between the two datasets. Significant SST deviations (1-2° C) in both the 2 and 5 yearly resolution datasets may relate to the relatively poor analytical precision achieved for the analyses. Average SSTs are unlikely to shift by as much as 1-2º C over an average 2-5 year period. This problem is discussed further in section 7.2.4.

Table 6.1. Summary of SST reconstructions for the modern and mid-Holocene corals. The SST proxies display positive replication for most of the corals and indicate that SST conditions during the mid-Holocene were similar to today. * mid-Holocene coral.

	Proxy temperature (° C)			
Coral record	**Sr/Ca**	**Mg/Ca**	**U/Ca**	**O isotopes**
1980-1984 (ACQUIRE)	26.50 ± 1.67	26.30 ± 1.84	27.13 ± 1.84	25.71 ± 3.31
1992-1996 (QHSS)	24.16 ± 1.14	25.84 ± 0.51	N/A	N/A
NEL03D (two-monthly resolution)*	26.78 ± 1.78	27.18 ± 2.33	25.91 ± 1.76	28.00 ± 3.28
1812-1986 (ACQUIRE)	25.01 ± 3.12	26.21 ± 0.98	27.45 ± 0.75	N/A
1810-1985 (QHSS)	25.09 ± 0.76	24.62 ± 0.37	N/A	25.81 ± 1.21
NEL01D (ACQUIRE)*	24.99 ± 0.82	26.95 ± 1.54	24.66 ± 1.61	N/A
NEL01D (QHSS)*	24.44 ± 0.80	24.79 ± 0.47	N/A	25.15 ± 1.71
NEL03D (ACQUIRE)*	26.40 ± 0.58	26.26 ± 0.78	25.24 ± 0.86	N/A
NEL03D (QHSS)*	25.43 ± 0.83	24.96 ± 0.27	N/A	26.60 ± 0.78
NEL06A (ACQUIRE)*	25.57± 0.58	25.26 ± 2.11	25.67 ± 1.20	N/A
NEL07C (ACQUIRE)*	26.28 ± 0.74	26.07 ± 0.81	25.77 ± 1.12	N/A

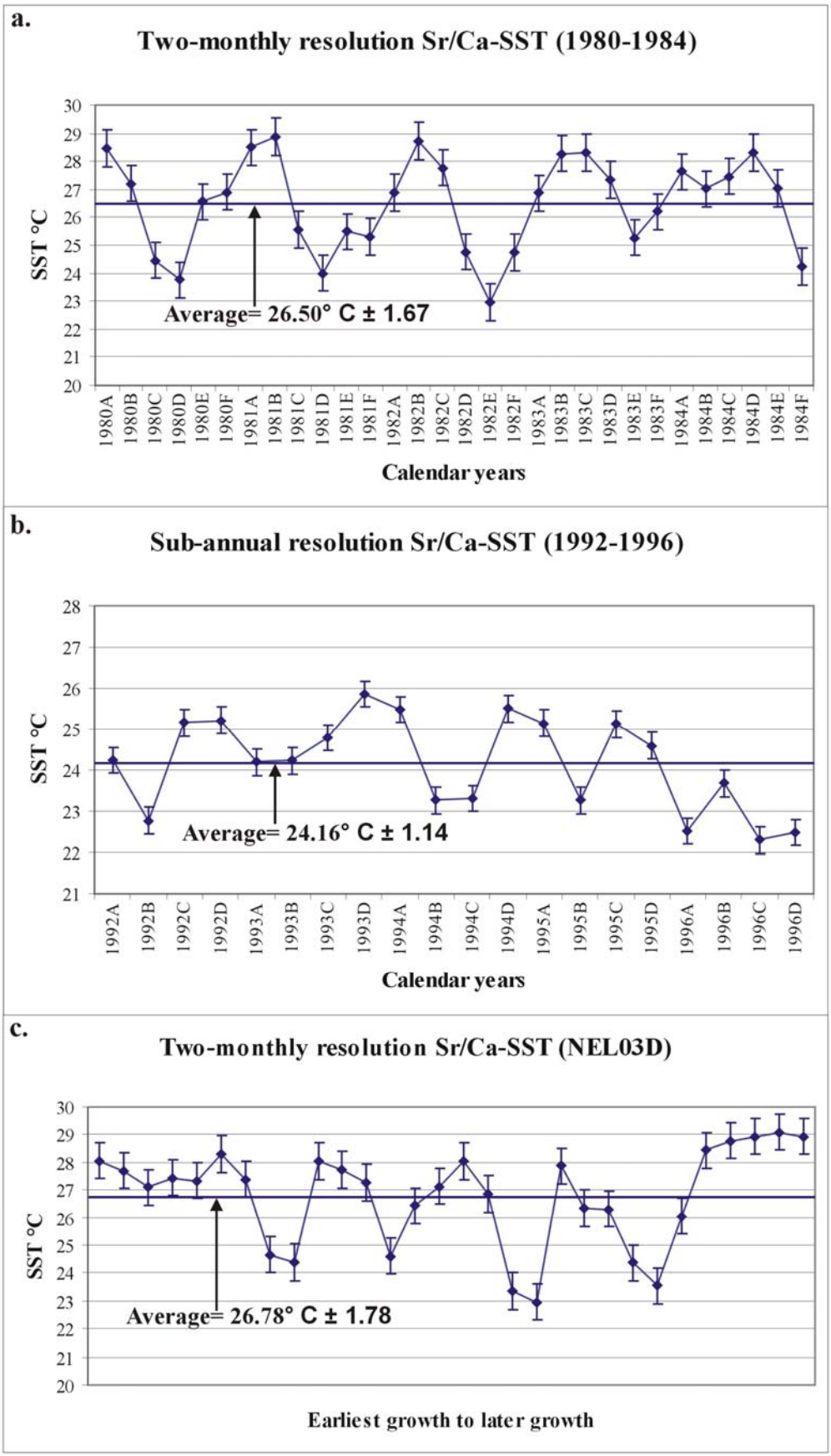

Figure 6.5 (a-c). Sub-annual resolution Sr/Ca-SST reconstructions for the modern (a-b) and mid-Holocene (c) corals. The records displayed a strong seasonality; however, the 1992-1996 record (b) should be rejected from further discussion as the coral was not sampled along the major growth axis.

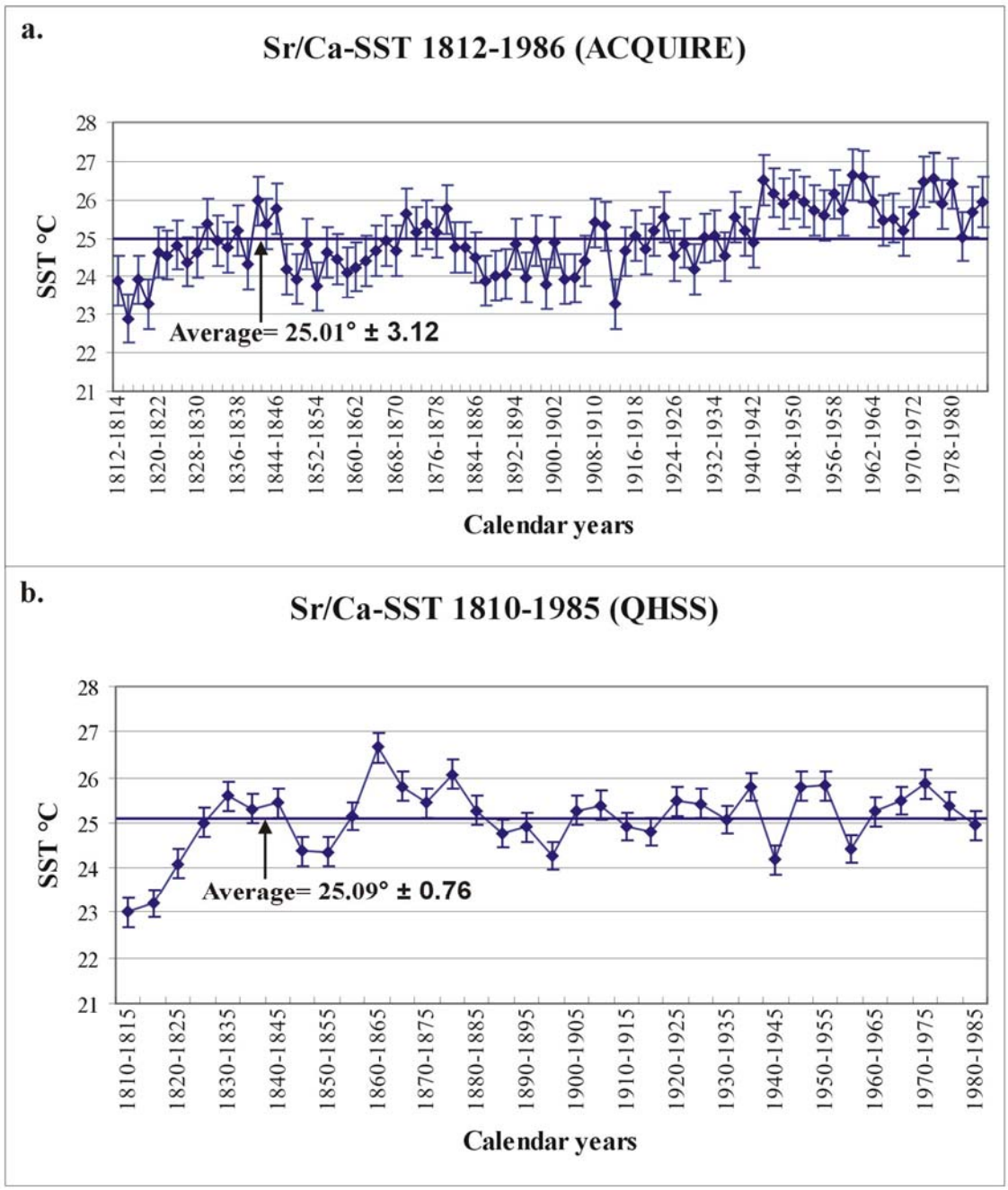

Figure 6.6 (a-b). Sr/Ca-SST reconstruction for the MAG01D modern coral record. The apparent "cooling" indicated by the 1810-1820 samples may, in fact, be a juvenile coral signature and this data may need to be rejected. Both the records displayed similar SST averages and suggest that there was an excellent replication between the two laboratories. The warming trend displayed in the ACQUIRE record after the 1930s is not supported by the QHSS dataset. It appears that the QHSS Sr/Ca-SST reconstruction has not been affected by the H_2O_2 treatment.

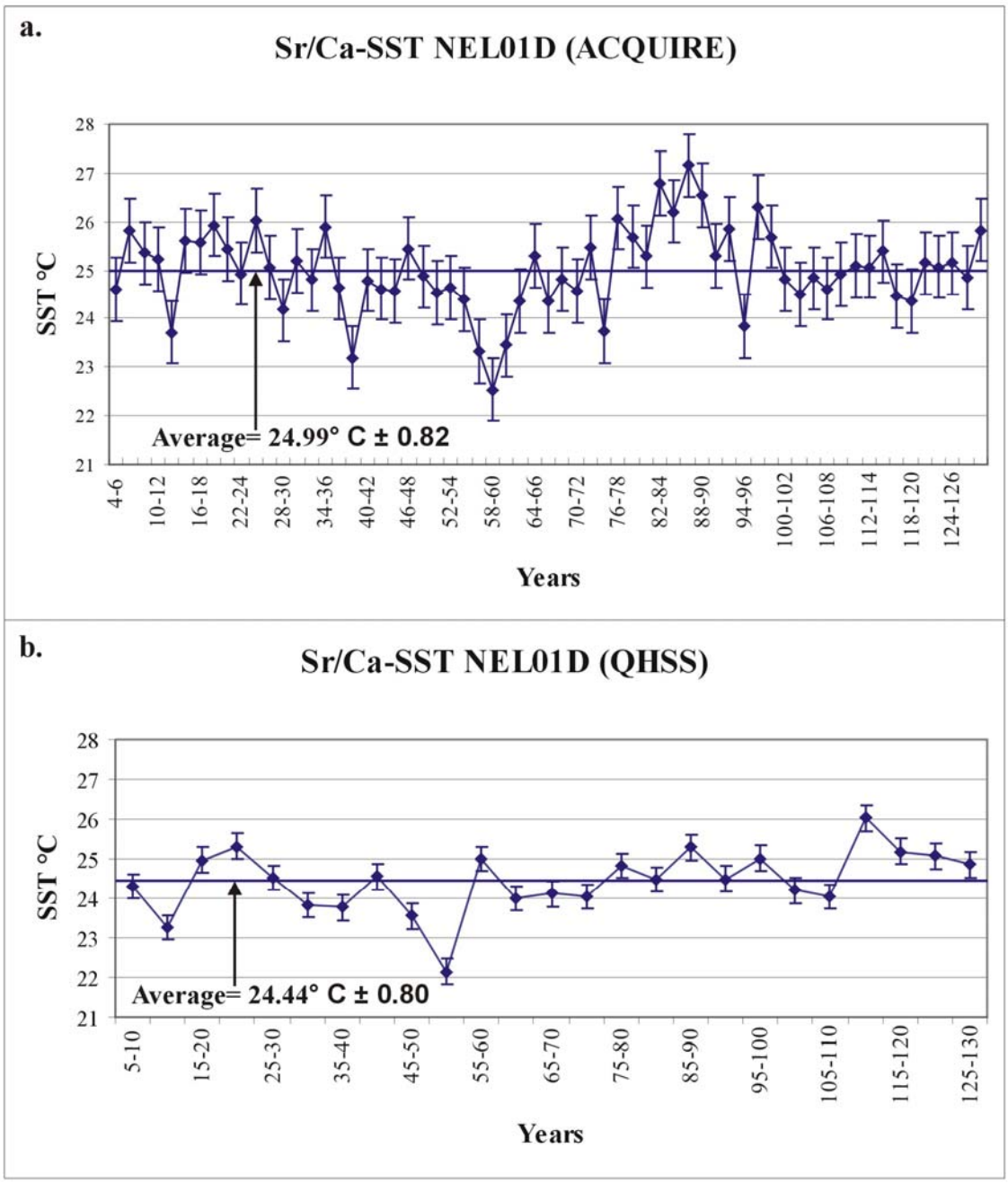

Figure 6.7 (a-b). Sr/Ca-SST reconstructions for the mid-Holocene corals. The averages were indistinguishable from the modern records which suggest that SSTs in the waters surrounding Magnetic Island 6,000 years ago were similar to today. However, some of the variations in SST of up to 1-2° C between 2 and 5 yearly periods are unlikely and may be a product of analytical or sampling error.

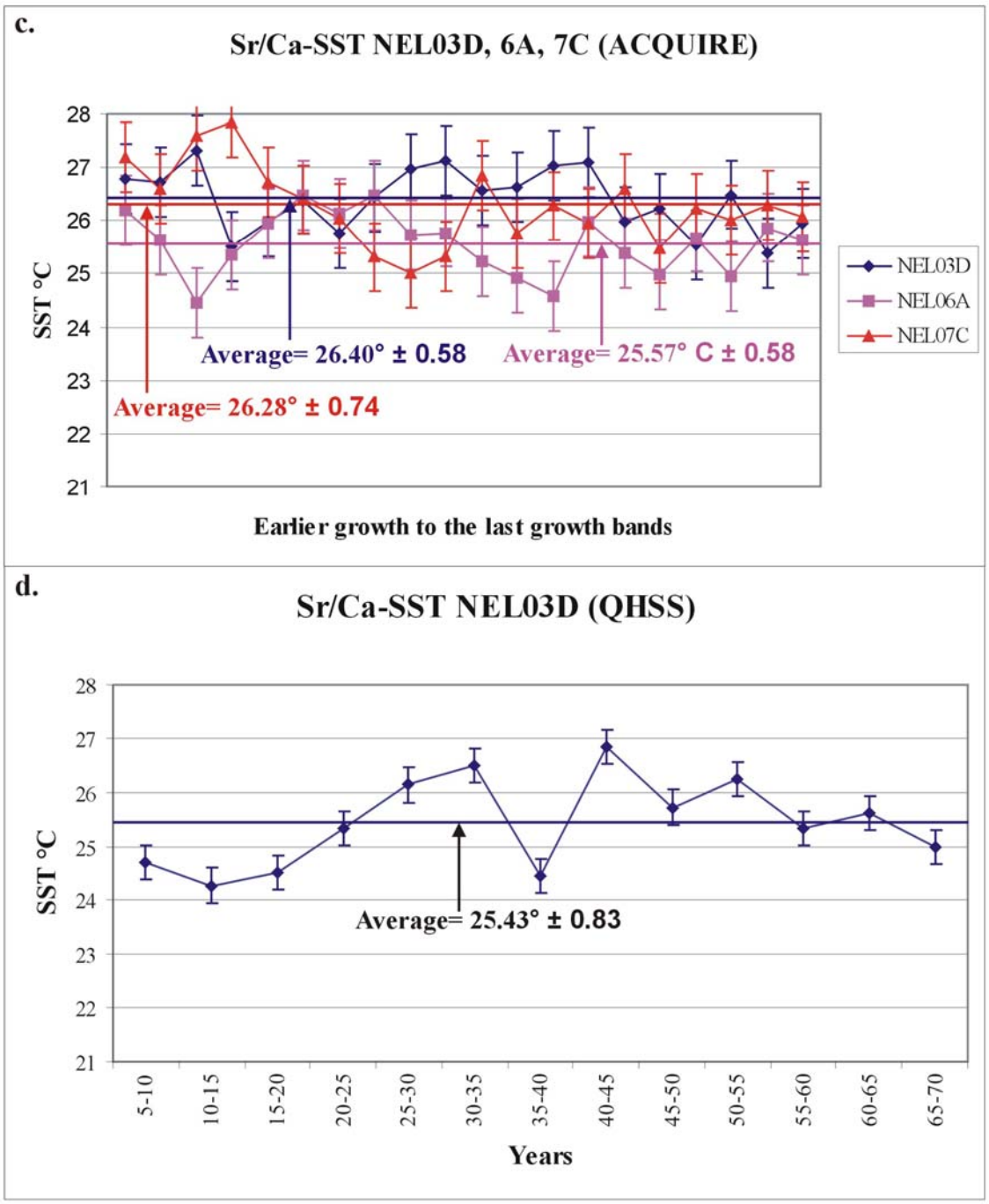

Figure 6.7 (c-d). Sr/Ca-SST reconstructions for the mid-Holocene corals (continued). The SSTs towards the final growth bands were similar to the early growth measurements (c) which indicate that extreme SST was unlikely to have caused the death of these corals.

6.4.3. Mg/Ca ratios

The average coral Mg/Ca-SST estimates for the 1980-1984 and 1992-1996 periods were 26.30 ± 1.84º C and 25.84 ± 0.51º C, respectively (Fig 6.8a-b). Both datasets exhibit seasonal variations; however, the Mg/Ca-SST estimates for the 1992-1996 period did not match the range of the instrumental SST records. The 1992-1996 data were rejected

as this coral slice (NEL09C) has a poor growth record (Fig 4.11) and could not be sampled along the major growth axis. The average of the two-monthly resolution Mg/Ca-SST record for the mid-Holocene coral (27.18 ± 2.33º C; NEL03D; Fig 6.8c) was slightly higher than for the 1980-1984 record. Both records displayed similar seasonality but the upper range for the mid-Holocene record was approximately 1º C higher than the 1980-1984 reconstruction.

The long-term Mg/Ca-SST estimates for the 1812-1986 period averaged 26.21 ± 0.98º C and 24.62 ± 0.37º C for the 2 and 5 yearly sampling resolutions, respectively (Table 6.1; Fig 6.9a-b). The significant difference in the average SSTs were probably related to the different Mg/Ca-SST calibrations that were applied to account for the H_2O_2 treatment. In addition, the untreated samples displayed considerable SST variability and may be influenced by an organic component (Fig 6.9a). Both the Mg/Ca and Sr/Ca-SST records displayed a warming trend of ~2° C from the 1860s-1880s but the Sr/Ca-SST variations may be accounted for by the 1σ standard deviation. This trend was also observed in the H_2O_2-treated Mg/Ca-SST 5 yearly resolution record. The Mg/Ca-SST reconstruction for the untreated ACQUIRE dataset revealed anomalous cooling "pulses" of up to 3° C that cannot be accounted for by the 1σ analytical error. These Mg/Ca shifts may derive from organic matter which could be distributed heterogeneously in the coral skeleton; the pre-treated samples display relatively flat trends over the 5 yearly resolution periods (Fig 6.9b). Alternatively, the SST fluctuations in the 2 yearly dataset may be an artefact of the Mg/Ca-SST calibration curve that was applied to the untreated samples. This calibration curve contained a steeper slope than the curve applied for the pre-treated samples (Fig 4.15). Therefore, any deviations in the coral Mg/Ca ratios would produce larger fluctuations in the reconstructed SST for the untreated dataset compared to the calibration curve applied to the pre-treated samples.

As with the Sr/Ca ratio, the average Mg/Ca-SST reconstructions agreed with both the mid-Holocene and modern coral records (Table 6.1). The average Mg/Ca-SST reconstructions were also systematically higher in the untreated 2 yearly ACQUIRE samples compared to the H_2O_2 treated 5 yearly resolution dataset for the mid-Holocene coral records (Table 6.1; Fig 6.10). This difference might be due to the alternative calibrations for the two datasets or because the untreated samples may have been affected by an organic component.

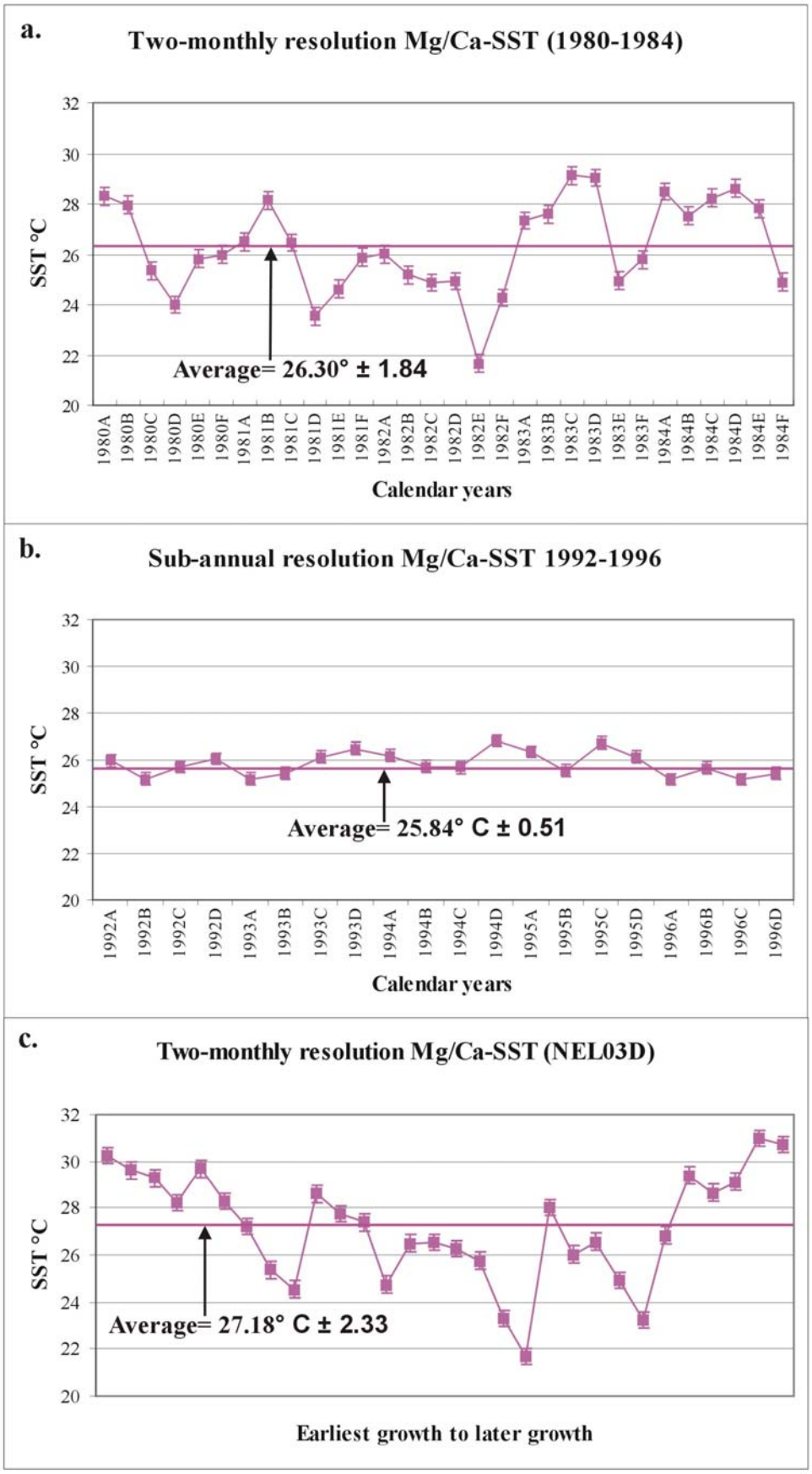

Figure 6.8 (a-c). Sub-annual resolution Mg/Ca-SST reconstructions for the modern (a-b) and mid-Holocene corals (c). Both the 1980-1984 and mid-Holocene records displayed a similar range and average. The 1992-1996 record was rejected as the coral was not sampled along the major growth axis.

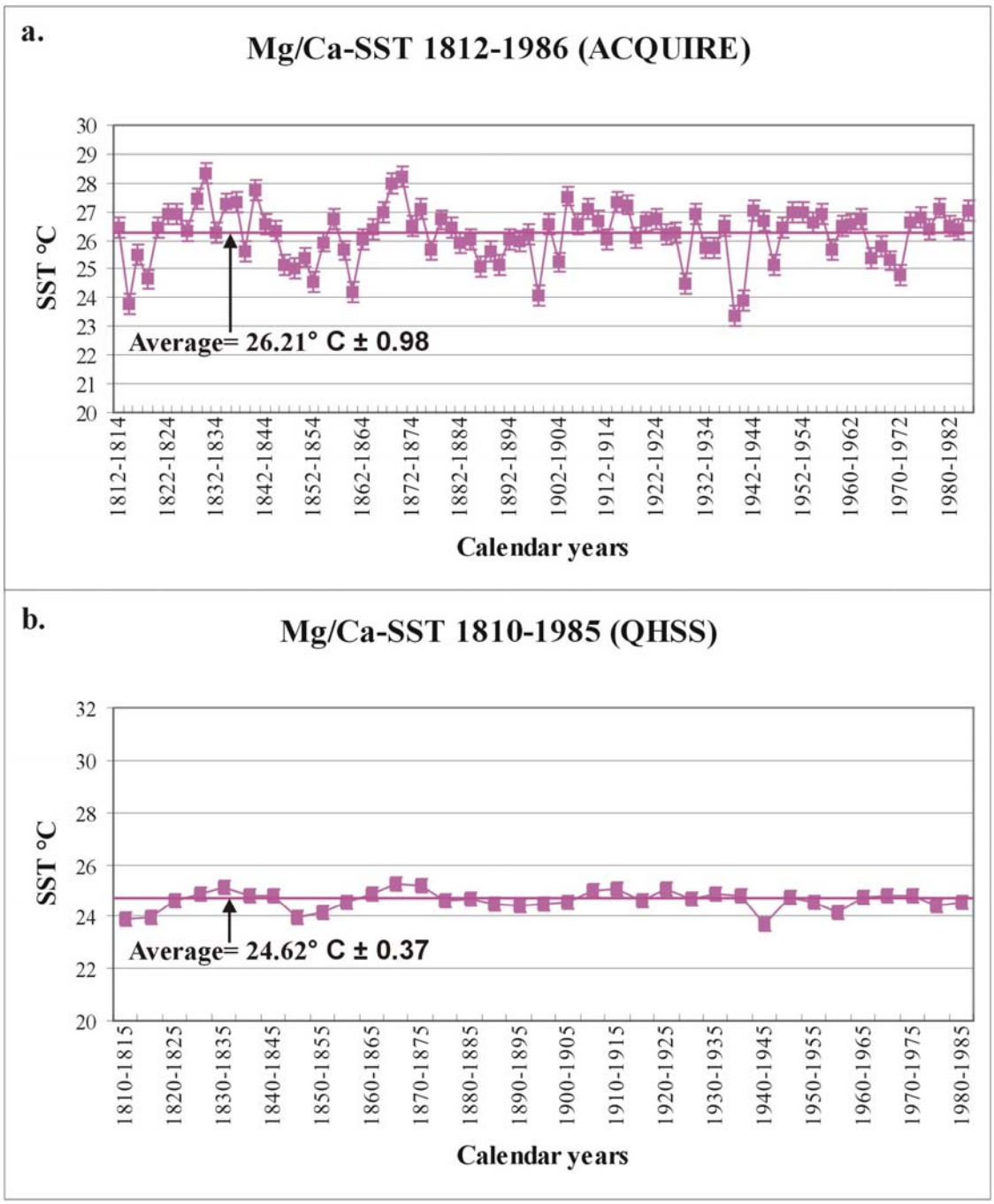

Figure 6.9 (a-b). Mg/Ca-SST reconstructions for the MAG01D coral slice (1812-1986). The SST reconstructions reveal a warming trend between 1860 and 1870. The variability observed in (a) compared to (b) might be related to the different Mg/Ca-SST calibrations or that the untreated samples (a) may be affected by an organic component.

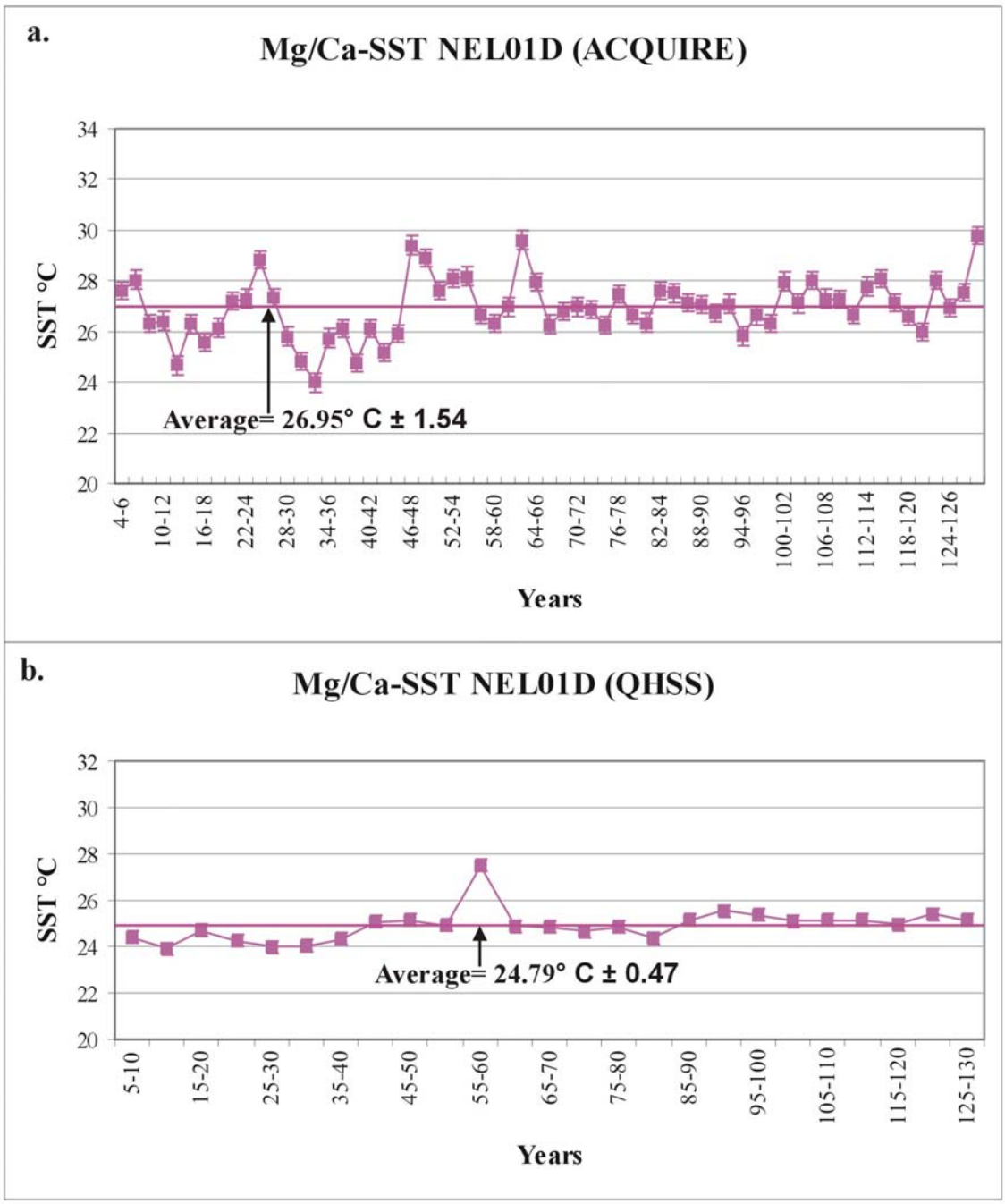

Figure 6.10 (a-b). Mg/Ca-SST reconstructions for the mid-Holocene corals. Similarly to Sr/Ca, the Mg/Ca ratios displayed a consistent trend and contained average SSTs that were similar to the modern record. The large SST variability in (a) is probably due to an organic influence as the coral was analysed untreated.

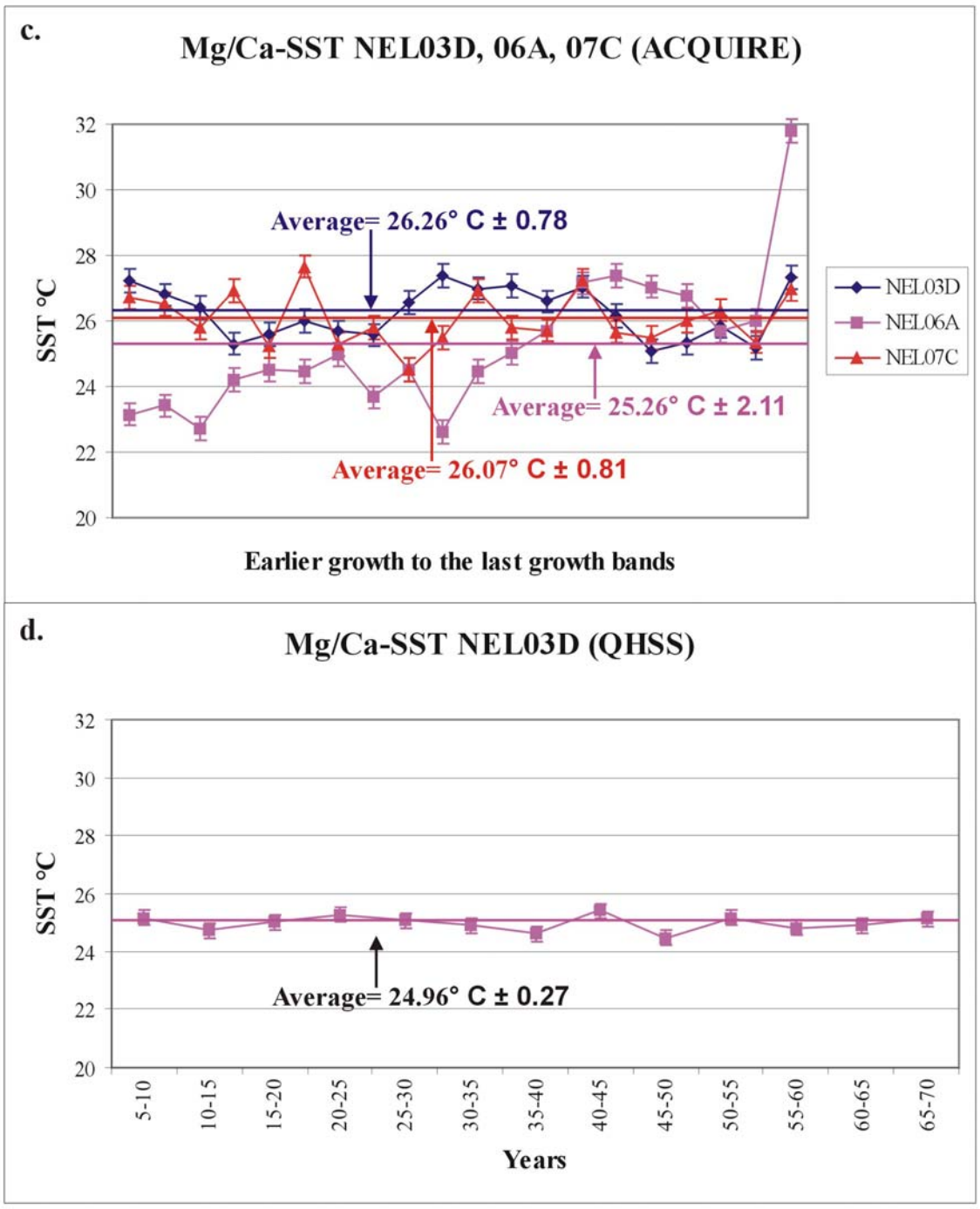

Figure 6.10 (c-d). Mg/Ca-SST reconstructions for the mid-Holocene corals (continued). With the possible exception of the NEL06A coral, there was no evidence of extreme temperature recorded in the final growth bands of the mid-Holocene corals. The Mg/Ca-SST reconstruction for the NEL06A coral slice displayed highly variable SSTs which may suggest that Mg in this record may have been influenced by another component or may be a product of sampling and/or calibration error. The large SST variability in (c) is probably affected by an organic component as these samples were analysed untreated. An alternative possibility for the large SST variability in (a) and (c) is that the calibration curve for the untreated samples contained a significantly steeper slope than the H_2O_2 treated curve (see Fig 4.15).

6.4.4. U/Ca ratios

The 1980-1984 coral U/Ca-SST record showed a seasonal cycle similar to both the Sr/Ca and Mg/Ca datasets (Fig 6.11a; Table 6.1). The average U/Ca-SST reconstruction for the 1980-1984 record (27.13 ± 1.84º C) was higher than the two-monthly resolution mid-Holocene record (25.91 ± 1.76º C; Fig 6.11b), but the datasets were within the 1σ standard deviation. The SST range of the mid-Holocene data was also similar to the modern record but did not display convincing seasonal variations. One of the mid-Holocene samples contained an anomalously high U concentration which strongly affected the SST estimate (-24.36° C). It is unlikely that excess U was incorporated into the coral lattice during a large flood event as the corresponding O isotope value does not display a significant shift towards lower salinity (Fig 6.14b). This data point corresponds to an elevated Mn concentration; therefore, an oxide/hydroxide phase or sediments may have been incorporated in this sample.

The 2 yearly 1812-1986 U/Ca-SST reconstruction averaged 27.45 ± 0.75º C (Fig 6.12) which was higher than the average Sr/Ca and Mg/Ca-SST estimations, although the results were within the 1σ standard deviation error (Table 6.1). The U/Ca-SST record did not display the trends (e.g. the apparent 1860s warming) in the Sr/Ca and Mg/Ca reconstructions.

The average U/Ca-SST reconstructions for the mid-Holocene corals were lower in the mid-Holocene records compared to the modern coral; however, they were within analytical error of the mid-Holocene SST estimates produced by the Sr/Ca and Mg/Ca ratios (Table 6.1). As with the Sr/Ca-SST estimates the U/Ca-SST data displayed warming and cooling trends for the mid-Holocene corals that were not apparent in the H_2O_2-treated Mg/Ca record (Fig 6.13a-b). The likelihood of these large SST variations over averaged 2 and 5 yearly records is doubtful, and the poor reproducibility of the analyses may explain this variability. However, the long-term SST averages for the modern coral appears to match the range that would be expected for Magnetic Island. These results are discussed further in section 7.2.

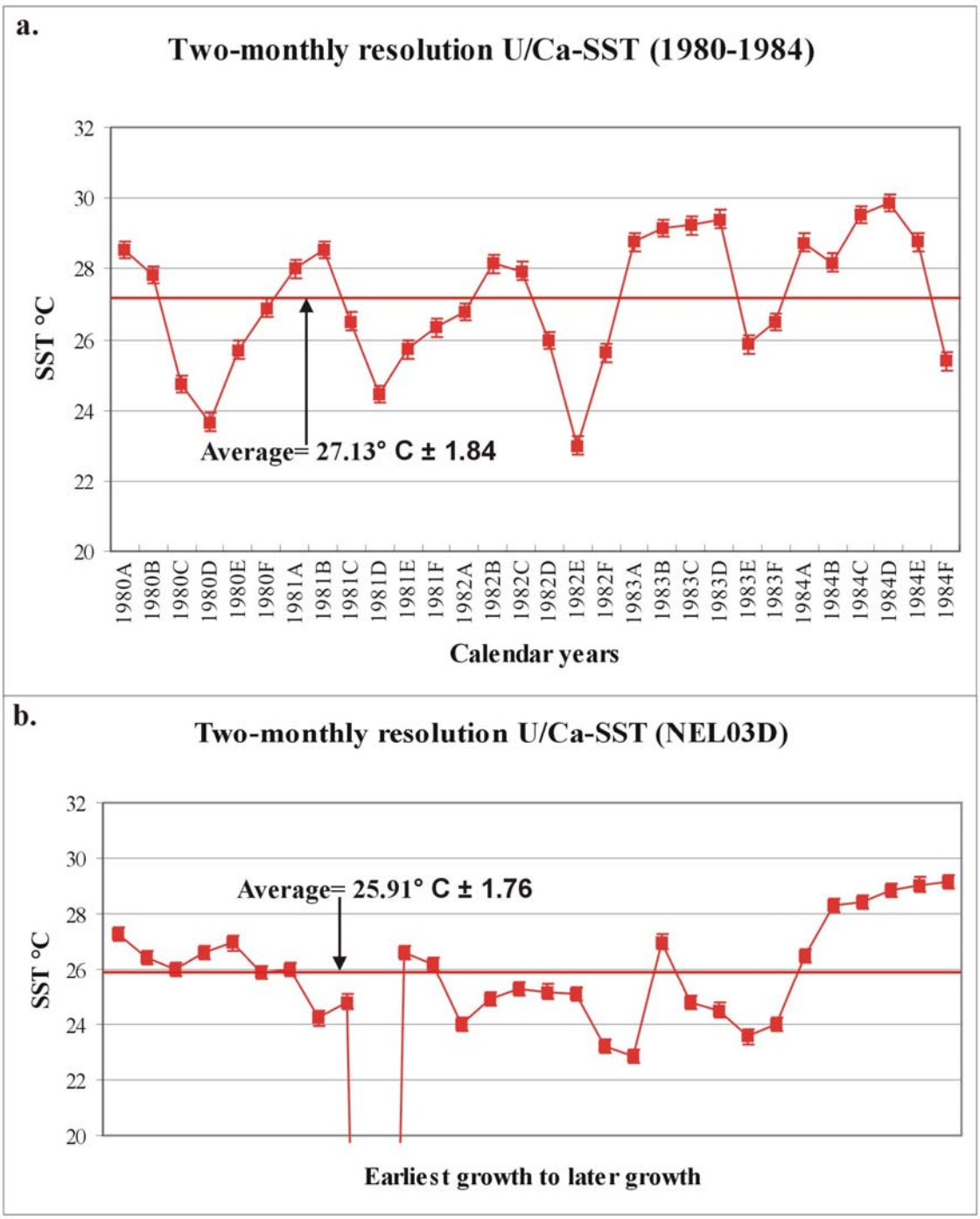

Figure 6.11 (a-b). The two-monthly resolution U/Ca-SST reconstruction for the 1980-1984 record (a) displayed strong seasonality. However, the seasonality for the mid-Holocene record (b) was not convincing with an inconsistent reading (-24.36°) due to excess U incorporated in the coral. Interestingly, this point also corresponds to a significant increase in Mn. The oxygen isotopes reveal that there was no major flood during this time; therefore, the excess U may be derived from detrital material trapped within the coral skeleton.

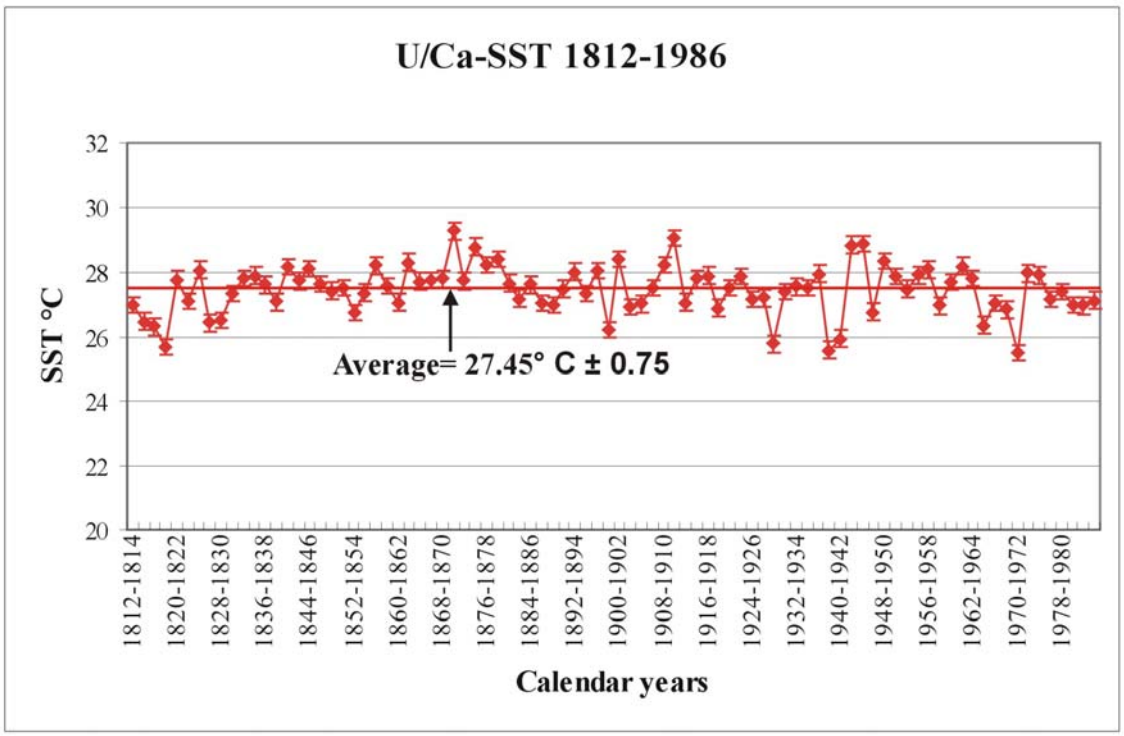

Figure 6.12. U/Ca-SST reconstruction for 1812-1986. The U/Ca ratios did not display the warming trend from 1860-1880 that was apparent in the Sr/Ca and Mg/Ca ratios. The ratios showed significant variations of 1-2° C which was unlikely given the homogenised 2 yearly sampling employed in this study.

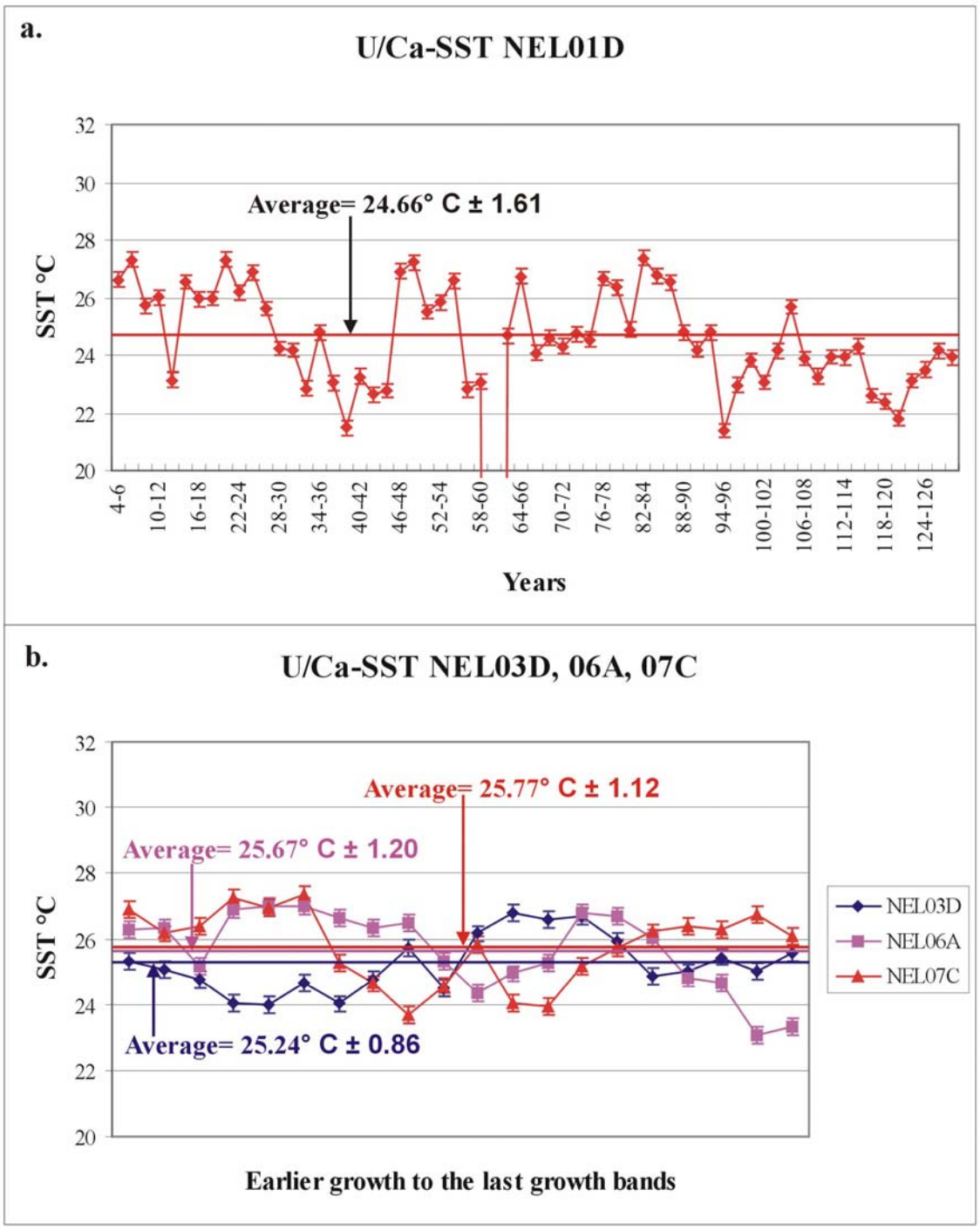

Figure 6.13 (a-b). U/Ca-SST reconstructions for the mid-Holocene coral heads. These records displayed large SST variability that did not appear to be reasonable. The reproducibility of the analyses may account for some of these large variations in the SST estimates. Like the Sr/Ca and Mg/Ca ratios, the final growth bands for the mid-Holocene corals (b) did not show any large shifts in SST, which suggests that extreme temperatures did not contribute to the corals death.

6.1.1. O isotopes

The average O isotope-SST reconstruction for 1980-1984 (25.71 ± 3.31º C; Fig 6.14a) was similar to the other SST proxies; the data also displayed seasonal variations. However, the SST range (18.13-33.22º C) was significantly higher than the other proxy SST estimates and outside the modern instrumental range. These data have been affected by freshwater input and evaporation as oxygen isotopes are affected by a combination of SST and seawater salinity (see section 2.2.2). The two-monthly resolution mid-Holocene record has also been influenced by seawater salinity which is evident from the considerably higher average temperature (28.00 ± 3.28º C) compared to the other SST proxies (Fig 6.14b; Table 6.1). Major flood events can be observed in the coral record by plotting the Sr/Ca-SST estimates alongside the corresponding O isotope data (Fig 6.14).

The average 5 yearly δ^{18}O-SST reconstruction from 1810-1985 (25.81± 1.21º C; Fig 6.15) was similar to the other coral SST proxies. The 1810-1985 δ^{18}O data appeared to display some warming and cooling trends; however, changes in freshwater inputs/seawater salinity may have significantly influenced this record. The addition of the corresponding Sr/Ca-SST reconstruction to the O isotope record provides an assessment of wetter and drier periods over this timeframe. These data suggest that the 1830-1880 and 1930-1960 periods were drier while 1880-1930 and the 1970s were wetter. There may be a relatively wetter period during 1810-1830; however, the Sr/Ca ratios may have been affected by a juvenile coral signature (see section 6.4.2).

The averages of the mid-Holocene O isotope-SST reconstructions were similar to the modern 1810-1985 record (6.16a-b) and also closely corresponded to the averages of the other SST proxies (Table 6.1). There were also variations between wetter and drier periods during the mid-Holocene which are highlighted by overlying the Sr/Ca ratios to the O isotope record.

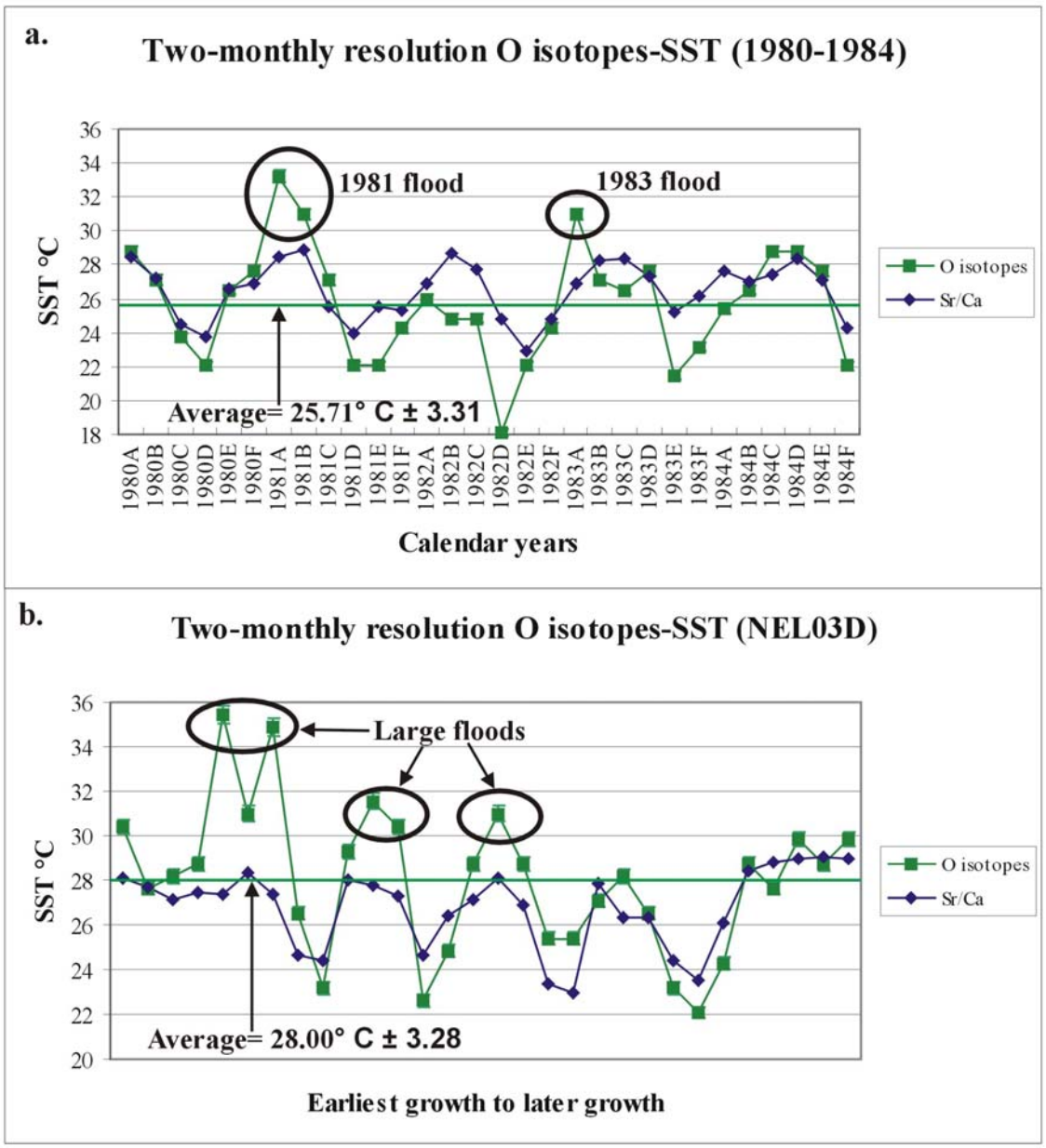

Figure 6.14 (a-b). Two-monthly O isotope-SST reconstructions for the 1980-1984 (a) and the mid-Holocene (b) coral records. The O isotope records both displayed excellent seasonality, although the SST range is outside that predicted by the Sr/Ca ratio. Presumably, this range was due to variations in salinity as the O isotopes record the flood events of 1981 and 1983 as well as what appeared to be three to four large floods in the mid-Holocene record. Despite the influence of floods on these records, the O isotopes displayed a significant correlation with the Sr/Ca ratios.

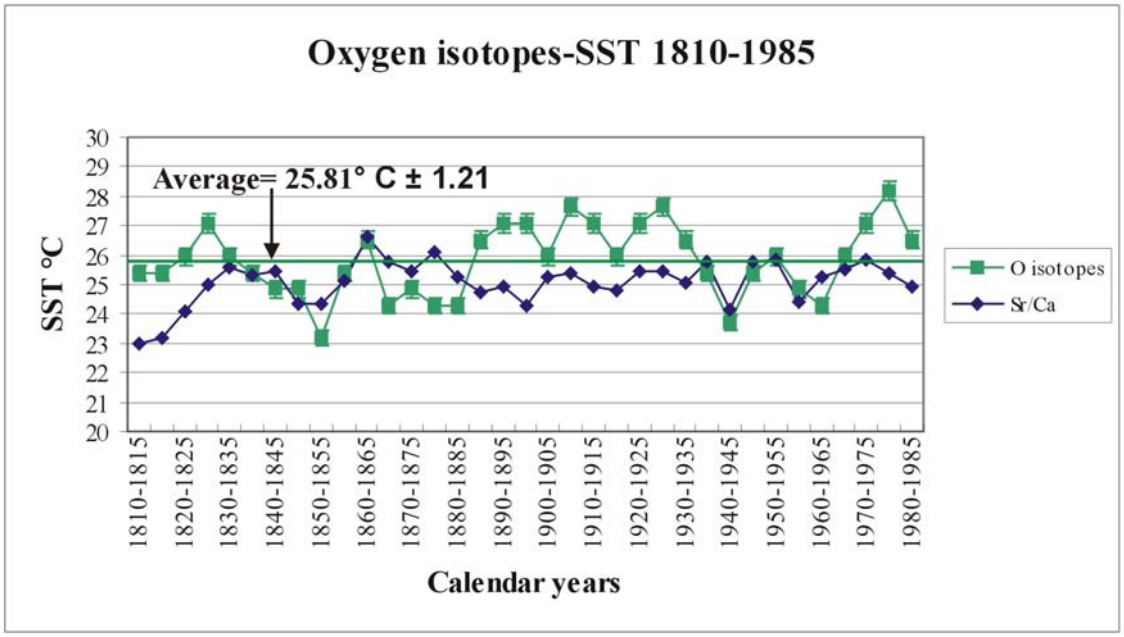

Figure 6.15. Coral oxygen isotope-SST reconstruction for 1810-1985. The O isotopes provide average SST estimates comparable to the other coral proxies. Wetter and drier periods over the last 200 years can be identified by overlying the Sr/Ca SST estimates to the O isotope record.

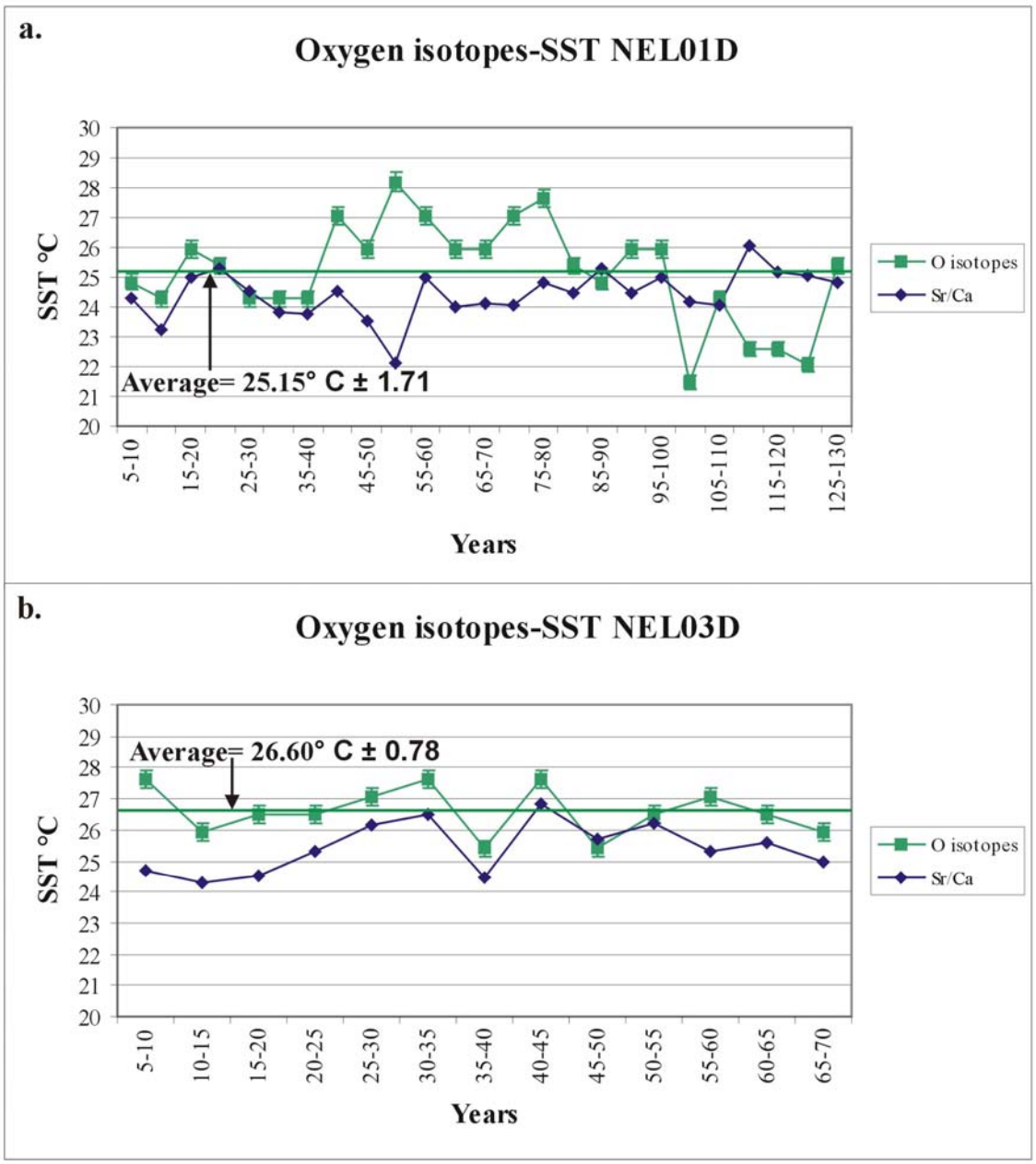

Figure 6.16 (a-b). Oxygen isotope-SST reconstructions for the mid-Holocene coral heads. Similarly to the modern records, the O isotope-SST reconstructions follow a similar trend to the Sr/Ca ratios.

6.1.2. Summary

The long-term averages from the different coral proxy SST reconstructions were similar with a few notable exceptions. The coral proxy SST reconstructions for the two-monthly resolution 1980-1984 record displayed seasonal variations and the proxies all contained a similar SST average and range to each other and to the instrumental SST records. The inconsistent results for the 1992-1996 record reflect the coral's poor growth record and should be rejected from further discussion. The coral Mg/Ca-SST reconstructions for the untreated samples also displayed inconsistent results.

6.2. $\Delta^{18}O$ results

6.2.1. Overview

This section reconstructs seawater salinity ($\Delta^{18}O$) by subtracting the Sr/Ca SST estimates from the corresponding O isotopic-SST data for the two-monthly resolution and 5 yearly resolution datasets. Coral $\Delta^{18}O$ reconstructions of seawater salinity reveal flood events in the two-monthly resolution records, while long-term trends between wetter and drier periods can be identified in the 5 yearly resolution records.

6.2.2. Oxygen isotopes

The two-monthly resolution $\Delta^{18}O$ data for 1980-1984 (Fig 6.17a) displayed 2 notable negative excursions that corresponded to flood events during the summer months of 1981 and 1983. Aside from these two "events", the majority of $\Delta^{18}O$ measurements remained in the positive portion of the graph and there was a significant shift towards strong positive values during late 1982. These strongly positive $\Delta^{18}O$ values coincided with the 1982-1983 ENSO event.

The $\Delta^{18}O$ values for the mid-Holocene records were consistently more negative (average= -0.22‰) compared to the 1980-1984 record (+0.14‰; Fig 6.17). The difference in the average $\Delta^{18}O$, however, was not significant when the standard deviation was taken into account (± 0.44‰). There were also two distinct spikes toward

strongly negative $\Delta^{18}O$ values in the mid-Holocene record which suggest significant freshwater influx (Fig 6.17b).

The 5 yearly resolution 1810-1985 $\Delta^{18}O$ data displayed oscillations from relatively positive to negative values (Fig 6.18). The coral record contained mostly positive $\Delta^{18}O$ values between the 1840s and 1880s and from the 1930s to the 1960s, while a shift toward more negative values occurred from the 1880s to the 1930s and the 1970s. The modern coral $\Delta^{18}O$ record averaged -0.13‰ ± 0.24. The $\Delta^{18}O$ record during 1810-1830 may have been compromised by the Sr/Ca ratio which, in turn, may have been affected by a juvenile coral signature.

The majority of the mid-Holocene $\Delta^{18}O$ data were negative and averaged -0.13‰ ± 0.38 (NEL01D; Fig 6.19a) and -0.21‰ ± 0.15 (NEL03D; Fig 6.19b). The NEL01D coral record displayed a large negative shift in the "50-55" sample and then shifted to more positive $\Delta^{18}O$ values towards the end of the growth record. In contrast, the NEL03D record was consistently within negative $\Delta^{18}O$ values with no major deviations in the record.

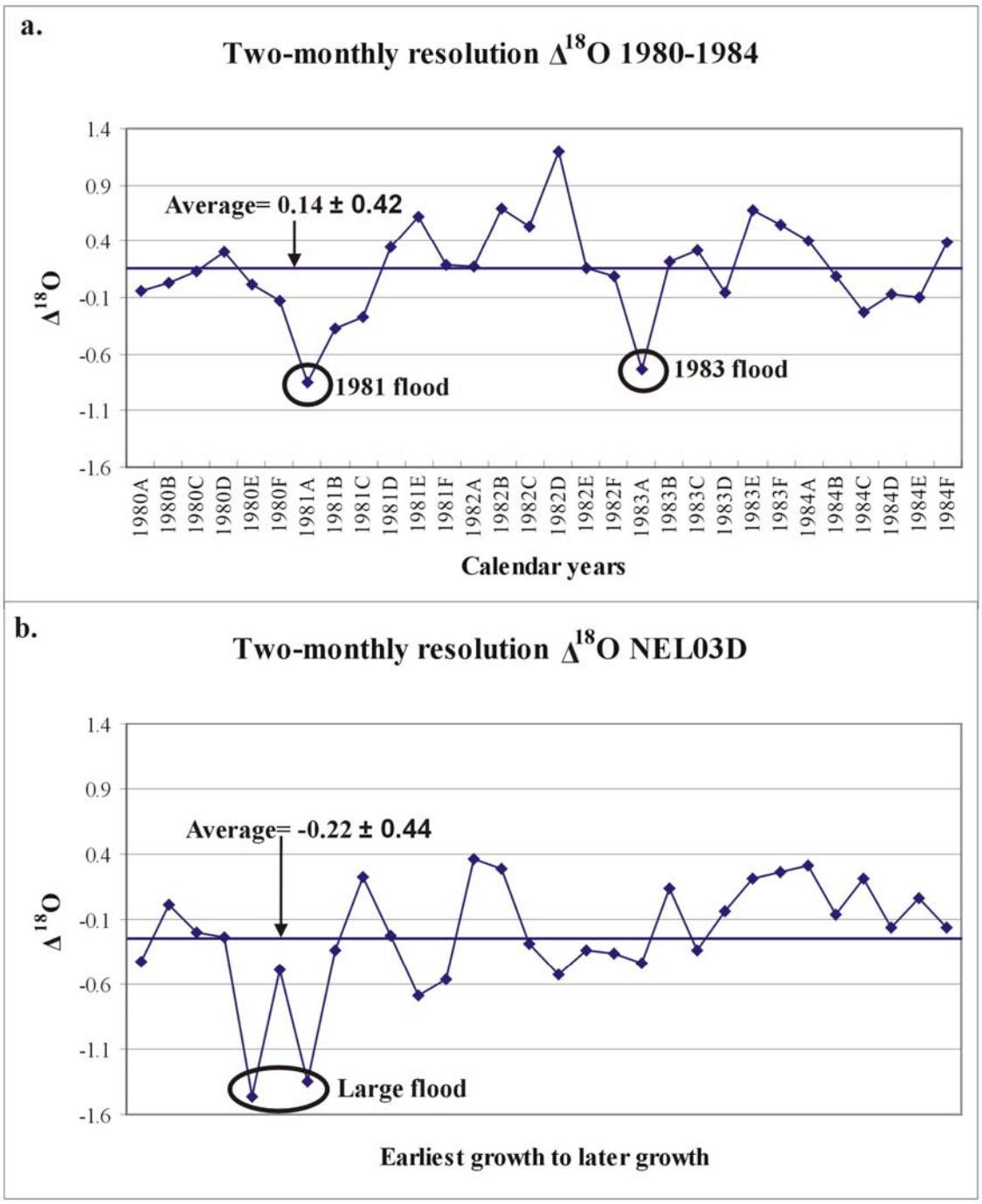

Figure 6.17 (a-b). A record of seawater salinity ($\Delta^{18}O$) was produced by subtracting the SST component from the O isotope record using the Sr/Ca ratios. Large negative excursions in $\Delta^{18}O$ were consistent with lowered salinity due to flood events. The $\Delta^{18}O$ values were particularly negative during the floods of 1981 and 1983 (a) as well as some large flood events in the mid-Holocene record (b).

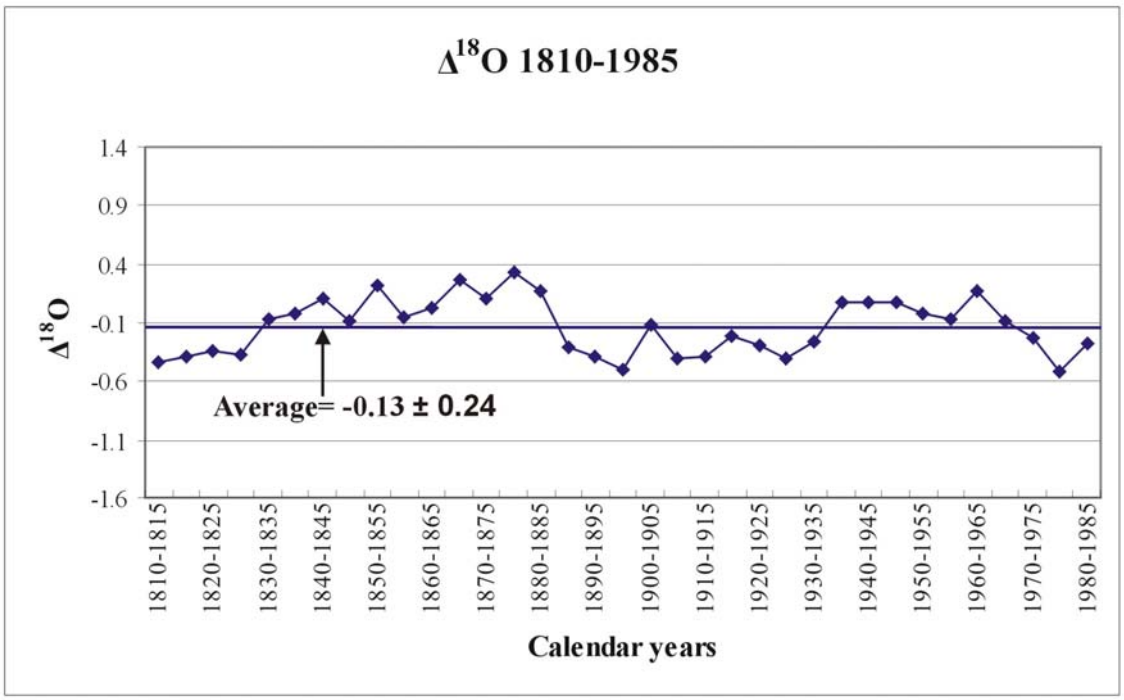

Figure 6.18. The coral $\Delta^{18}O$ record for 1810-1985. Using the Sr/Ca ratios to subtract the SST component from the O isotopes reveals the seawater salinity conditions that the corals endured. The record indicated that there were drier periods during 1830-1880 and 1935-1970, while wetter years persisted during 1885-1935 and the 1970s.

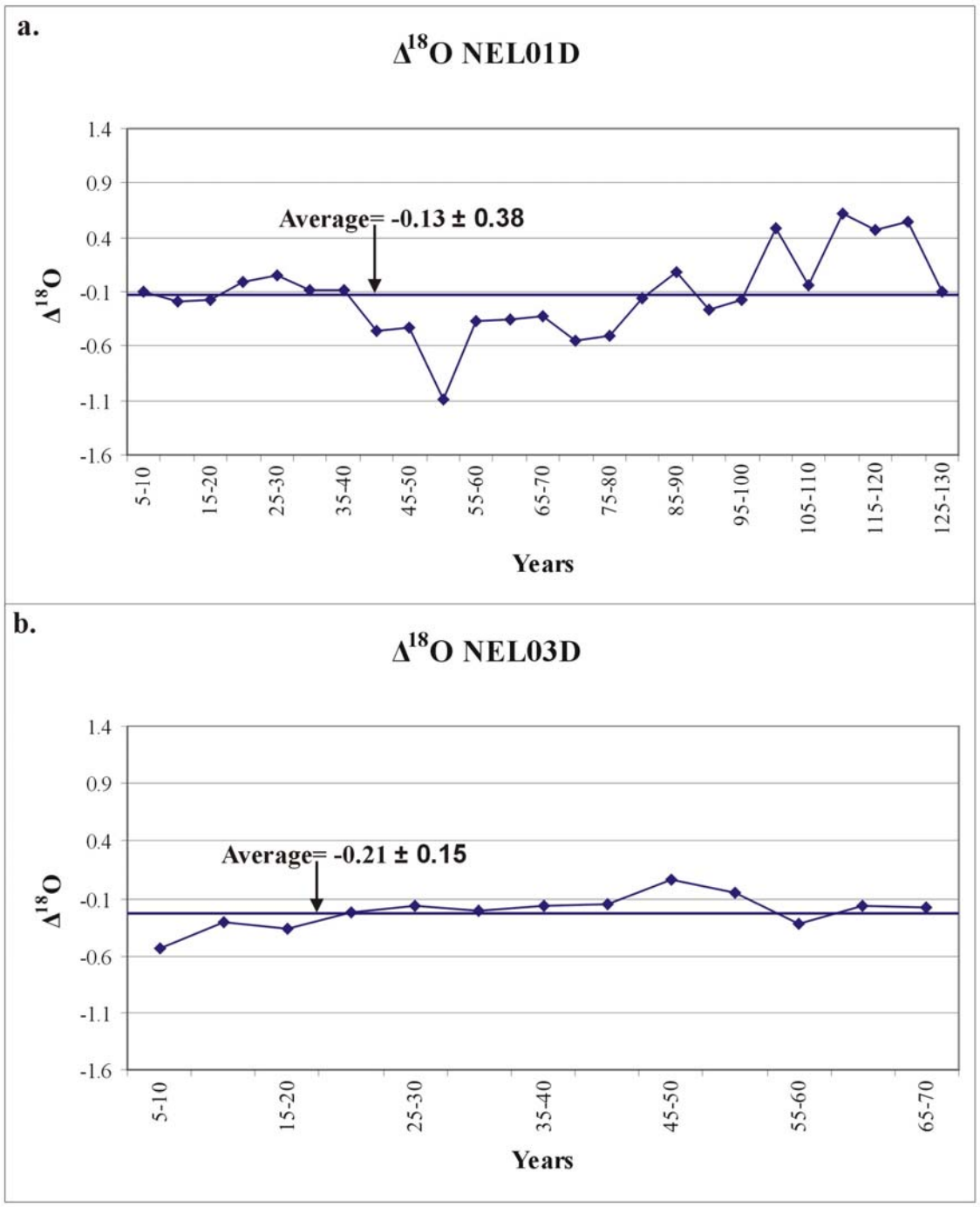

Figure 6.19 (a-b). The $\Delta^{18}O$ record for the mid-Holocene coral heads. The NEL01D coral showed some variability in seawater salinity while the NEL03D record did not reveal any significant salinity variations.

6.2.3. Summary

The two-monthly $\Delta^{18}O$ reconstructions were significantly influenced by the 1981 and 1983 flood events as well as by the 1982-1983 ENSO event in the 1980-1984 coral record. In addition, the two-monthly mid-Holocene coral record also displayed evidence of large flood events. The coral $\Delta^{18}O$ records at the 5 yearly sampling

resolution revealed long-term trends of relatively wetter and drier years in both the 1810-1985 and the mid-Holocene NEL01D coral records; the average $\Delta^{18}O$ values were similar in these two records.

6.3. Trace element results

6.3.1. Overview

This section presents the results for the possible coral proxies of water quality including the Ba/Ca ratio, Mn concentration, rare earth elements and Th concentration. The impact of European settlement in the region on these coral proxies will be assessed in the 1812-1986 modern coral record by examining their pre and post-1850 averages. In addition, the mid-Holocene corals will provide an independent perspective on what should be considered as "baseline/natural" values.

6.3.2. Ba/Ca ratios

The average Ba/Ca ratios were similar for both the sub-annual 1980-1984 ($4.06 \times 10^{-6} \pm 1.05 \times 10^{-6}$) and 1992-1996 ($3.19 \times 10^{-6} \pm 4.94 \times 10^{-7}$) records; however, the two-monthly resolution mid-Holocene record had significantly higher coral Ba/Ca ratios (average= $7.33 \times 10^{-6} \pm 1.70 \times 10^{-6}$; Fig 6.20a-c). The 1980-1984 record contained two excessive Ba/Ca ratios above 6.00×10^{-6} that did not correspond to the negative $\Delta^{18}O$ excursions (flood events). Another source of Ba (other than river discharge) is required to explain the elevated Ba/Ca ratios (e.g. see Sinclair, 2005b). In addition, the flood events of 1981 and 1983 did not correspond to higher coral Ba/Ca ratios. This may be due to the sampling resolution in this study (6 samples per year) as additional work on coral luminescent lines have shown Ba to be enriched in these "flood bands" (see section 8.4.4). Interestingly, the majority of the Ba/Ca ratios for the two-monthly resolution mid-Holocene coral record were consistently above 6.00×10^{-6} and subsequently had a considerably higher average than the modern corals (Fig 6.20c). These "anomalous" coral Ba/Ca ratios are discussed further in section 8.4.

Significant increases in coral Ba/Ca after 1850 were observed in both the 2 and 5 yearly records of the 1812-1986 coral (Fig 6.21a-b). The 2 yearly resolution coral record

showed a rise in average Ba/Ca after 1850 from $2.07 \times 10^{-6} \pm 3.11 \times 10^{-7}$ to $3.65 \times 10^{-6} \pm 1.00 \times 10^{-6}$ after 1850; the 5 yearly record displayed a shift from $1.54 \times 10^{-6} \pm 7.42 \times 10^{-8}$ to $2.79 \times 10^{-6} \pm 5.25 \times 10^{-7}$. This data represents an average Ba increase of 76% and 81% for the 2 and 5 yearly records, respectively.

Despite the increase in coral Ba/Ca in the modern coral record after 1850, the mid-Holocene corals displayed significantly higher average values (Table 6.2). The lowest average Ba/Ca ratios of the mid-Holocene coral records was NEL01D ($3.66 \times 10^{-6} \pm 3.87 \times 10^{-7}$) compared to NEL06A which had the highest average Ba/Ca ratios ($1.02 \times 10^{-5} \pm 3.17 \times 10^{-6}$; Fig 6.22a-d).

Table 6.2. Summary of the Ba/Ca and Mn concentrations in the modern and mid-Holocene corals. The Ba/Ca ratios were significantly higher in the mid-Holocene coral compared to the modern coral; while Mn concentrations in the coral were similar during the mid-Holocene compared to the post 1850 record.

	Trace elements	
Coral record	**Ba/Ca (atomic)**	**Mn (ppm)**
1980-1984 (ACQUIRE)	$4.06E^{-06} \pm 1.05E^{-06}$	0.43 ± 0.09
1992-1996 (QHSS)	$3.19E^{-06} \pm 4.94E^{-07}$	0.88 ± 0.67
NEL03D (two-monthly resolution)	$7.33E^{-06} \pm 1.70E^{-06}$	1.35 ± 0.53
1812-1850 (ACQUIRE)	$2.07E^{-06} \pm 3.11E^{-07}$	0.58 ± 0.12
1850-1986 (ACQUIRE)	$3.65E^{-06} \pm 1.00E^{-06}$	1.66 ± 2.09
1810-1850 (QHSS)	$1.54E^{-06} \pm 7.42E^{-08}$	0.10 ± 0.12
1850-1985 (QHSS)	$2.79E^{-06} \pm 5.25E^{-07}$	1.53 ± 1.85
NEL01D (ACQUIRE)	$4.32E^{-06} \pm 1.02E^{-06}$	0.86 ± 0.23
NEL01D (QHSS)	$3.66E^{-06} \pm 3.87E^{-07}$	1.34 ± 1.12
NEL03D (ACQUIRE)	$7.89E^{-06} \pm 1.60E^{-06}$	1.38 ± 0.52
NEL03D (QHSS)	$5.50E^{-06} \pm 9.20E^{-07}$	1.11 ± 0.49
NEL06A	$1.02E^{-05} \pm 3.17E^{-06}$	1.95 ± 0.51
NEL07C	$5.80E^{-06} \pm 2.17E^{-06}$	2.01 ± 0.67

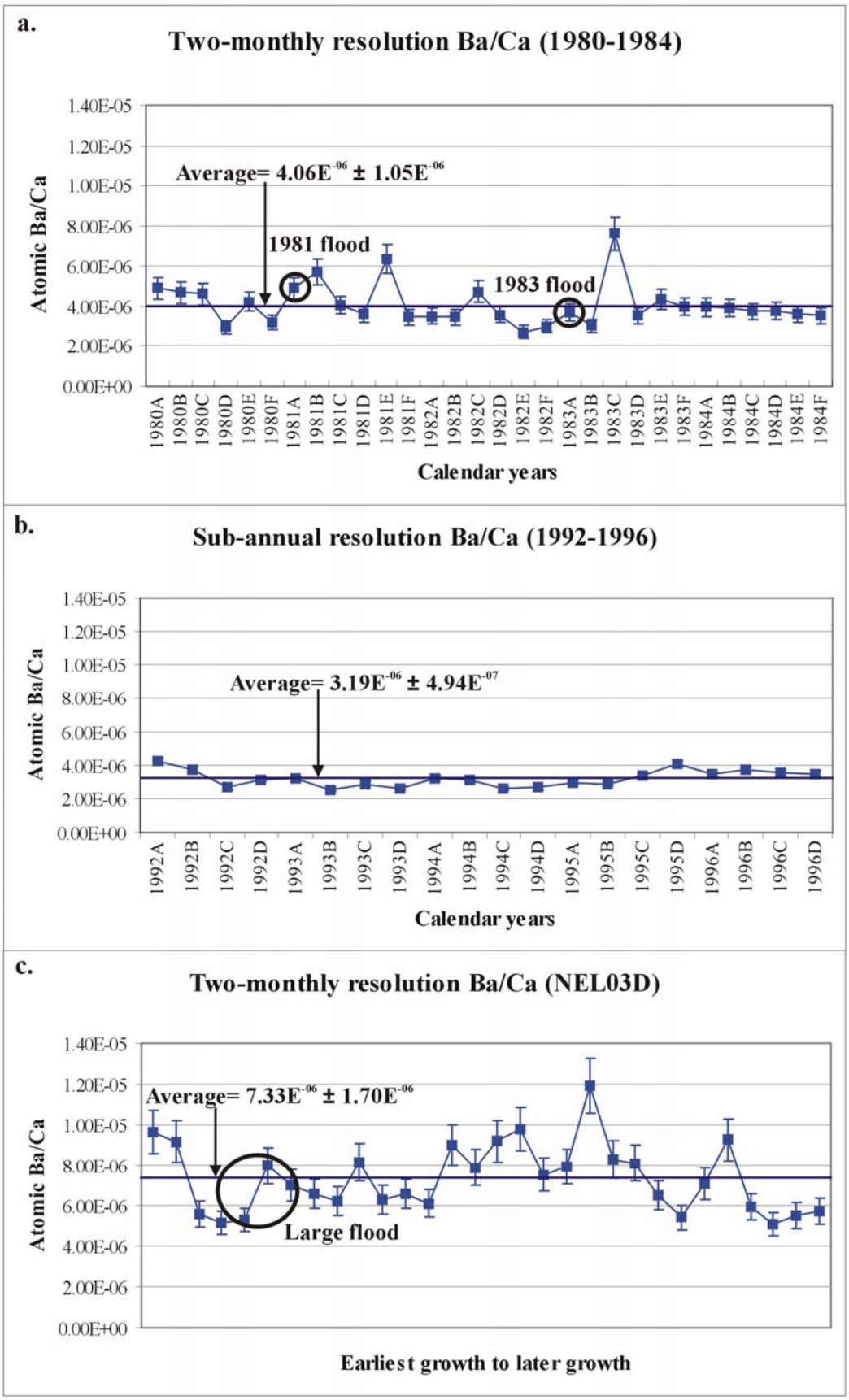

Figure 6.20 (a-c). Sub-annual Ba/Ca records for the modern and mid-Holocene corals. Interestingly, the Ba/Ca ratios did not display any significant enrichment during the floods of 1981 and 1983 or the large flood in the mid-Holocene record. This may be due to the sampling resolution employed on the corals as additional studies of luminescent lines revealed significantly elevated Ba concentrations (see section 8.4.4).

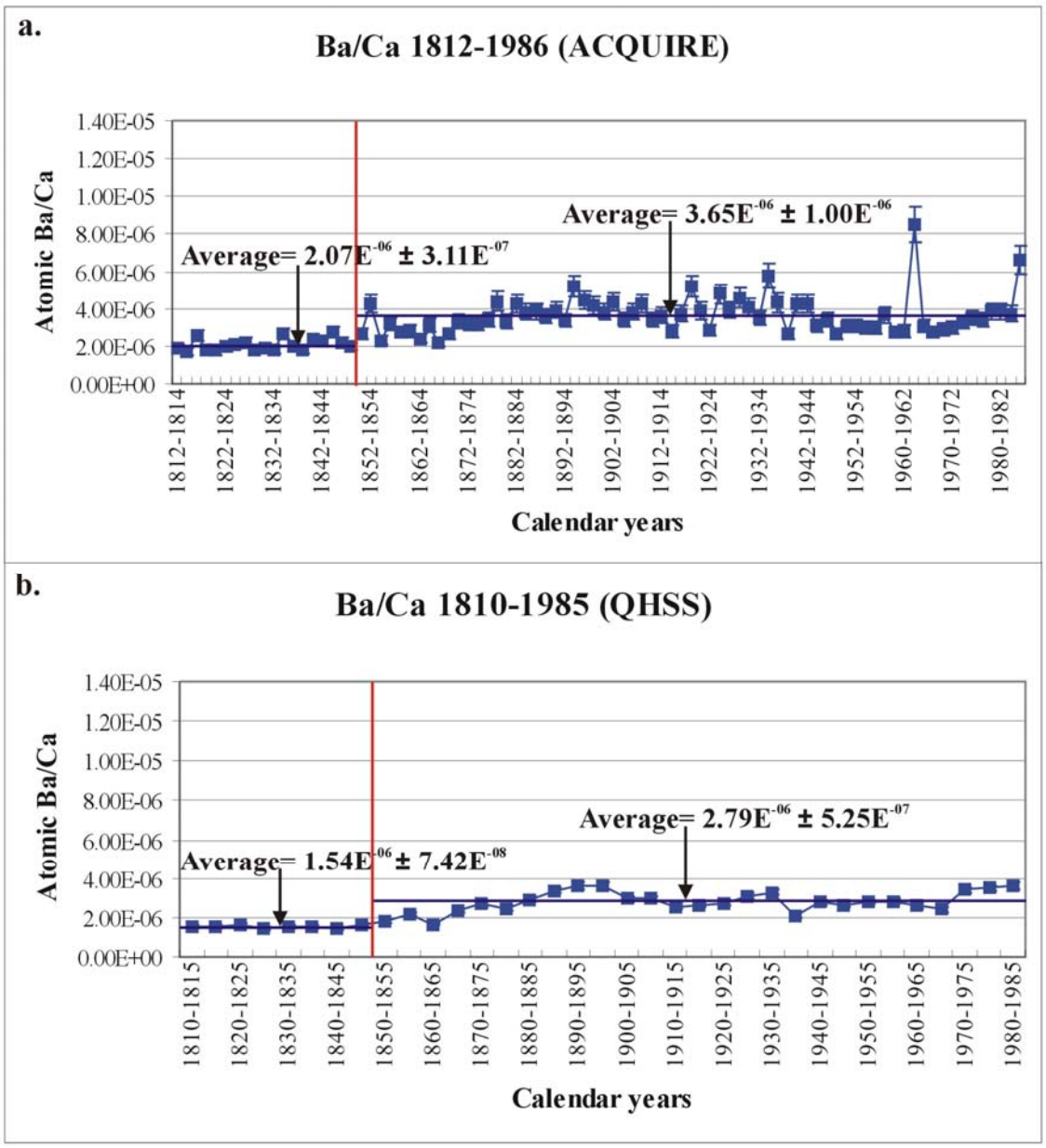

Figure 6.21 (a-b). Ba/Ca ratios in the MAG01D (1812-1986) coral slice for the 2 and 5 yearly sampling resolutions. There was strong replication between the 2 records, with a significant increase in coral Ba/Ca ratios occurring shortly after 1850. The replication between the two records suggests that the coral Ba/Ca ratio is not affected by the H_2O_2 treatment procedure (b).

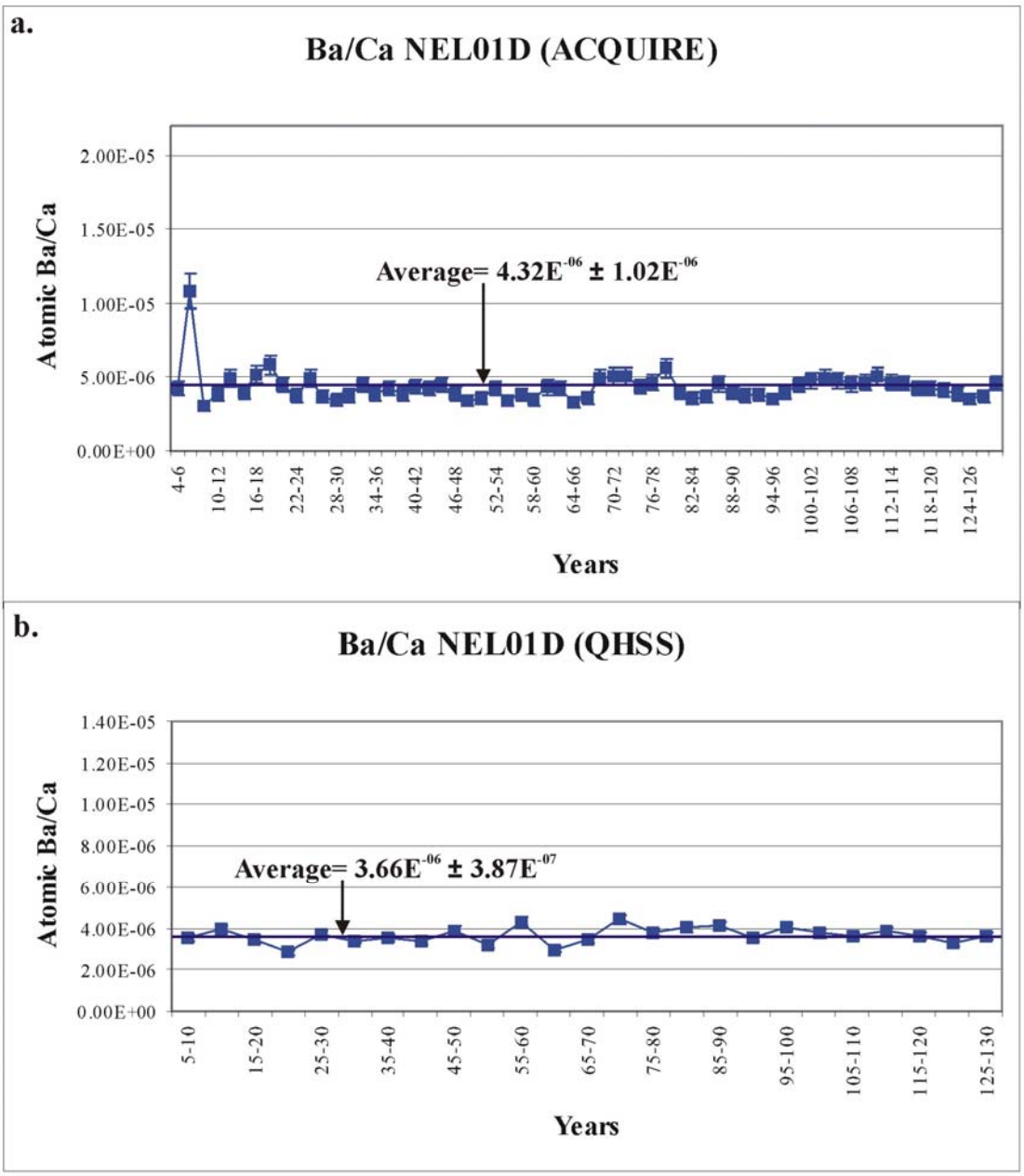

Figure 6.22 (a-b). Ba/Ca ratios for the mid-Holocene corals. Like the long modern Ba/Ca record, the 2 and 5 yearly records displayed excellent replication. The Ba/Ca ratios during the mid-Holocene were considerably elevated compared to the modern coral records.

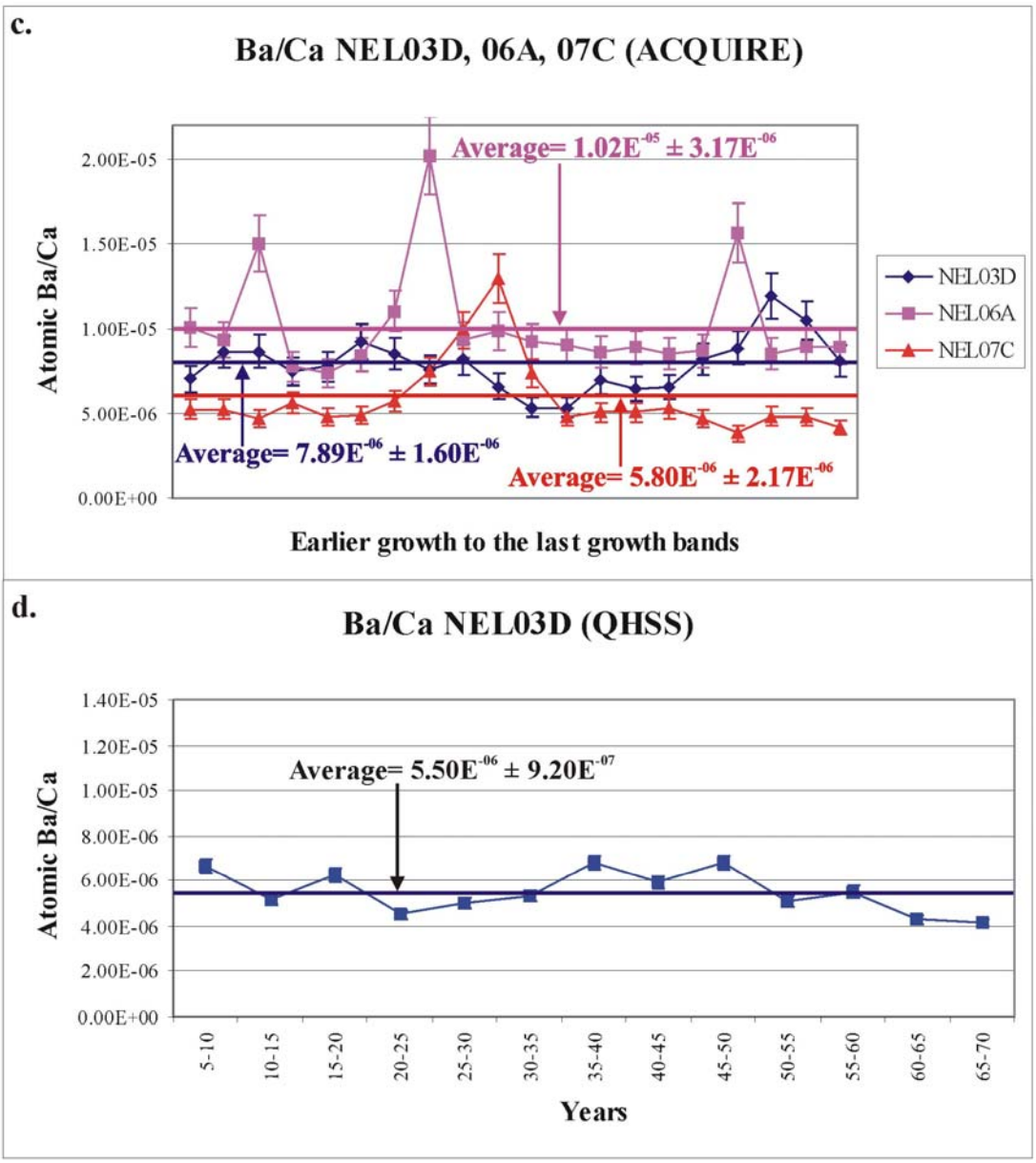

Figure 6.22 (c-d). Ba/Ca ratios in the mid-Holocene coral heads (continued). There were also elevated Ba/Ca ratios in the additional mid-Holocene corals compared to the modern record, including some significant Ba peaks in the NEL03D, NEL06A and NEL07C coral slices. However, it should be noted that towards the final growth bands there are no considerable deviations in coral Ba/Ca (c).

6.3.3. Mn concentrations

The average Mn concentrations were similar for both the 1980-1984 (0.43 ± 0.09 ppm) and the 1992-1996 (0.88 ± 0.67 ppm) coral records (Table 6.2; Fig 6.23a-b). Both records showed relatively flat trends and had relatively low Mn concentrations (Table 6.2). In comparison, the mid-Holocene coral contained slightly higher Mn concentrations (average= 1.35 ± 0.53 ppm; Fig 6.23c).

Significant increases in coral Mn concentrations occur shortly after 1850 in both the 2 and 5 yearly datasets. There was an excellent replication between the 2 datasets and the Mn concentrations in the QHSS dataset appeared to be unaffected by the H_2O_2 pre-treatment procedure. The initial Mn increase occurred in the 1854-1856 (ACQUIRE) and the 1850-1855 (QHSS) samples and was over an order of magnitude compared to the background Mn concentrations. After European settlement, average coral Mn concentrations increased by 286% and 1530% for the 2 and 5 yearly records, respectively. Unlike the Ba/Ca ratios, the Mn data were punctuated by a sharp increase shortly after 1850 and elevated concentrations continued until the early 1900s. Another minor increase in coral Mn concentrations occurred during the 1940-50s. However, in the more recent coral records, the Mn concentrations had returned to the pre-1850 baseline levels.

The Mn concentrations in mid-Holocene coral were considerably lower than in the 1850-1900 levels but they closely matched the post 1850 average for both the 2 and 5 yearly records (Table 6.2; Fig 6.25a-d). Anomalous Mn concentrations are observed in the NEL01 (sample 55-60) and the NEL06 (last sample) coral samples taken from the dead tissue layer of the coral slices. Sediments may have been trapped in the pore spaces of these tissue layers and resulted in elevated Mn. Therefore, these anomalies were excluded from the average calculations.

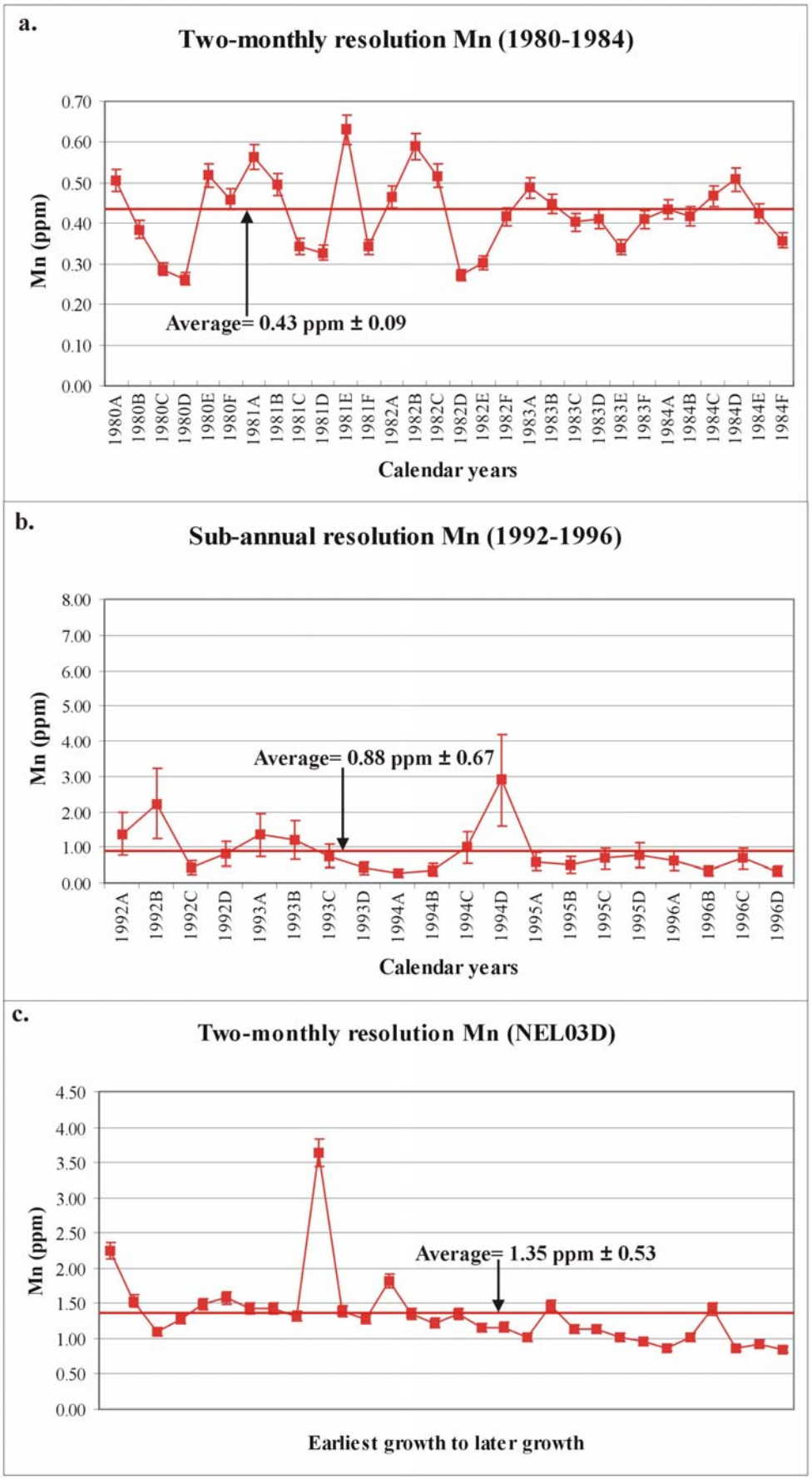

Figure 6.23 (a-c). Sub-annual resolution coral Mn concentrations. The Mn concentrations for the 1980-1984 record (a) displayed what appeared to be seasonality while the other records (b-c) failed to display any seasonal trends.

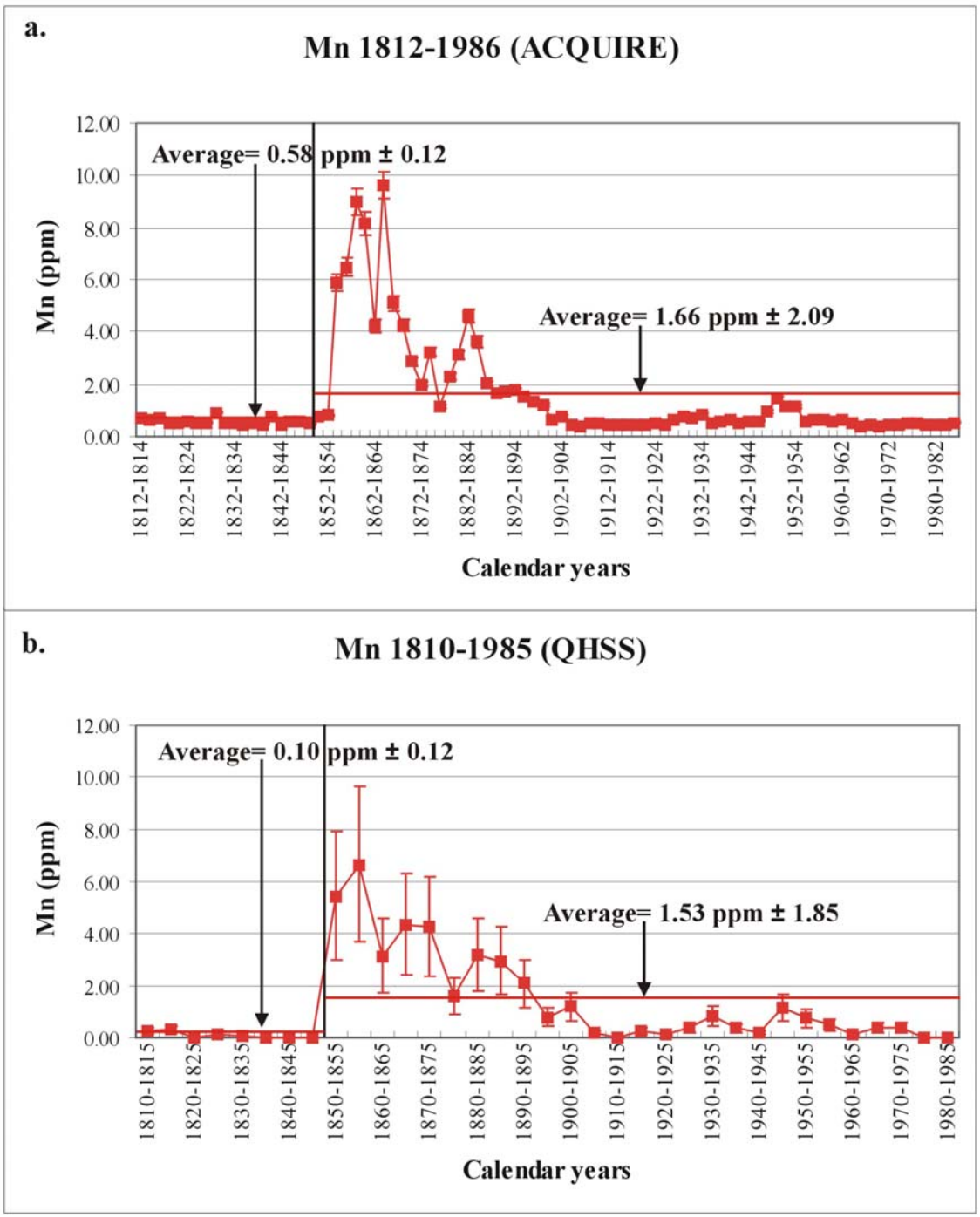

Figure 6.24 (a-b). Coral Mn concentrations for the 2 and 5 yearly resolution 1812-1986 datasets. Both records displayed excellent replication with significant Mn elevations occurring shortly after 1850 and suggest that the coral Mn concentration is unaffected by the H_2O_2 treatment (b). The enhanced coral Mn concentrations continued until approximately 1900 when they returned to baseline values. Elevated coral Mn concentrations also occurred shortly after World War II.

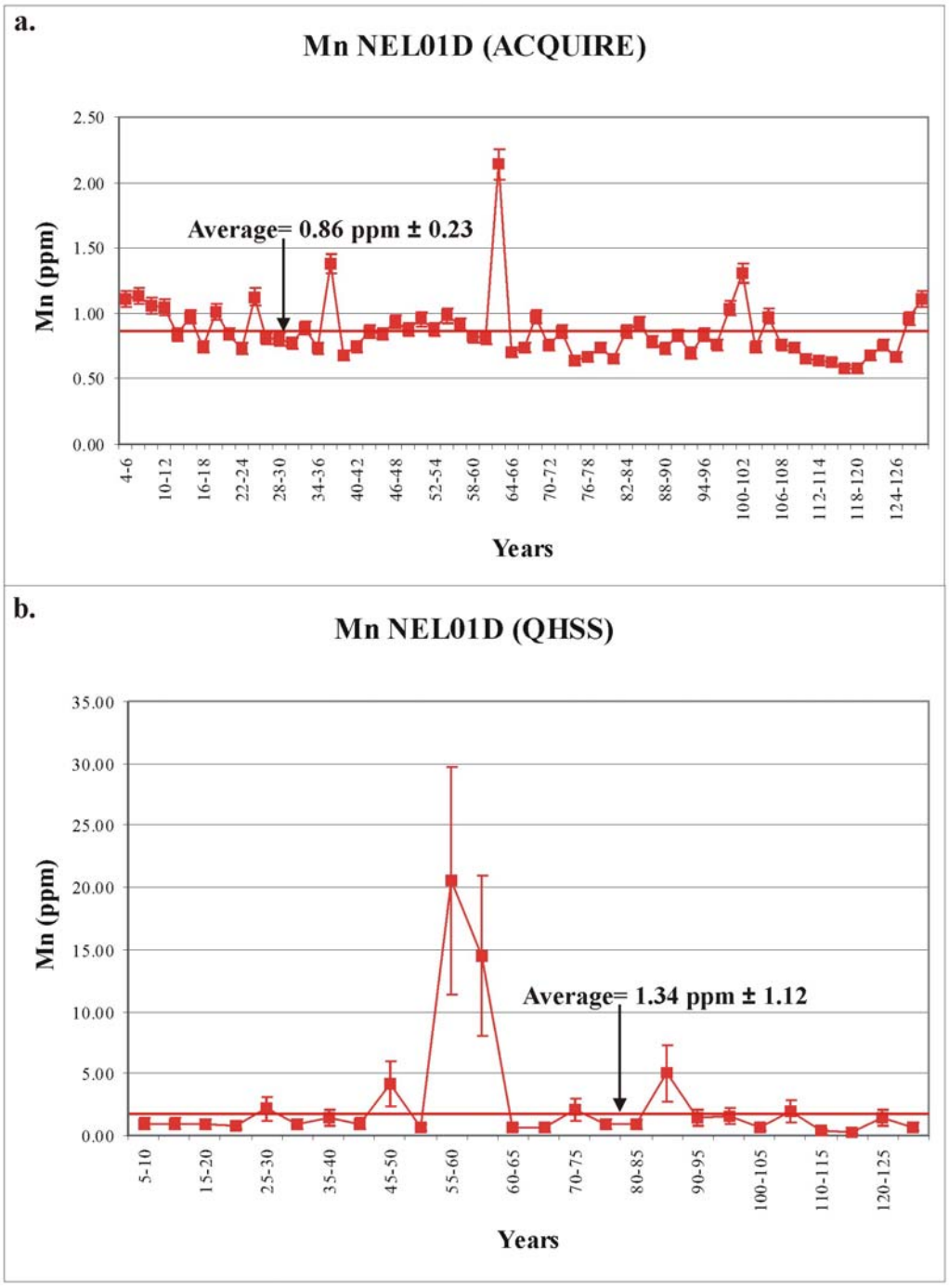

Figure 6.25 (a-b). Mn concentrations for the fossil mid-Holocene corals. The concentrations were similar to the post 1850 averages in the modern record. Sampling within the tissue layer of the QHSS record (b) may account for the significantly elevated Mn concentrations in excess of 10 ppm. These tissue layers contain sediment trapped within the coral pore space; Mn may have been leached from these sediments during the acid digestion stage for the preparation for ICP-MS analysis.

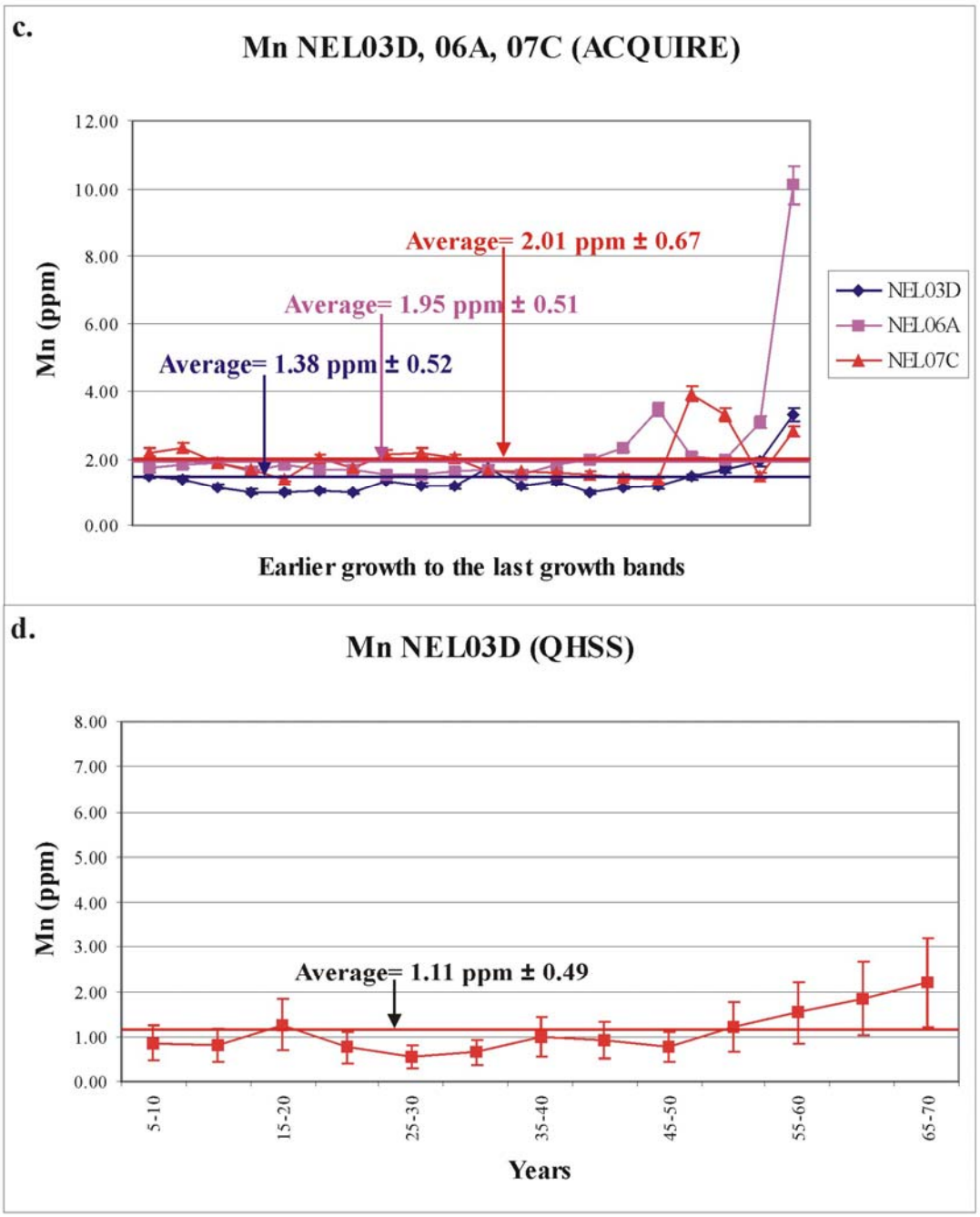

Figure 6.25 (c-d). Mn concentrations for the mid-Holocene corals (continued). The additional mid-Holocene corals analysed had consistently flat trends and averages similar to those measured in the post 1850 period of the long modern record. It is noted that there was an elevated Mn concentration in the last sample taken in the NEL06A coral slice which was affected by sediments.

6.3.4. Rare earth elements

Relatively consistent yttrium (Y: Fig 6.26), praseodymium (Pr: Fig 6.27), samarium (Sm: Fig 6.28) and holmium (Ho: Fig 6.29) concentrations were found for the 1968-1973 and 2000-2003 periods in the NEL21A coral. Minor variations in these elements were probably the result of floods; Y and Ho displayed enrichments during early 1972 which coincided with Tropical Cyclones Althea and Bronwyn, while elevated Pr and Sm concentrations also occurred in early 1972 as well as during the 1973 flood. These data are discussed further in section 8.6.

All 4 REEs (Y, Pr, Sm and Ho) measured in the 1812-1986 modern coral record increased significantly after 1850 (Fig 6.30-6.33a). The Y, Pr, Sm and Ho concentrations averaged 154.24 ± 9.66, 6.67 ± 1.82, 6.60 ± 1.98 and 2.53 ± 0.34 ppb, respectively, prior to 1850 and displayed a substantial increase after 1850 (196.99 ± 25.19, 9.57 ± 2.01, 9.27 ± 2.29 and 3.32 ± 0.54 ppb respectively). This signifies a 28% increase in Y, 43% for Pr, and 40% and 31% rises in Sm and Ho, respectively. These results may suggest an enhanced terrestrial influence on the MAG01D coral. It must be noted, however, that in the 2000-2003 coral record, the REE concentrations were identical or even slightly lower than the averages for the 1850-1986 period (Table 6.3).

As with the 1812-1986 modern coral record, the Y, Pr, Sm, Ho concentrations displayed similar trends with each other in the mid-Holocene records (Fig 6.30-6.33b-c). While the modern 2 yearly REE record showed consistent baseline levels (with the possible exception of Sm), the mid-Holocene REE concentrations were more variable. The REE values were significantly elevated in the samples “36-38”, “62-64” and “128-130” in the NEL01 coral and towards the last growth periods for the other mid-Holocene records (Figs 6.30b-c-6.33b-c). The average data, presented in Table 6.3, revealed that REE concentrations in the mid-Holocene corals were similar or slightly higher than the post 1850 data. Sampling into the coral tissue layer in the NEL01D “62-64” and the last sample in the NEL06A coral slice may explain these extreme data points and these have been excluded from the average calculations.

Table 6.3. Summary of the average REE concentrations for the corals that were analysed.

	Rare earth elements (ppb)			
Coral record	**Y**	**Pr**	**Sm**	**Ho**
1968-1973	200.39 ± 23.78	6.31 ± 1.33	6.36 ± 1.15	3.24 ± 0.46
2000-2003	205.03 ± 20.48	6.79 ± 1.07	6.97 ± 1.03	3.30 ± 0.40
1812-1850	154.24 ± 9.66	6.67 ± 1.82	6.60 ± 1.98	2.53 ± 0.34
1850-1986	196.99 ± 25.19	9.57 ± 2.01	9.27 ± 2.29	3.32 ± 0.54
NEL01D	203.70 ± 28.78	7.33 ± 4.06	7.35 ± 3.71	3.36 ± 0.88
NEL03D	226.92 ± 79.88	8.55 ± 6.55	8.96 ± 5.90	3.89 ± 2.35
NEL06A	268.25 ± 38.28	9.70 ± 3.31	9.76 ± 4.38	4.76 ± 1.48
NEL07C	195.03 ± 35.28	9.11 ± 4.77	8.44 ± 3.74	3.42 ± 1.00

The REE and Y (REY) distribution plots for the 1968-1973 and 2000-2003 records (Fig 6.34 a-b), normalised to the mud from Queensland sediment standard (MUQ; Kamber et al., 2005), displayed a similar pattern to modern seawater which indicated that the coral was preserving a genuine seawater REE distribution. These records both contained periods of enhanced REE which could be linked to flood events. The 2 yearly REE and Y data systematically increased after 1850 (Fig 6.34c). The 2 yearly resolution record for the mid-Holocene (Fig 6.34d) coral had similar concentrations to the modern 2 yearly coral record, with the exception of the "62-64" sample which was more consistent with a sediment-related pattern.

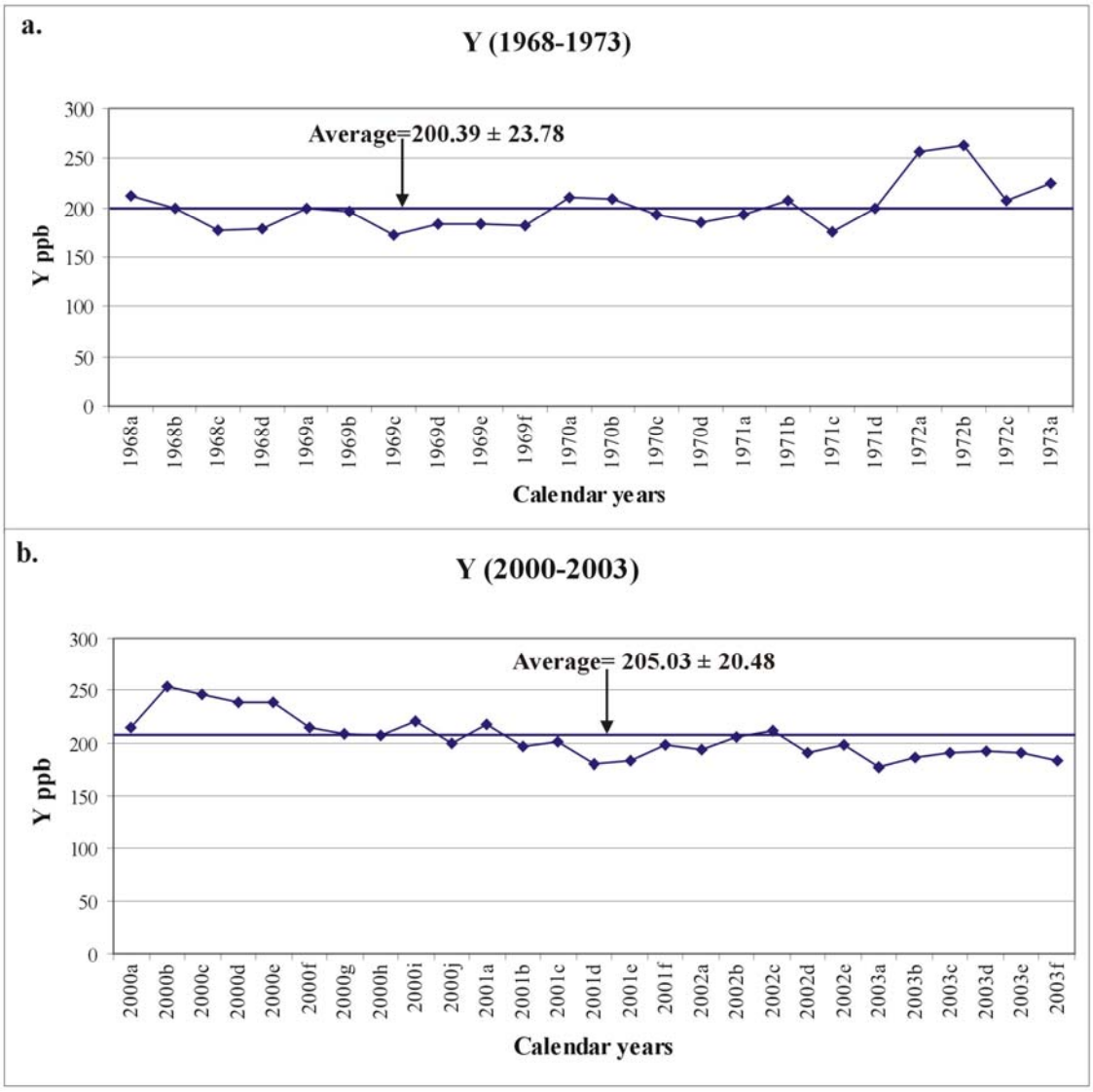

Figure 6.26 (a-b). Yttrium concentrations for the 1968-1973 (a) and 2000-2003 (b) coral records. The Y concentrations were slightly elevated in early 1972 (a) coinciding with Cyclones Althea and Bronwyn but, in most cases, displayed little variation in both records.

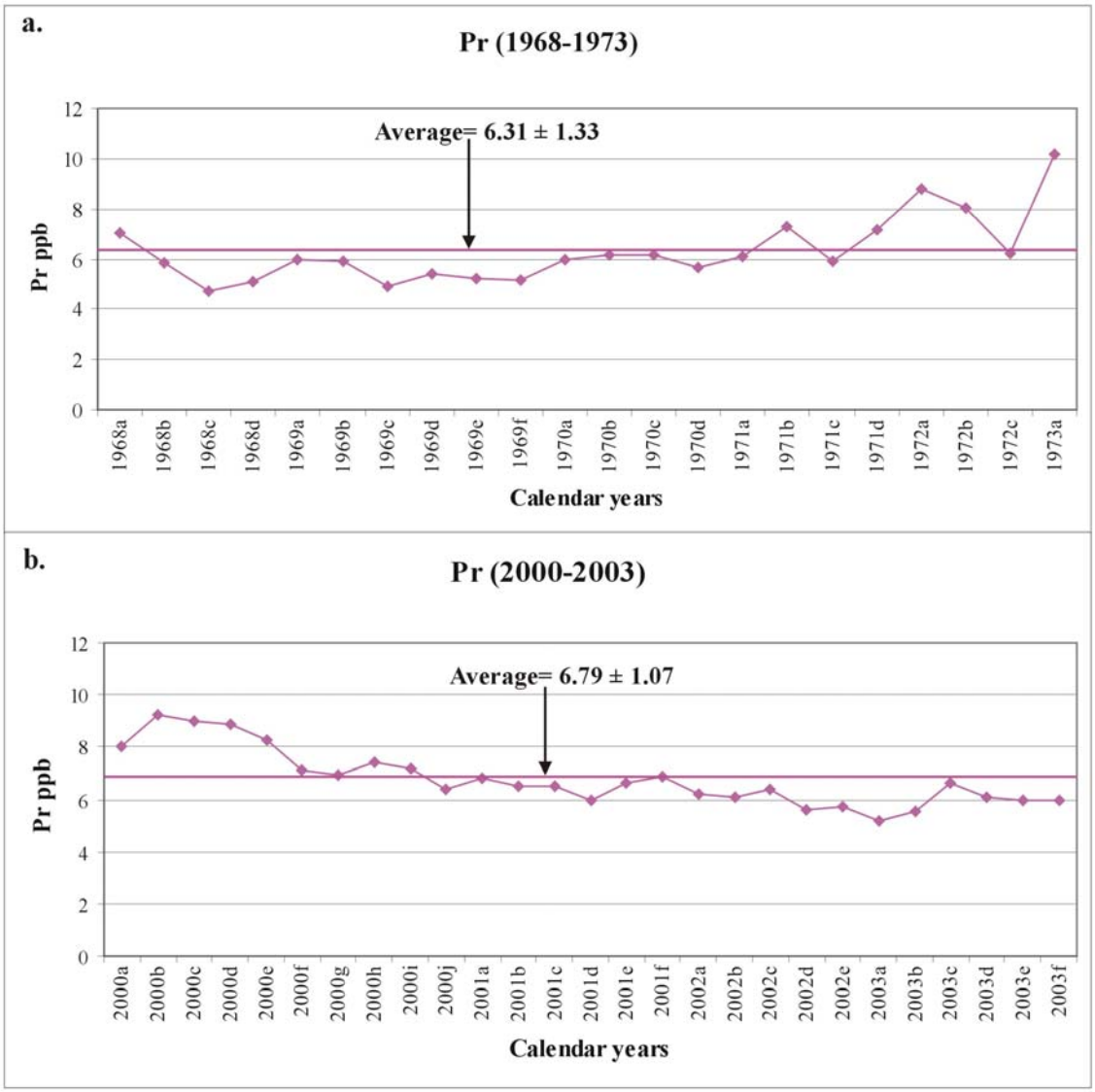

Figure 6.27 (a-b). Pr concentrations for the 1968-1973 (a) and 2000-2003 (b) coral records. Similarly to Y, the Pr concentrations showed little deviation, but appeared to be affected by Cyclones Althea and Bronwyn. Coral Pr concentrations were also elevated at the time of the 1973 flood.

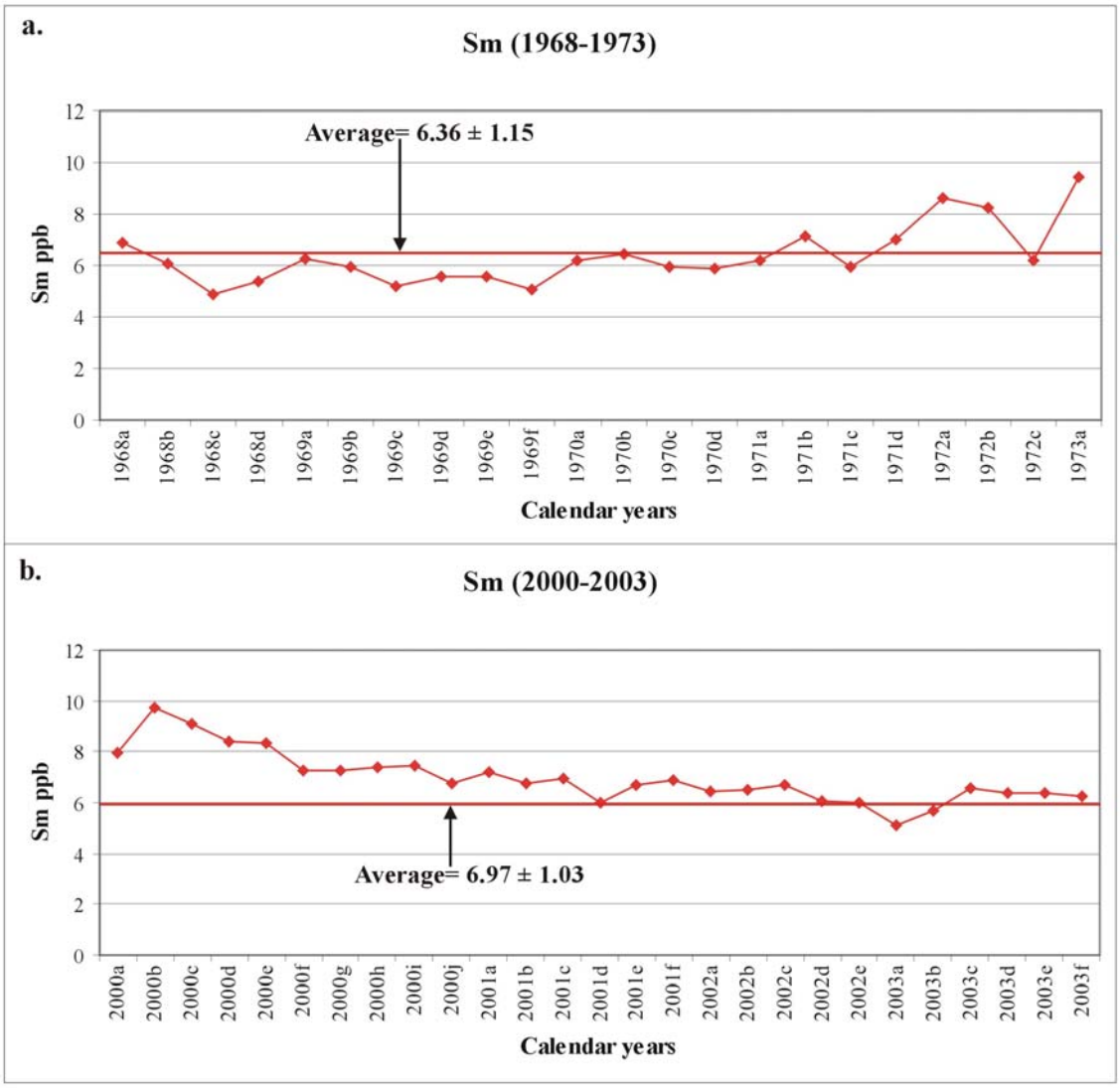

Figure 6.28 (a-b). Sm concentrations for the 1968-1973 (a) and 2000-2003 (b) coral records. The Sm concentrations displayed consistent trends and were elevated during the cyclonic events during early 1972 as well as during the 1973 flood.

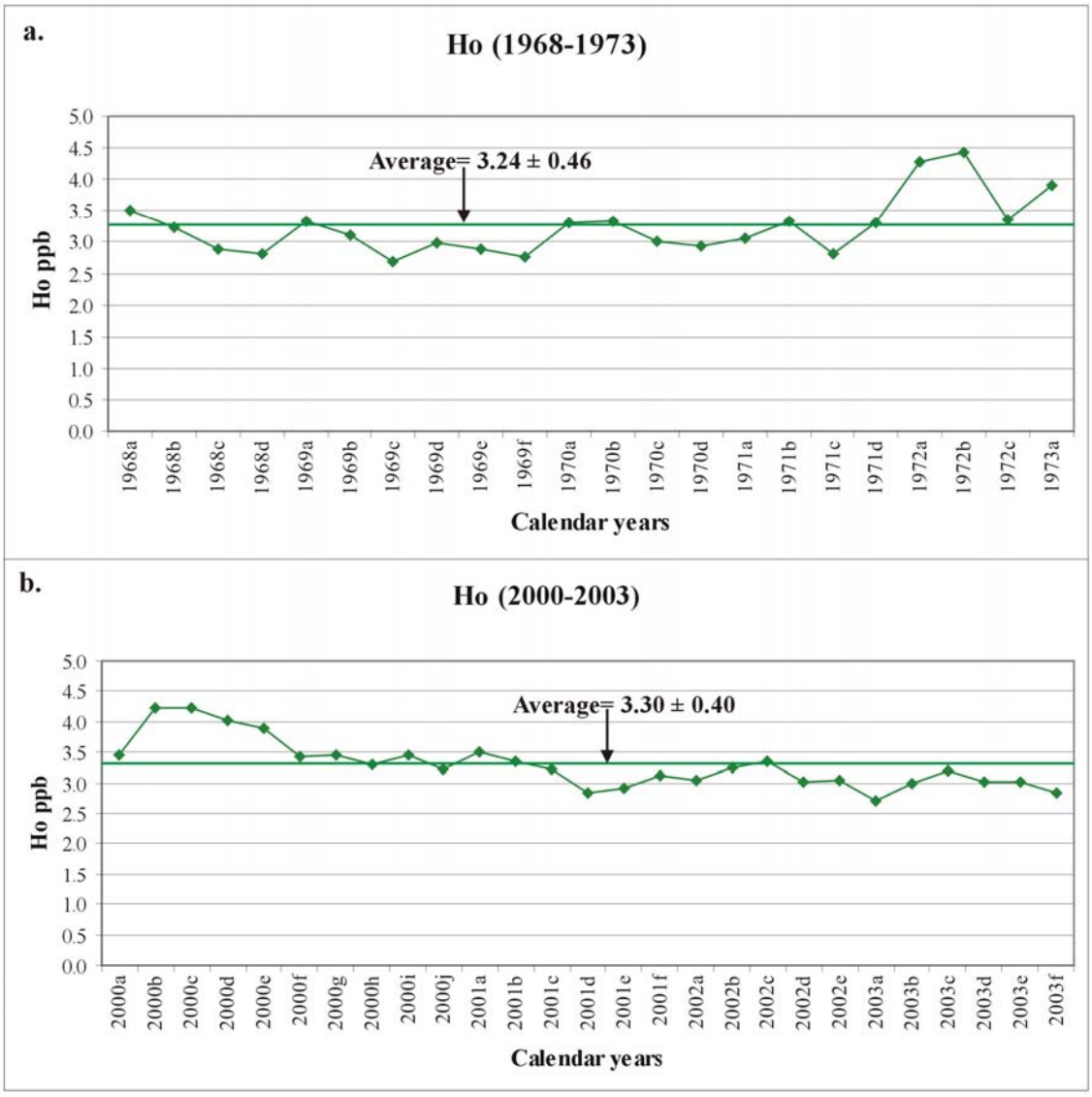

Figure 6.29 (a-b). Ho concentrations for the 1968-1973 (a) and 2000-2003 (b) coral records. The Ho concentrations also displayed little variation in these records and were only elevated during the cyclonic events. Ho was also slightly enriched during the 1973 flood.

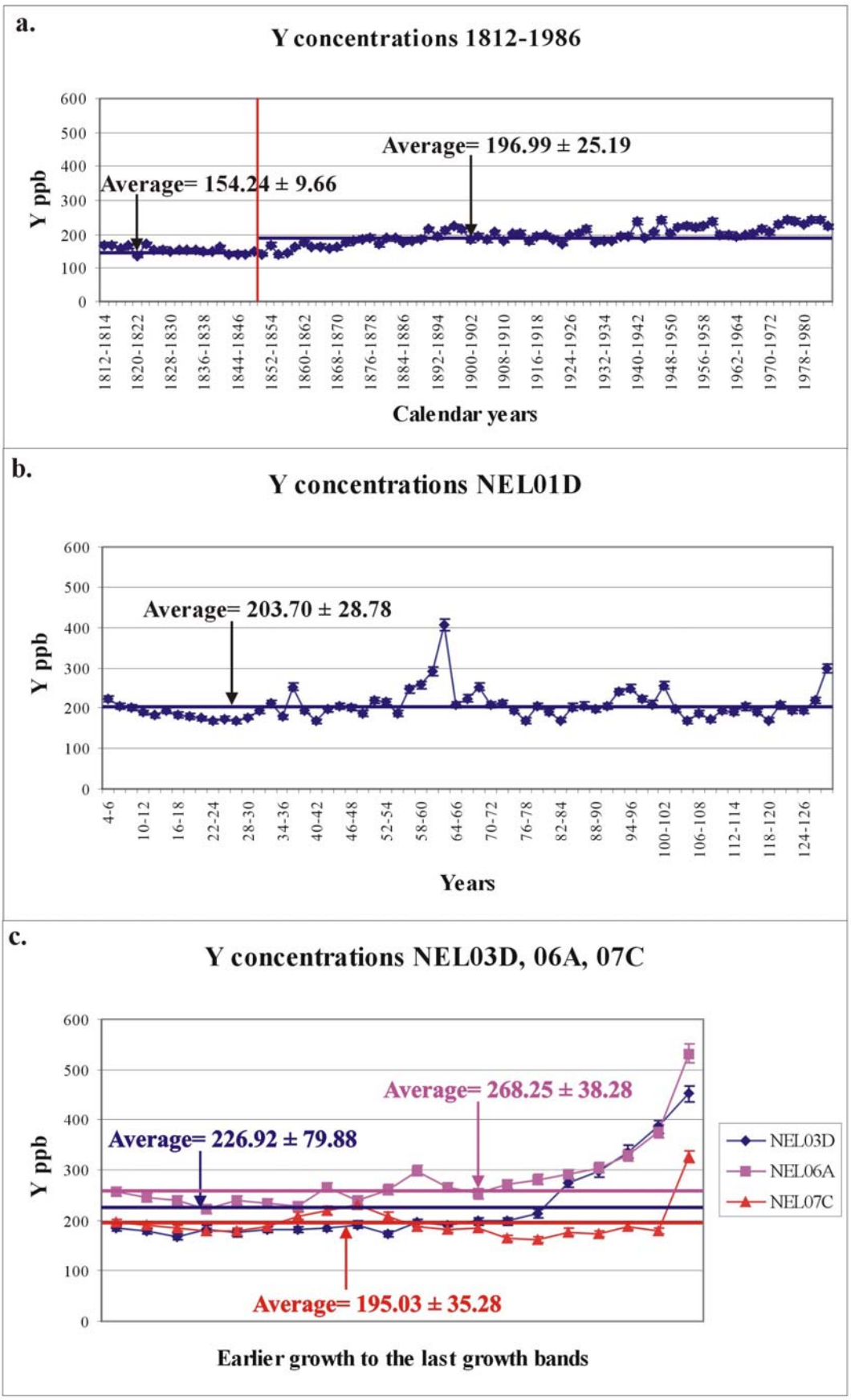

Figure 6.30 (a-c). Y concentrations in the modern and mid-Holocene corals. The modern 1812-1986 record (a) displayed a significant increase in Y concentrations after 1850. The mid-Holocene corals, however, had Y concentrations similar to the post 1850 averages (b-c). The final growth bands for the mid-Holocene corals (c) also contained elevated Y concentrations.

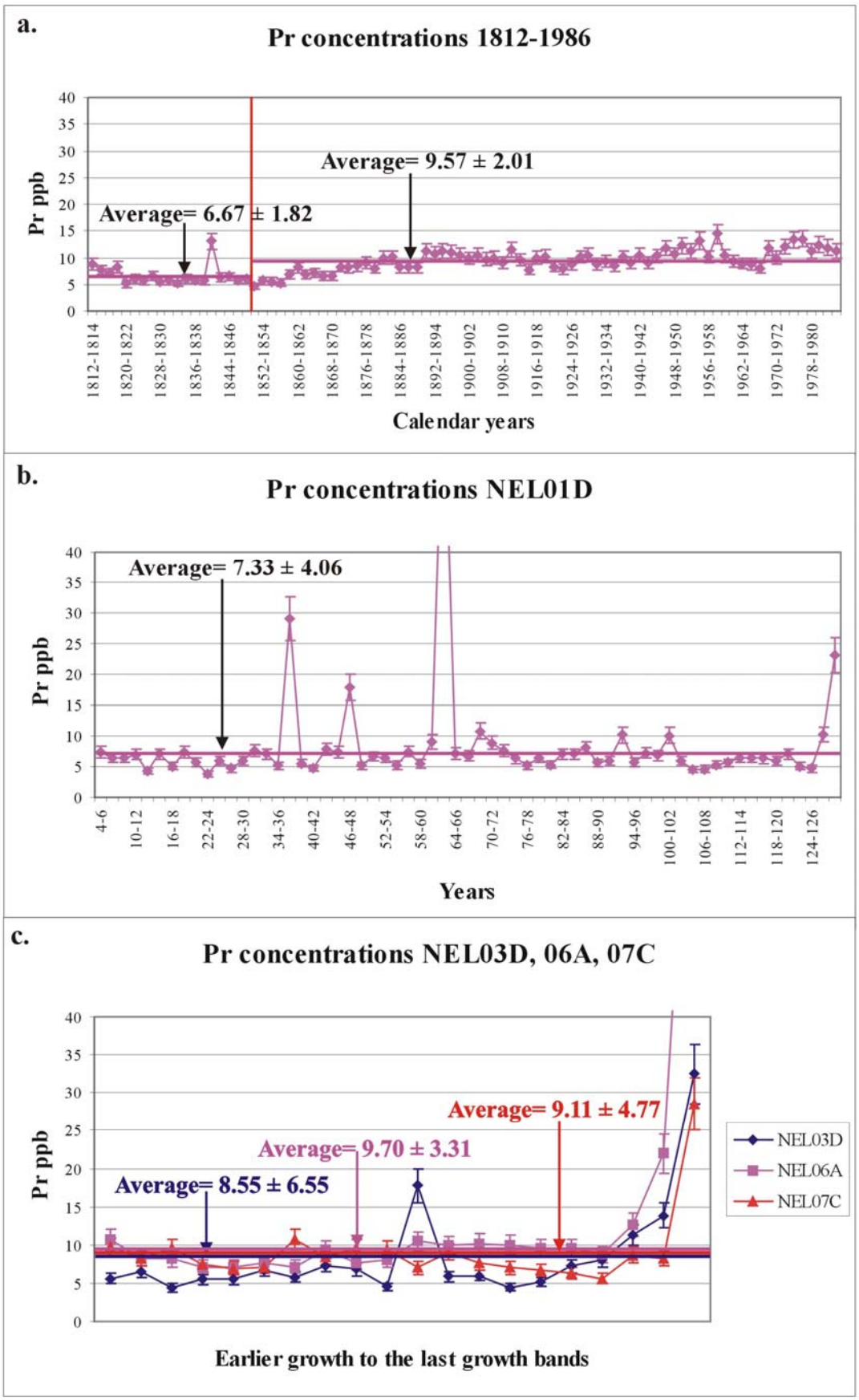

Figure 6.31 (a-c). Pr concentrations for the modern (a) and mid-Holocene corals (b-c). Like Y, the Pr concentrations were elevated after 1850. The mid-Holocene corals had Pr concentrations comparable to the post 1850 average and Pr became significantly elevated during the final growth bands of NEL01D, NEL03D, NEL06A and NEL07C.

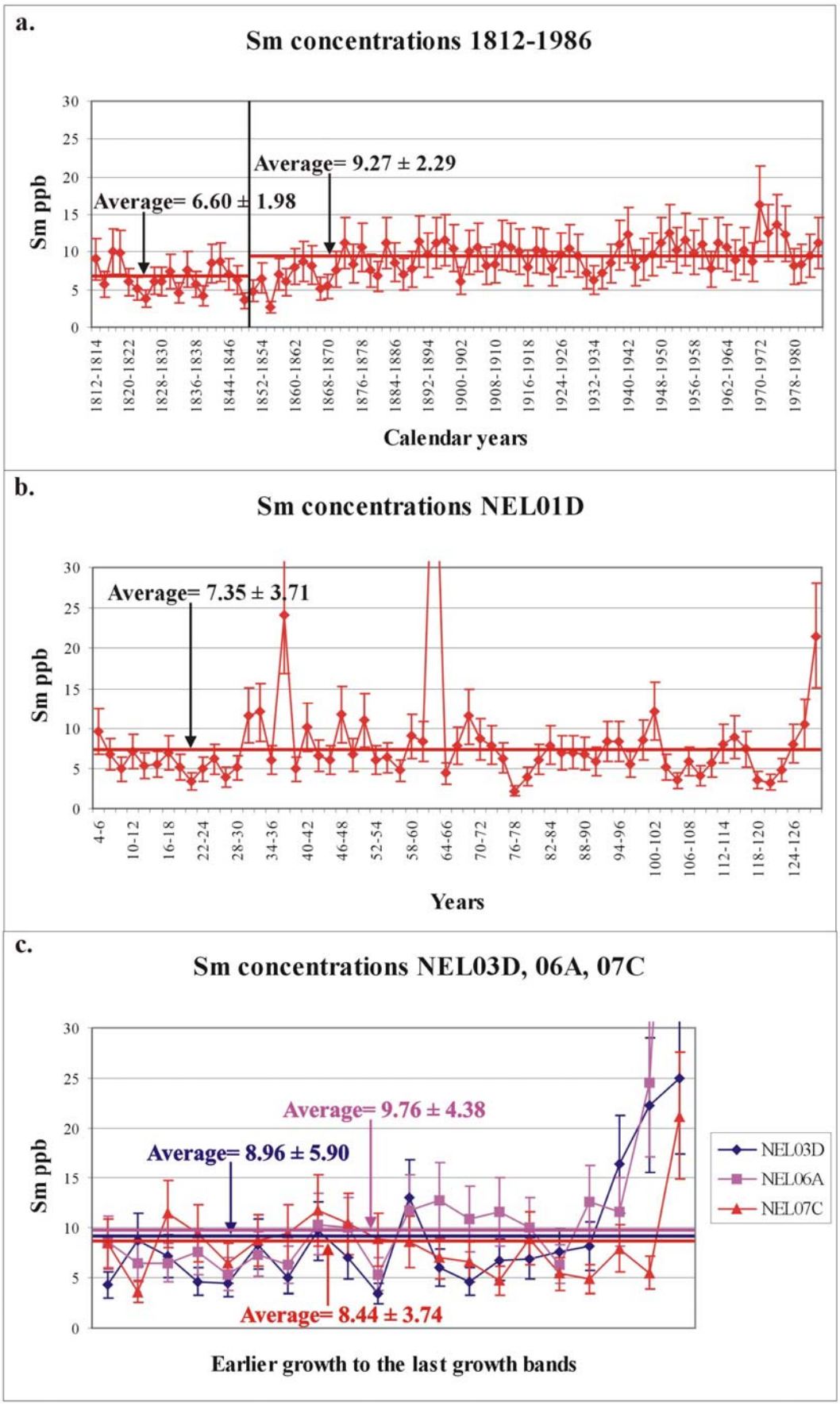

Figure 6.32 (a-c). Sm concentrations for the modern (a) and mid-Holocene corals (b-c). The analytical precision for Sm was poorer compared to Y, Pr and Ho. However, the trends were similar to the other REE records (a). Significantly elevated Sm concentrations occurred in the mid-Holocene corals just before their demise (b-c).

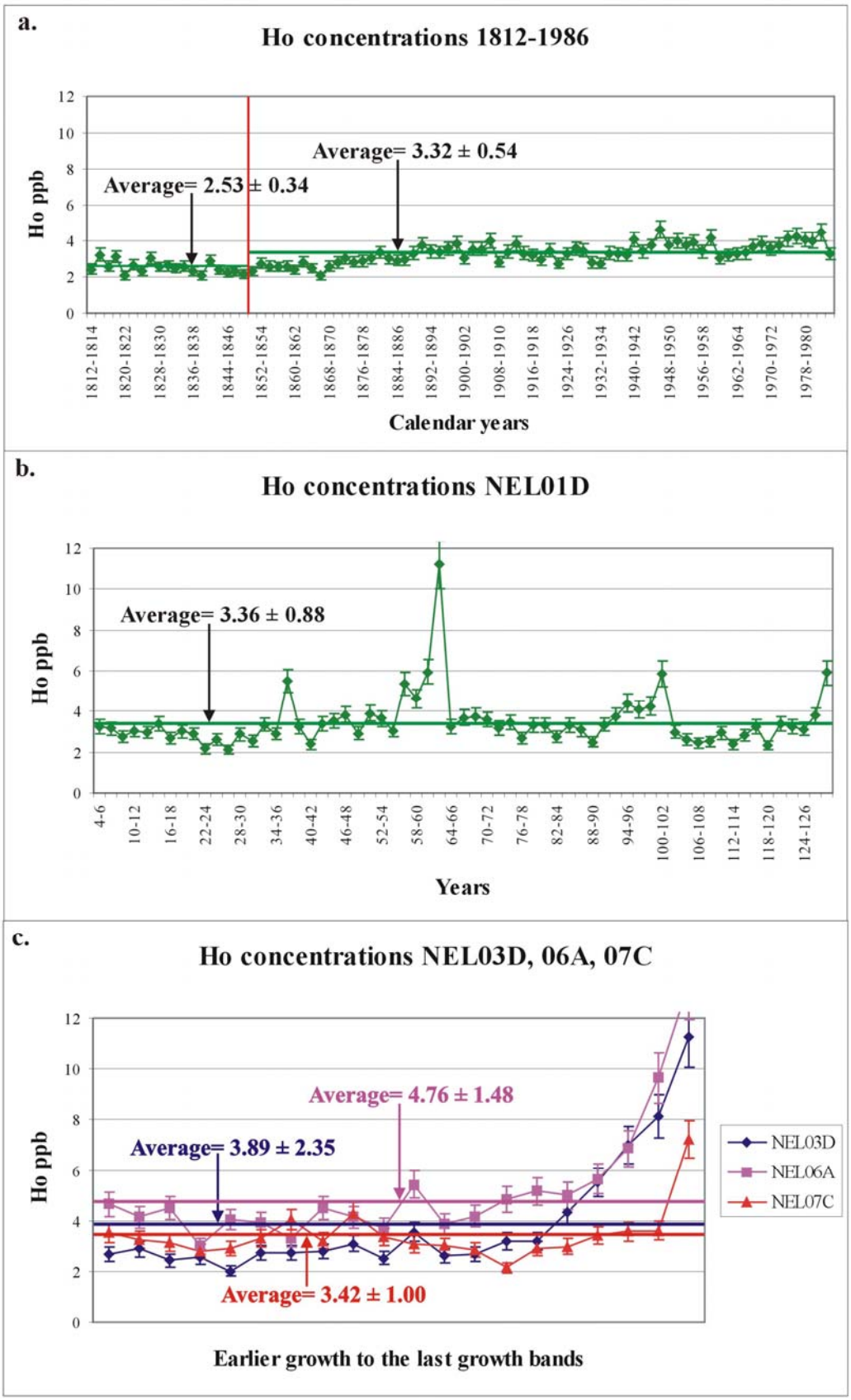

Figure 6.33 (a-c). Ho concentrations for the modern (a) and mid-Holocene corals (b-c). Ho concentrations were significantly elevated after 1850 in the modern coral record (a). Similarly to the other REE, there were also elevated Ho spikes throughout the NEL01D slice, particularly in the "62-64" sample where the coral tissue layer was sampled (b). There were also significantly elevated Ho concentrations in the final growth bands of the mid-Holocene corals.

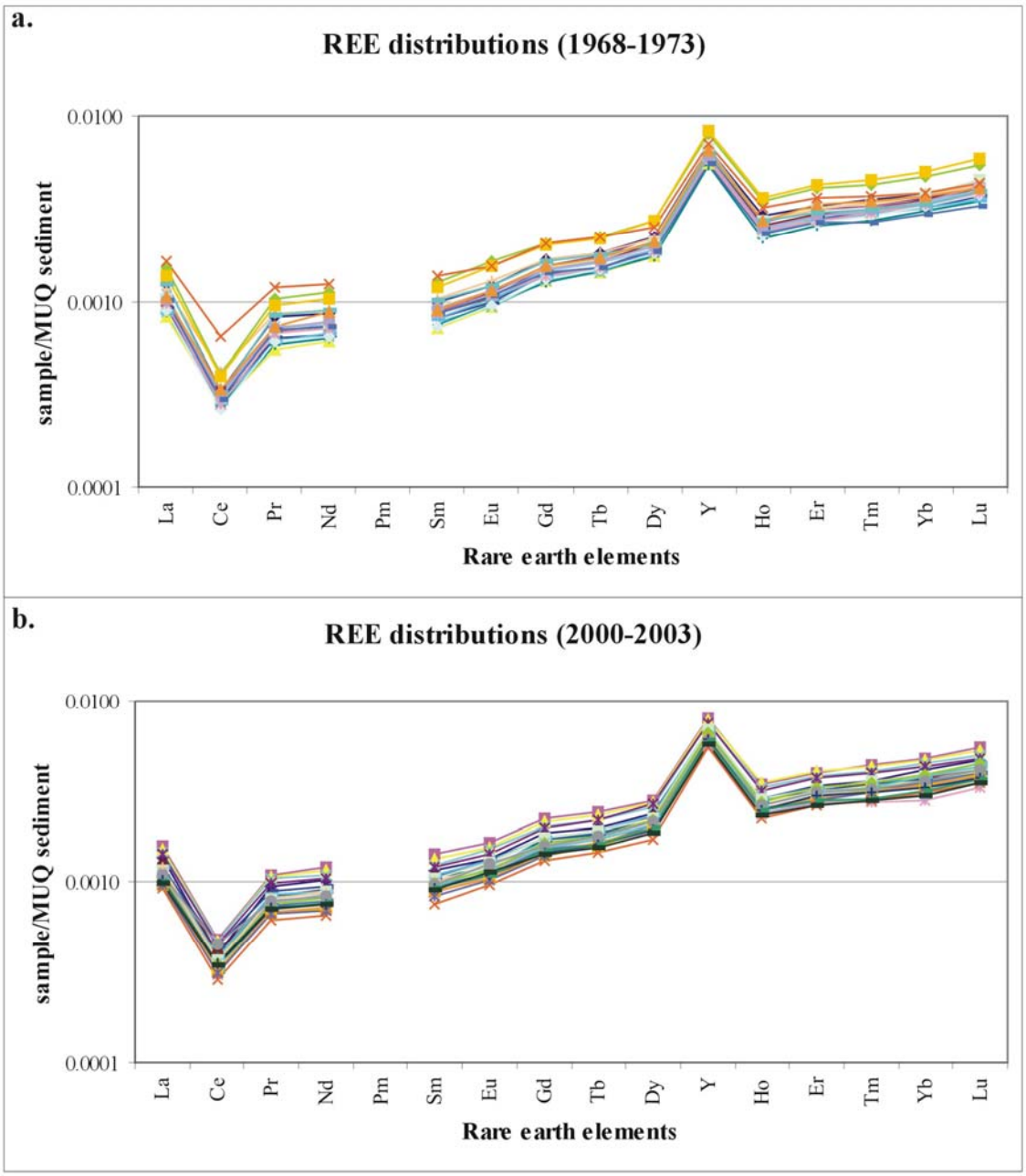

Figure 6.34 (a-b). REE and Y distributions for 1968-1973 and 2000-2003. The records show the "baseline" REE pattern which was similar to modern seawater REE distribution. Terrestrial runoff during flood events could alter the REE pattern (such as the Ce anomaly; a) as well as result in relatively elevated REE concentrations.

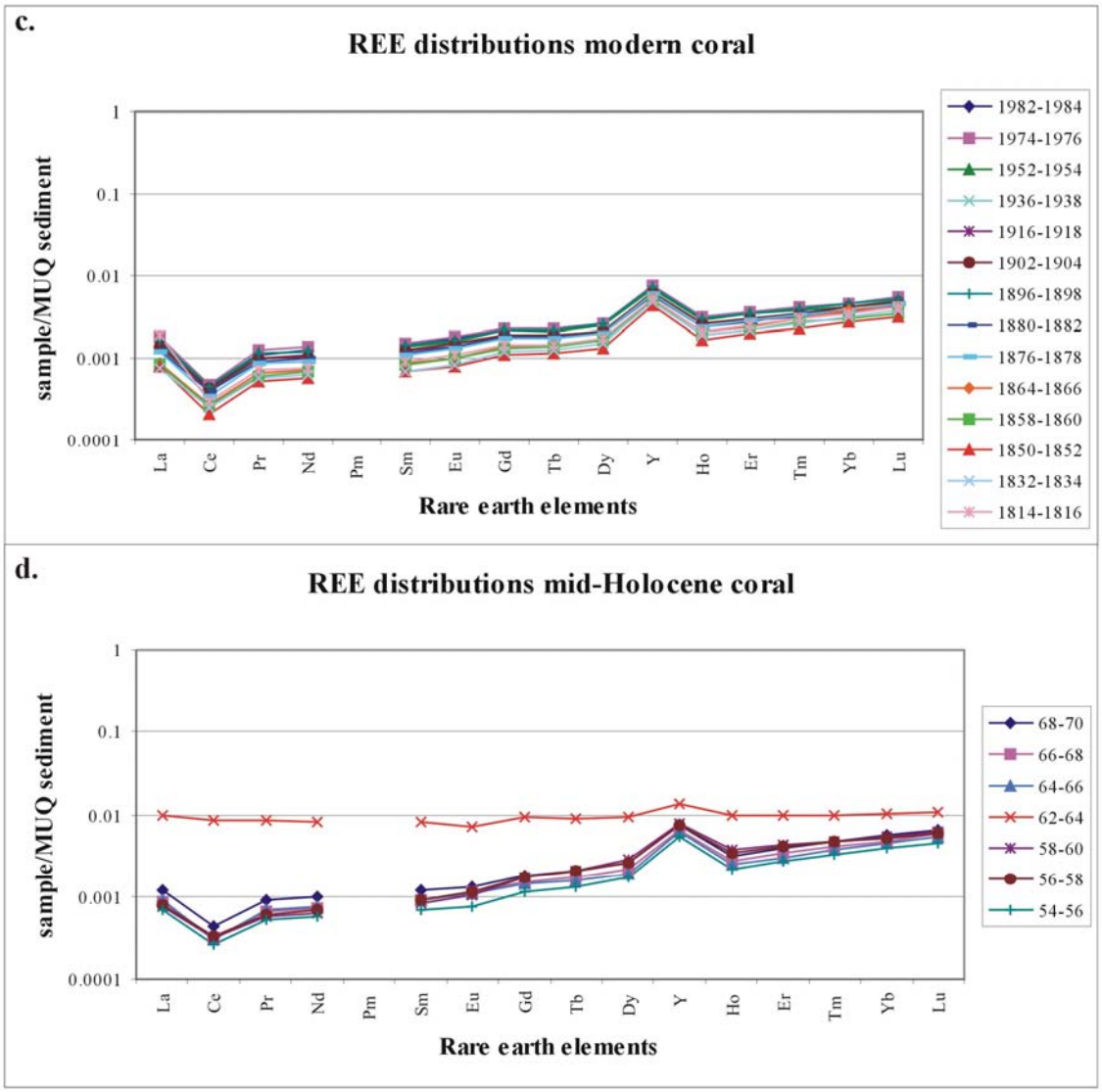

Figure 6.34 (c-d). REE and Y distributions for the modern and mid-Holocene corals. The modern coral record (c) displayed a systematic increase in REE over time which suggested that there has been an increased terrestrial influence after 1850. The mid-Holocene coral record (d) had a similar REE pattern to the modern REE distributions with the exception of the 62-64 sample which displayed a sediment-related pattern.

6.3.5. Thorium concentrations

Coral Th concentrations were all consistently below 1 ppb in both the 1968-1973 and 2000-2003 records with only 3 exceptions (Fig 6.35). The highest Th concentration of 2.40 ppb was recorded during the 1973 flood, which may indicate a minor influx of sediment that was incorporated into the coral skeleton. Coral Th concentrations are discussed further in sections 8.2 and 8.3.

The 1812-1986 Th record demonstrated that there was negligible sediment/detrital material incorporated into the coral skeleton, with the possible exception of the 1840-1842 sample. The average pre-1850 Th concentration (1.92 ± 1.17 ppb) was similar to the post-1850 concentration (1.13 ± 1.17 ppb; Fig 6.36a). The abnormally high Th concentrations in the "62-64" sample (NEL01D) and the last sample in NEL06A were indicative of sediment incorporated into the dead coral tissue layers (Fig 6.36b-c). The anomalous spikes in sample "36-38" and the 2nd point in NEL06A are also thought to be the result of sediments trapped within the coral skeleton; these samples were excluded in the average calculations.

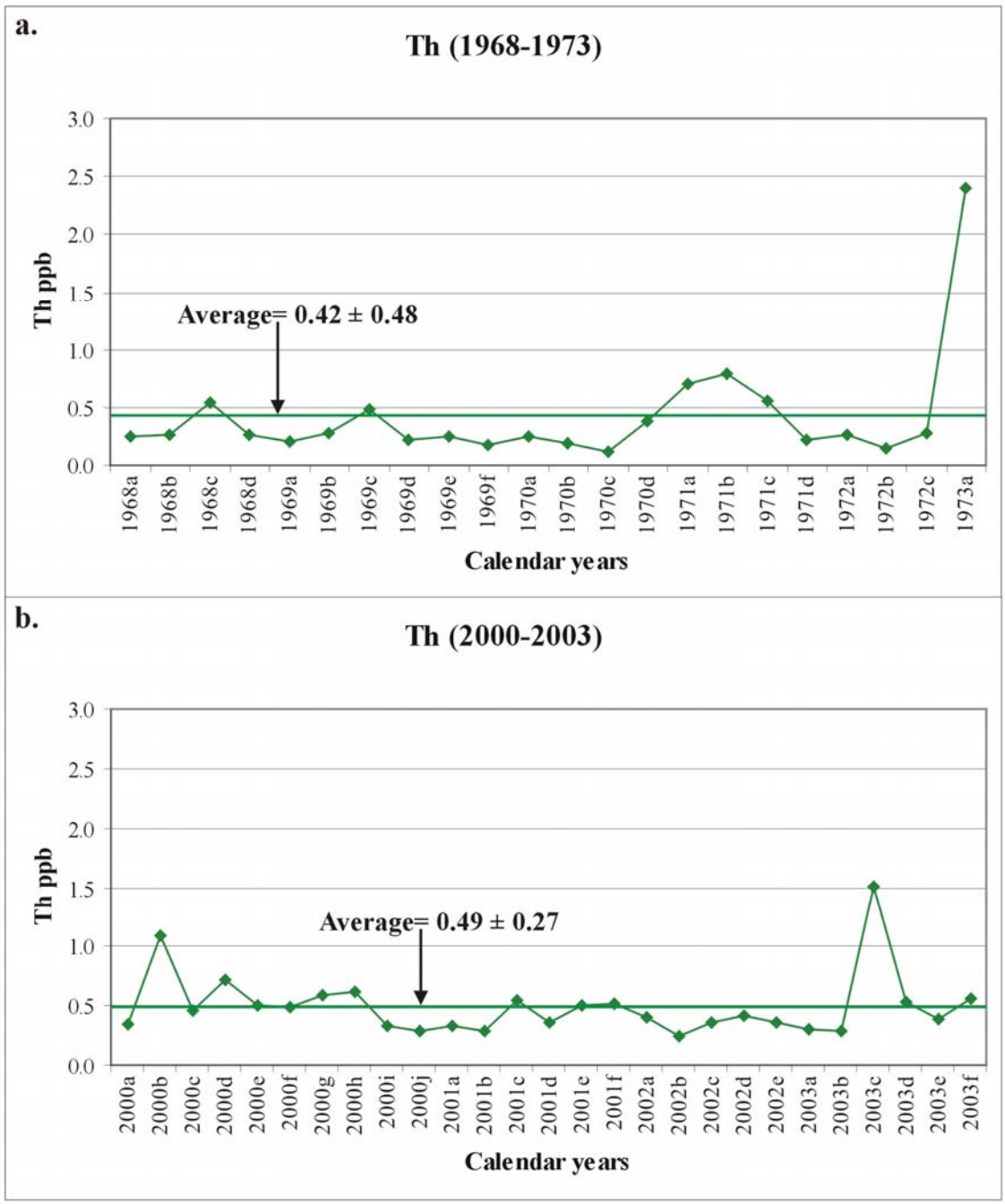

Figure 6.35 (a-b). Th concentrations for 1968-1973 (a) and 2000-2003 (b). The Th concentrations in the coral were negligible and a peak occurred during the 1973 flood. Interestingly, Th was not elevated during the cyclonic events of early 1972 (a).

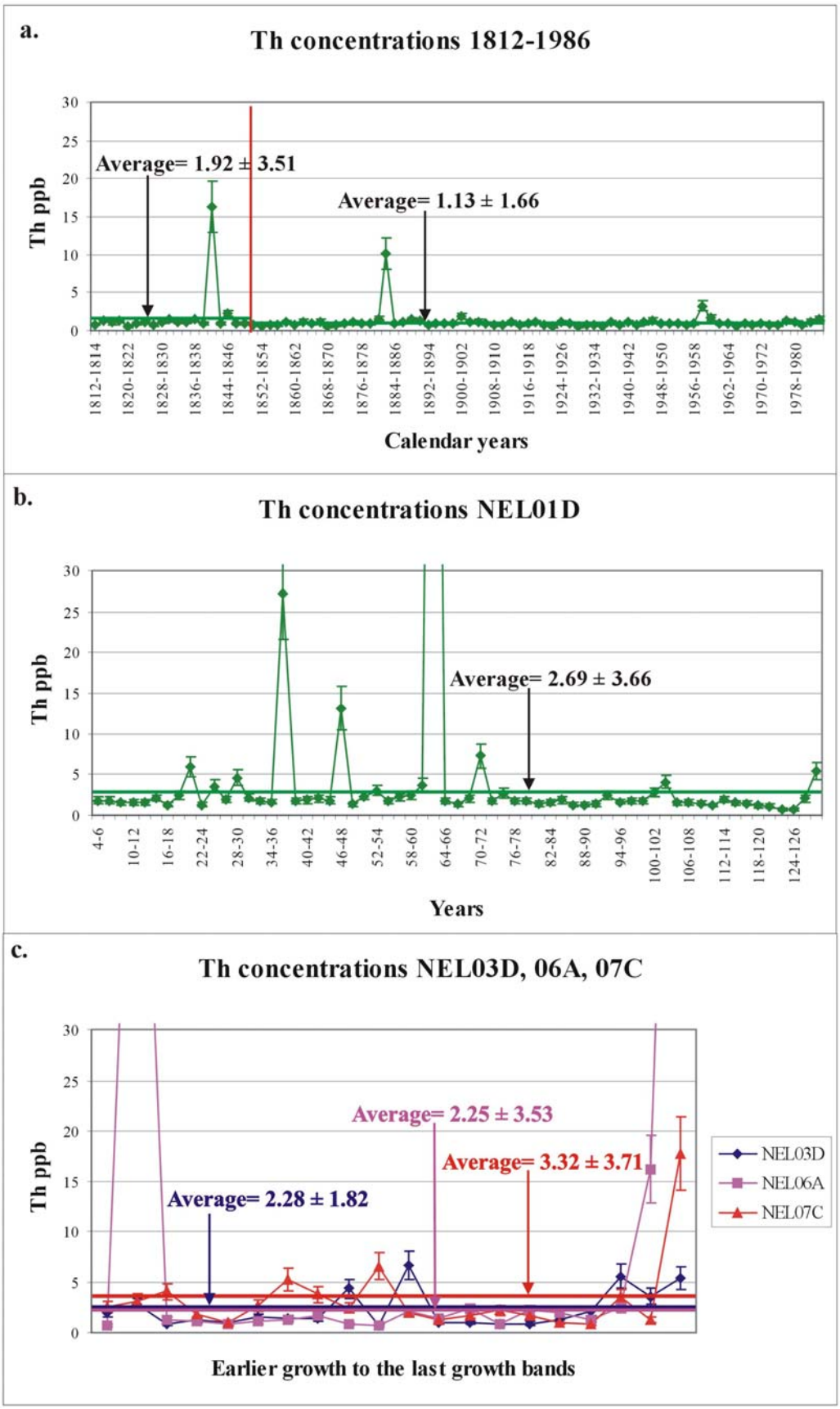

Figure 6.36 (a-c). Th concentrations for the modern (a) and mid-Holocene corals (b-c). There was no significant difference in average Th concentrations between the modern and mid-Holocene corals. The elevated Th "spikes" in the mid-Holocene corals suggest that these samples have been influenced by sediment. Interestingly, there were elevated Th concentrations recorded in all the final growth bands of the mid-Holocene corals.

6.3.6. Summary

Significant increases in the coral Ba/Ca ratio, Mn concentrations and rare earth elements were discovered after European settlement in the region (c. 1850). Interestingly, the Ba/Ca, Mn and REE coral proxies significantly increased after 1850, although each proxy displayed different trends. This difference suggests that these proxies are responding to different environmental parameters. However, the Ba/Ca ratio and the rare earth elements in the mid-Holocene corals displayed averages similar to the post-1850 coral. In addition, coral Th concentrations were significantly elevated in the final samples of the mid-Holocene coral in comparison to the negligible levels throughout the modern coral record.

6.4. Chapter Summary

- Microanalytical analyses indicated that the corals were free of any obvious diagenesis and therefore were acceptable for trace element and isotope analyses.
- The coral Sr/Ca, U/Ca and Ba/Ca ratios as well as the Mn concentrations were relatively unaffected by the H_2O_2 treatment. In comparison, the Mg/Ca and Ni concentrations were greatly affected by the treatment which suggests that these proxies were influenced by an organic component.
- The Sr/Ca-SST reconstructions for the two-monthly 1980-1984 and mid-Holocene corals displayed seasonal variations and had a similar range and average. The long-term average for the 2 and 5 yearly resolution Sr/Ca 1812-1986 records also displayed a similar average to the mid-Holocene coral records.
- The Mg/Ca-SST reconstruction displayed seasonal variations in both the two-monthly resolution 1980-1984 and mid-Holocene records. There was, however, a systematic difference between the average estimates for the untreated and pre-treated samples in the 2 and 5 yearly resolution records. This difference is probably from organic material which has affected the Mg/Ca ratio in the untreated coral samples.
- The U/Ca-SST reconstruction for the 1980-1984 record displayed strong seasonal variations; however, this was not particularly evident in the two-monthly resolution mid-Holocene record.

- The O isotope-SST reconstruction displayed seasonal variations in both the two-monthly 1980-1984 and mid-Holocene records. In addition, the 5 yearly resolution modern and mid-Holocene records displayed similar averages to the Sr/Ca SST reconstruction. However, the O isotopes were affected by variations in salinity.
- The subtraction of the SST component from the O isotopes allowed seawater salinity to be reconstructed. The two-monthly resolution records displayed large fluctuations which coincided with flood and El Niño Southern Oscillation events. The $\Delta^{18}O$ reconstructions for the 5 yearly resolution 1810-1985 and mid-Holocene records reveal trends towards wetter and drier years.
- Coral Ba/Ca ratios in the 1812-1986 record displayed a significant increase after European settlement; however, the post 1850 average was similar to that of the mid-Holocene corals.
- Coral Mn concentrations rose significantly after 1850 and were considerably higher than in the mid-Holocene coral records.
- Coral REE (Y, Pr, Sm and Ho) concentrations and distributions increased after 1850; however, as with the Ba/Ca ratios, the average mid-Holocene values were comparable to the post 1850 averages.
- Coral Th concentrations consistently remained at low values throughout the 1812-1986 record. This suggested that there was a negligible detrital component incorporated into the coral, whereas the mid-Holocene coral heads had significantly higher Th concentrations which indicated that these corals had been influenced by sediment or other detrital matter.

Chapter 7

Coral geochemistry discussion: Proxies of climate

7.1. Chapter overview

Several geochemical and physical coral proxies have been used in this study to reconstruct SST and seawater salinity. This chapter will discuss the results of each coral proxy and evaluate their reliability for reconstructions of past climate on the GBR. The chapter will be presented in the following order:

1) Section 7.2 examines the reconstruction of SST from the modern and mid-Holocene corals using the Sr/Ca, Mg/Ca, U/Ca ratios and $\delta^{18}O$ isotopes. In addition, the average coral calcification rate is investigated to estimate long-term SSTs.
2) Section 7.3 explores the seawater salinity records produced by the $\Delta^{18}O$ in the modern and mid-Holocene corals. The coral luminescence data is compared with the $\Delta^{18}O$ records to allow an assessment of wetter and drier periods for the last 200 years and during the mid-Holocene.

7.2. Proxies of sea surface temperature

7.2.1. Overview

Coral Sr/Ca, Mg/Ca, U/Ca ratios and $\delta^{18}O$ isotopes were used in section 6.4 to reconstruct sea surface temperature (SST) from the modern (1812-1986) and the mid-Holocene corals. Potential problems with each thermometer, which include the considerably different calibrations curves that have been developed, are discussed in this section. The correlations between each proxy with instrumental SST, other elemental ratios and coral calcification are examined. The SST proxies are also compared to previous reconstructions of GBR SST with a particular focus on the research of Hendy et al. (2002) and Gagan et al. (1998).

7.2.2. Background and calibration

Coral Sr/Ca ratio

Sr/Ca ratios are considered the most reliable coral SST proxy and have been widely applied on the GBR (e.g. McCulloch et al., 1994; Alibert and McCulloch, 1997; Gagan et al., 1998; Fallon et al., 2003); however, this SST proxy has been associated with many potential problems (see Table 2.1). Published Sr/Ca-SST calibration curves for the GBR display considerable variability, particularly the intercept of each curve (Fig 2.3b). The most noteworthy example is the significantly different calibration curves, developed for *Porites* corals from Orpheus Island (Fig 2.3b), by Gagan et al. (1998) and Fallon et al. (2003). Failure to sample along the major growth axis (Alibert and McCulloch, 1997), the use of juvenile corals (Marshall and McCulloch, 2002), variation between species (Smith et al., 1979), analytical error (Beck et al., 1992), statistical errors (Solow and Huppart, 2004), biological/metabolic effects (Cohen et al., 2002; Meibom et al., 2004), calcification/light effects (Cohen et al., 2002; Reynaud et al., 2004) and coral diagenesis (Müller et al., 2001) have been suggested as possible reasons for the variability in the numerous Sr/Ca-SST calibration curves (see section 2.2.3; Table 2.1), although it is not obvious which of these factors has the major influence on the different calibration curves from Orpheus Island. The coral Sr/Ca-SST calibrations of Gagan et al. (1998) and Fallon et al. (2003) were applied to reconstruct SST for the two-monthly resolution 1980-1984 Sr/Ca record from the Magnetic Island coral. Gagan et al.'s (1998) equation provides SST estimates approximately 3° C higher than Fallon et al.'s (2003) calibration (Fig 7.1a). The intercept-adjusted curve of Gagan et al. (1998) has been applied to the corals of Magnetic Island because of the stronger linear regression with instrumental SST from the higher precision TIMS analysis (r^2= 0.98; Gagan et al., 1998) compared to LA-ICP-MS (r^2= 0.79; Fallon et al., 2003). In addition, the adjusted curve closely matches the SST range from Magnetic Island measured since the 1990s (Fig 7.1b) and also provides a better average SST estimate for the 1980-1984 coral record from Magnetic Island. The slope of Fallon et al.'s (2003) calibration was significantly steeper than the curves produced from TIMS (Fig 4.14) which provides cooler SST estimates when the coral Sr/Ca ratio exceeds 0.0090.

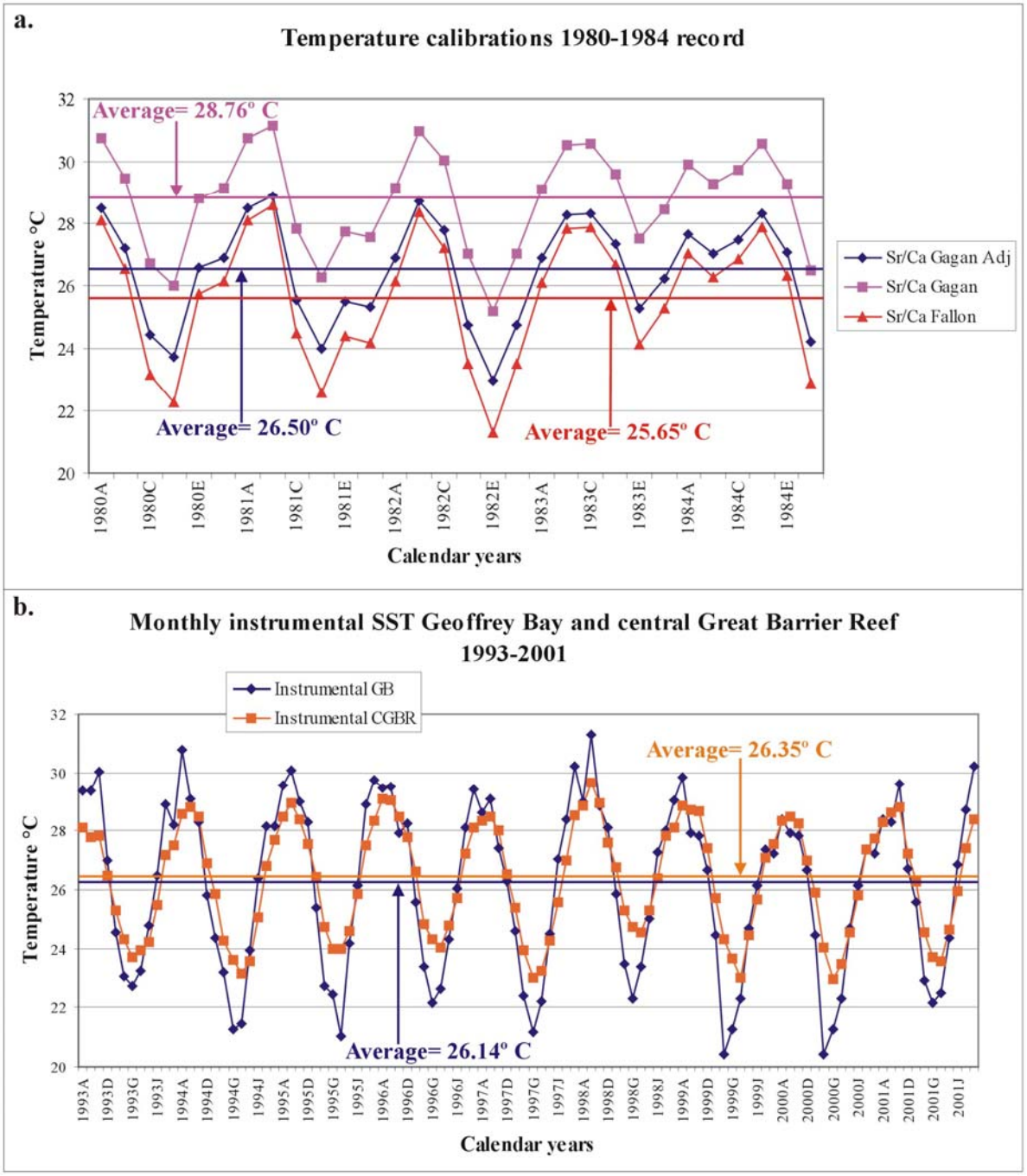

Figure 7.1a. Sr/Ca-SST reconstructions for the 1980-1984 Magnetic Island coral record from the calibrations of Gagan et al. (1998), Fallon et al. (2003) and this study (Gagan adj). The Gagan et al. (1998) calibration produces SST estimates that are approximately 2-3° C higher than the monthly instrumental range from Geoffrey Bay (GB), Magnetic Island from 1993-2001 (b). The SST reconstruction from the adjusted calibration by Gagan et al. (1998; a) produces similar SST estimates to the instrumental dataset (b). The instrumental SST range in Geoffrey Bay for 1993-2001 (b) is higher than the central Great Barrier Reef (CGBR; 15.5-19.5° S); however, the average SST estimates are similar, which suggests that the Magnetic Island corals will provide a reliable estimate of regional SST variations.

Coral Mg/Ca ratio

Previous studies have demonstrated that the Mg/Ca thermometer may be strongly influenced by organic matter incorporated into the coral skeleton (e.g. Watanabe et al., 2001). Microanalysis revealed that Mg can be concentrated by as much as 10 times in the centre of calcification relative to the outer coralline wall (Meibom et al., 2004). Therefore, the incorporation of Mg in corals may be biologically controlled (Allison, 1996; Meibom et al., 2004). The Mg/Ca-SST calibrations for the GBR display a significant difference between inshore and offshore sites, which suggests that a terrestrial source may be influencing this SST proxy (Fallon et al., 2003). In addition, the problems associated with the Sr/Ca ratio (see Table 2.1) may also apply for the coral Mg/Ca ratio, although few studies have thoroughly examined this SST proxy. Despite these potential problems, coral Mg/Ca ratios commonly display significant correlations with SST.

Two different Mg/Ca-SST calibrations were applied to separate the H_2O_2 treated corals from the untreated coral samples (Fig 4.15). The intercept of the Mg/Ca-SST calibration curve of Watanabe et al. (2001) was slightly adjusted to match the SST range of Magnetic Island; this curve was used to reconstruct SST for the H_2O_2 treated samples. The Mitsuguchi et al. (1996) Mg/Ca-SST calibration was also intercept-adjusted and used to reconstruct SST for the untreated samples. Interestingly, the slope of the H_2O_2-treated calibration is much shallower than the untreated curve (Fig 4.15). Therefore, the range of the Mg/Ca-SST reconstructions for the untreated samples should be greater than the corresponding H_2O_2-treated samples.

Coral U/Ca ratio

The U/Ca thermometer is considered one of the better coral SST proxies and has been applied to reconstruct historical SST on the GBR (Hendy et al., 2002). Nevertheless, despite the coral thermometer's obvious potential, few studies have thoroughly examined this proxy or have established a reliable SST calibration curve for the GBR, with the exception of Fallon et al. (2003). As with the Mg/Ca thermometer, there is a significant variation in the U/Ca-SST calibration curves from inshore to offshore sites on the GBR, which indicates that U may be influenced by terrestrial sources (Fallon et al., 2003).

Uranium is thought to substitute for the CO_3^{2-} ion in the coral skeleton (e.g. Shen and Dunbar, 1995) and, therefore, could also be affected by the coral calcification rate and *p*H (Min et al., 1995). Another potential problem is that the U/Ca-SST calibration curve produced from the TIMS technique (Min et al., 1995) is significantly different to the curves from the LA-ICP-MS method (Fallon et al., 2003; Fig 2.8). Corals from New Caledonia and Tahiti were used to construct Min et al.'s (1995) U/Ca-SST calibration curve. It is unclear if these corals were responding to their own environment, which may be different to the corals from the GBR, or if the different calibration curves were a product of the analytical technique (Table 2.1).

For this study, the high precision TIMS U/Ca-SST calibration of Min et al. (1995) was adjusted to match the instrumental SST range from the waters surrounding Magnetic Island. Both the slope and intercept of Fallon et al.'s (2003) U/Ca calibration curve differed significantly from that of Min et al. (1995) and produced SST estimates that were much higher than the expected range from Magnetic Island.

Coral $\delta^{18}O$ composition

The coral O isotope composition is influenced by both SST and seawater salinity (e.g. McCulloch et al., 1994; Gagan et al., 1998). Therefore, the coral O isotope composition is reliable for SST reconstructions at localities where seawater salinities are constant. However, the $\delta^{18}O$ composition of corals from the inshore GBR, such as Magnetic Island, is affected by seawater salinity, particularly during the summer months. Because the $\delta^{18}O$-SST calibration relationship is fixed, seawater salinity can be confidently reconstructed from inshore GBR corals provided that a reliable thermometer can be applied to subtract the SST component from the O isotope data (section 7.3).

7.2.3. Comparison of the two-monthly SST proxies and the instrumental dataset

Coral Sr/Ca ratio

The two-monthly resolution 1980-1984 coral Sr/Ca-SST reconstruction had a similar range and average (within 1° C) to the SST record from Magnetic Island (Fig 7.1b). This proxy

indicates that the SST record concluded during the winter of 1984 (June-July; Fig 7.2a), and suggests that the estimation of the chronology from the visible luminescent "flood" lines was slightly inaccurate. The luminescent line observed in the 1983 coral growth record was incorrectly interpreted to have formed in January. The major Burdekin River discharge in 1983 actually occurred in May.

Coral Mg/Ca ratio

The 1980-1984 Mg/Ca-SST reconstruction displayed a similar average to the 1993-2001 instrumental SST data from Magnetic Island, except for the 1982 summer, which coincided with a particularly strong ENSO year (e.g. Jones et al., 1997; Figs 7.1b; 7.2). Overall, the coral Mg/Ca ratios did not record the expected range of SST variability for the two-monthly resolution SST records and appear to be inferior to the Sr/Ca and U/Ca thermometers in reconstructing SST.

Coral U/Ca ratio

The 1980-1984 coral U/Ca-SST reconstruction contained a similar SST range and average to the instrumental record from 1993-2001 (Figs 7.2a; 7.1b). Like the Sr/Ca and Mg/Ca SST reconstructions, the U/Ca thermometer suggests that the 1980-1984 record terminated during the winter months of 1984. These SST reconstructions also suggest that the coral may have grown faster during the summer months. This finding was evident in the two-monthly resolution (6 samples per year) 1980-1984 coral record where within the one year periods, 4 of 6 samples commonly showed higher than average SSTs (Fig 7.2a). Therefore, the coral should provide, theoretically, a more reliable record of a "short-pulsed event" during the summer months than an event during "cooler" SSTs (e.g. Taylor et al., 1995).

Coral $\delta^{18}O$ composition

The coral $\delta^{18}O$-SST reconstruction for 1980-1984 has a similar average to instrumental SST records from Magnetic Island from 1993-2001; however, the SST range is considerably higher than would be expected at Magnetic Island over two-monthly periods. This $\delta^{18}O$ record has been clearly influenced by fluctuations in seawater salinity.

7.2.4. Comparison between the SST proxies at 2 and 5 yearly resolutions and the instrumental dataset

Coral Sr/Ca ratios

There was a significant correlation between the 2 yearly Sr/Ca-SST estimates and the instrumental SST record extending back to the 1870s ($r= 0.48$; $p <0.000$; $n= 58$; Table 7.1); however, the correlation between the 5 yearly resolution Sr/Ca reconstruction and the instrumental SST record was not significant ($r= 0.05$; $p >0.05$; $n= 23$). The instrumental SST dataset may not be as reliable particularly during the late 19th and early 20th centuries, because earlier "ships of opportunity" SST records are fewer and not directly from Magnetic Island. In addition, the 2 and 5 yearly sampling strategies represented a sample that approximated a two and five year growth period, respectively. This strategy could have produced sampling errors and may account for some of the variability observed in the Sr/Ca-SST reconstructions. For example, when 1.5 instead of 2.0 years is averaged in the instrumental SST record from Magnetic Island, an error of around 0.5° C is produced, while averaging 4.5 instead of 5.0 years produced an error within 0.1° C. The ranges of the 2 and 5 yearly Sr/Ca-SST reconstructions were 3.72° C and 3.65° C, respectively. In comparison, the range for the 2 and 5 yearly averaged instrumental data from 1870 were 1.04° C and 0.65° C, respectively. This relatively low instrumental range was within the combined limits of analytical precision and sampling inaccuracy.

There was excellent agreement between the long-term averages produced for the Sr/Ca-SST reconstructions for both the 2 and 5 yearly records (24.97 ± 0.81 ° C and 25.09 ± 0.76 ° C respectively) as well as for the instrumental data from 1870-1986 (25.84 ± 0.24° C). The good agreement between the two sampling resolutions analysed at different laboratories supports the validity of long-term estimates of SST using the coral Sr/Ca ratio. The apparent warming trend in the 2 yearly 1812-1986 Sr/Ca-SST reconstruction after the 1940s (Fig 7.4a) was not evident in the 5 yearly dataset (Fig 7.5a). This trend is probably an artefact of sampling, analytical and calibration errors.

Coral Mg/Ca ratio

There was no significant correlation between the Mg/Ca ratios for both the 2 (r= 0.03; p >0.05; n= 58) and 5 (r= 0.27; p >0.05; n=23) yearly sampling resolutions with instrumental SSTs for the central GBR since 1870 (Figs 7.4-7.5; Table 7.1). The range for the coral Mg/Ca-SST reconstructions in the 1812-1986 record was 4.97° C, and 1.59° C for the 2 and 5 yearly resolutions, respectively. However, the instrumental SST range for the central GBR since 1870 at 2 and 5 year averages is 1.04° C and 0.65° C. Therefore, errors relating to the coral sampling procedure, analytical precision and calibration as well as biological effects may explain why the correlation between the coral Mg/Ca-SST reconstruction and instrumental SST was insignificant (see Table 2.1).

Coral U/Ca ratio

The correlation between the coral U/Ca-SST reconstruction and instrumental SST since 1870 was also insignificant (r= 0.07; p >0.05; n= 58). As with the coral Mg/Ca ratio, the range of the U/Ca-SST reconstruction at the 2 yearly sampling resolution was considerably higher (3.77° C) than the corresponding instrumental range since 1870. This finding was probably the result of sampling, analytical or calibration errors.

Coral $\delta^{18}O$ composition

There was no significant correlation between the coral $\delta^{18}O$-SST reconstruction and instrumental SST from the central GBR since 1870 (r= 0.28; p >0.05; n= 23). This correlation may have been insignificant because of the low number of samples or because the coral $\delta^{18}O$ has been affected by seawater salinity.

7.2.5. Correlation coefficients between the SST proxies

Sr/Ca and Mg/Ca

The coral Sr/Ca and Mg/Ca-SST reconstructions for the two-monthly and long-term 2 and 5 yearly resolution records were all significantly correlated with the exception of the QHSS NEL01D record (Table 7.1). This record was taken at 5 yearly resolution and the correlation may have been insignificant due to the limited number of samples (25) in the

dataset. The two-monthly resolution records contained a higher correlation coefficient than the 2 and 5 yearly resolution samples, although the H_2O_2-treated 5 yearly resolution 1810-1985 record had a considerably higher correlation coefficient than the untreated 2 yearly records.

Sr/Ca and U/Ca

The Sr/Ca and U/Ca-SST reconstructions were also significantly correlated in all the coral records (Table 7.1). The two-monthly resolution records, like the Sr/Ca-Mg/Ca correlation, had higher correlation coefficients than the 2 yearly resolution records. Excess U had been incorporated into the coral skeleton in one of the mid-Holocene two-monthly resolution samples (Fig 7.3) and also the 2 yearly resolution NEL01D coral ("60-62"; Fig 7.6) which significantly affected the SST estimates. The O isotope-SST reconstruction suggests there was no significant salinity variation in these samples and rules out freshwater influx as a possible U source. Possible explanations for these inconsistent data include sedimentation, sample contamination and instrumental error. Unfortunately, no sedimentation proxies were measured in the two-monthly resolution record but the adjacent "62-64" sample in the 2 yearly resolution NEL01D dataset contained excessive Th concentrations, although this sample provided a reasonable U/Ca-SST estimate. Therefore, sedimentation is unlikely to influence the U/Ca-SST reconstruction.

Sr/Ca and $\delta^{18}O$

The Sr/Ca and δ^{18}O-SST reconstructions for the two-monthly resolution records were significantly correlated, although the correlation coefficients were comparably lower than the Sr/Ca-Mg/Ca and Sr/Ca-U/Ca relationships (Table 7.1). The correlations between Sr/Ca and δ^{18}O for both the 5 yearly resolution coral records were insignificant (Table 7.1).

Mg/Ca and U/Ca

Significant correlations between the Mg/Ca and U/Ca-SST reconstructions were observed in all the coral records (Table 7.1). The correlation coefficient was higher in the two-monthly resolution records compared to the 2 and 5 yearly datasets, as it was with the other records. The lower correlation coefficients for the 2 and 5 yearly resolution records were

probably influenced by the coarser sampling resolutions; once the seasonal resolution is removed (range ~ 8° C; Fig 7.1b) there is little variability in the SST range (range ~ 1° C for instrumental data). Therefore, analytical, calibration and sampling errors can produce relatively large errors that exceed the "natural" SST range for individual samples (Table 2.1). These errors, in turn, may affect the correlation coefficients between the geochemical coral SST proxies.

Mg/Ca and $\delta^{18}O$

Like the Sr/Ca-δ^{18}O relationships, the Mg/Ca and δ^{18}O-SST reconstructions were significantly correlated in the two-monthly resolution coral records, while the correlations in the 5 yearly resolution records were insignificant (Table 7.1). The insignificant correlations in the 5 yearly resolution records may have been produced by the coarse sampling resolutions (lower SST range) as well as by a combination of analytical, calibration and sampling errors. Alternatively, the δ^{18}O-SST reconstructions may have been influenced by seawater salinity, which has affected the SST correlation with elemental proxies.

U/Ca and $\delta^{18}O$

The U/Ca and δ^{18}O-SST reconstructions were significantly correlated in the two-monthly resolution coral records (Table 7.1). Unfortunately, U was not measured in the QHSS dataset; therefore, U/Ca could not be compared to δ^{18}O in either the 2 or 5 yearly resolution records.

Summary

Significant linear correlations between the coral geochemical SST proxies were found for all the two-monthly resolutions datasets, while only the Sr/Ca and Mg/Ca-SST reconstruction was significantly correlated in the 5 yearly 1810-1985 record. The 2 yearly resolution Sr/Ca, Mg/Ca and U/Ca-SST reconstruction were all significantly correlated with each other. However, the slopes of all the linear correlations were different to the 1:1 relationship that would be expected if the geochemical coral SST proxies were solely influenced by SST (Figs 7.2-7.7). The Mg/Ca and U/Ca thermometers may be affected by

factors other than SST and, for these reasons, the Sr/Ca ratio is currently the most reliable coral SST proxy (e.g. Gagan et al., 2000). In addition, the accuracy of the coral SST proxies could also be affected by sampling, calibration and analytical errors.

Table 7.1. Summary of correlation coefficients (r) between the coral geochemical and physical SST proxies and the instrumental dataset from the central GBR for both the modern and mid-Holocene corals sampled at different resolutions (number of data points given in brackets).

	Coral Record					
Correlation variables	**Two-monthly 1980-1984**	**Two-monthly NEL03D**	**2 yearly 1812-1986 ACQUIRE**	**5 yearly 1810-1985 QHSS**	**2 yearly NEL01D ACQUIRE**	**5 yearly NEL01D QHSS**
Sr/Ca-Mg/Ca	**0.79**** (30)	**0.91**** (30)	**0.46**** (87)	**0.71**** (35)	**0.26*** (63)	0.29 (25)
Sr/Ca-U/Ca	**0.90**** (30)	**0.89**** (29)	**0.44**** (87)	N/A	**0.54**** (62)	N/A
Sr/Ca-$\delta^{18}O$	**0.75**** (30)	**0.69**** (30)	N/A	0.16 (35)	N/A	0.32 (25)
Sr/Ca-instrumental	N/A	N/A	**0.48**** (58)	0.05 (23)	N/A	N/A
Sr/Ca calcification	N/A	N/A	**0.30**** (86)	**0.47**** (35)	N/A	N/A
Mg/Ca-U/Ca	**0.90**** (30)	**0.90**** (29)	**0.65**** (87)	N/A	**0.48**** (62)	N/A
Mg/Ca-$\delta^{18}O$	**0.69**** (30)	**0.61**** (30)	N/A	0.28 (35)	N/A	0.18 (25)
Mg/Ca-instrumental	N/A	N/A	0.03 (58)	0.27 (23)	N/A	N/A
Mg/Ca calcification	N/A	N/A	0.04 (86)	0.14 (35)	N/A	N/A
U/Ca-$\delta^{18}O$	**0.70**** (30)	**0.52**** (29)	N/A	N/A	N/A	N/A
U/Ca-instrumental	N/A	N/A	0.07 (58)	N/A	N/A	N/A
U/Ca calcification	N/A	N/A	0.08 (86)	N/A	N/A	N/A
$\delta^{18}O$-instrumental	N/A	N/A	N/A	0.28 (23)	N/A	N/A
$\delta^{18}O$-calcification	N/A	N/A	N/A	0.09 (35)	N/A	N/A
Instrumental-calcification	N/A	N/A	0.13 (58)	0.08 (23)	N/A	N/A

Note: *= $p < 0.05$; **= $p < 0.01$; (n)= number of samples.

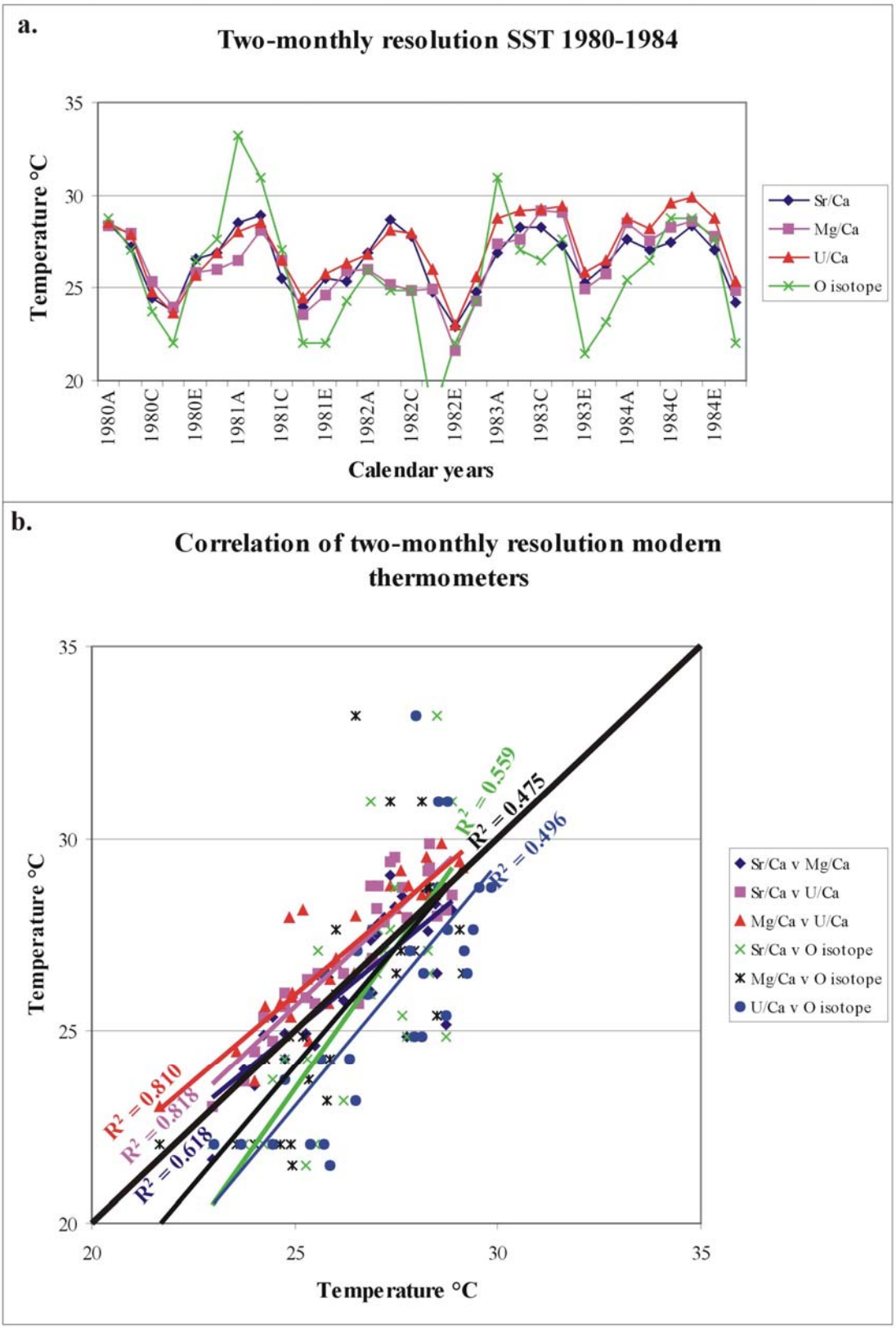

Figure 7.2 a-b. SST reconstruction for 1980-1984 using the Sr/Ca, Mg/Ca, U/Ca and O isotope thermometers. The proxies were all significantly correlated with each other (b) and display a temperature range expected for Magnetic Island.

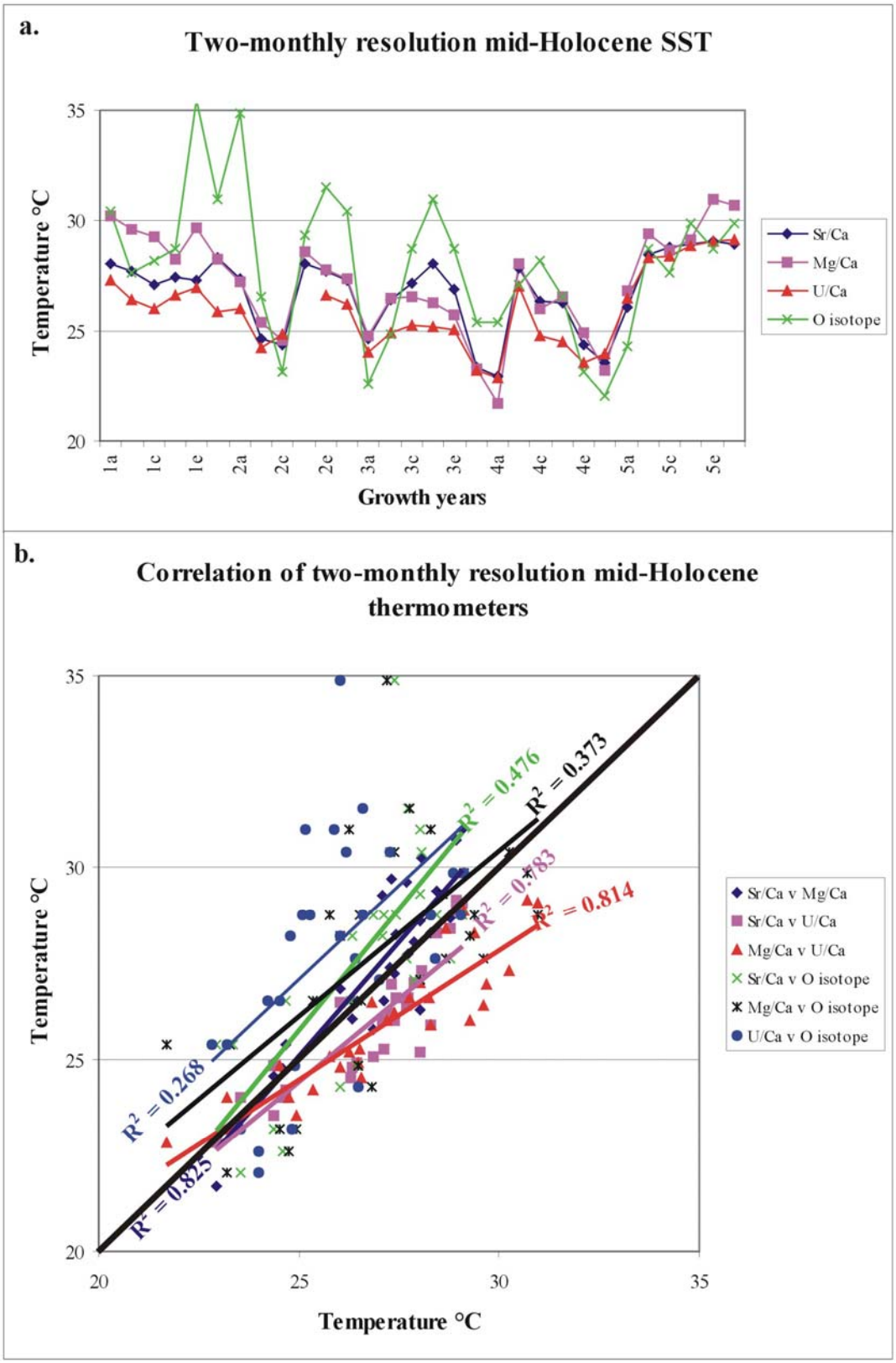

Figure 7.3 a-b. SST reconstructions for the 1980-1984 two-monthly resolution record using the Sr/Ca, Mg/Ca, U/Ca and O isotope thermometers. The proxies were positively correlated with each other (b) and demonstrate that they have potential in reconstructing historical SST.

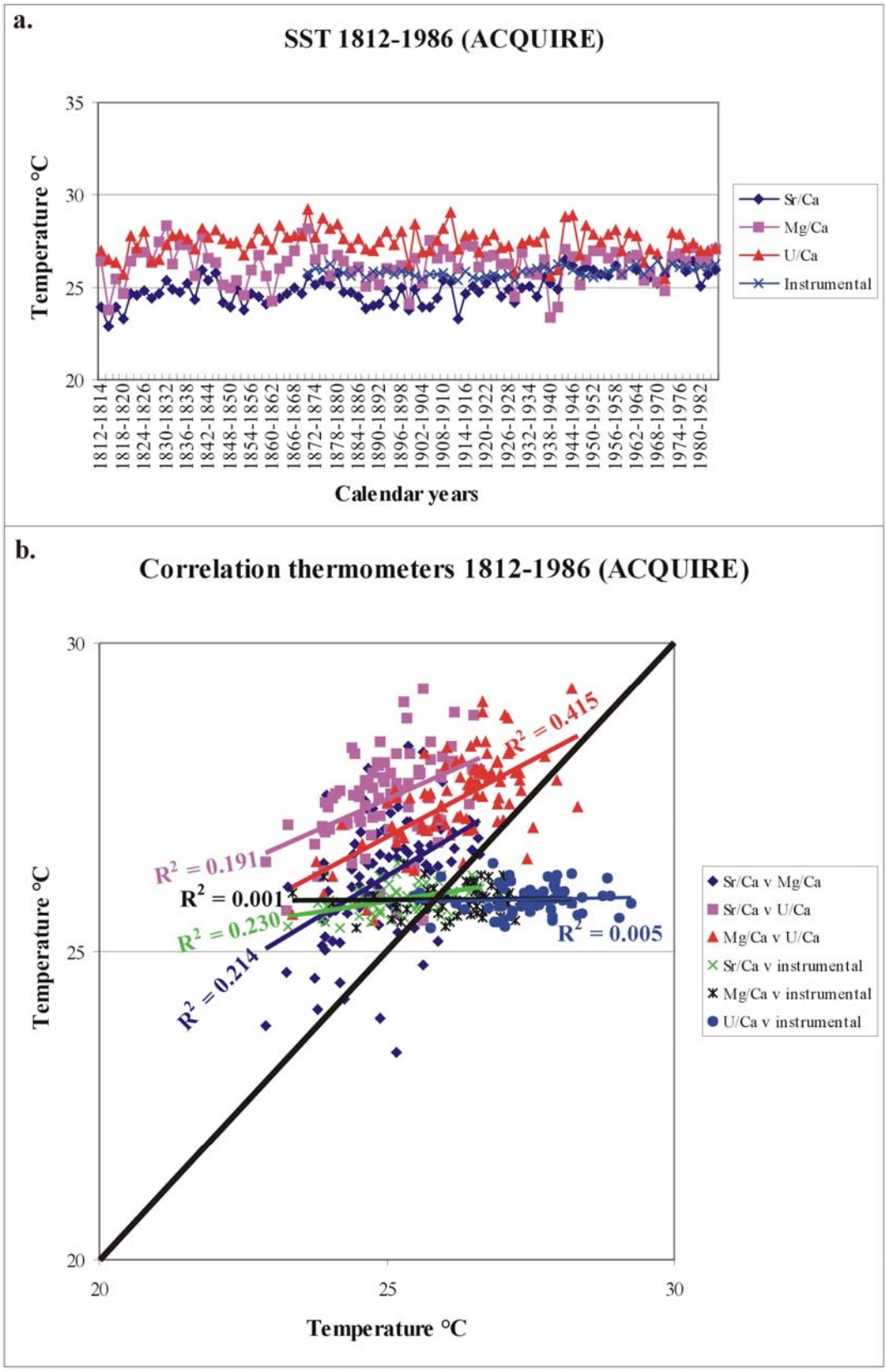

Figure 7.4 a-b. SST reconstruction for the 2 yearly resolution 1812-1986 (ACQUIRE) record using the Sr/Ca, Mg/Ca and U/Ca thermometers. The proxies were poorly correlated with each other (b) which probably reflects a combination of analytical, sampling and calibration errors.

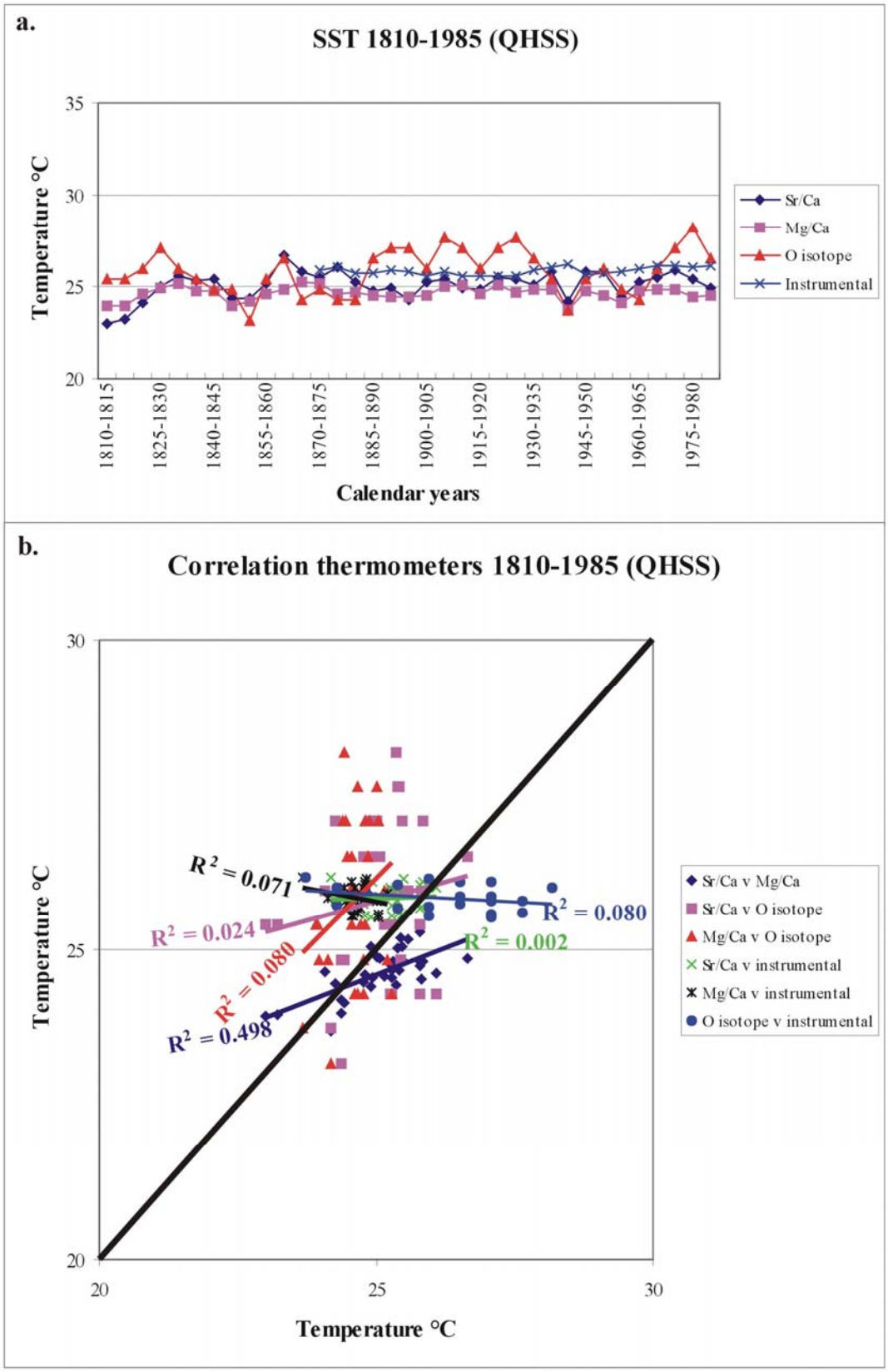

Figure 7.5 a-b. SST reconstruction for the 5 yearly resolution 1810-1985 (QHSS) record using the Sr/Ca, Mg/Ca and O isotope thermometers. The proxies were poorly correlated with each other (b) which probably reflects a combination of analytical, sampling and calibration errors.

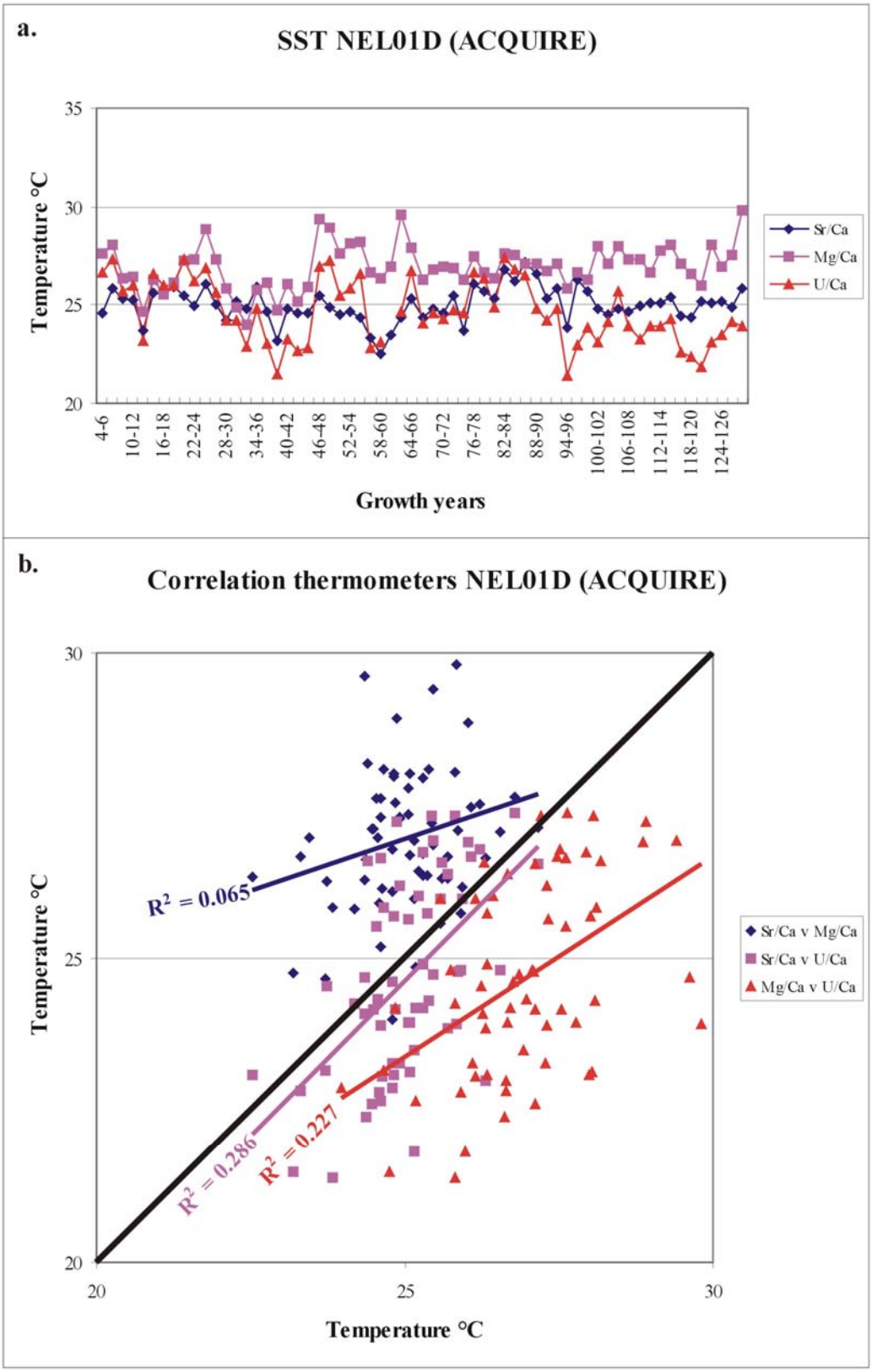

Figure 7.6 a-b. SST reconstruction for the 2 yearly resolution mid-Holocene (ACQUIRE) record using the Sr/Ca, Mg/Ca and U/Ca thermometers. The proxies were poorly correlated with each other (b) which probably reflects a combination of analytical, sampling and calibration errors.

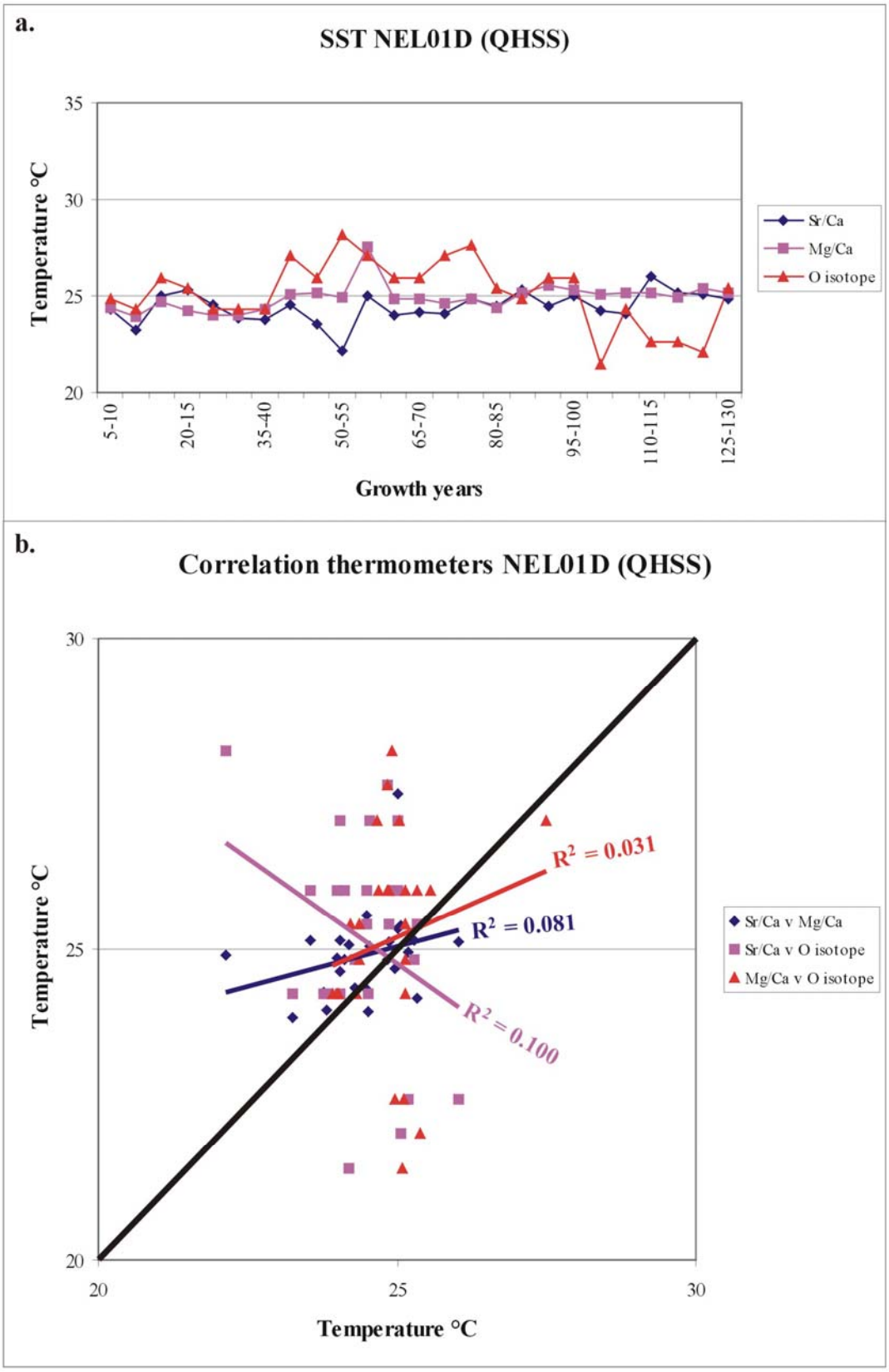

Figure 7.7 a-b. SST reconstruction for the 5 yearly resolution mid-Holocene (QHSS) record using the Sr/Ca, Mg/Ca and O isotope thermometers. The proxies were poorly correlated with each other (b) which probably reflects a combination of analytical and sampling errors.

7.2.6. Correlations between the geochemical SST proxies and coral calcification rates

The correlations between the geochemical SST proxies and calcification rates were only calculated for the 2 and 5 yearly modern records because the calcification rate was measured at annual intervals. In addition, the geochemical (Sr/Ca, Mg/Ca, U/Ca and $\delta^{18}O$) and physical (calcification rate) SST proxies were measured independently and therefore a reliable chronology for the mid-Holocene corals could not be established to compare the 2 and 5 yearly resolution records. The SST temperature estimates (Fig 7.8a-c) were produced using the calibration of Lough and Barnes (2000) which indicated that for every 1° C rise in SST, calcification increases by 0.33 g/cm^2 per year [SST= 3.0303 × annual calcification rate (g/cm^2 per year) + 21.485]. The calcification-SST reconstructions displayed considerable variability and contained large SST ranges for the averaged 2 (3.33° C) and 5 (2.97° C) year samples that were outside the corresponding instrumental measurements since 1870 (1.04 and 0.65° C, respectively; Fig 7.8 d-e). Coral calcification rates can also be affected by changes in light, salinity, nutrient levels, seawater *p*H and distortions in coral growth (e.g. Lough and Barnes, 2000; Kinsey, 1991b; Kleypas et al., 1999) which may significantly contribute to the annual variability.

The Sr/Ca-SST reconstruction was the only geochemical proxy that showed a significant correlation with the average calcification data; this significant correlation was observed in both the 2 ($r= 0.30$; $p <0.00$; $n= 86$) and 5 ($r= 0.47$; $p <0.00$; $n=35$) yearly records (Table 7.1). The better analytical precision for the coral Sr/Ca ratio in the 5 yearly record may explain the higher correlation coefficient compared to the 2 yearly dataset. Alternatively, the correlation coefficient may have been improved by the longer-term averages and thus may have 'smoothed' the 5 yearly dataset.

The coral calcification-SST reconstruction closely matched the average SST values produced from the paleothermometers when the datasets were averaged over the entire coral record. The average annual calcification for the 1812-1986 record is 1.42 g/cm^2 per year, which equates to a SST of 25.80° C. The average calcification rates for the fossil mid-Holocene coral heads are 1.48 (25.98° C), 1.61 (26.35° C), 1.34 (25.55° C) and 1.52

(26.09° C) g/cm^2 per year for NEL01, NEL03, NEL06 and NEL07 corals, respectively, and produce SST estimations similar to the modern coral record. These values are also similar to the SST reconstructions from the geochemical proxies.

7.2.7. Comparisons between the modern coral SST reconstructions and previous studies

The range of the atomic Sr/Ca (8.89 to 9.12 × 10^{-3}: 3.65° C) for the 5 yearly resolution coral record from Magnetic Island is higher than Hendy's (2003) nearby Havannah Island coral dataset (Sr/Ca= 8.98 to 9.10 × 10^{-3}: 1.88° C). The lower Sr/Ca range in Hendy (2003) may be the result of the higher precision TIMS analysis compared to the ICP-AES data from this study. However, the coral U/Ca range for the 2 yearly Magnetic Island record (1.14 to 1.31 × 10^{-6}: 3.77° C) is lower than the 5 yearly resolution Havannah Island dataset (U/Ca= 1.10 to 1.30 × 10^{-6}: 4.30° C; Hendy, 2003). The SST range in both studies is larger than observed for the instrumental 2 and 5 yearly resolution records from the central GBR since 1870 (1.04 and 0.65° C, respectively). This result implies that the measurement of the Sr/Ca and U/Ca ratios for these two coral records may have been affected by calibration, analytical and sampling errors, diagenesis or a possible biological/metabolic effect. In addition, the relatively high reconstructed SST ranges for the 1812-1986 Magnetic Island coral record makes it difficult to identify any genuine SST variations in the coral record. However, an apparent warming event after the 1880s from the Sr/Ca and Mg/Ca ratios (sections 6.4.2 and 6.4.3) is supported by Hendy et al. (2002).

7.2.8. Comparisons between the mid-Holocene coral SST reconstructions and previous studies

Multi-proxy SST reconstructions from four mid-Holocene corals suggest that average SSTs in the waters surrounding Magnetic Island 6,000 years ago were indistinguishable from the 1812-1986 SST reconstructions (Fig 7.6a-7.7a). The mid-Holocene coral from Orpheus Island in the Gagan et al. (1998) study was approximately 700 years younger than the Magnetic Island corals and contained significantly higher Sr/Ca ratios, which are indicative of a cooler environment; however, Gagan et al. (1998) argued that SSTs were approximately 1° C warmer during the mid-Holocene. Their result was based on a SST

calibration that was developed from a modern Orpheus Island coral. Fallon et al. (2003) also produced a coral Sr/Ca-SST calibration from Orpheus Island using the LA-ICP-MS technique. This SST calibration closely resembles other studies from the GBR and produces SST estimates around 3° C cooler than the coral Sr/Ca ratios measured by Gagan et al. (1998). Marshall et al. (2000) also found evidence of cooler SST (2° C) on the GBR approximately 6.20 ka. However, Gagan et al. (1998) showed a close correlation between oxygen isotopes and the Sr/Ca-SST estimates in the modern record. The O isotopes in the mid-Holocene coral provide similar summer SST estimates to the modern Orpheus Island record; while the winter SST estimations are approximately 1.5° C cooler. The fossil Magnetic Island corals provide a more reliable estimate of mid-Holocene SST compared to Gagan et al. (1998) and Marshall et al. (2000) because the Magnetic Island coral records cover a significantly longer timeframe (~100 years) compared to the previous studies (~10 years). In addition, this study employed multi-proxy records of SST, including the Sr/Ca, Mg/Ca and U/Ca ratios, as well as oxygen isotopes and annual calcification rate compared to only Sr/Ca ratios and O isotopes in the previous studies.

Fossil coral heads can contain relatively higher Sr/Ca values (therefore lower SST estimations) if partially infilled with secondary aragonite (e.g. Enmar et al., 2000). The Sr/Ca-SST relationship might also be compromised by differing light conditions (Cohen et al., 2002; Reynaud et al., 2004). In addition, the corals from the previous studies were taken from different locations (environments) and are of different ages (around 200-700 years apart). Therefore, these Sr/Ca-SST estimates may reflect a genuine cooling trend during the mid-Holocene.

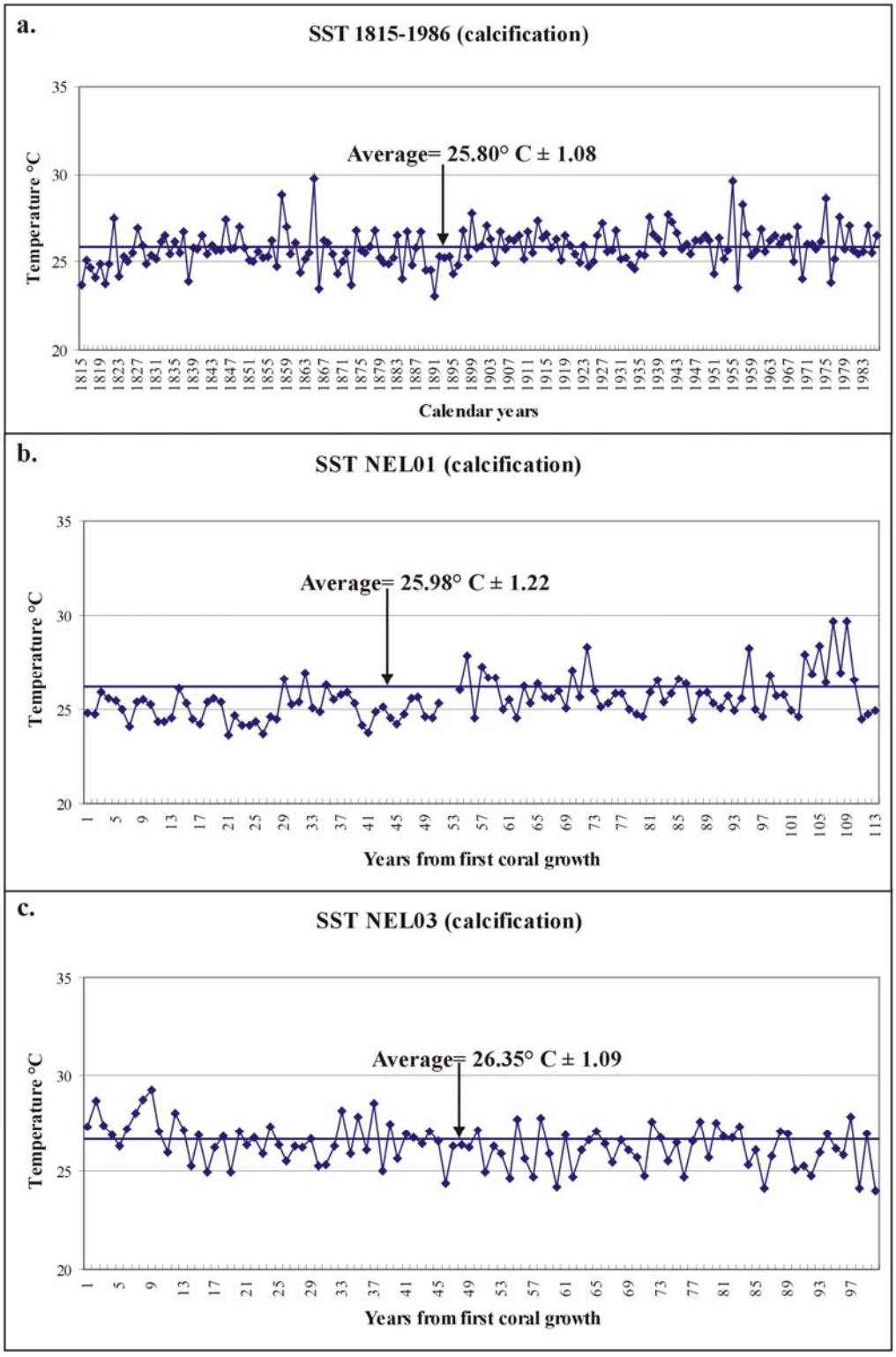

Figure 7.8 a-c. Annual coral calcification-SST reconstructions for the modern (a) and mid-Holocene (b-c) coral records using calibration of Lough and Barnes (2000). While the long-term SST average is consistent with the estimates from the geochemical thermometers, the calcification-SST reconstructions display significant annual variability that could not all be attributed to SST fluctuations. This variability suggests that the annual coral calcification rate may be influenced by other parameters.

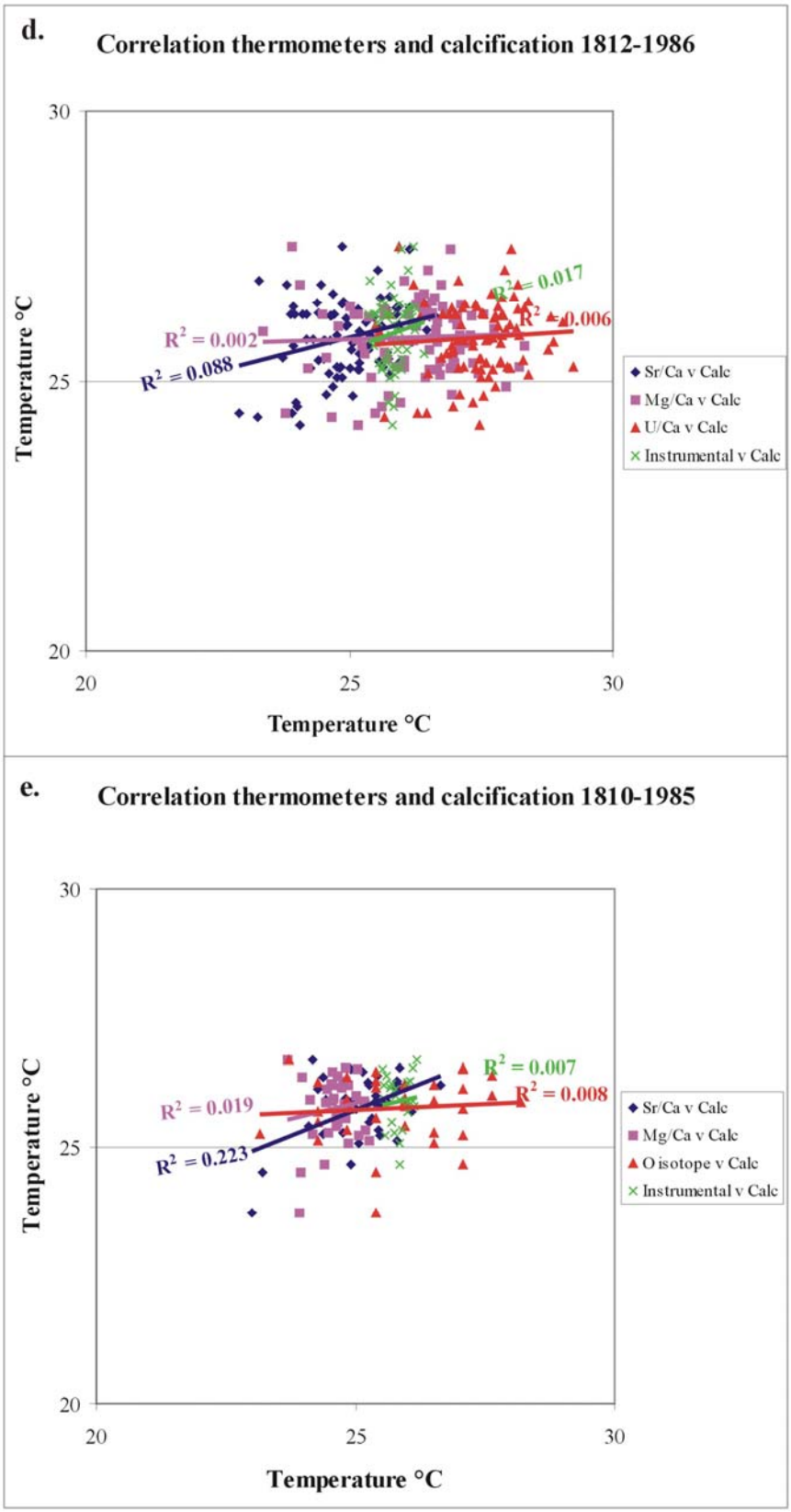

Figure 7.8 d-e. Correlations between the calcification data with the Sr/Ca, Mg/Ca, U/Ca and O isotope thermometers for the 2 (d) and 5 (e) yearly resolutions. The poor correlations are not surprising as calcification can be affected by parameters other than SST.

7.2.9. Summary: proxies of sea surface temperature

Generally, the SST proxies provided reliable estimates of average SST despite the numerous problems associated with them (Table 2.1). The data show that the Sr/Ca ratio is the best of the thermometers as it was the only coral proxy that was significantly correlated with instrumental SST records from the central GBR since 1870. For future reconstructions, the full suite of SST proxies (Sr/Ca, U/Ca, Mg/Ca, O isotopes, B/Ca and coral calcification) should be analysed. Multi-proxy analyses would significantly improve both the reliability of the data and the understanding of the individual systematics of the proxies. The SST proxies provided similar mean temperature estimates in both the modern and mid-Holocene coral records which suggests that SSTs 6,000 years ago were similar to today. These results were inconsistent with previous studies on the GBR and more research is required to validate these data. This study indicates that the mid-Holocene corals employed in this study were largely in an unaltered form, an interpretation which was justified by microanalytical investigations (section 6.2). Significantly, this study applied a number of proxies on four long-lived (~100 years) fossil corals to reconstruct mid-Holocene SST, whereas previous studies measured Sr/Ca and O isotopes only, and also based their results on a much shorter coral record (~10 years).

7.3. Seawater salinity ($\Delta^{18}O$)

7.3.1. Overview

The $\Delta^{18}O$ was calculated for the modern and mid-Holocene coral records at both two-monthly and 5 yearly resolutions to examine short (flood events) and long-term (wetter and drier) fluctuations in seawater salinity, respectively. The Sr/Ca ratio, despite its potential problems, is currently the most reliable coral SST proxy and has been applied to reconstruct coral $\Delta^{18}O$ for this study. In addition, the annual luminescence of the corals was investigated to assess long-term climate variations and was compared to the coral $\Delta^{18}O$ variations. The $\Delta^{18}O$ and luminescence records will be combined to examine climate variations during the mid-Holocene.

7.3.2. Two monthly resolution records

Significant negative excursions in the 1980-1984 two-monthly coral $\Delta^{18}O$ record coincided with large discharge events from the Burdekin River (Fig 7.9a). The $\Delta^{18}O$ value of -0.85 ± 0.25 ‰, recorded during the large 1981 flood closely matches McCulloch et al.'s (1994) peak value (~ -0.90 ‰) for this flood, sampled from a Pandora Reef coral record, about 60 km north of Magnetic Island (Fig 2.11). In comparison, the 1983 flood has a more negative $\Delta^{18}O$ value (-0.74 ± 0.25‰) compared to McCulloch et al.'s (1994) value (~ -0.30 ‰). This finding is not unexpected as corals from Magnetic Island are closer to the mouth of the Burdekin River channel. Burdekin floods of lower intensity may exert a greater influence on Magnetic Island compared to Pandora Reef. This is evident from the flood plume modelling data of King et al. (2001) for the Burdekin, Herbert, Tully and Johnstone Rivers (see Fig 8.10). These models suggest that Pandora Reef may also be strongly influenced by the Herbert River as well as by the Burdekin. During the 1983 flood, the Herbert River plume did not reach Pandora Reef, while the freshwater plume from the Burdekin was considerably diluted by the time it reached this area. In addition, local flooding in the Townsville region could have also reduced the salinity in the waters surrounding Magnetic Island during 1983.

There was a large excursion towards more positive $\Delta^{18}O$ values during mid-1982 (Fig 7.9a). This excursion was probably due to the 1982 ENSO event where higher than average evaporation rates may have resulted in a positive shift in $\Delta^{18}O$. This event is currently the only plausible explanation for the significant $\Delta^{18}O$ excursion.

As with the SST reconstructions, the $\Delta^{18}O$ record displayed a slight sampling error where the chronology was misjudged. The luminescent line in the 1983 coral growth band was incorrectly assumed to have formed in January; however, it is now interpreted to be linked to the Burdekin River flood in May 1983. The 1981 flood, which occurred in January, concurred with the chronology estimation that was made during the sampling procedure (Fig 7.9a).

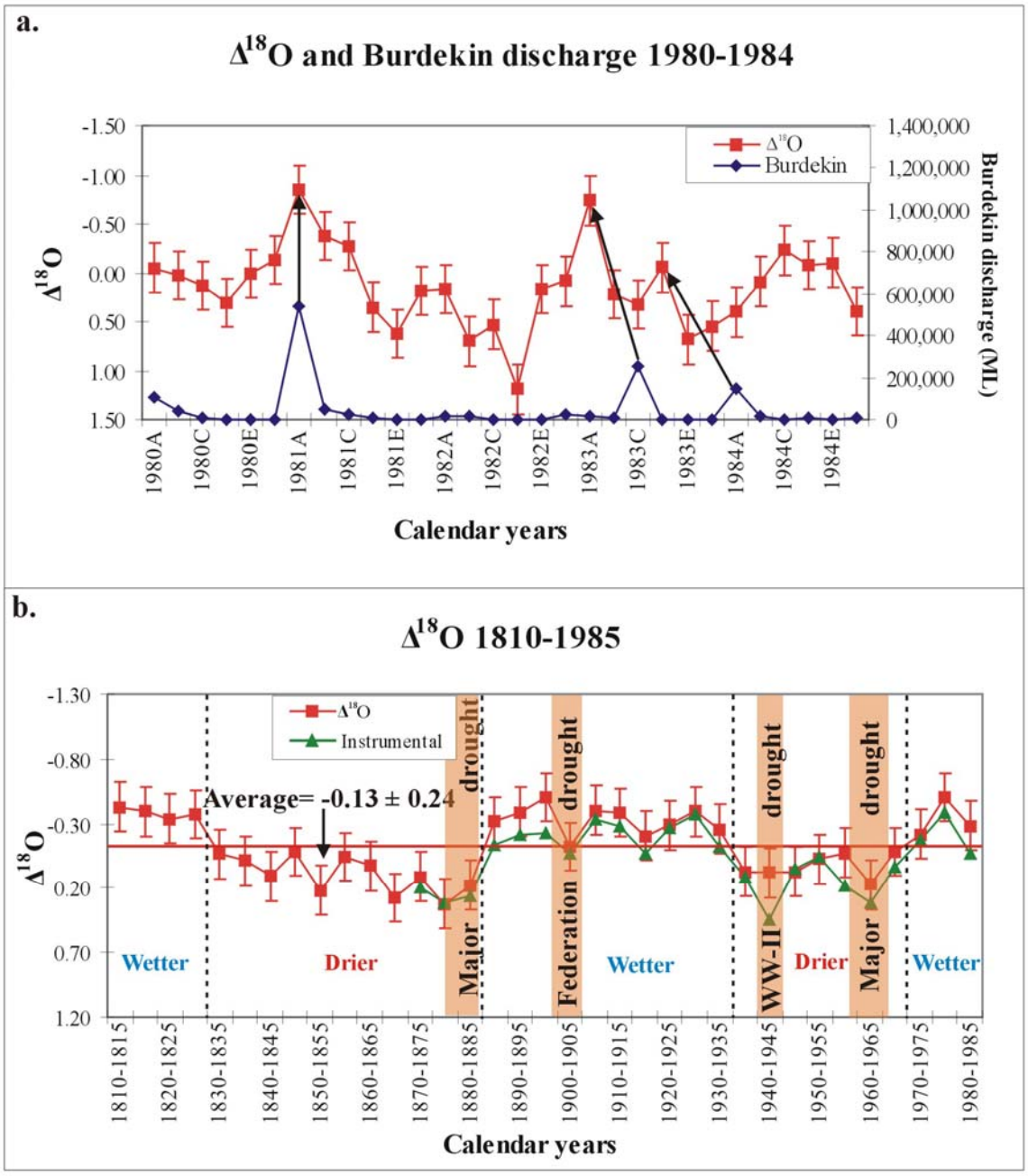

Figure 7.9 a-b. Coral $\Delta^{18}O$ reconstructions for the two-monthly resolution 1980-1984 (a) and 5 yearly resolution 1810-1985 (b) records. The relatively poor analytical uncertainty for the two-monthly $\Delta^{18}O$ values (± 0.25‰) largely relates to the precision of the Sr/Ca SST estimates. However, the trends in these records were genuine, with large negative $\Delta^{18}O$ excursions coinciding with the 1981 and 1983 floods and a large positive excursion in mid-1982 which may be related to enhanced evaporation during the 1982 ENSO event (a). Due to inaccuracies in the estimation of timing when sampling this coral, there is an offset between the negative $\Delta^{18}O$ excursions and the Burdekin discharge of the 1983 and 1984 flood events. The arrows highlight the actual chronology. The 1810-1985 record (b) displays periods of relatively wetter (1885-1935 and post 1970) and drier conditions (1830-1885 and 1935-1970) in the GBR lagoon. The 1810-1830 period may have been relatively wetter; however, the coral Sr/Ca ratios may have been affected by a juvenile coral signature (see section 6.4.2) which may have, in turn, affected the $\Delta^{18}O$ calculation. Interestingly, the $\Delta^{18}O$ "cycles" between relatively wetter and drier years fluctuate on 50-70 year periodicities (b) which appear to be related to the Pacific Decadal Oscillation. In addition, major droughts also coincide with more positive $\Delta^{18}O$ values.

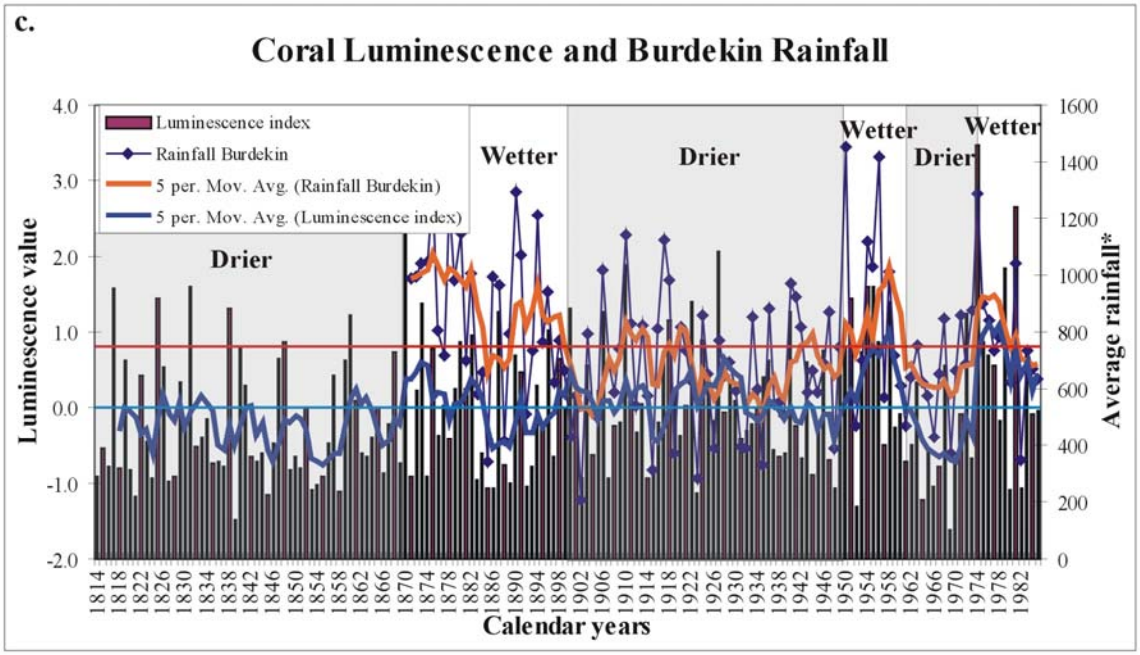

Figure 7.9c. The coral luminescence data and average rainfall in the Burdekin River catchment produced similar estimations to the coral $\Delta^{18}O$ reconstruction of relatively drier and wetter intervals. There was a significant correlation (r= 0.54) between the coral luminescence and rainfall records (Fig 7.11b). In this record, drier periods were identified during 1814-1870, 1900-1950 and 1960-1970 while wetter periods persisted during 1870-1900, 1950-1960 and 1970-1985. note *= average rainfall was produced using rainfall data throughout the Burdekin River catchment (Fig 4.16). The catchment was divided into a series of sub-catchments and the average rainfall data from these were used to produce the average rainfall (units are in mm).

The two-monthly resolution mid-Holocene record displayed 3-4 large negative $\Delta^{18}O$ excursions in successive years (Fig 6.14b; 6.17b). The timing of these excursions suggests that the floods occurred during the summer wet season of north Queensland. The first $\Delta^{18}O$ excursion (-1.46 ‰) is considerably larger in comparison to the 1981 flood (-0.85 ‰) which, from the coral luminescent record, was the 3rd largest flood in the 1812-1986 Magnetic Island coral record. During the mid-Holocene, the Burdekin River channel discharged in closer proximity to Magnetic Island than at present, which may explain the lower salinities recorded in flood events (Fig 3.1). The mid-Holocene corals also grew near the mouth of Gustav Creek and its plume may have significantly reduced the seawater salinity in the local area. The Eu anomaly in the mid-Holocene corals may provide additional evidence of a Gustav Creek freshwater influence (Appendix 2). Alternatively, the wet seasons during the mid-Holocene may have been more intense. However, this high

resolution record only extends for 5 years and this short timeframe may not be representative of the mid-Holocene.

The mid-Holocene coral $\Delta^{18}O$ record does not support Gagan et al.'s (1998) interpretation of a positive enrichment of $\Delta^{18}O$ values for the waters of the GBR. Their study was based on a mid-Holocene coral from Orpheus Island, and the $\Delta^{18}O$ range of Gagan et al.'s (1998) study is between 0.0 and + 0.5 ‰ which accounts for the natural variation in the 1980-1984 salinity record. However, the Sr/Ca-SST calibration of Gagan et al. (1998) was different from other curves developed for the GBR including Fallon et al.'s (2003) calibration from an Orpheus Island coral. An alternative Sr/Ca-SST calibration would lower the SST estimate and shift the $\Delta^{18}O$ record towards more negative values. If this hypothesis is correct, the more negative $\Delta^{18}O$ values in the Orpheus Island record may support the idea that the Burdekin River channel had a greater influence when it discharged further northwards during mid-Holocene times (Hopley, 1970a; Fielding et al., 2003; Fielding et al., 2006; see section 3.2.2).

7.3.3. The 5 yearly sampling resolution records

The 5 yearly $\Delta^{18}O$ 1810-1985 record indicates that relatively drier environments persisted during 1830-1885 and 1935-1970, with wetter conditions during 1885-1935 and post 1970. These data were in good agreement with the studies of Isdale et al. (1998) and Hendy et al. (2003) who measured luminescent lines in corals from the GBR. The coral luminescence record indicates that drier conditions occurred during the mid 19th and mid-20th centuries while wetter conditions prevailed in the late 19th century (Fig 7.10). The results are also similar to the rainfall records of Tucker (1975), who suggested that drier conditions occurred between 1941 and 1970. However, the rainfall records of Lough (1991) indicate that summer rainfall increased significantly from the 1919-1948 timeframe to the 1949-1978 30 year period which was not evident in the $\Delta^{18}O$ coral record.

Unfortunately, the precision limits for the 5 yearly $\Delta^{18}O$ 1810-1985 record (± 0.19‰) accounts for much of the variation in the dataset. The Sr/Ca-SST reconstruction suggests

that SST increased after the 1940s, which was not evident in the instrumental dataset for the central GBR or the other coral SST thermometers. The $\Delta^{18}O$ signal has a trend towards more saline (drier) conditions, but this may have been influenced by the Sr/Ca-SST reconstruction. However, in any case, applying the instrumental data for the central GBR to subtract the SST component from the O isotopes produces similar trends in $\Delta^{18}O$ (Fig 7.9b). Therefore, it is considered that these trends are real and not an artefact of the precision or calibration of the Sr/Ca ratio, with the possible exception of the 1810-1830 $\Delta^{18}O$ record. This section may have been affected by the Sr/Ca ratios, which could have been influenced by a juvenile coral signature (see section 6.4.2).

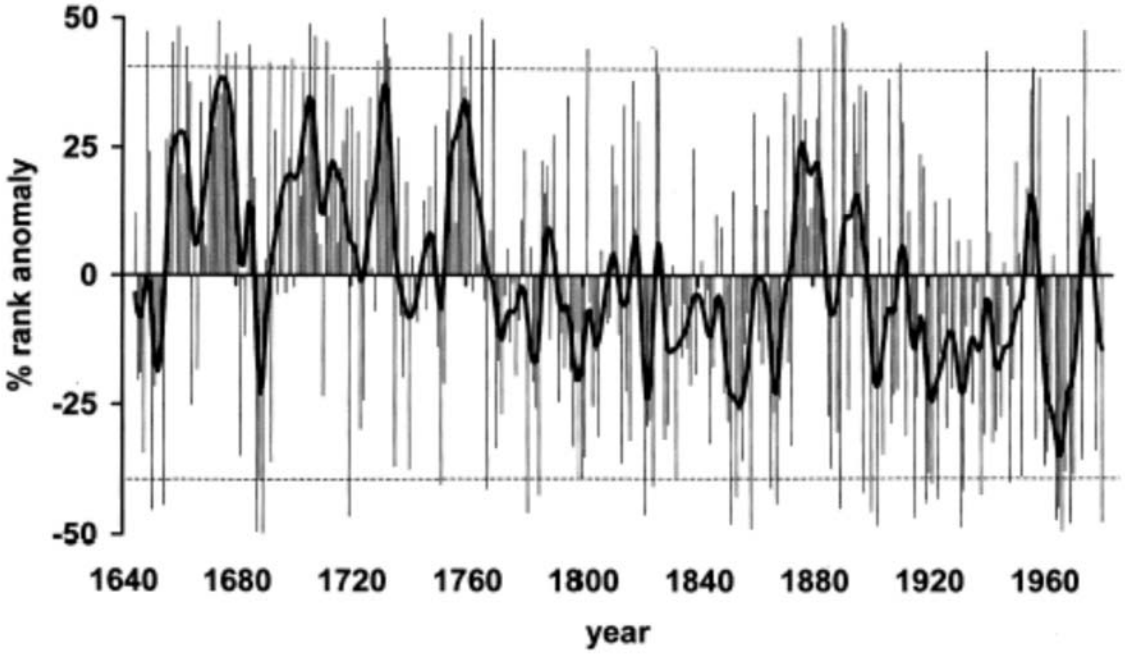

Figure 7.10. Coral luminescence record (Pandora Reef and Havannah Island corals) from Isdale et al. (1998). The record displayed similar trends to that observed in the $\Delta^{18}O$ record and luminescence record in this study: i.e. the drier periods which occurred during 1800-1870, 1900-1940 and wetter years from 1870-1900, 1940-1950s and 1970s.

The correlations between coral $\Delta^{18}O$ data with luminescence, rainfall and Burdekin discharge were not significant; however, the luminescence record, rainfall data, Burdekin discharge and the Hendy et al. (2003) luminescence master set were all significantly correlated with each other (Table 7.2; Figs 7.11-7.12). This finding may suggest that coral luminescence provides a more reliable proxy of climate than this $\Delta^{18}O$ record, which was only measured at 5 yearly resolution compared to the luminescence dataset which was

measured annually. The 5 yearly resolution coral $\Delta^{18}O$ record shows long-term, but subtle, trends in seawater salinity whereas the luminescence data reveal large, short-term salinity variations from rainfall and river discharge events. Therefore, the coral $\Delta^{18}O$ and luminescence datasets are recording different environmental conditions and explain the insignificant correlation between the two records. While there was no significant correlation between the coral $\Delta^{18}O$ data and the luminescence record, the long-term trends in both records appear to be similar. The significant correlation between the coral luminescence and Hendy et al.'s (2003) luminescence master set confirms that the Magnetic Island coral recorded a regional signal and was strongly influenced by the Burdekin River (Fig 7.12b). The coral luminescence record reveals that wetter conditions occurred during the 1950s and 1970s as was previously observed by Lough (1991; Fig 7.9c).

Table 7.2. Correlation coefficients between the coral $\Delta^{18}O$, luminescence data, rainfall records, Burdekin River and Herbert River discharge and Hendy et al.'s (2003) coral luminescence master set. Significant correlations are shown in bold.

Correlation variables	Correlation coefficient (r)	Significance (p)	Number of samples (n)
$\Delta^{18}O$ v Luminescence	0.21	> 0.05	35
$\Delta^{18}O$ v Rainfall	0.21	> 0.05	23
$\Delta^{18}O$ v Burdekin discharge	0.02	> 0.05	13
Luminescence v Rainfall	**0.54**	< 0.00	115
Luminescence v Burdekin discharge	**0.81**	< 0.00	64
Luminescence v Hendy et al. (2003)	**0.72**	< 0.00	172
Rainfall v Burdekin discharge	**0.75**	< 0.00	64
Rainfall v Hendy et al. (2003)	**0.63**	< 0.00	115
Hendy et al. (2003) v Burdekin discharge	**0.84**	< 0.00	64
Hendy et al. (2003) v Herbert discharge	**0.72**	< 0.00	70
Burdekin discharge v Herbert discharge	**0.72**	< 0.00	64

The 5 yearly $\Delta^{18}O$ 1810-1985 dataset records long-term seawater salinity variations and partially agrees with previous climatic research for north Queensland. Although the $\Delta^{18}O$ record supports a "freshening" of the GBR lagoon which coincided with the end of the Little Ice Age (1870), as suggested by Hendy et al. (2002), the $\Delta^{18}O$ values returned to pre-1870 values between 1935 and 1970. This result indicates a natural 50-70 year cyclic

salinity variation on the GBR which could be related to the Pacific Decadal Oscillation (PDO; Mantua and Hare, 2002). The timing of these $\Delta^{18}O$ cycles also coincided with fluctuations between "warm" and "cool" phases of the PDO. "Cool" PDO phases occurred between 1890-1924 and 1947-1976 and "warm" regimes prevailed between 1925-1946 and from 1977 (Mantua and Hare, 2002). In addition, the 5 yearly resolution $\Delta^{18}O$ dataset appears to record major drought events in north Queensland such as the 1880-1886 drought, the Federation Drought (1895-1903), the World War II drought (1939-1945) and the 1958-1968 drought (Young, 2000; Fig 7.9b).

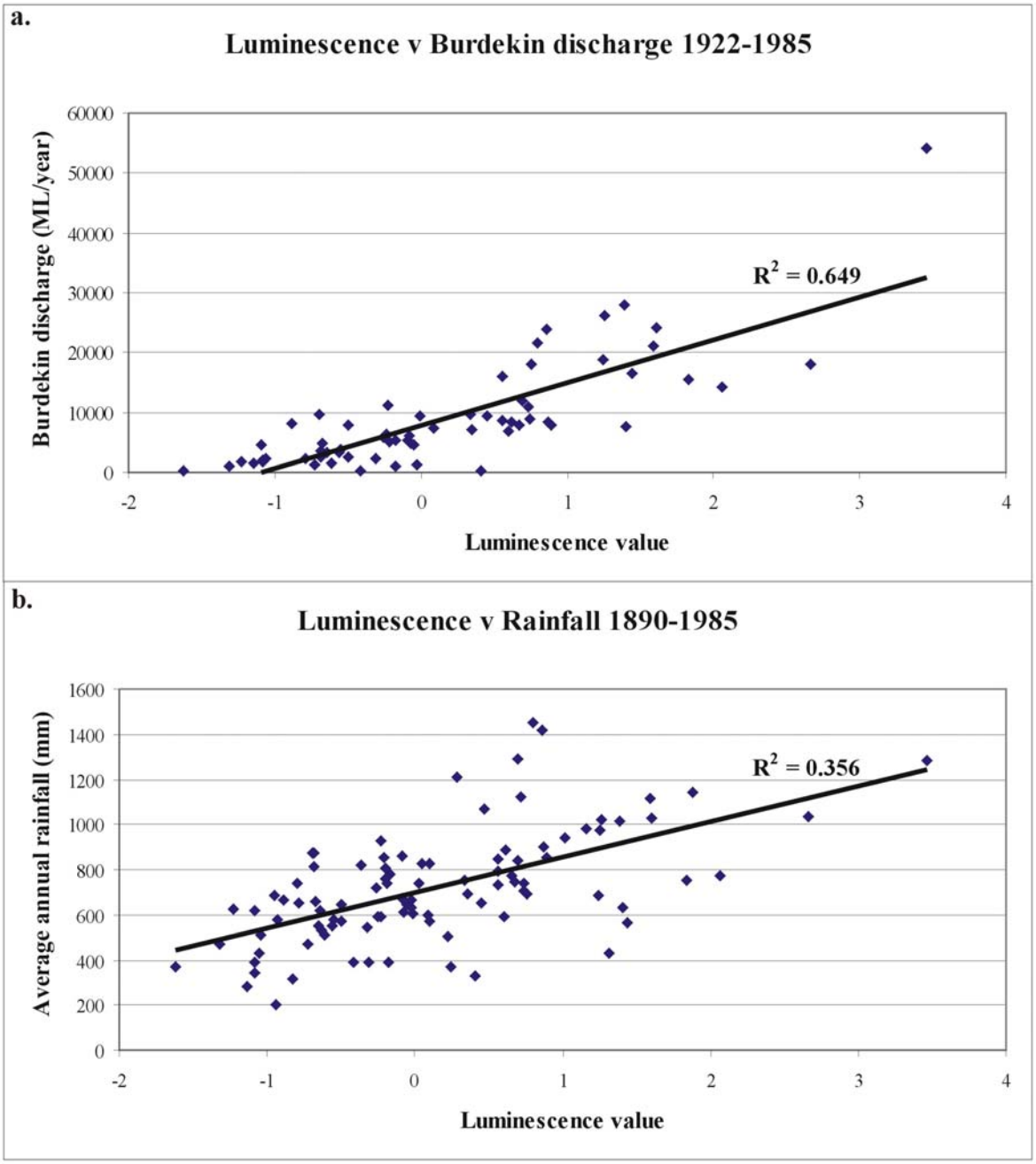

Figure 7.11 a-b. The Magnetic Island coral luminescence record was significantly correlated with Burdekin River discharge since 1922 (a) and rainfall in the Burdekin catchment (b) (see locations in Fig 4.16). This correlation suggests that the Magnetic Island coral record was influenced by the Burdekin River plume and thus recorded regional climate trends.

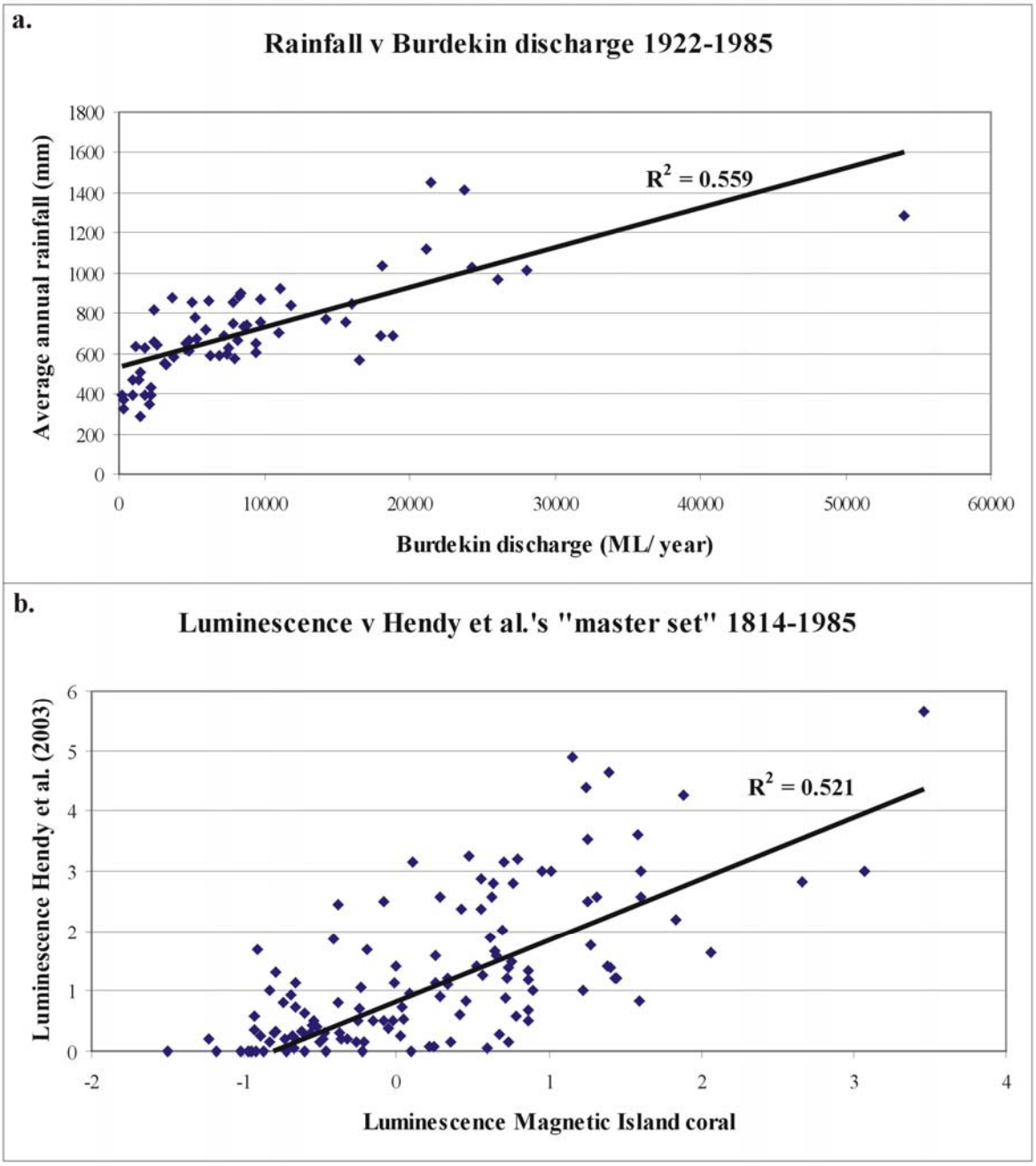

Figure 7.12 a-b. The Burdekin discharge data was significantly correlated with a compilation of rainfall records from the extensive Burdekin River catchment (a; see Fig 4.16 for locations). The coral luminescence record was also significantly correlated with the luminescence "master set" compiled for 8 long coral cores from the GBR by Hendy et al. (2003). This result suggests that the Magnetic Island coral recorded at least part of a regional signal.

The two mid-Holocene records displayed similar average $\Delta^{18}O$ values compared to the modern record (Fig 7.13 a, c). Although the two monthly resolution $\Delta^{18}O$ values may have been significantly affected by the closer proximity of the Burdekin River during the mid-Holocene, the 5 yearly resolution records would essentially average out these flood events which are represented in only approximately 1/6 of coral growth (assuming annual river discharge of 30 days, which is typical for the Burdekin system, and faster coral growth during summer or annual luminescent lines of 2 mm in thickness). The final growth record for the mid-Holocene corals displayed no large $\Delta^{18}O$ excursions which suggest that the sudden mortality of these corals was not the result of freshwater influx.

Interestingly, the mid-Holocene salinity record for the NEL01D coral displays similar $\Delta^{18}O$ variability to the modern record (Fig 7.13a). In addition, the $\Delta^{18}O$ fluctuations in the NEL01D record occur on a 50-70 year periodicity, which may indicate that the Pacific Decadal Oscillation (PDO) may have also influenced the mid-Holocene corals. However, the NEL03D $\Delta^{18}O$ record does not display this variability (Fig 7.13c) and more data is required to examine the influence of the PDO during the mid-Holocene.

Because the coral $\Delta^{18}O$ record and the luminescence dataset were analysed independently, an accurate chronology for the mid-Holocene corals could not be established. Therefore, these datasets could not be directly compared. It appears that these two proxies do not display the same trends in the mid-Holocene records (Fig 7.13a-d) and thus may be responding to different environmental parameters.

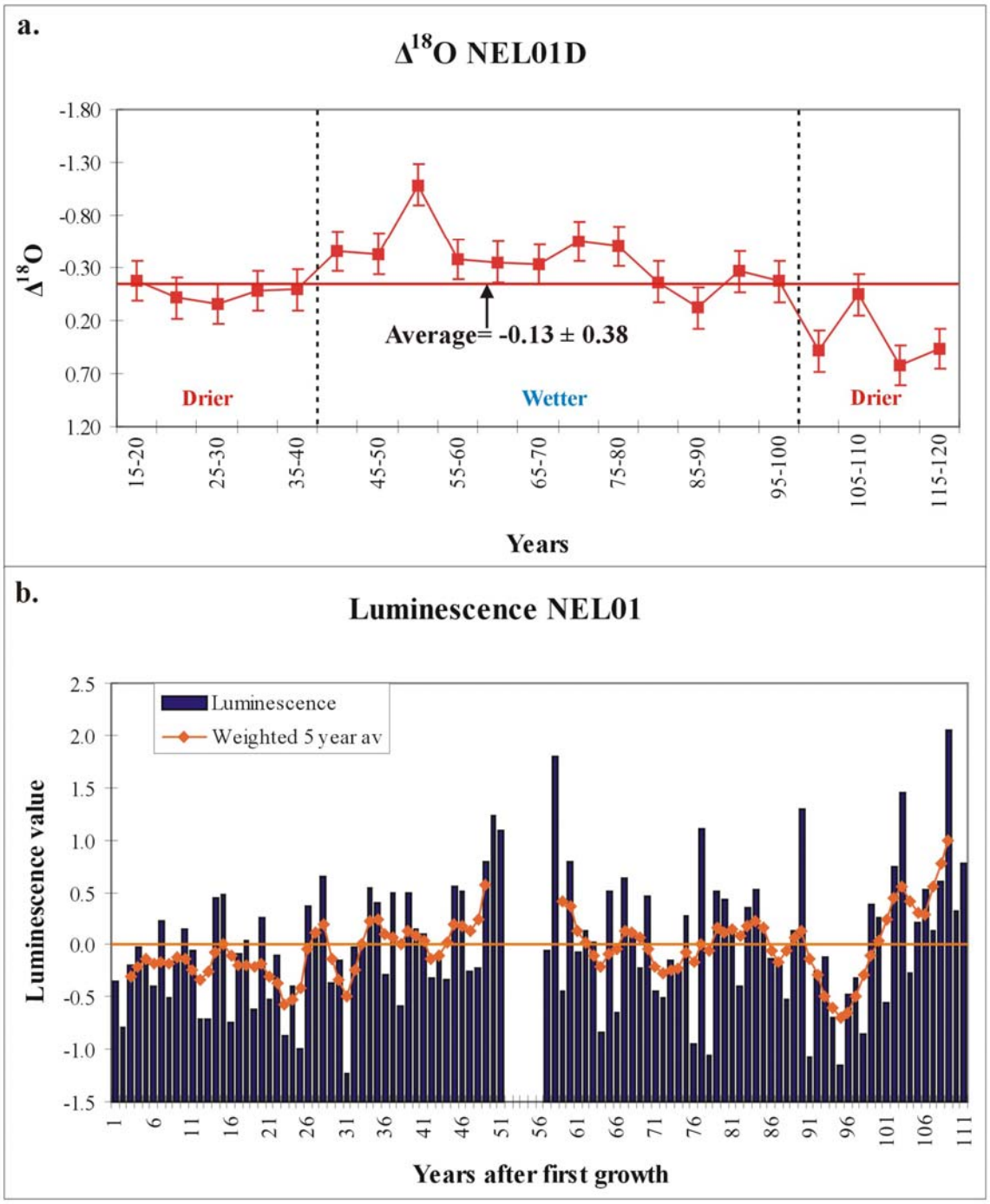

Figure 7.13 a-b. Coral $\Delta^{18}O$ reconstruction for the NEL01D (a) 5 yearly resolution mid-Holocene record and the corresponding luminescence data (b). The NEL01D salinity record displayed similar wetter and drier trends to the 1810-1985 modern record; however, these trends were not observed in the coral luminescence record (b). Therefore, coral luminescence may also be influenced by other parameters. A recent study has shown that coral luminescence is related to increased coral pore space which may occur during stressful environmental conditions (Barnes and Taylor, 2001; 2005).

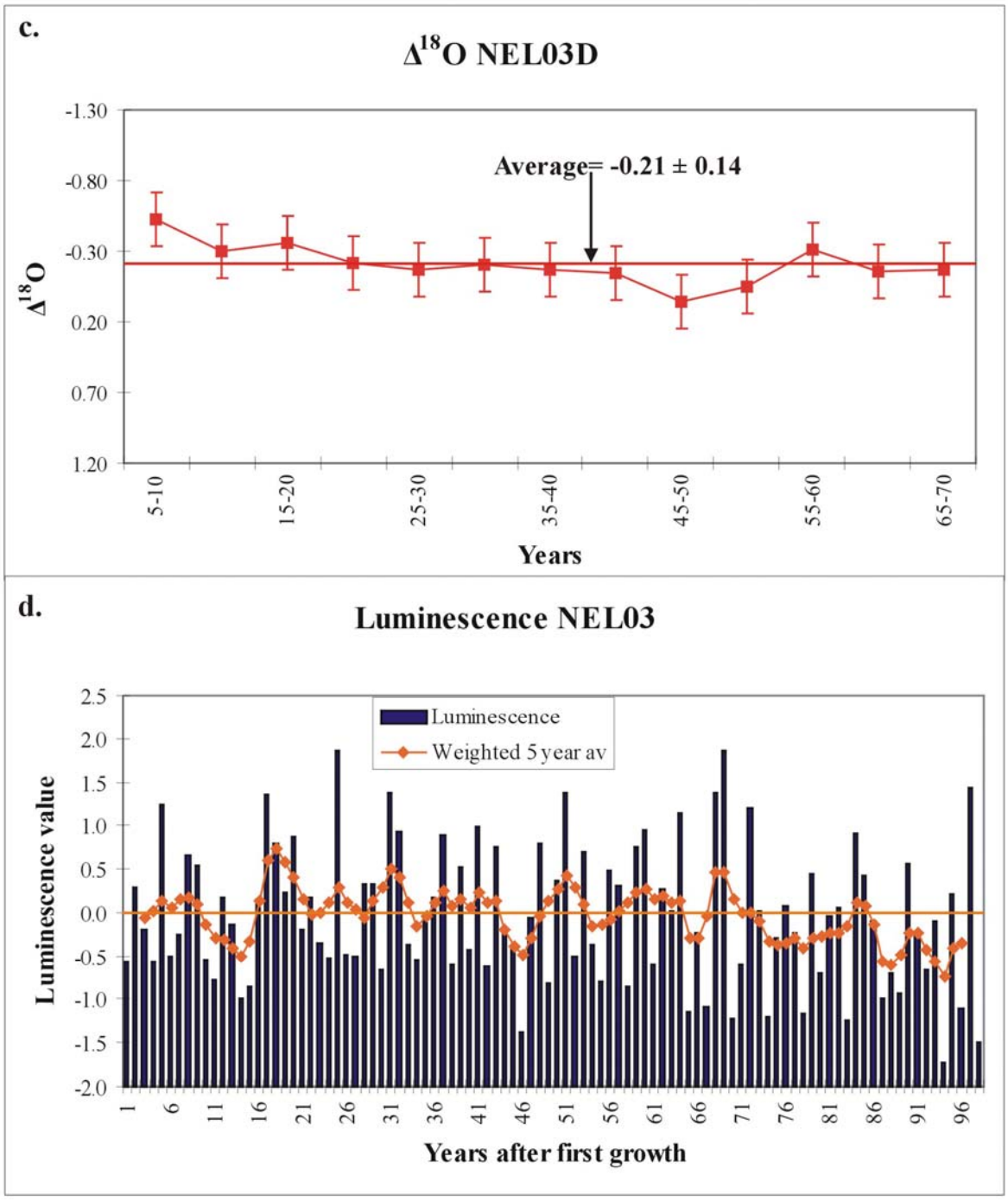

Figure 7.13 c-d. Coral $\Delta^{18}O$ reconstruction for the NEL03D (c) 5 yearly resolution mid-Holocene record and the corresponding luminescence data (d). In comparison to the NEL01D dataset, the NEL03D record displayed a relatively flat trend with no apparent shifts from wetter to drier conditions. The luminescence data displayed variable trends and does not appear to be related to the $\Delta^{18}O$ record.

7.3.4. Summary

The two-monthly resolution $\Delta^{18}O$ records suggest that the mid-Holocene corals may have experienced lower salinity during flood events compared to the modern record. The Burdekin River channel discharged closer to Magnetic Island during the mid-Holocene which may explain this finding. Alternatively, Gustav Creek may also have influenced the fossil corals, but it is difficult to draw firm conclusions from this limited record. The 5 yearly coral $\Delta^{18}O$ records suggested that seawater salinity during the mid-Holocene varied on a similar magnitude to today, and that the long-term average was indistinguishable from the modern coral record. This result contradicts Gagan et al.'s (1998) $\Delta^{18}O$ record from Orpheus Island that suggested there was a 0.5‰ enrichment in salinity during the mid-Holocene. Additional analyses of mid-Holocene corals are required to substantiate these findings.

7.4. Chapter summary

- The coral Sr/Ca, Mg/Ca, U/Ca ratios and the O isotopes produce modern SST estimates comparable to previous studies, despite potential sampling, analytical and calibration errors. The Sr/Ca ratio was the most reliable coral SST proxy and was the only geochemical coral SST proxy significantly correlated with instrumental SST records from the central GBR. However, it should not be used exclusively to reconstruct SST. The long-term SST averages for the geochemical proxies and the calcification dataset agreed with the instrumental SST dataset since 1871.
- The SST proxies suggest that SST in the four mid-Holocene coral records were indistinguishable from the 1812-1986 modern coral record. This finding contradicts previous mid-Holocene coral SST studies from the GBR.
- The coral $\Delta^{18}O$ records suggest that seawater salinities were highly variable and reflect drier and wetter periods. The long-term $\Delta^{18}O$ average for the mid-Holocene coral was similar to the modern coral record; however, the mid-Holocene records may have experienced lower salinities during flood events. This finding contradicts

the mid-Holocene coral $\Delta^{18}O$ dataset of Gagan et al. (1998) who argued for a positive enrichment of $\Delta^{18}O$ values (higher salinity) during this period.

- The coral $\Delta^{18}O$ was not significantly correlated with the coral luminescence record, the rainfall records or the Burdekin River discharge. This finding suggests that the coral $\Delta^{18}O$ record and the luminescence records may have responded to different environmental parameters. The 5 yearly resolution coral $\Delta^{18}O$ record shows subtle, long-term (50-70 year) trends in seawater salinity that coincide with the Pacific Decadal Oscillation. In contrast, the coral luminescence dataset reveals large, short-term variability in salinity from rainfall and river discharge events. Both records display some similar long-term trends.
- The coral luminescence data, rainfall records from the Burdekin River catchment, the Burdekin River discharge and the coral luminescence master set of Hendy et al. (2003) were all significantly correlated with each other. This result suggests that the Magnetic Island coral has recorded regional rainfall and river discharge signals.

Chapter 8

Coral geochemistry discussion: environmental proxies

8.1. Chapter overview

Geochemical proxies of environmental change were measured in modern and mid-Holocene corals from Magnetic Island. These proxies are discussed in this chapter together with an evaluation of their reliability in reconstructing historical water quality on the Great Barrier Reef. This chapter is composed of the following sections:

1) Section 8.2 examines the potential of coral Th concentrations and other trace elements as proxies for sedimentation and to investigate the cause of death of the fossil mid-Holocene corals.
2) Section 8.3 explores the threat of sedimentation to the modern Magnetic Island coral reef from the sedimentation proxies identified in section 8.2.
3) Section 8.4 reviews the coral Ba/Ca ratios as a proxy for sediment export to the GBR lagoon. Ba/Ca ratios in the 1812-1986 Magnetic Island coral record were compared to the studies of McCulloch et al. (2003) and Hendy (2003). The ratio was measured at different sampling resolutions to identify the major influences on the incorporation of Ba into the coral skeleton.
4) Section 8.5 presents Mn concentrations in the 1812-1986 coral record and compares this dataset with records of past land-use changes in the Burdekin River catchment.
5) Section 8.6 examines the potential of the rare earth element and yttrium (REY) group to reconstruct terrestrial runoff to the GBR lagoon. In addition, the REY group and the associated La and Ce anomalies are investigated as coral proxies of water quality.

8.2. Sedimentation: Th concentrations and other elemental proxies

8.2.1. Overview

The sediment cores and radiocarbon data suggest that the cause of mortality for the massive, long-lived fossil mid-Holocene *Porites* coral heads was the burial of the corals by biogenic and terrigenous sediments from a prograding reef flat (see Chapter 5). Further geochemical evidence is required to validate independently this hypothesis. In this study, sedimentation is defined as terrigenous fine-grained sediments settling out of suspension onto corals. Corals have the capacity to tolerate relatively low sediment accumulation rates; however, if the degree of sediment settling continues unabated, corals may eventually succumb to a suffocating blanket of sediment (reviewed in Fabricius, 2005). The development of a coral proxy for sedimentation would be invaluable to assess the current risk of sedimentation to the inshore reefs of the GBR. This section will examine the geochemistry of the final growth layers of the fossil mid-Holocene coral heads and the distinctive growth hiatus observed in the NEL01D coral slice (see Fig 4.6) to investigate the cause of death of these corals.

8.2.2. The geochemistry of the final growth layers from the mid-Holocene corals

The final 2 years of growth in each of the fossil mid-Holocene coral heads had higher Th concentrations than the 1812-1986 coral record (average= 1.30 ppb), particularly the NEL06A slice which was sampled into the remnants of the coral tissue layer (99.37 ppb; Fig 6.40). These "dead" coral tissue layers are significantly more porous than the typical coral skeleton and the numerous pore spaces could trap sediment. Thorium concentrations in seawater and stream water are extremely low (6×10^{-8} and $<1 \times 10^{-4}$ ppm respectively; Taylor and McLennan, 1985) compared to the concentrations of Th in sediments, which are elevated by many orders of magnitude (11.13 ppm Kamber et al., 2005- MUQ; average 16.27 ppm- this study). The corals of this study have baseline Th concentrations of approximately 1 ppb which was considerably lower that that reported for carbonate rocks (1.7 ppm; Turekian and Wedepohl, 1961). Since it is unlikely that Th is substituted into the

coral aragonitic lattice due to its different ionic structure (size and charge), the only conceivable explanation for elevated coral Th concentrations is sediment trapped within the coral skeleton. Any fine-grained particles in the coral skeleton might be partially dissolved (leaching Th) in nitric acid during the sample preparation for ICP-MS analysis. Indeed, the coral samples which had elevated Th concentrations also contained sediment residue in the bottom of the polystyrene centrifuge tubes after the nitric acid digestion.

Yttrium, Pr, Sm and Ho concentrations were also highly elevated in the final years of growth for the mid-Holocene corals (Fig 6.30-6.33 b-c). Interestingly, these concentrations steadily increased over a longer period (~ 10 years) in contrast to Th which, typically, was only elevated in the final 2 years of growth. This indicates that Th records fine-grained sediment trapped within the coral skeleton while the enhanced coral REY concentrations may reflect an increasing terrestrial influence which is not necessarily related to sedimentation. Unlike Th, the REY group is thought to substitute into the coral lattice (Sholkovitz and Shen, 1995; Wyndham et al., 2004; Luo and Byrne, 2004) and, therefore, may record deteriorating water quality conditions, such as turbidity, long before sediment settles out onto the corals. This interpretation was supported by the variable REY concentrations in the long NEL01D record (Figs 6.30b; 6.31b; 6.32b; 6.33b) compared to the relatively consistent baseline Th concentrations (Fig 6.40b). One exception in this record was the highly elevated Th concentration in the "62-64" sample (Fig 6.40b). This sample was partially taken from the growth hiatus present in the coral which contained sediments trapped within the coral skeleton (Fig 4.6).

Additional investigations revealed that this sample also contained elevated concentrations of Be, Sc, Ti, Ga, Zr, Rb, W and Nb (Fig 8.1). These elements were also indicative of a sediment signature as they all have relatively low seawater concentrations compared to sediments. It is conceivable that sediments may have been incorporated within outer growth layers of the coral head after burial, but it is unlikely that the sediments trapped in the growth hiatus (centred mainly towards the middle of the coral head) would have been included post burial. A thorough geochemical investigation of this growth hiatus was conducted to further the understanding of the demise of the mid-Holocene corals.

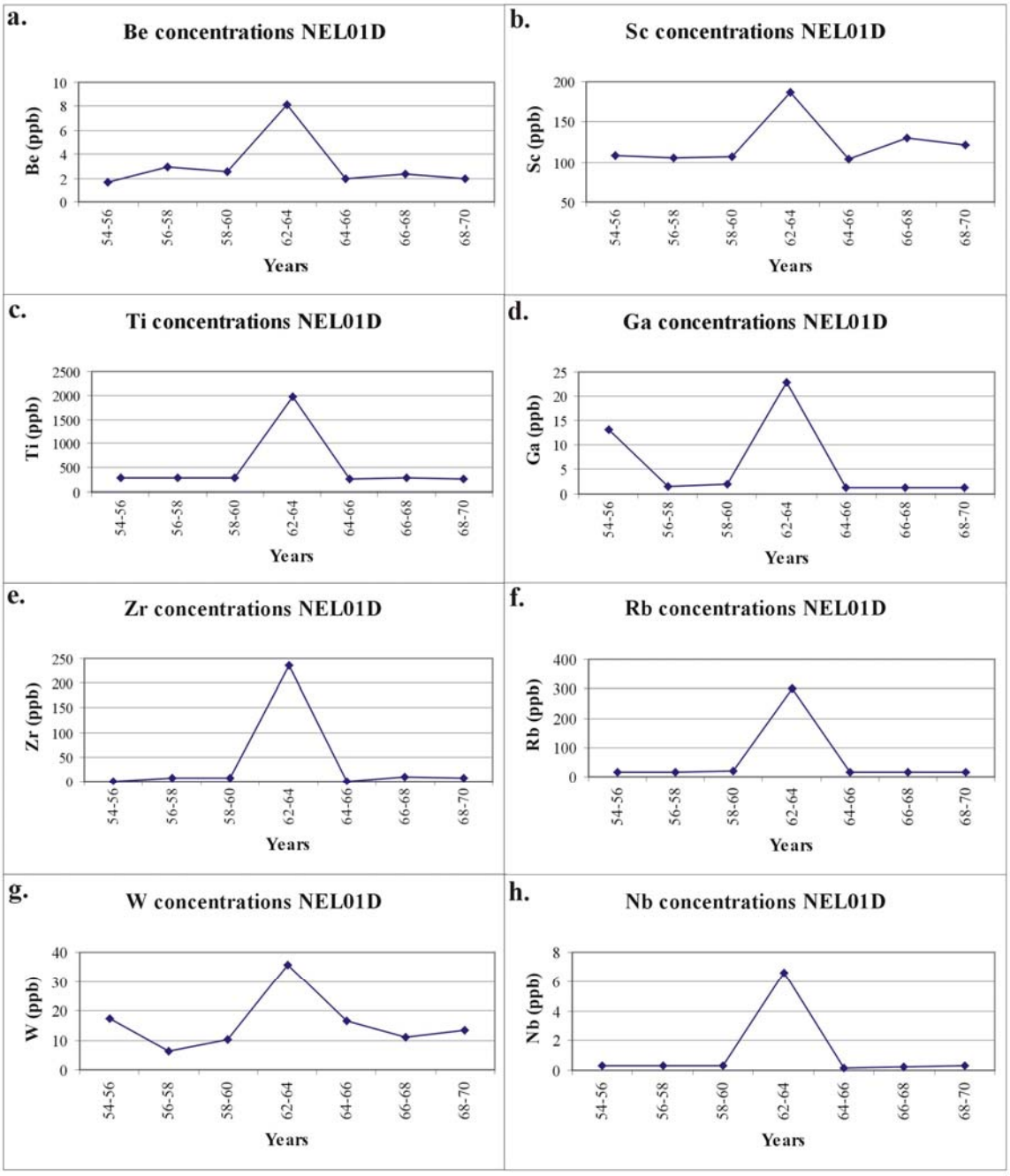

Figure 8.1 a-h. A high performance ICP-MS technique was employed on 7 samples from the 2 yearly resolution NEL01D mid-Holocene coral record which incorporated the "62-64" sample. This sample was enriched in elements which are relatively low in seawater compared to sediment. Therefore, sediment has been incorporated in the 62-64 sample.

8.2.3. The NEL01D growth hiatus

Seven samples that corresponded to a 2 year period were taken near the distinct growth hiatus observed in the NEL01D coral core, which included one sample into the former tissue layer which represented the hiatus. This coral Th record began at slightly elevated (3.76 ppb) concentrations and ramped up to the excessive value in the sample from the growth hiatus (676.97 ppb; Fig 8.2a). The observation of sediment residue in the majority of these samples after the nitric acid digestion confirms that the Th concentrations provide a record of fine-grained sediment trapped within the coral skeleton. Therefore, elevated Th concentrations appear to be a reliable coral proxy to determine detrital sediments that have been incorporated into the coral and could possibly be used to indicate periods of stress and subtle growth hiatuses caused by sedimentation.

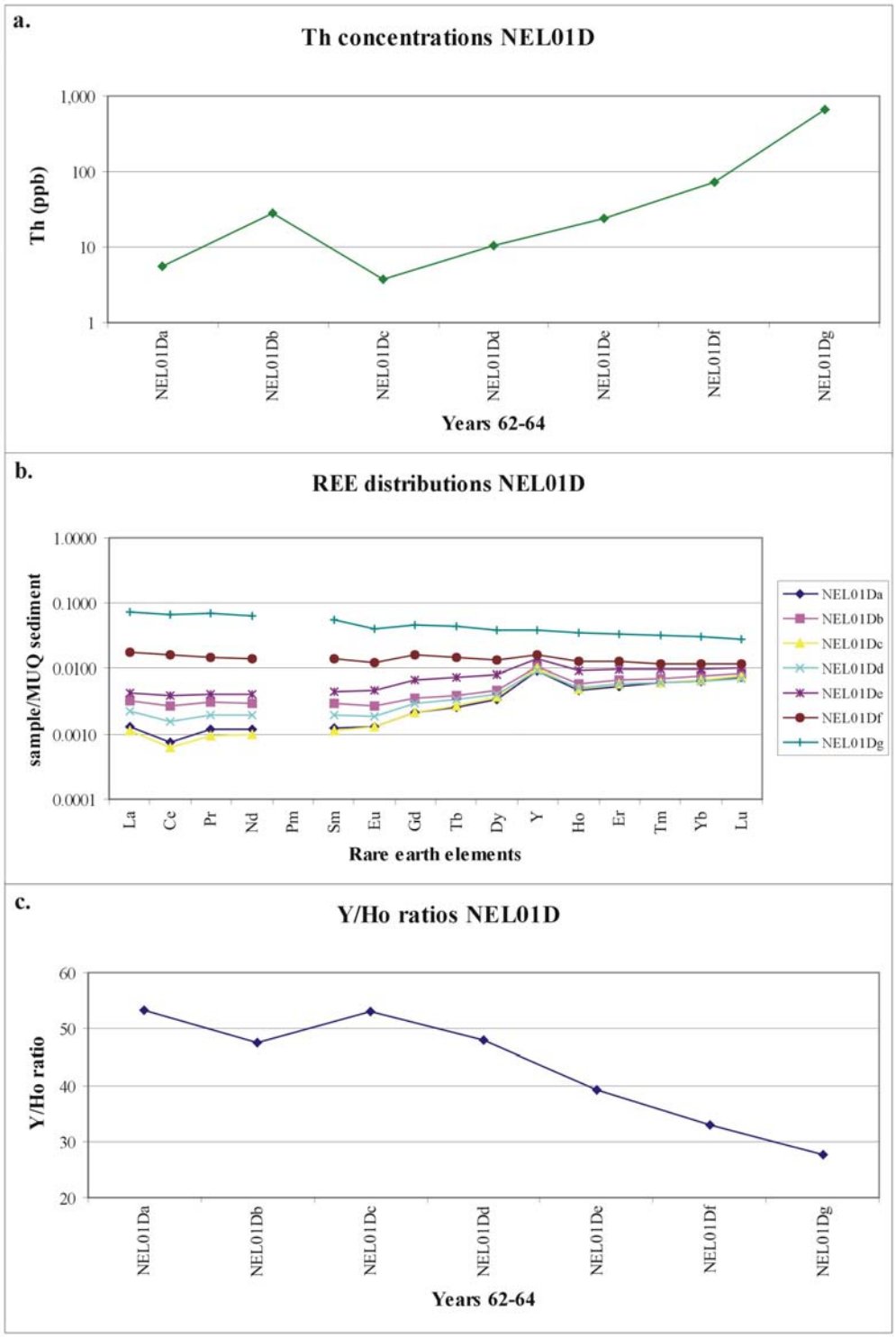

Figure 8.2 a-c. An investigation of the growth hiatus in the mid-Holocene NEL01D coral suggests that the coral was suffocated by sediments. The Th concentrations (a; note log scale) ramped up to excessive levels in the last four samples to values in excess of 10 ppb, an order of magnitude above the "baseline" concentrations in the modern corals. The "flattening" pattern of the REY distributions (b) was also indicative of an increased sediment influence. The coral Y/Ho ratios (c) progressively fall from a typical seawater ratio to common sediment values.

8.2.4. Rare earth element and Y (REY) distribution to examine the provenance of the sediments incorporated into the mid-Holocene corals

The normalised (MUQ sediment; Kamber et al., 2005) coral REY distributions displayed increasing concentrations towards the growth hiatus and contained a progressively "flatter" pattern (Fig 8.2b). A flat REY distribution is characteristic of a sediment or freshwater influence (e.g. Fig 2.11; Wyndham et al., 2004). The increase in Th and REY concentrations indicates that water quality conditions (that relate to turbidity and sedimentation) gradually declined over this 2 year period until the corals succumbed to sedimentation. This finding also suggests that the elevated Th and REY concentrations in the final growth of the mid-Holocene corals are probably not an artefact of post burial sediment accumulation, but rather reflect a genuine water quality signature.

The REY group may provide a tool to assess the source of the sediments incorporated in the mid-Holocene corals. Possible sediment sources include the Burdekin and Ross Rivers, Gustav Creek, and sediments in Nelly Bay. Fortunately, these sediments all contain a distinctive REY fingerprint which can, in theory, be mixed with a coral (or seawater) REY "end member" to match the sediment-affected patterns in the mid-Holocene corals.

The sediments incorporated within the NEL01D "62-64" mid-Holocene coral sample were probably derived from Nelly Bay. The 1850-1852 REY distribution was applied as the "coral end member" for the REY mixing plots as it represented the "most pristine" REY seawater signature. A mixture of 0.50% NEL13A sediment to the 1850-1852 coral end member produced a similar REY pattern to the "62-64" NEL01D sample. Therefore, the NEL13A sediment was the most probable source of sediment incorporated in the mid-Holocene corals (Fig 8.3a). However, a mixture of 0.40% Gustav Creek and 0.60% Nelly Bay sediments produced a similar REY pattern and could also explain the sediment trapped within this sample. The REY signatures preserved in the NEL01D growth hiatus also confirm that local sediments from Nelly Bay were the probable source. A 50-50% combination of the "NEL01De" and "NEL01Df" samples produced a similar pattern to the "62-64" sample (Fig 8.3b). The NEL01Da and g samples were more difficult to model (Fig

8.3b); however, the presence of a relatively large negative Eu anomaly in these coral samples was similar to the sediments from Gustav Creek and Nelly Bay (Fig 5.12a).

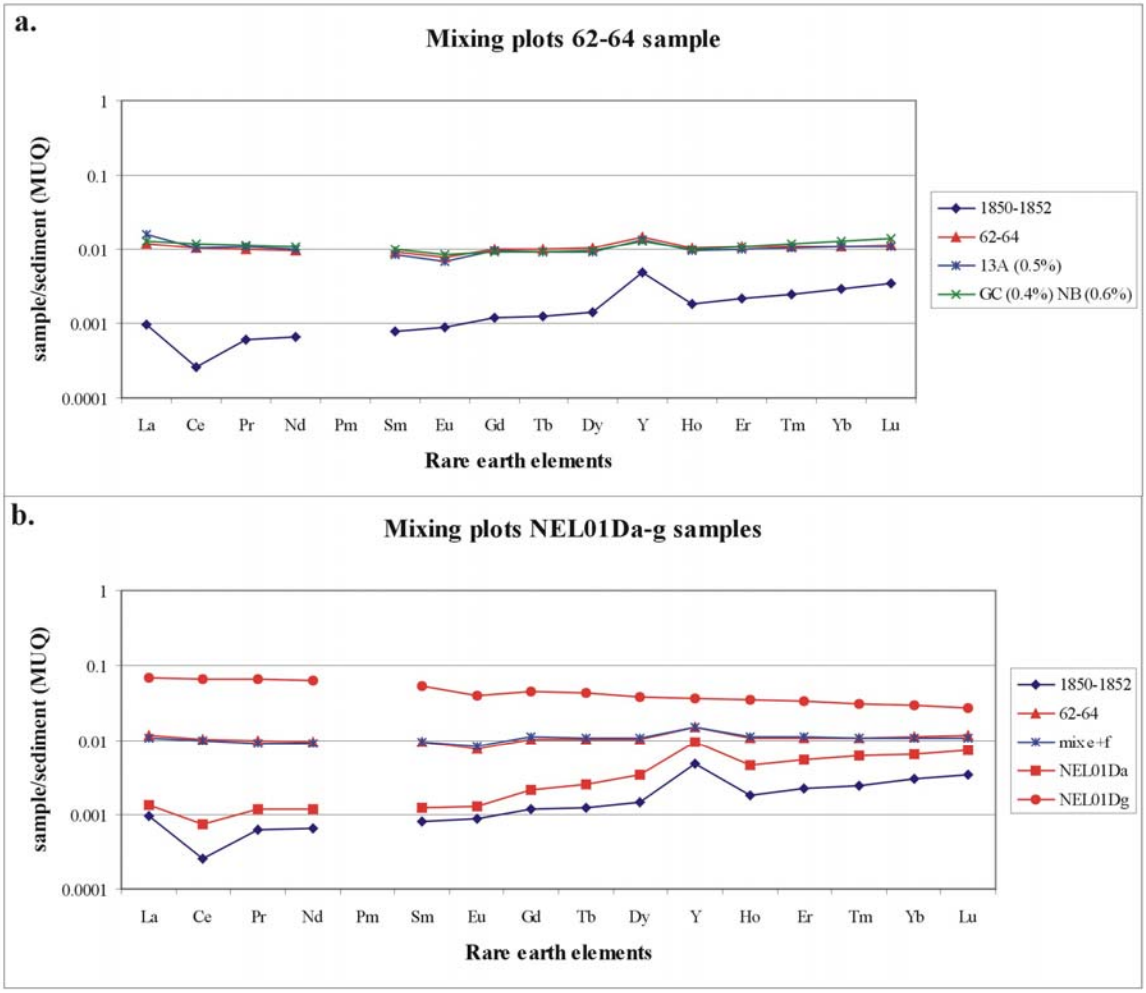

Figure 8.3 a-b. Mixing plots were constructed to investigate the source of the sediment incorporated into the mid-Holocene corals. The mixture of 0.50% of NEL13A sediment to a pristine coral REY distribution (1850-1852 sample) produced a similar REY pattern to the "62-64" sample (a). This result suggests that the NEL13A sediment has been trapped in the coral lattice and may have contributed to the demise of the mid-Holocene corals. The high-resolution mid-Holocene REY distributions were more difficult to model; however, a mixture of the "NEL01De" and "NEL01Df" samples produced a similar pattern to the "62-64" sample. In addition, the negative Eu anomaly also matched the sediments from Nelly Bay (Fig 5.12).

8.2.5. The Y/Ho ratio

The gradual demise of the fossil corals was evident in the Y/Ho ratios. The Y/Ho ratios declined towards the final growth in all the mid-Holocene coral records and thus provide

evidence of a gradual deterioration of living conditions before their death (Fig 8.2c; 8.4). The Y/Ho ratio of "healthy" corals and other marine carbonates record genuine seawater ratios (Bau, 1996) between 44 and 74 (Webb and Kamber, 2000; this study). Possible influences on the coral Y/Ho ratio include salinity, sedimentation and turbidity as the Y/Ho ratio of freshwater and sediments is considerably lower (~20-30) than seawater (Taylor and McLennan, 1985; Kamber et al., 2005; Lawrence et al., submitted). Interestingly, the coral Y/Ho ratio did not appear to be influenced by changes in salinity as the ratio was unaffected in coral luminescent lines or "flood bands" (Fig 8.5b; 8.6d). Therefore, any deviation in the coral Y/Ho ratio is thought to derive from a sediment/colloidal influence.

Evidence that the coral Y/Ho ratio responds to sedimentation was highlighted by the growth hiatus of the NEL01D mid-Holocene coral. The Y/Ho ratio steadily declined in these samples, while coral Th concentrations increased (Figs 8.1a; 8.1c). The coral Th concentration is a proxy of sedimentation (see section 8.2.2) and the coral Y/Ho ratio was also influenced by sediment trapped within the coral skeleton; the ratio from the former tissue layer is consistent with sediment values (27.67; Fig 8.1c).

However, there is also evidence that the coral Y/Ho was influenced by parameters other than sedimentation and may be a proxy of turbidity. The Y/Ho declined significantly over the last 10 years of growth in all the mid-Holocene records (Fig 8.4); however, sedimentation in these coral records was not apparent until the final 4-6 years of growth from the coral Th concentration (Fig 6.36b-c). In addition, the Y/Ho ratios in the 2 yearly NEL01D coral record displayed marked fluctuations throughout the 130-year record which also did not coincide with the Th sedimentation proxy (Fig 8.4a). It is hypothesised that the other major control on the Y/Ho ratio may be related to increased turbidity levels (see Appendix 12).

Interestingly, the Y/Ho ratio fluctuated in the NEL01D coral on cycles of about 10-15 years (Fig 8.4a). These cycles might be related to sea-level fluctuations. A stabilisation of sea level may result in the corals growing towards, and reaching, the mean low water spring zone which is characteristic of a highly turbid environment. This stable sea level may have

been followed by a minor sea-level transgression where the conditions improved and the coral continued to grow. If this hypothesis is correct, then the mid-Holocene sea levels were considerably more complex than previously thought. However, the limitations of C-14 dating and the variability of the sea-level indicators over this period can not substantiate this hypothesis of decadal sea-level fluctuations during the mid-Holocene.

The geochemical signature of the growth hiatus in the NEL01D coral provided further evidence for environmental conditions during the mid-Holocene. The coral geochemistry suggests that the colony initially succumbed to sedimentation, but managed to regenerate and survive for a further 60-70 years. This finding highlights the coral's capacity to recover from the effects of sedimentation, provided that conditions were suitable for regeneration.

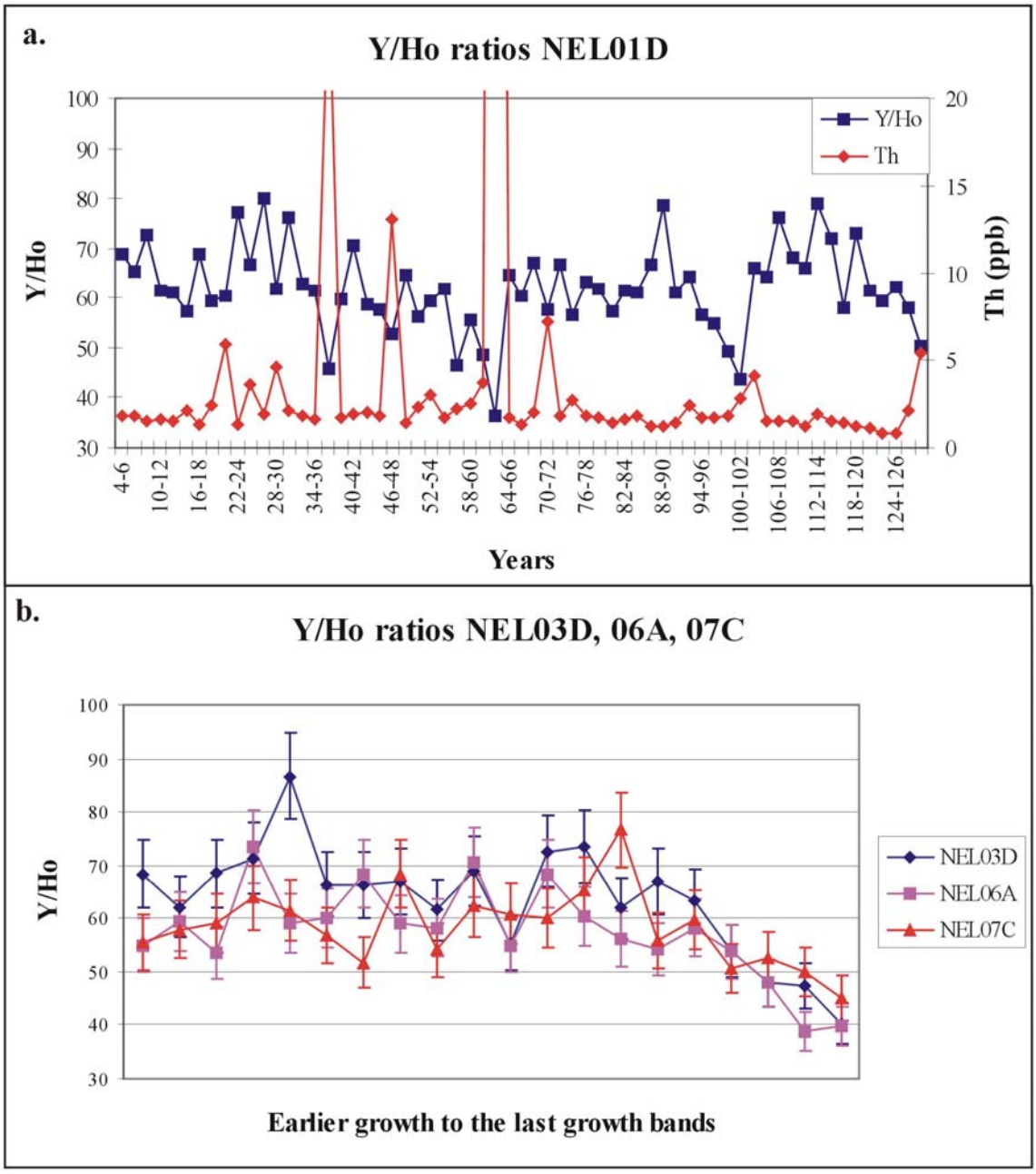

Figure 8.4 a-b. The declining Y/Ho ratios measured towards the final growth records of the mid-Holocene coral suggest that water quality conditions deteriorated in the last decade of their lives. Th concentrations indicate that sediment was only trapped in the last 2-4 years of growth, and therefore the Y/Ho ratio must be influenced by other processes. The declining Y/Ho ratios may indicate highly turbid conditions which is characteristic of a high energy environment. This highly turbid environment, in turn, was probably within or near the zone of the lowest astronomical spring tide. The four notable Y/Ho excursions in the NEL01D record (a) may reflect a complex step-like sea-level transgression during the mid-Holocene.

8.2.6. Summary

The final 2-4 years of growth of the mid-Holocene corals all contained elevated Th concentrations (>2 ppb) which were indicative of sediment trapped within the coral skeleton. Thorium and other trace elements including Be, Sc, Ti, Ga, Zr, Rb, W and Nb were also elevated significantly in the growth hiatus of the NEL01 mid-Holocene coral. REY coral-sediment mixing plots suggest that the sediments in the mid-Holocene corals were sourced from the local Nelly Bay area. The coral Y/Ho ratio declined significantly in the NEL01 growth hiatus as well as in the final growth years of the mid-Holocene corals. This ratio falls well before the rise in the coral Th concentration and may indicate that the coral Y/Ho ratio recorded the declining water quality conditions (such as elevated turbidity) before the mid-Holocene corals were overcome by sedimentation.

8.3. Using coral Th and REY concentrations to assess the threat of sedimentation to the modern inshore reefs of the GBR

8.3.1 Overview

Increased sedimentation is considered a major threat to inshore coral reefs of the GBR (Wolanski and Spagnol, 2000; Duke and Wolanski, 2001; Fabricius, 2005) and has already caused widespread damage to reefs around the world (reviewed in Fabricius, 2005). The significant increase in sediment export from the coastal river catchments draining into the GBR lagoon since European settlement may have resulted in increased turbidity levels and an enhanced threat of sedimentation along the inshore reefs (e.g. McCulloch, 2003; Fabricius, 2005). However, Hopley (1994) believes that any increase in turbidity and sedimentation at inshore reefs may be related to the natural process of coastal progradation over the last 3,000 years. Nonetheless, the significant increase in sediment export to the inner GBR may have accelerated coastal progradation rates and, in turn, may have reduced the “natural” life of these inshore coral reefs. This section will apply the coral proxies applied in section 8.2 to investigate the perceived threats of sedimentation to the inshore coral reefs.

8.3.2 The modern threat of sedimentation to inshore coral reefs

The threat of sedimentation to the fringing reefs of Magnetic Island can be evaluated from the coral Th proxy. Thorium concentrations in the 1812-1986 2 yearly resolution modern coral record displayed little variation from the baseline level (~1 ppb) which suggests that this coral was not affected significantly by sedimentation. A Th spike in the 1840-1842 sample (16.33 ppb; Fig 6.40a) is minor when compared to the Th values in excess of 20 ppb in the last 3 samples of the mid-Holocene record (Fig 8.1a). In addition, the 1840-1842 deviation occurred approximately 10 years before European settlement in the region and this value may represent either a "natural" variation or an analytical error. Sedimentation was also negligible in the 1968-1973 and 2000-2003 coral records as the coral Th concentrations displayed little variation from the "baseline" levels (Fig 6.36). Moreover, sedimentation after major floods was negligible in the coral record, with the exception of the 1974 flood (Fig 8.5a; 55.82 ppb). The 1974 flood was the largest in the Burdekin instrumental data record, in terms of the total volume of water discharged in the year, and coincides with the highest coral luminescence value in coral records over the last 400 years (Hendy et al., 2003). Substantial loads of sediments were exported from the creeks and rivers of north Queensland to the inshore coral reefs during this flood event. The Th concentrations in the 1974 coral "flood band" indicated that at least some inshore coral reefs experienced sedimentation during this severe flood. REY mixing plots appear to support the hypothesis that the sediment trapped in the 1974 band was derived from the Burdekin River (or Ross River; Fig 8.5c).

While sedimentation in the 1812-1986 coral record may have been negligible, the coral Th concentration could be insensitive to conditions that precede sedimentation. This finding was evident from the mid-Holocene coral records (e.g. section 8.2). The REY distributions and the Y/Ho ratios were of greater value as they are more sensitive and are capable of detecting changes in water quality conditions over a longer period.

The REY distributions displayed an increasing terrestrial influence after European settlement in the modern coral record (Fig 6.34). This increase was also apparent in the

elevated Y, Pr, Sm and Ho concentrations observed in the 1812-1986 modern coral record (Figs 6.30a-6.33a), although these levels may have stabilised in the more recent records (6.34a-b). In addition, while the REY concentrations have increased markedly since European settlement, the Y/Ho ratio has remained stable throughout the 1812-1986 and 2000-2003 records (Fig 8.6 c-d). Therefore, turbidity levels may have been relatively constant during the 191 year period, and the sedimentation rate on Magnetic Island's fringing coral reefs over this time appears unchanged (Fig 8.6). The coral Y/Ho ratios were not affected by flood events with the exception of the 1974 flood when sediment was trapped within the coral skeleton (Fig 8.6a-b). The acceptable Y/Ho ratio for *Porites* corals from *inshore* coral reefs should be between 60 and 70. Any deviation below these values is due to either sedimentation or elevated turbidity (Fig 8.6a-b; see Appendix 12).

As with the coral Y/Ho ratios, heavy metal concentrations (Ni, Zn, Pb) in the coral skeletons have not significantly increased since European settlement. This finding suggests that industrial contamination to Magnetic Island's coral reefs from mining in the Burdekin River catchment and from the nearby Townsville Port is negligible (see Appendix 15). However, elements that were associated with mining in the Charter Towers district such as Hg were not measured in the coral.

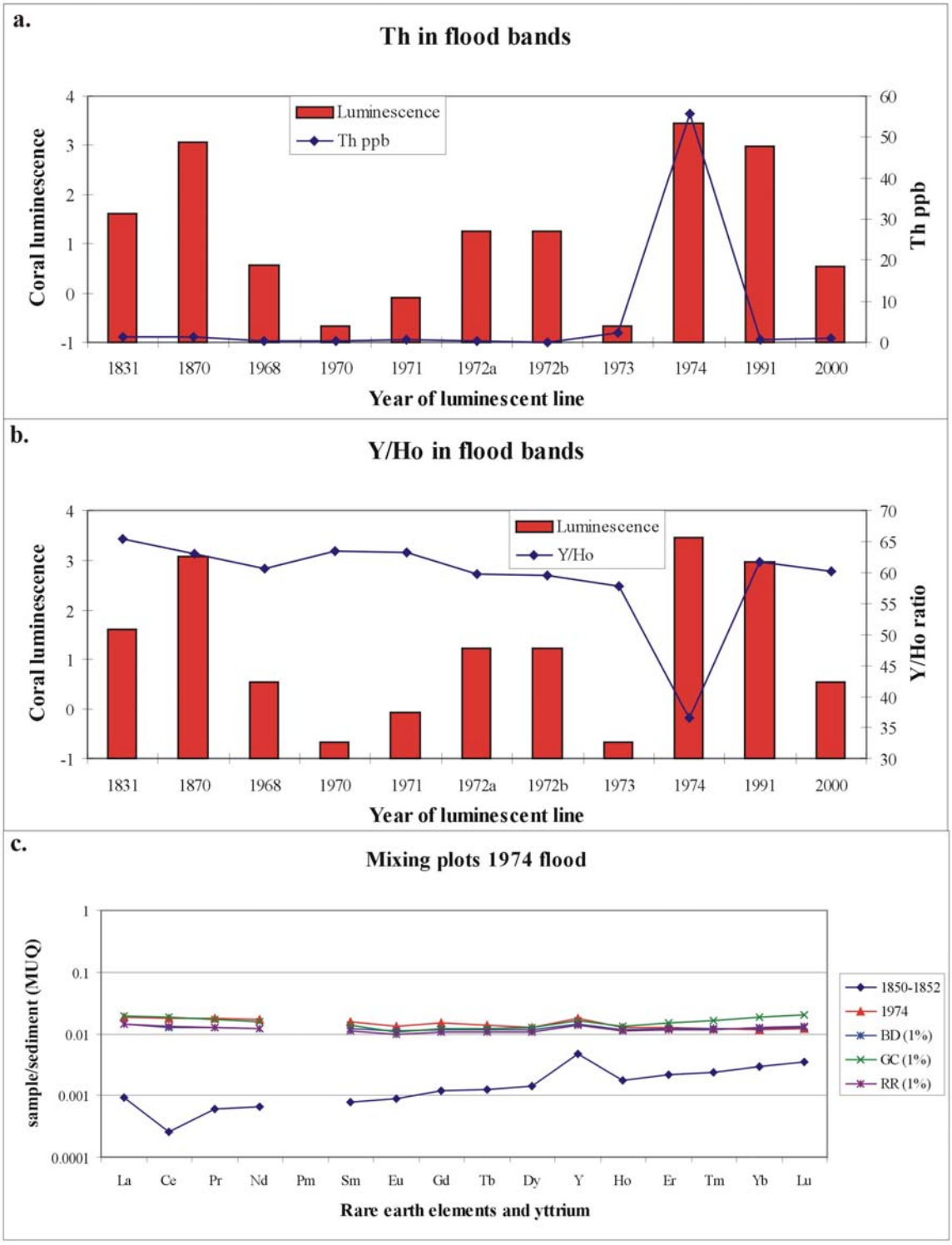

Figure 8.5 a-c. The Th concentrations (a) and the Y/Ho ratios (b) in coral luminescent lines ("flood bands") remained at the background levels and were not influenced by sediments. The exception was the 1974 flood where Th concentrations and the Y/Ho ratios indicated that sediment was trapped in the coral skeleton. The source of the sediment incorporated within the coral was probably derived from the Burdekin River (BD) or Ross River (RR; c). The sediment-coral REY mixing plots indicates that any sediment influence from Gustav Creek (GC) in the 1974 coral luminescent line would have been negligible.

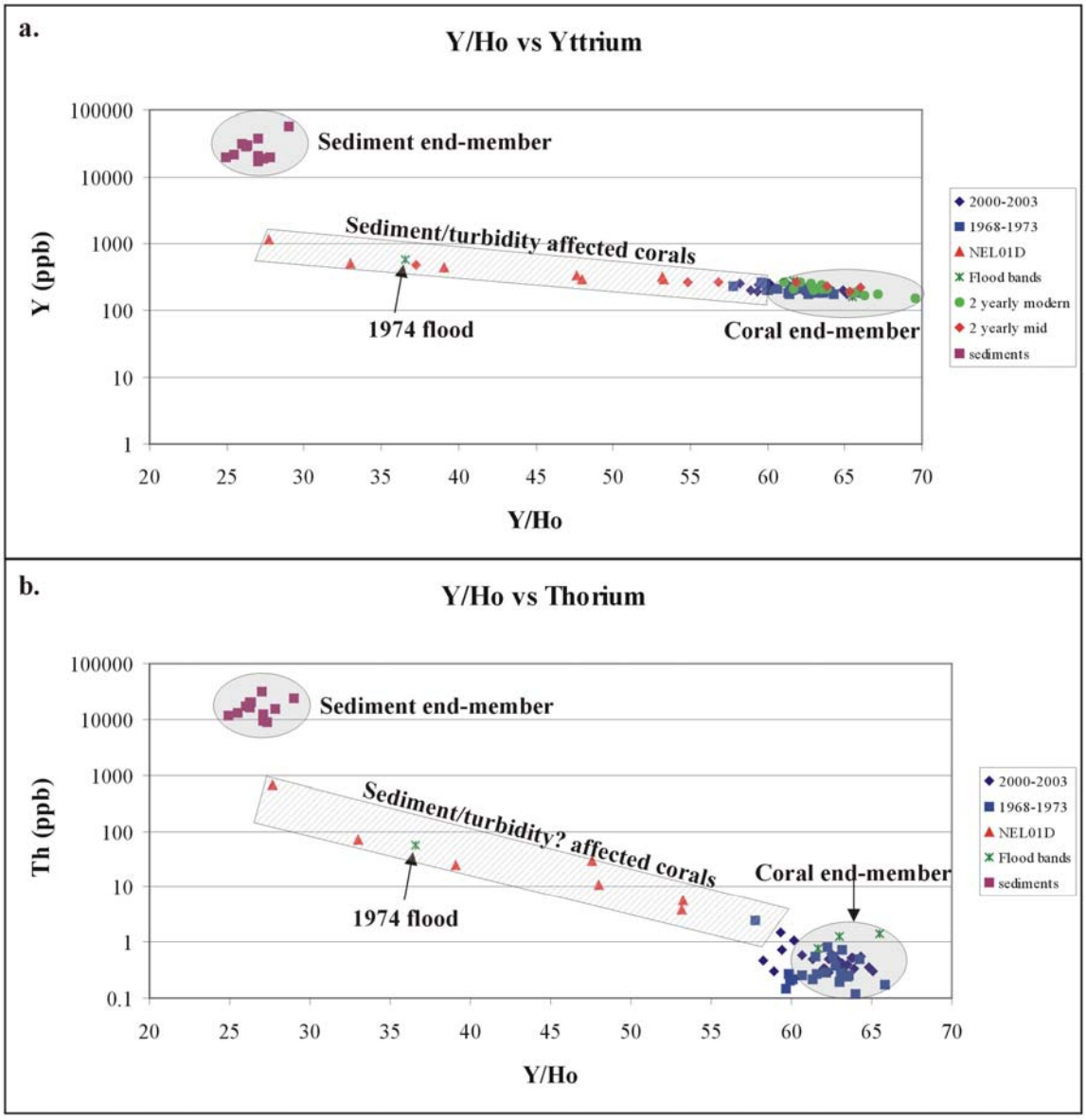

Figure 8.6 a-b. Y/Ho v Y (a) and Y/Ho v Th (b) plots. These data indicate that the Y/Ho ratio for *Porites* corals growing in ambient seawater conditions at inshore reefs is between 60 and 70. Sediments in the local area contain Y/Ho ratios of 25-30 and the plots suggest that sedimentation, with the exception of the 1974 flood event, is not a major problem for the modern fringing coral reefs of Magnetic Island.

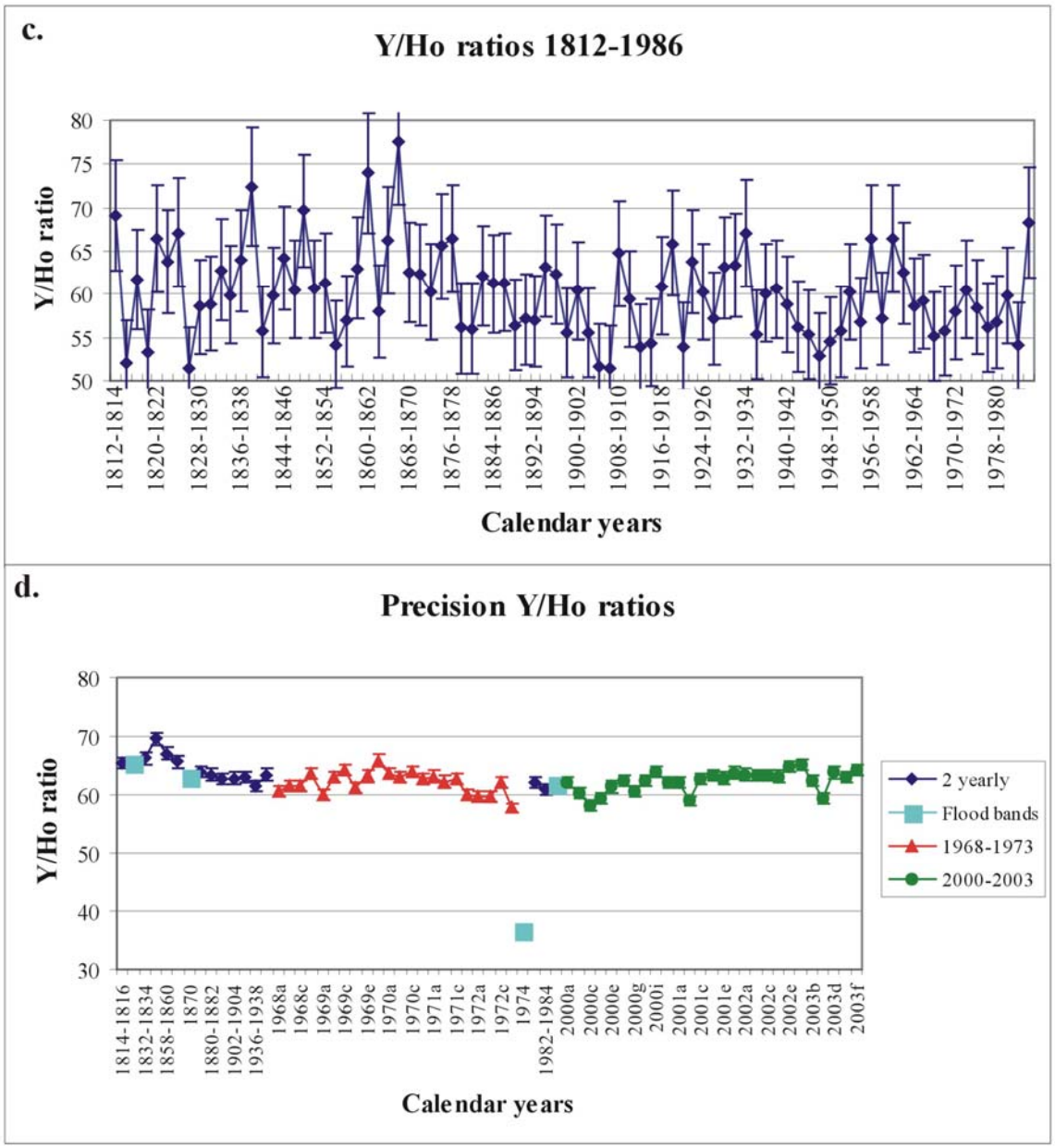

Figure 8.6 c-d. The Y/Ho ratios in the modern coral records were consistent with pre-settlement values and it appears that the corals of Magnetic Island are currently under no particular threat of sedimentation. The Y/Ho ratios in (c), unfortunately, were marred by relatively poor analytical precision and trends were difficult to interpret in this record. However, the incomplete high precision ICP-MS analytical record (d) provided a better insight into the Y/Ho ratio and suggests that water quality conditions, such as turbidity and sedimentation, have not significantly changed since European settlement in the Burdekin River catchment.

8.3.3 Bivariant plots

To investigate further the changes in sedimentation, sediment export from rivers and turbidity on the fringing reefs of Magnetic Island, a series of bivariant plots were constructed from the high precision ICP-MS coral dataset. These plots included Y/Ho v Th, Th v Ba, Y/Ho v Ba and Y/Ho v Mn (Fig 8.7a-e).

Sedimentation can be assessed from the Th v Y/Ho plot (Fig 8.7a). These proxies displayed a significant linear correlation ($r= 0.64$; $p <0.00$; $n= 60$) and can be fitted with a strong power regression ($r^2= 0.85$; Fig 8.7a), although this regression is only defined by one data point. The Y/Ho ratios below 55 were all from the mid-Holocene corals (with the exception of the 1974 flood) and display progressively elevated Th concentrations as this ratio declines. This plot provides further evidence that the mid-Holocene corals died from sedimentation and that sedimentation has been negligible in the modern coral records.

If sediment export to the GBR has increased since European settlement, one would expect that there would be an enhanced threat of sedimentation on inshore coral reefs (e.g. Fabricius, 2005). The coral Ba concentration provides a proxy to assess the amount of fine-grained sediment exported from rivers (e.g. McCulloch et al., 2003; section 8.4), while the coral Th concentration reveals sedimentation on coral reefs (section 8.2). The Ba v Th bivariant plot indicates that, while sediment export (Ba) has increased significantly since European settlement, sedimentation (Th) has been negligible on coral reefs (8.7b-c). In addition, the sediment-affected mid-Holocene corals did not display enhanced Ba concentrations, and so Ba is unlikely to be an indicator of sedimentation (Fig 8.7b-d). Interestingly, the 1831 flood contained higher Th concentrations compared to the majority of floods after European settlement (Fig 8.7c), so it seems that there has been no increased threat of sedimentation to the fringing reefs of Magnetic Island during flood events since the arrival of Europeans. The one exception was the extreme 1974 flood which contained both highly elevated Ba and Th concentrations (discussed in section 8.3.2).

If sediment export to the GBR has increased since European settlement, one would also expect turbidity levels to have increased at inshore coral reefs (e.g. McCulloch, 2003; Fabricius, 2005). The coral Y/Ho ratio may be a reliable proxy of turbidity (see section 8.2.5; Appendix 12), while Ba is a proxy of fine-grained sediment exported to the GBR (e.g. McCulloch et al., 2003; section 8.4). The Ba v Y/Ho bivariant plot (Fig 8.7d) displayed similar trends to the Th v Ba plot; however, there were some important, but subtle, exceptions that demonstrate that the Y/Ho ratio is not just a sedimentation proxy and that turbidity may have increased in flood plumes after European settlement. Although the 1831 and 1870 floods contained relatively higher Th concentrations compared to most floods after the cattle industry expanded in the Burdekin catchment (Fig 8.7c; Fig 3.13), the Y/Ho ratios were higher in both the 1831 and 1870 flood bands compared to most floods occurring after the rise of the cattle industry (Fig 8.7d). This finding suggests that flood plumes may have become slightly more turbid since the arrival of Europeans, which is not unexpected when the increase of fine-grained sediments exported from rivers are considered. However, turbidity is dominantly controlled by the resuspension of fine sediment particles during rough weather, and suspended sediment concentrations in river plumes are considerably lower than the levels in storm-like events (e.g. Larcombe, 2001). In addition, the Th v Ba bivariant plot (Fig 8.7b-c) suggests that no additional sediment has settled around or on the coral reefs of Magnetic Island during flood events. Therefore, it appears that no extra sediment is being deposited in the Magnetic Island area and no additional sediment is available to be resuspended during rough weather conditions.

There was a significant linear correlation between the coral Y/Ho and Mn ($r= 0.71$; $p <0.00$; $n= 60$) which suggests that high coral Mn concentrations may be influenced by sediments trapped within the coral skeleton. This interpretation was supported by the elevated Mn concentrations in the sediment-affected mid-Holocene corals. One exception was the 1870 flood band when the coral Mn concentration was excessively high whereas the coral Y/Ho ratio was at “normal” levels. The increased coral Mn may coincide with land-use in the Burdekin River catchment (see section 8.5).

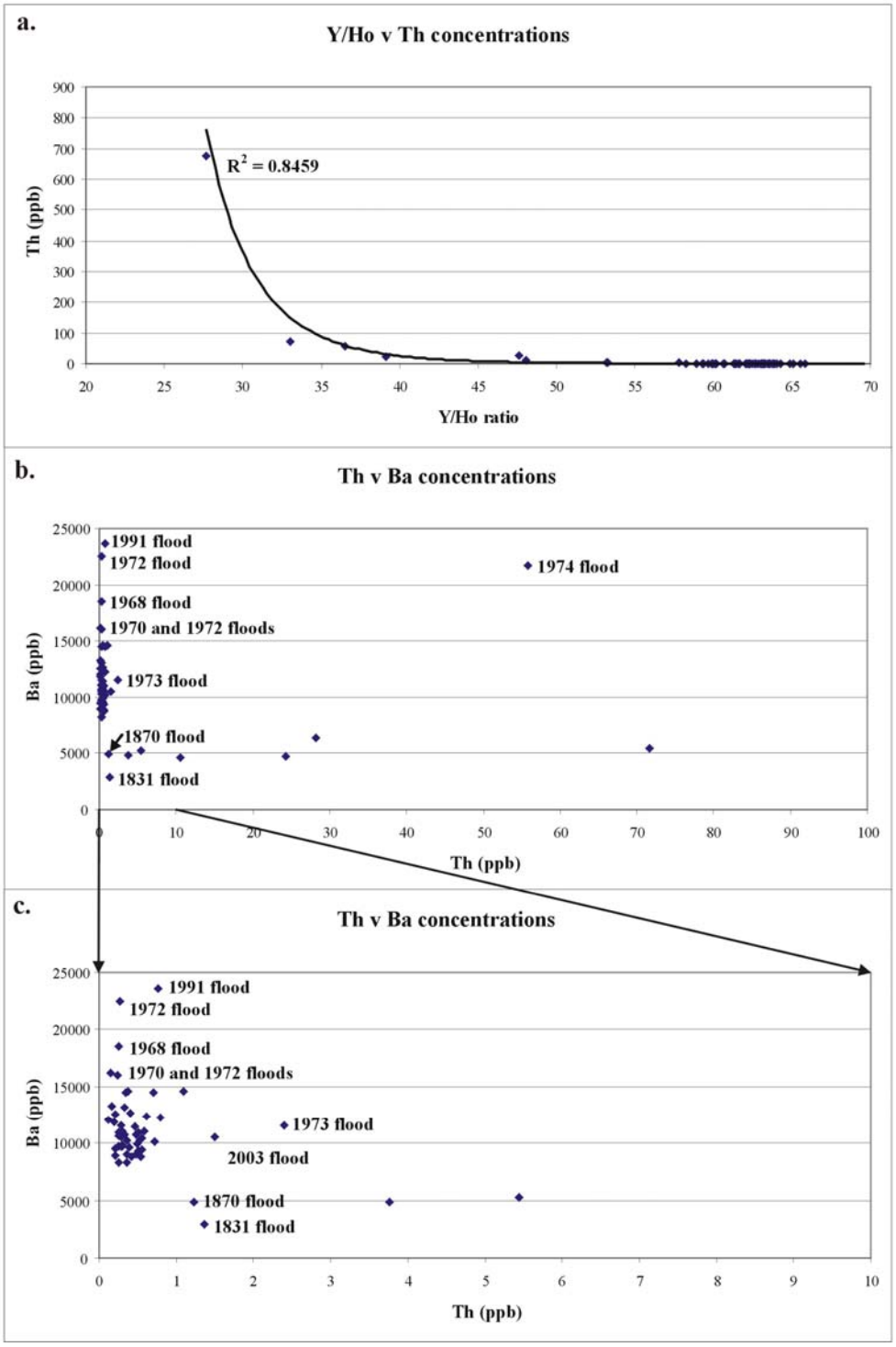

Figure 8.7 a-c. Bivariant plots allow the data to be presented from an alternative perspective which reveals additional trends. The Y/Ho v Th plot (a) demonstrates the positive relationship between the two proxies and highlights their potential as sedimentation indicators. The Th v Ba plots (b-c) reveals that, while the coral Ba concentrations have increased since European settlement, there has been no increased threat of sedimentation (coral Th concentrations) to the fringing reefs of Magnetic Island. The plot also demonstrates that Ba is not responding to sediment trapped within the coral skeleton and therefore is not an indicator of sedimentation.

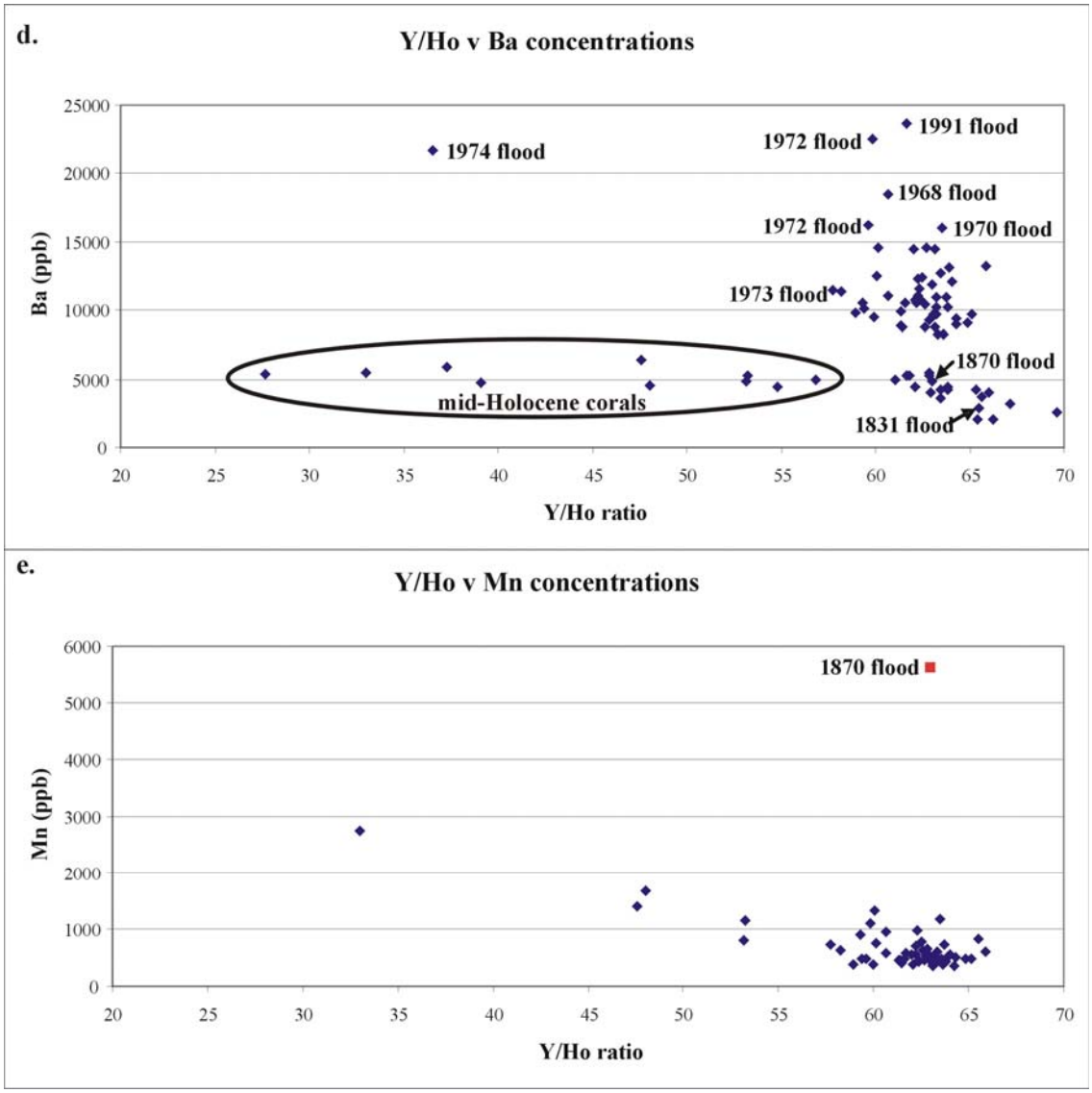

Figure 8.7 d-e (continued). The Y/Ho v Ba bivariant plot (d) also suggests that Ba is not a coral sedimentation proxy. The declining Y/Ho ratios were, however, indicators of sediment trapped within the coral skeleton and possibly a turbidity proxy. Coral Ba concentrations have significantly increased since European settlement, but there has been little change in the Y/Ho ratio. The coral Y/Ho ratio may have declined in flood events following European settlement. The majority of samples in the Y/Ho v Mn plot are clustered with coral Y/Ho ratios between 55 and 65 and Mn concentrations typically lower than 1 ppm. In most cases, high concentrations of Mn coincide with a lower Y/Ho ratio and are indicative of a sediment influence. The exception is the 1870 flood when Mn may have increased because of increased agricultural land-use in the Burdekin River catchment.

8.3.4 Summary and directions for future research

The geochemical coral proxies indicate that the fringing coral reefs surrounding Magnetic Island are not threatened by sedimentation. Preliminary data suggest that while the REY concentrations have increased since the 1850s, the Y/Ho ratio has remained constant. This finding indicates an increased terrestrial influence on the fringing coral reefs around Magnetic Island; however, turbidity levels appear to have remained constant. The coral REY distributions and the Y/Ho ratio seem to provide reliable assessments of sedimentation, changes in terrestrial runoff and turbidity on the GBR. Nevertheless, additional study needs to be done on these coral proxies from other coral colonies to confirm their reliability. Inshore reefs of the Cairns region where increased turbidity/sedimentation have been reported would be an ideal locality to further develop these coral proxies (e.g. Wolanski and Spagnol, 2000).

8.4 An evaluation of the Ba/Ca ratio

8.4.1 Overview

Barium is desorbed from fine-grained terrigenous sediments within the 10‰ mixing zone in river plumes (Coffey et al., 1997) and, subsequently, the coral Ba/Ca ratio has proven a reliable proxy to assess the quantity of fine riverine sediment particles exported to the GBR lagoon (section 2.4.2; McCulloch et al., 2003; Alibert et al., 2003; Sinclair and McCulloch, 2004). The landmark work of McCulloch et al. (2003) was among the first studies to demonstrate that corals can provide proxies of sediment erosion from river catchments. Ba/Ca ratios were measured in a long coral record from Havannah Island, which contained a growth record from 1760-1998. The coral Ba/Ca ratios increased significantly after 1870, and were linked to soil erosion from the growth of the cattle industry in the Burdekin River catchment (McCulloch et al., 2003). The modern coral core taken from Magnetic Island provides an opportunity to replicate the work of McCulloch et al. (2003) and to develop the Ba/Ca proxy. The Ba concentrations of fine-grained sediments from the rivers and creeks which influence Nelly Bay are compared to sediments from the Nelly Bay sediment cores

and Cleveland Bay to investigate how much Ba is released in the 10‰ mixing zone. In addition, the Ba/Ca ratio will be examined in the mid-Holocene corals and from coral luminescent lines in order to gain additional insights into this proxy.

8.4.2 Barium in sediments

Soluble Ba in sediments is completely desorbed in the 10‰ salinity zone (e.g. Coffey et al., 1997; Sinclair and McCulloch, 2004) and therefore the Ba concentration of sediments in the freshwater zone should be higher than sediments from the marine environment. This hypothesis is supported by this study which found that sediments from the seawater zone contain substantially less Ba than riverine sediments. The average Ba concentration of fine-grained sediments (<80 μm) in the freshwater zone (average of the Burdekin Dam, Ross River Dam and Gustav Creek: 494 ± 60 ppm; Fig 8.8) was higher than the MUQ measurements of Queensland alluvial sediments (396 ppm; Kamber et al., 2005), although the result was consistent with the Ba concentration from fine sediment in the Burdekin (475 ppm) and the Belyando (509 ppm) Rivers (Kamber et al., 2005).

In contrast, the terrigenous sediments from the marine environment (Cleveland Bay) which were originally derived from the Burdekin River, Ross River and Gustav Creek (and therefore have the same mineralogical composition) contain significantly lower Ba concentrations (average 199 ± 27 ppm; Fig 8.8) than the riverine sediments. The average Ba concentration from the marine sediments compares favourably with previous work from Cleveland Bay (239 ± 80 ppm; Ward et al., 1995). Previous studies have demonstrated that the mobile Ba component in sediments was readily desorbed within the 10‰ salinity zone (Coffey et al., 1997; Sinclair and McCulloch, 2004 and references therein) and so it is unlikely that additional Ba is released from sediment during resuspension events. The sediments in Cleveland Bay contain approximately 200 ppm of insoluble Ba. They also have appreciable quantities of feldspar (both plagioclase and microcline) which could be the major insoluble host of Ba (Ward et al., 1995; Table 5.3). Therefore, it appears that ~ 300 ppm of Ba is readily desorbed from sediment and colloidal particles within the 10‰ salinity zone and Ba would then be transported in the dissolved phase of the river plume.

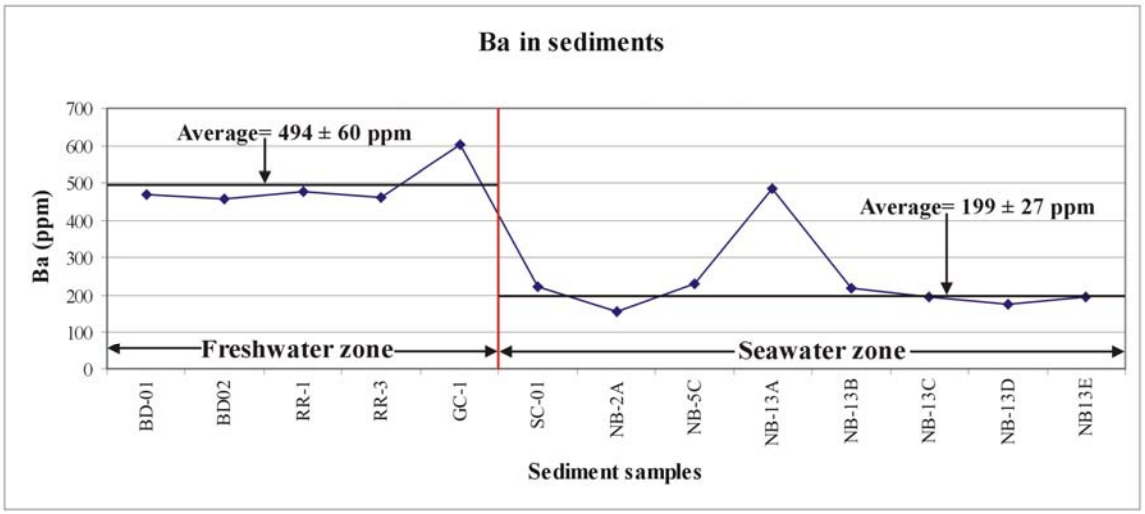

Figure 8.8. Ba concentrations in sediments from the freshwater and seawater zones. BD= Burdekin Dam; RR= Ross River Dam; GC= Gustav Creek (Nelly Bay); SC= Shipping Channel; NB= Nelly Bay. The sediments from the seawater zones have substantially less Ba than the riverine sediments which supports the model that Ba is desorbed within the 10‰ salinity zone. Note that the NB-13A sample has been excluded from the average calculation as this sample was thought to have been mixed with alluvial Pleistocene sediments (see section 5.5.9).

8.4.3 The modern coral Ba/Ca records

The Ba/Ca ratios from the 2 yearly resolution Magnetic Island coral record were correlated significantly with the Havannah Island record (McCulloch et al., 2003; r= 0.47; p <0.00; n= 87; Table 8.1). The 2 yearly averaged Havannah Island Ba/Ca record displayed a smoother curve than the Magnetic Island record, as 1 data point represented the mean of approximately 100 Ba/Ca measurements in the McCulloch et al. (2003) dataset (Fig 8.9a). The magnitude of the Ba increase was much greater in the Magnetic Island coral record where the Ba/Ca ratio doubles from 1850 to 1900; however, McCulloch et al.'s (2003) record contained significantly higher baseline Ba/Ca ratios than this study. Both records increase after the 1870s and plateau around the 1890s. However, the Magnetic Island Ba/Ca record decreased after the 1930s as opposed to the Havannah Island record, where the Ba/Ca ratios remained consistent (Fig 8.9a). Unfortunately, the 2 yearly sampling resolution employed for the Magnetic Island coral was insufficient to estimate the quantity of extra sediment supplied from the Burdekin River since European settlement.

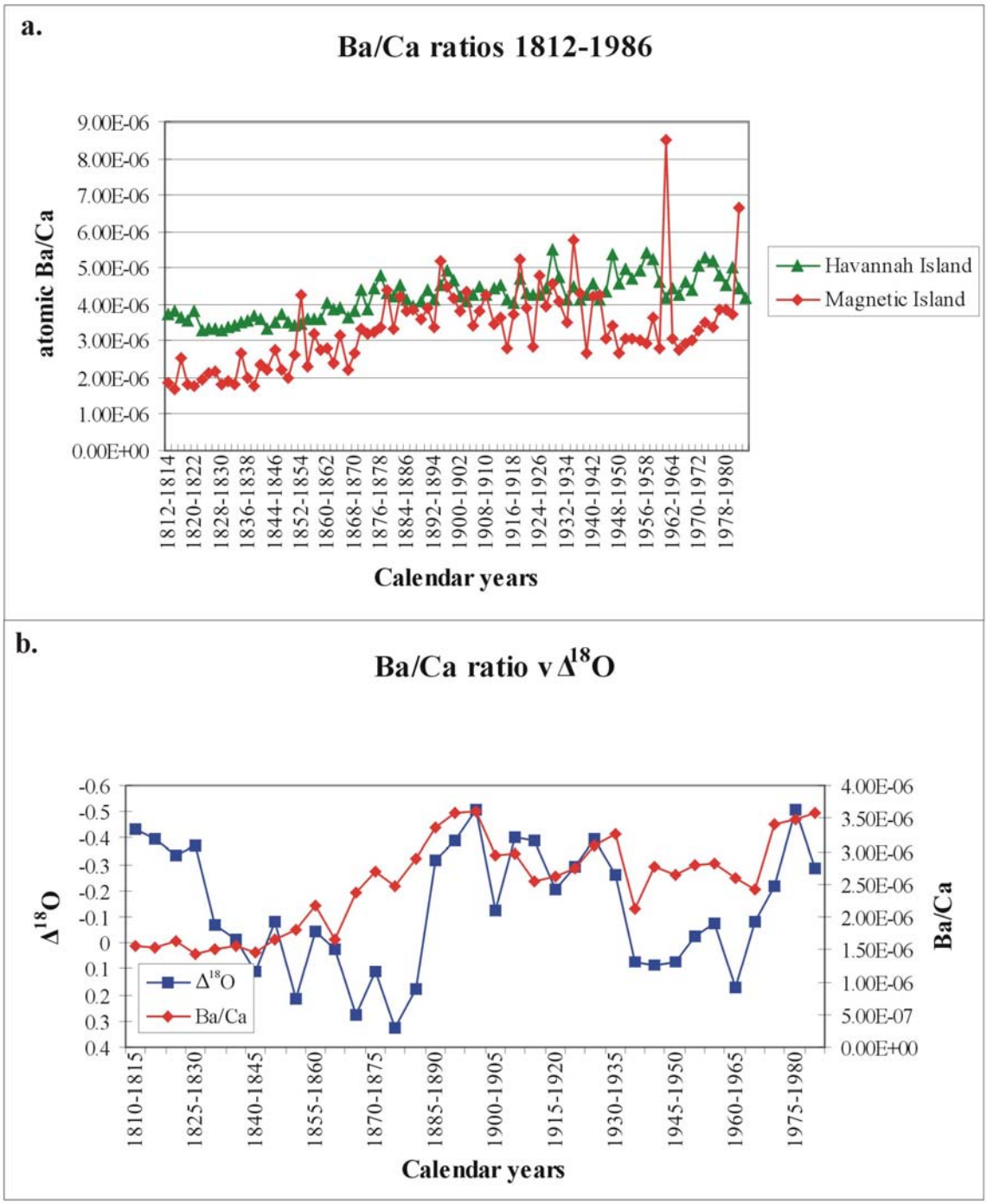

Figure 8.9 a-b. Ba/Ca ratios from this study compared with the averaged data of McCulloch et al. (2003; a). While a significant correlation was observed between the 2 datasets, the Ba/Ca ratios displayed slightly different trends. Both coral Ba/Ca datasets increased after 1870; however, the ratios plateau around the 1890s and while the Havannah Island dataset remained at consistent levels, the Magnetic Island record decreased after the 1930s. (b) The Ba/Ca ratios in this study compared to the $\Delta^{18}O$ record. The decline in the coral Ba/Ca ratios after the 1930s in the Magnetic Island record coincided with a positive excursion in $\Delta^{18}O$ values. This finding suggests that the Magnetic Island Ba record may be influenced by long-term wet/dry cycles (b).

There are two possible explanations for the different Ba/Ca trends in these datasets and the higher Ba concentrations in the Havannah Island coral. The first explanation is that Havannah Island may be strongly influenced by the Herbert River, which discharges considerably closer to Havannah Island than the Burdekin River (Fig 8.10). The two major terrestrial sources of Ba are in the dissolved fraction from rivers and desorbed Ba from fine-grained silt and clay particles within the 10‰ salinity zone (Sinclair and McCulloch, 2004). Once Ba is desorbed from the sediment, it becomes progressively diluted as the river plume becomes mixed with seawater and the concentration of Ba in the river plume mixes conservatively in proportion to the salinity of the water (Coffey et al., 1997; Sinclair and McCulloch, 2004). Therefore, Ba is enriched in the lower salinity zones close to river mouths. Indeed, the Havannah Island coral Ba/Ca record from McCulloch et al. (2003) is near the Herbert River delta and Crystal Creek, both of which strongly influence salinity in the region (Fig 8.10; J. Brodie personal communication, 2005). They (and local creeks in the proximity) may have a more dominant influence on the Ba concentrations in the Havannah Island coral than the Burdekin River.

However, McCulloch et al. (2003) found that the Ba/Ca peaks and coral luminescent lines were significantly correlated with the Burdekin discharge records, although a large flood in the Burdekin catchment typically coincides with widespread rainfall throughout northern Queensland. In fact, the Burdekin River discharge was correlated significantly with discharge from the Herbert River ($r= 0.75$; $p <0.00$; $n=77$; Fig 8.11) and therefore the Herbert River discharge is probably also correlated with the coral Ba/Ca ratios and luminescent lines from McCulloch et al.'s (2003) Havannah Island coral. Indeed, the increase in the coral Ba/Ca ratio after 1870 in the Havannah Island record coincides better with land settlement in the Herbert catchment (~ 1865) rather than the Burdekin, which was settled during the early 1850s.

On the other hand, the second explanation for the higher Ba/Ca ratios in the Havannah Island coral is that the Burdekin River plume has a greater influence on Havannah Island than the geographically closer Magnetic Island which, in turn, may be influenced by additional parameters. Models of the Burdekin River discharge for the wet seasons from

1966-1995 (King et al., 2001) suggest that the plume may occasionally exert a greater influence on Havannah Island, particularly when the winds were predominantly from a southerly or westerly direction during peak discharge. The Havannah Island coral Ba/Ca record was also significantly correlated with cattle numbers in the Burdekin River catchment ($r= 0.49$; $p <0.00$; $n=52$), whereas the Magnetic Island Ba/Ca-cattle correlation was insignificant (Table 8.1). Therefore, the Havannah Island Ba/Ca record may reflect regional trends in the Burdekin River catchment, while the Magnetic Island coral Ba/Ca ratios may be influenced by additional factors. The coral Ba/Ca ratio from Magnetic Island was not correlated with the $\Delta^{18}O$ record, but it appears to partially follow the long-term salinity trends (Fig 8.9b). The coral Ba/Ca ratios were elevated during the "wet" 1885-1935 period, but declined after 1935, which was a "drier" period marked by the $\Delta^{18}O$ record. A return to wetter conditions after 1970 in the coral $\Delta^{18}O$ record coincided with another increase in the Ba/Ca ratio (Fig 8.9b). In addition, elevated coral Ba/Ca ratios were not always correlated with river discharge events; coral Ba/Ca may also be influenced by barite trapping following phytoplankton blooms, decaying blooms of *Trichodesmium*, physiological perturbations associated with coral spawning and bottom sediment resuspension following dredging (Sinclair, 2005b; Esslemont et al. 2004).

Table 8.1. Correlation coefficients between Ba/Ca ratios, Mn, Y, $\Delta^{18}O$ from the 1812-1986 Magnetic Island (MI) coral record, as well as the Ba/Ca ratios from Havannah Island (HI; McCulloch et al., 2003) and sheep and cattle numbers in the Burdekin River catchment (Statistics for the Colony/State of Queensland. Note: Bold denotes a significant correlation, while the values listed in bold and grey are inversely correlated.

Correlation variables	Correlation coefficient (r)	Significance (p)	Number of samples (n)
Ba/Ca (MI) v Ba/Ca (HI)	**0.47**	< 0.00	87
Ba/Ca (MI) v $\Delta^{18}O$	-0.28	> 0.05	35
Ba/Ca (MI) v Sheep	0.09	> 0.05	52
Ba/Ca (HI) v Sheep	**-0.28**	0.04	52
Ba/Ca (MI) v Cattle	0.21	> 0.05	52
Ba/Ca (HI) v Cattle	**0.49**	< 0.00	52
Ba/Ca (MI) v Mn	-0.09	> 0.05	87
Ba/Ca (HI) v Mn	-0.19	> 0.05	87
Ba/Ca (MI) v Y	**0.48**	< 0.00	87
Ba/Ca (HI) v Y	**0.86**	< 0.00	87
Mn v $\Delta^{18}O$	**0.43**	0.01	35
Mn v Sheep	0.05	> 0.05	52
Mn v Cattle	**-0.64**	< 0.00	52
Mn v Y	**-0.27**	0.01	87
Y v Sheep	**-0.39**	< 0.00	52
Y v Cattle	**0.64**	< 0.00	52

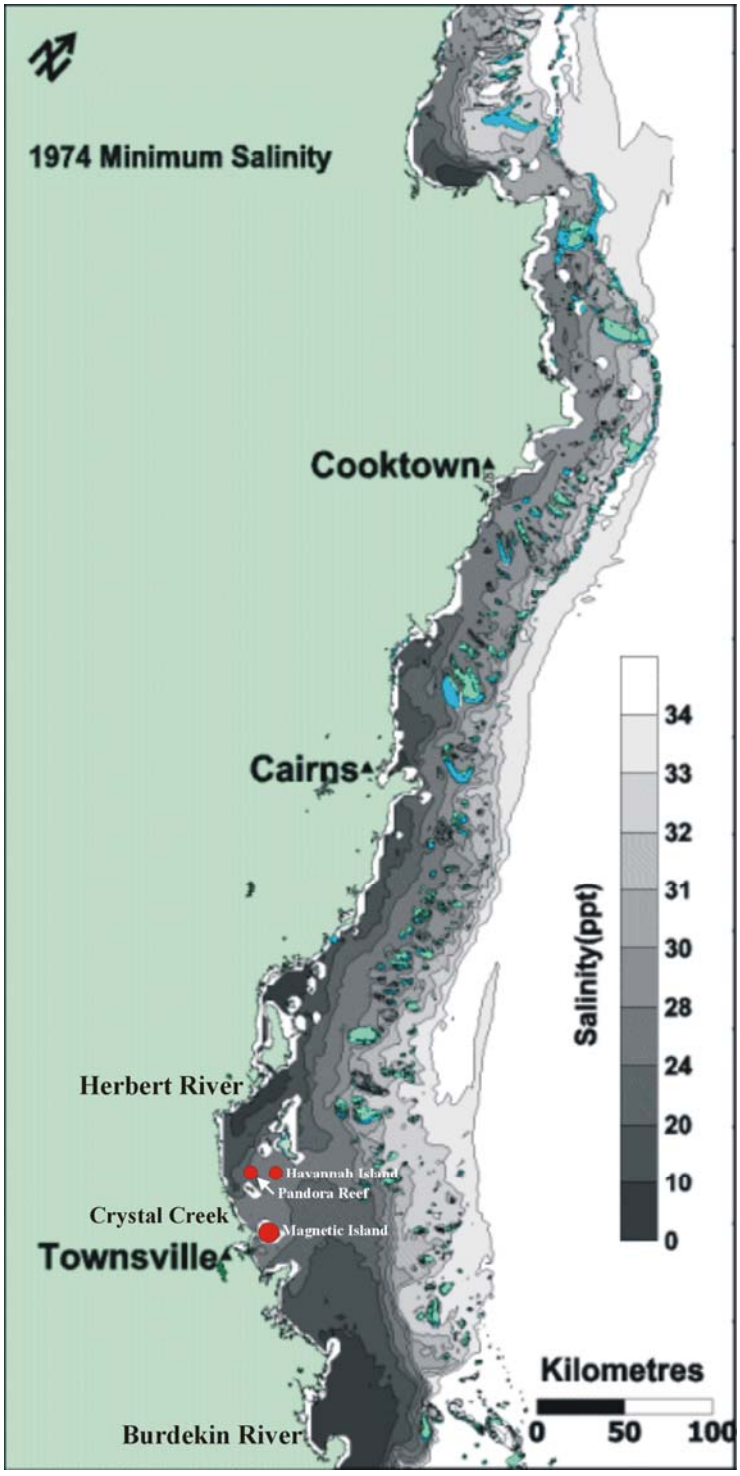

Figure 8.10. Flood plume modelling of north Queensland's major rivers suggest that salinity in the Havannah Island area may, in fact, be dominantly influenced by the Herbert River rather than the Burdekin River. The lower salinities at Havannah Island compared to Magnetic Island during flood events may also explain why the Ba/Ca ratios are higher in the Havannah Island record (1974 flood model; modified from King et al., 2001). Note that the 0-10 ppt salinity zone for the Burdekin River is confined exclusively to Upstart Bay.

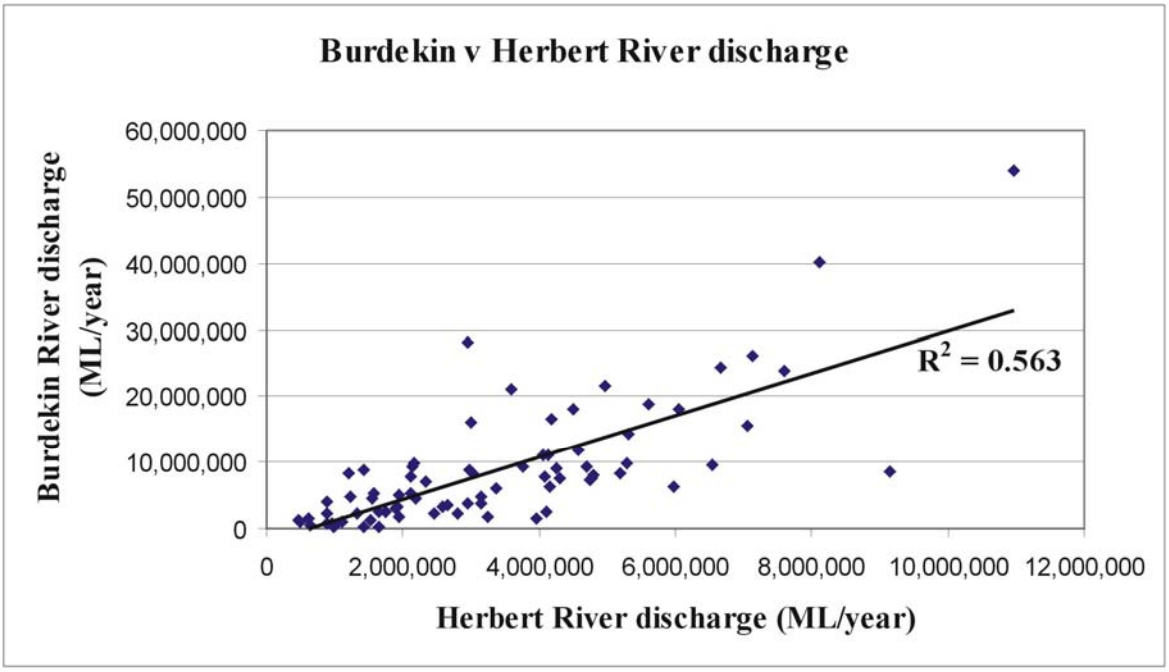

Figure 8.11. A significant correlation exists between the Herbert and Burdekin River discharge (r= 0.75) which suggests that the Herbert River had similar flood events to the Burdekin system in the same years. Therefore, coral luminescence records for the Havannah Island coral, initially thought to be influenced by the Burdekin River catchment may, rather, be related to the Herbert River discharge.

8.4.4 Ba concentrations in flood plumes

Barium concentrations in the luminescent lines of the Magnetic Island corals have increased significantly since European settlement and indicate that sediment export to the GBR lagoon has increased. The 1991 luminescent line contains the highest measured Ba concentration (23.62 ppm), which is approximately 5 times greater than a flood of similar magnitude in 1870 (4.90 ppm; Fig 8.12). In addition, the 1972 flood band (22.51 and 16.19 ppm) contained 6-8 times more Ba than the 1831 luminescent line (2.91 ppm) of similar intensity. The increase in coral Ba concurs with the estimations of McCulloch et al. (2003) who suggested that sediment supplied from the Burdekin River had increased 5 fold since 1870 in the Havannah Island coral Ba/Ca record. As previously discussed (section 8.3.3), elevated Ba concentrations do not necessarily indicate a greater threat of sedimentation to the inshore coral reefs as Ba is desorbed from sediments within the 10‰ salinity zone (Coffey et al., 1997). Nonetheless, coral Ba concentrations provide evidence of the

quantity of fine-grained sediment supplied from rivers and also provide a way to track the progressions of the dissolved phases of nutrients (such as nitrate) in flood plumes. Interestingly, the coral Ba/Ca ratios were not elevated during the 1981 and 1983 flood events in the 1980-1984 two-monthly resolution coral record (Fig 6.20a). This finding was inconsistent with the Ba samples from the luminescent lines and may relate to the coarser sampling resolution in the 1980-1984 record.

Flood events after prolonged dry periods, such as the 1970 and 1991 floods, coincided with relatively enriched coral Ba concentrations (Fig 8.12). The increased coral Ba was thought to reflect increased sediment erosion in the river catchments due to the lower vegetation cover produced during drought (e.g. Sinclair and McCulloch, 2004). These particular floods need to be considered when applying the coral Ba/Ca ratios to estimate the extra quantity of sediment exported from the river catchments. However, the 1870 flood also followed a dry period and was of a similar magnitude to the 1991 flood. Therefore, the estimate of a 5-fold increase in sediments exported from the Burdekin River since European settlement is reasonable.

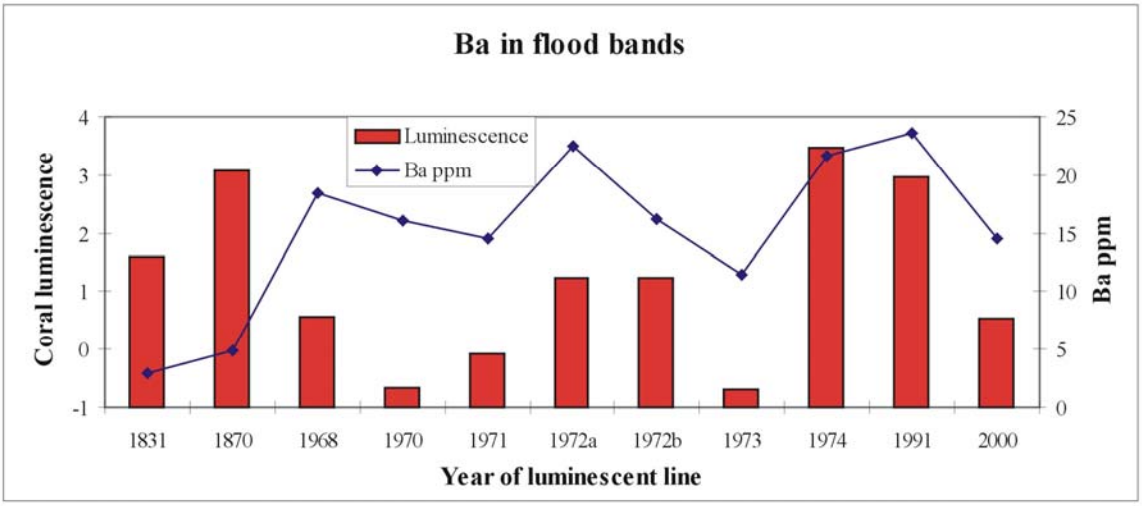

Figure 8.12. Ba concentrations in coral luminescent lines (flood bands) have increased significantly since European settlement. Ba concentrations have risen approximately 5-fold compared to the 1870 and 1991 floods, which were of similar magnitude and followed extended dry periods. Higher Ba concentrations also occurred after prolonged dry periods, which was evident in the relatively minor 1970 flood that followed the 1969 drought.

8.4.5 Baseline coral Ba concentrations

Elevated coral Ba/Ca ratios were commonly associated with the luminescent lines (flood bands; e.g. McCulloch et al., 2003), which have substantially increased since European settlement; however, it appears that the ratio has also increased in the baseline values that did not coincide with flood events. The 1831 flood band contained a Ba concentration of 2.91 ppm, which was considerably lower than the averages of the 1980-1984 (5.15 ppm), 1968-1973 (12.32 ppm) and 2000-2003 (10.72 ppm) coral records (Fig 8.13), although the 1968-1973 and 2000-2003 records were from a different coral cored in Nelly Bay. This high concentration suggests that seawater Ba concentrations have significantly increased since European settlement and that another source of Ba, other than from flood plumes, is required to explain the increase in baseline coral Ba/Ca ratios.

The seawater in Cleveland Bay is flushed every 40-60 days (P. Ridd personal communication, 2005) and the flood plume Ba would be quickly diluted in seawater and Ba would return to "background/baseline" levels. The significant baseline increase in coral Ba was probably not related to a regional Pacific Ocean signature because the ocean residence time for Ba is approximately 5,000 years (Taylor and McLennan, 1985). However, long-term salinity changes, observed in the coral $\Delta^{18}O$ record, may be related to the Pacific Decadal Oscillation and, in turn, may influence seawater Ba concentrations. Evidence for a salinity/climate signal on coral Ba concentrations was postulated by Hendy (2003). Another possible mechanism for elevated seawater Ba may be increased organic matter/phytoplankton which may retain and recycle Ba (e.g. Sinclair, 2005b).

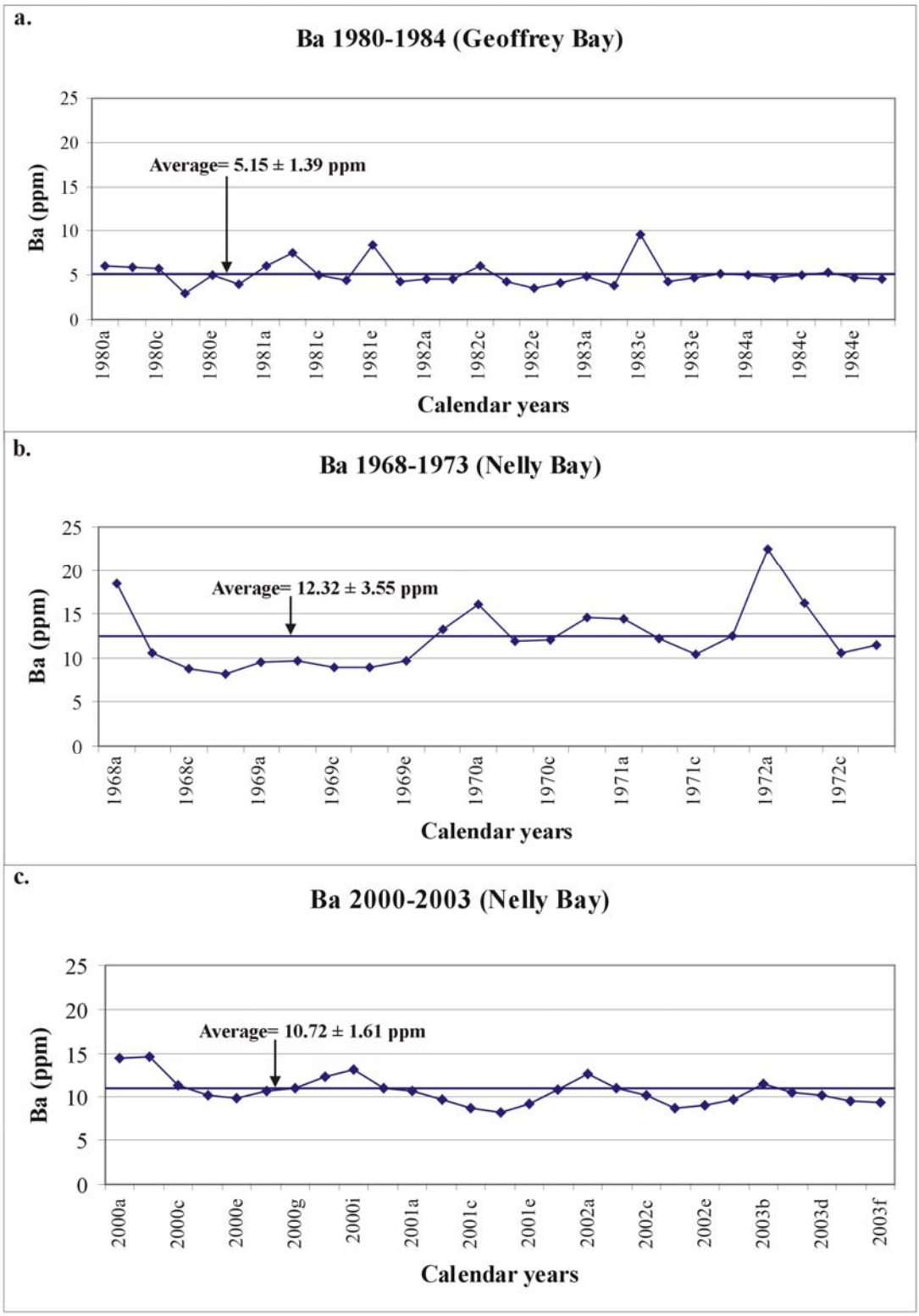

Figure 8.13. Ba concentrations in the 1980-1984 (a), 1968-1973 (b) and 2000-2003 (c). Interestingly, the average concentrations in these records were considerably higher than that for the 1831 and 1870 floods, which suggests that seawater Ba has increased significantly since European settlement. Another source for the increased Ba (other than from floods) is required to explain the increased baseline coral Ba concentrations.

8.4.6 Ba/Ca in the mid-Holocene corals

The Ba/Ca ratios in the mid-Holocene corals (Fig 6.22) are similar to the post-1850 averages (Fig 6.21), a time of extensive land-use in the Burdekin catchment and increased erosion from the Burdekin River. However, it is unlikely that the volume of sediment exported from north Queensland local rivers was similar during the mid-Holocene. There are three possible explanations for the elevated coral Ba/Ca ratios 6,000 years ago.

The Burdekin River once discharged into Bowling Green Bay during the Holocene and Pleistocene Epochs (Fig 3.1; Hopley, 1970a; Fielding et al., 2005b; 2006). Therefore, the Burdekin River delta was closer to Magnetic Island during the mid-Holocene and may have exerted a greater influence on the salinity in this area. This interpretation is supported by the two-monthly resolution mid-Holocene $\Delta^{18}O$ values which imply that salinity during flood events were significantly lower compared to the 1980-1984 record (Fig 6.17 a-b). In addition, Fielding et al. (2006) found evidence for increased sediment supply to the coast during the mid-Holocene compared to the last 3-4,000 years BP, a time when drier conditions prevailed. As previously discussed, (section 8.4.4) Ba concentrations in river plumes become progressively lower as the plume becomes diluted with seawater; therefore, the lower salinities recorded in the two-monthly mid-Holocene coral should result in relatively higher Ba/Ca ratios. However, the Ba/Ca ratios in this record were not significantly elevated during these flood events (Fig 6.20c), which does not support this hypothesis.

The second possible cause for the elevated Ba/Ca ratios in the mid-Holocene corals was their close proximity to Gustav Creek which discharges into Nelly Bay and the nearby Ross River. The fossil corals were recovered near the mouth of Gustav Creek; this creek is unlikely to have changed course due to the geomorphological constraints. The mid-Holocene corals would have grown near the mouth of this creek and, during flood events, the coral may regularly have experienced salinities within the 10‰ zone (where Ba is desorbed from sediments; Coffey et al., 1997). While this small creek system probably did not export appreciable quantities of sediment compared to the much larger Burdekin, it may

have significantly influenced the Ba/Ca ratios in the mid-Holocene corals. In addition, all the sediment exported from Gustav Creek is delivered to Nelly Bay, whereas only a fraction of fine Burdekin sediment reaches Magnetic Island, although the Burdekin River plume may carry significantly higher dissolved Ba.

The third hypothesis is that seawater Ba concentrations were higher during the mid-Holocene. Interestingly, the coral Ba/Ca ratios were not particularly elevated during the large flood events in the two-monthly resolution mid-Holocene record (Fig 6.20c), which suggests that another source of Ba, other than from land runoff, is required to explain the elevated baseline values. As sea-levels rose during the mid-Holocene, alluvial Pleistocene-early Holocene sediments would have been reworked extensively. This reworking may have released significant amounts of desorbed Ba into seawater.

8.4.7 Coral Ba "tails"

Another demonstration that elevated coral Ba/Ca ratios were not always related to seawater salinity or flood plumes is the gradual "tailing off" of the ratios well after the plume has been mixed and salinities returned to normal (Alibert et al., 2003), although this "tailing off" only occurs after select flood events. A few possible explanations have been offered to explain this prolonged decline, including a tidal/mangrove Ba source or submarine groundwater seeps (Alibert et al., 2003). However, these possibilities do not appear to explain why the Ba/Ca ratios "tail off" only after select flood events.

An alternative explanation is that phytoplankton/diatoms capture and store Ba. Phytoplankton has the capacity to absorb Ba; subsequently, the plankton decays and re-releases dissolved Ba into the seawater (Bishop, 1988; Stroobants et al., 1991; Bernstein and Byrne, 2004; Colbert and Manus, 2005). Phytoplankton outbreaks develop only after certain flood events and so reefs would only be affected intermittently as the outbreaks are restricted to particular turbidity (<10 mg/L) and salinity (~20-35 ppt) zones (Dagg et al., 2004; Devlin and Brodie, 2005). Sinclair (2005b) has also suggested that *Trichodesmium* blooms, which are common when the SE trade winds relax at the end of the winter months,

may consume and release Ba upon decay. These blooms do not rely on flood events. Sinclair's (2005b) suggestion explains the elevated coral Ba concentrations that do not coincide with freshwater influx (Sinclair, 2005b). Other potential reasons for Ba peaks, not related to salinity/floods, might include submarine groundwater seeps (Alibert et al., 2003), coral spawning (Sinclair, 2005b) or harbour dredging (Esslemont, 2000).

8.4.8 Ba as a sedimentation indicator

In some cases, the increased Ba signal in corals has been misinterpreted as a proxy for increased sedimentation at coral reefs (e.g. Cole, 2003). While the Ba/Ca ratio suggests there has been a significant increase in fine-grained sediment exported from rivers, this finding does not necessarily imply that there has been enhanced sedimentation at coral reefs. The Burdekin River delta is approximately 100 km from the fringing coral reefs surrounding Magnetic Island, which are among the first to be influenced by the Burdekin River plume. Recent research has demonstrated that the sediment exported from the Burdekin River is retained in Upstart Bay and Bowling Green Bay, and as little as 5% is deposited in Cleveland Bay (Orpin et al., 2004). This sediment is then either transported to northward embayments or deposited in inshore mangrove environments (Bryce et al., 1998; Lambeck and Woolfe, 1999; Orpin et al., 2004). While coral reefs are unlikely to suffer any increased effects of sedimentation as a direct result of the Burdekin River plume (see also section 8.3), reefs in close proximity to the river mouths in far north Queensland could be affected by an increased riverine sediment load. These reefs need to be the focus of future coral proxy studies to quantify the sediment export from rivers, turbidity and sedimentation on coral reefs.

8.4.9 Summary

The Ba/Ca ratio appears to be a reliable proxy to assess fine-grained sediment particles exported from rivers to the inshore GBR. Coral Ba/Ca ratios in the Magnetic Island coral were correlated significantly with the Havannah Island record of McCulloch et al. (2003). The coral Ba/Ca ratio increased after the 1870s in both records and indicated that the export

of fine-sediments from the Burdekin River may have increased by as much as 5-fold. However, these two coral Ba/Ca records displayed different trends during the 1930-1970 period; the Havannah Island record remained relatively constant compared to the Ba/Ca ratios in the Magnetic Island coral which declined over this period. These trends are difficult to explain. The Havannah Island coral Ba/Ca ratios were significantly correlated to the growth of the cattle industry in the Burdekin River catchment, but the Magnetic Island coral Ba/Ca ratios displayed no significant correlation with cattle numbers and appeared to follow long-term trends in seawater salinity. Elevated coral Ba/Ca ratios were not necessarily related to river discharge and have been linked to a tidal/mangrove source, submarine groundwater seeps, *Trichodesmium* blooms, coral spawning and harbour dredging (e.g. Alibert et al., 2003; Sinclair, 2005b; Esslemont, 2000). The mid-Holocene corals from Magnetic Island also displayed elevated Ba/Ca ratios, which may be explained by an increased influence from the Burdekin River and/or Gustav Creek, or because local seawater Ba concentrations were higher during the mid-Holocene.

8.5 Mn concentrations

8.5.1 Overview

The 1812-1986 coral Mn concentration increased from baseline levels of <0.8 ppm to values which exceeded 4 ppm (Fig 6.24a). These changes commenced in the 1854-1856 sample and continued to the early 1900s before they returned to baseline values. Elevated Mn also occurs after World War II. The extremely low coral Th concentrations (<1 ppb) suggest that there has been no significant incorporation of detrital particles into the coral (Wyndham et al., 2004). In addition, the chemically pre-treated coral Mn record displayed similar trends and concentrations to the untreated biennial resolution analysis conducted at the ACQUIRE laboratory (Fig 6.24). Therefore, this coral trace element record is considered to be genuine and probably lattice-bound.

Previous investigations have linked elevated coral Mn concentrations to a wide range of processes including ash fallout from fire (Abram et al. 2003), release from bottom

sediments (Shen et al. 1992b; Alibert et al. 2003; Wyndham et al. 2004), volcanic eruptions (Shen et al. 1991) and upwelling events (Shen et al. 1991). None of these studies have reported Mn concentrations as high as those reported here, and none of the above explanations can fully explain systematic trends in coral Mn levels on a decadal-scale. The initial coral Mn increase in 1854 – 1856 directly follows the opening of Port Curtis (Gladstone) and the very first sheep run in the Suttor and Belyando sub-catchments by Jeremiah Rolfe in the vicinity of Mistake Creek in 1854 (O'Donnell, 1989). Therefore, land-use changes within the Burdekin catchment are investigated as the most likely explanation for the Mn signature of the Magnetic Island coral.

8.5.2 Coral Mn concentrations and the history of land-use in the Burdekin River catchment

The dramatic increase in coral Mn after the 1852-1854 growth bands (Fig 6.24) coincides with the very first occupation of sheep in the Burdekin catchment where land was acquired in the Peak Downs/Clermont area in 1854 (Fox, 1919-1923; O'Donnell, 1989; Bode, 1984). This settlement was immediately followed by the rapid expansion of sheep runs in the Belyando and Suttor sub-catchments with much of the area being sub-divided for sheep and cattle farming by 1861 (Bolton, 1963; Cunningham, 1895). The rate of land take-up was in part fuelled by the land act of 1860, which required that the area be stocked within the first year of purchase (Bolton, 1963; Thorpe, 1996). For coral Mn to respond so swiftly to land-use changes, the sheep must have immediately triggered Mn release from that area of the catchment.

Because no undisturbed, regularly burnt area has remained it was not possible to study the chemistry, mineralogy and structure of pre-1850 soils in coastal Queensland. However, clues may be obtained from the nature of the underlying lithologies. The Peak Downs/Clermont area coincides with one of the largest basaltic provinces in Queensland: the Tertiary-age Peak Range Volcanics (Fig 3.12). Because basaltic soils are frequently Mn-rich (1750 ppm: Faure, 1998) and are commonly 2-3 times more enriched than granitic and most sedimentary rocks (e.g. Faure, 1998), it seems likely that this huge area of basalt bedrock supplied the Mn, which made its way to the inner GBR after European settlement.

It is proposed that Mn became further concentrated in coastal Queensland soils over 40,000 years because of the build up of ash from Aboriginal burning (Griffiths, 2002), and that native vegetation became accustomed to the biogeochemical balance provided by this ash. The natural tendency of ash to increase soil *p*H may have helped to build a substantial, but transient, Mn reservoir because of the relative immobility of Mn under alkaline *p*H (Chirenje and Ma, 2002).

The peak Mn concentration in 1864-1866 coincided with the end of the American Civil War and the drop in wool price caused by the lifting of the cotton embargo to Great Britain, a period that also marks the collapse of the sheep industry in coastal Queensland (Fig 3.13). Agricultural efforts turned instead to cattle grazing and the establishment of the sugarcane industry with strong expansion between 1870 and 1895, at which time the area experienced its worst drought on record (the "Federation Drought", 1895-1902), an event that drastically reduced livestock numbers (Fig 3.13) and coincided with Mn concentrations in the coral returning to the low pre-1850 levels (Fig 8.14). Another significant Mn peak coincided with the period immediately following World War II, when agriculture, including the cattle industry, intensified in part due to land release to war veterans and recent European immigrants, but mainly due to increased mechanisation of land clearing. The cattle industry was particularly prominent in the upper Burdekin sub-catchment, which appears to be the most recently settled land in the Burdekin. Cattle numbers also rose significantly in the Suttor and Bowen sub-catchments following World War II and the increase in coral Mn concentrations may coincide with release from soils covering large basalt provinces in these three sub-catchments (Fig 3.12). The period between 1945-1953 also saw the development of the tobacco industry when huge tracts of land in the lower Burdekin sub-catchment were cleared by the government following a major drought during World War II (Kerr, 1994). This extensive clearing in the lower reaches of the Burdekin is another possible reservoir for Mn; however, the banks of the lower Burdekin are typically at higher elevations than the surrounding landscape, and runoff from this lower catchment is commonly from local creek systems rather than from the Burdekin River (J. Brodie personal communication, 2005). Lowest coral Mn concentrations were found during the

major drought between 1958-1968 (Young, 2000) and coincide with a drastic decline in sheep numbers in the Burdekin catchment (Fig 3.13).

The post 1868 drop off in sheep numbers was most severe in the coastal districts and it appears that the lower coral Mn concentration was a response to this decline in sheep numbers from the coastal districts. The swiftness of the initial rise in Mn after the introduction of sheep and its subsequent decline may suggest the original existence of a large, but transient reservoir of Mn in the soil cover of the Burdekin catchment, which quickly became depleted. The timing of the second and third spikes in coral Mn concentration exactly corresponds to the growth of cattle herds, which replaced sheep (Figs 3.13; 8.14). However, the magnitude of Mn response declined with each stockage and the observation that growing herds after the Federation Drought never produced a comparable response in terms of Mn levels confirms the transient nature of this topsoil Mn reservoir.

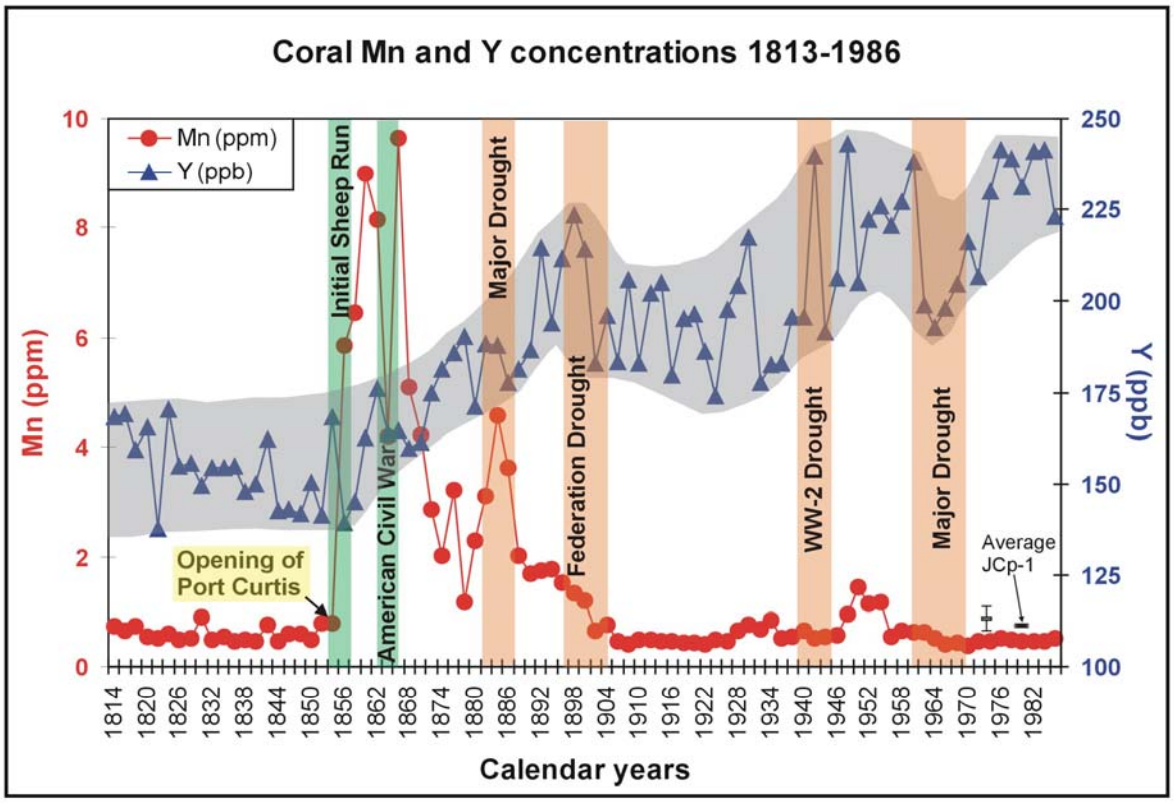

Figure 8.14. Mn and Y concentrations in the coral core from 1813-1986. Yttrium concentration, like Ba, is interpreted to be an erosion indicator, steadily increasing after 1860-70. Manganese defines a different history. Elevated Mn concentrations coincide with major land settlement in the Burdekin catchment. The initial Mn spike in 1854-1856 was related to the establishment of the first sheep run in the Burdekin catchment. The peak Mn concentration coincided with the end of the American Civil War and the climax of rapid expansion of the sheep industry in the Burdekin catchment. The second major Mn peak in 1882-1884 coincided with, and may thus be related to, the expansion of the cattle industry or the beginning of the sugar cane industry on the lower Burdekin catchment. The return of Mn concentrations to pre-1850 levels coincides with the Federation Drought, which decimated sheep and cattle numbers throughout the catchment. An increase in Mn after WWII may be related to the further development of the cattle industry. Reproducibility of Mn is shown for the (slightly heterogeneous) G.S.J. coral standard JCp-1. Also shown for comparison are average and standard deviation of Mn in a mid-Holocene coral recovered from Nelly Bay, Magnetic Island.

8.5.3 The environmental significance of the coral Mn record

Identification of the environmental parameters responsible for the historic release of an apparently transient Mn reservoir will remain tentative because no land conservation measures protected any comparable soils in eastern Australia from grazing. Nonetheless, it is remarkable that the fluctuations of Mn concentration in this coral appear to be so decoupled from the Y concentration and Ba/Ca ratio records, both in timing and in amplitude. If the proposal that Ba/Ca (McCulloch et al., 2003) and Y concentrations

(Sinclair, 2005b) of nearshore GBR seawater are proxies for fine sediment release holds up, then the much more dramatic response of Mn cannot relate to physical erosion and soil loss but to the release of Mn, dissolved in run-off.

Although the surface seawater inventory of Mn, which is concentrated in plant ash, can be influenced by wildfires (Abram et al., 2003), the fluctuations found in this study are not related to bush fires. Across the entire 130-year growth period of the mid-Holocene specimen that was analysed for comparison, there was no significant deviation in Mn concentration from the mean (0.86 ± 0.23 ppm; Fig 6.25a). The mid-Holocene mean, which corresponds to a time of known Aboriginal inhabitation was, within error to the pre-1850 mean of the recent coral (0.58 ± 0.12 ppm; Fig 6.24a), which argues against wildfire influences from Aboriginal back-burning practices.

Manganese distribution in soils reflects a complex balance between mineralogical, biological, textural (grain size) and physicochemical (redox, state, *p*H) parameters (Post, 1999), most of which would have been affected by sheep grazing. Unlike native terapods, sheep not only disturb the soil texture with their hooves but also crop plants low and pull shrubs and grasses out of the soil by the roots. Exposure of disrupted soil cover to air, the efficient recycling of topsoil via sheep faeces (the volume of which would have initially overwhelmed indigenous dung beetles) and the loss of pH buffering ash, resulted in conditions under which Mn was rapidly lost to run-off. The paucity of carbonate in the catchment soils may have also contributed to the reduced Mn-holding capacity of the disturbed soils (Mania et al., 1989). The combination of these factors would have effectively mobilised Mn, making it more available to plants and possibly even toxic to the pre-existing native vegetation. It may be speculated that the rapid loss of native vegetation was triggered not only by the more obvious physical impacts of grazing and seed dispersal via the introduced sheep, but also by more subtle changes to the existing micronutrient balance, which is strongly related to Mn-mineral surface chemistry (Post, 1999).

In the modern inner Great Barrier Reef, Mn is consumed rapidly in the water column by phytoplankton (Alibert et al., 2003), but the large release of dissolved Mn in the 19th

century was evidently sufficient to reach certain nearshore reefs such as those surrounding Magnetic Island. However, Mn was not necessarily transported solely as a dissolved (Mn II) phase through the catchment because Mn is commonly photo-chemically reduced from Mn (IV) in particulate matter to soluble Mn (II) species in the estuarine zone or at the ocean's surface (Morel and Price, 2003). Further studies of corals in similar proximity to significant catchments need to be investigated for Mn, Y and Ba/Ca to refine understanding of the details of land-use practices on nearshore seawater quality and its consequences for the health of the reef.

8.5.4 Mn concentrations in flood plumes

The 1870 and 1974 luminescent lines contained elevated Mn concentrations compared to the other flood bands which lie within the baseline (~ 1 ppm) range (Fig 8.15). The coral Mn concentration in the 1974 luminescent line was influenced by sediment (Fig 8.5a), while the 1870 flood coincided with the time of land disturbance in the Burdekin River catchment. Interestingly, the 1870 flood band has a similar Mn concentration (5.63 ppm) to the 2 yearly resolution samples (4.23 ppm and 2.87 for the 1868-1870 and 1870-1872 samples, respectively; Fig 8.15). This finding suggests that, while Mn was originally derived from the river catchment, it has been retained and recycled in the system over some time.

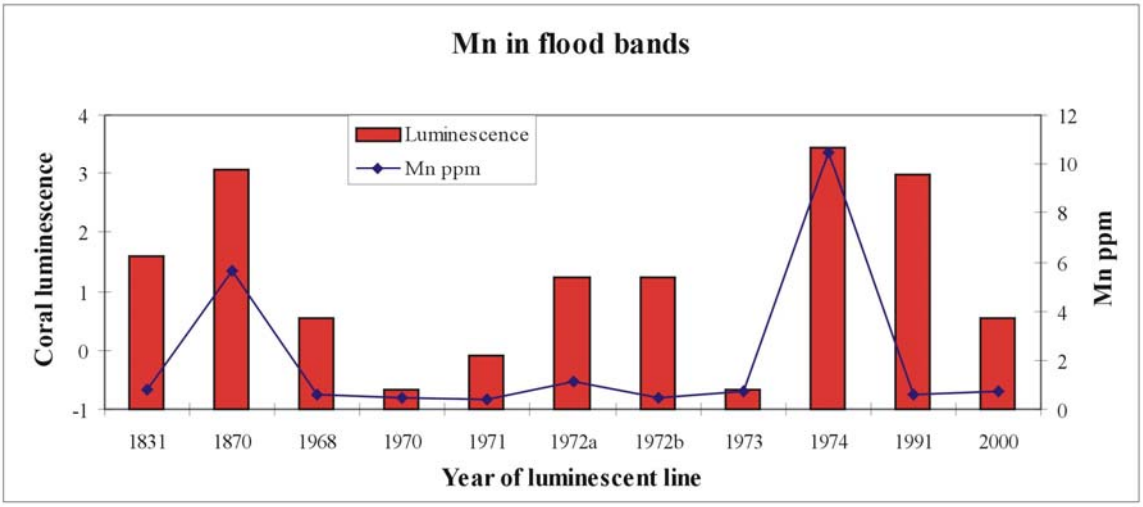

Figure 8.15. Coral Mn concentrations in coral luminescent lines typically were at low "baseline" levels except for the 1870 and 1974 flood. The 1870 flood was related to the disturbance of virgin land in the Burdekin River catchment, while the elevated concentrations in the 1974 flood were due to sediment trapped within the coral skeleton.

8.5.5 Summary

Elevated coral Mn concentrations coincide with the rapid exploitation of virgin land in the Burdekin catchment particularly from the sheep and cattle industries. The coral record provides an extensive, but incomplete, insight into the vast changes in soil chemistry in the Burdekin catchment as a result of these industries. In addition, the concentration of Mn in this coral was significantly elevated compared to previous studies which have linked elevated coral Mn concentrations with ash fallout from fire, upwelling events, release from bottom sediments and volcanic eruptions (e.g. Alibert at al., 2003; Abram et al., 2003; Shen et al., 1991; Shen et al., 1992b). Manganese is an important trace element for phytoplankton production (e.g. Millero, 1996) and is rapidly consumed in the water column (Alibert et al., 2003). Phytoplankton blooms consume oxygen in the water column and are thought to provide the reducing conditions necessary to convert Mn oxide particles to a dissolved phase (Abram et al., 2003). The coral Mn concentrations appear to have remained elevated well after flood events and Mn may have been retained and recycled in the system by phytoplankton (e.g. Colbert and McManus, 2005).

8.6 Rare earth elements/anomalies and Y concentrations

8.6.1 Overview

The REE plus Y (REY) display interesting trends in both the mid-Holocene and modern coral records which have previously been described in sections 8.2 and 8.3. Other studies have demonstrated that the REY group is incorporated into the coral aragonite lattice and preserve genuine seawater REE signatures when normalised to a shale standard (Sholkovitz and Shen, 1995; Wyndham et al., 2004; Akagi et al., 2004). The typical marine REE signature comprises a positive La anomaly, a negative Ce anomaly and an increasing trend from the light REE (Pr) to the heavy REE (Lu). The majority of coral REE studies have been unable to measure the full suite of REY, including important elements such as Pr, Tb and Nb because of analytical constraints (e.g. Wyndham et al., 2004). The absence of these elements renders less certain the calculation of the La, Ce, Eu and Gd anomalies. This

section will discuss the possible influences on the REY group in seawater and their incorporation into the coral skeleton as well as the anomalies that are associated with this important elemental group. In addition, the REY group (Y, Pr, Sm and Ho) will be examined as a coral proxy of sediment export (erosion) to the GBR and their correlation with land-use in the Burdekin River catchment.

8.6.2 Rare earth elements and Y concentrations

Y and the REEs (REY), like Ba, shows promise as an indicator of fine-grained sediment input into the inner GBR (Sinclair, 2005b); theoretically, the REY should be a better indicator than Ba because of the more conservative behaviour of REY during estuarine mixing due to the formation of strong aqueous carbonate complexes in seawater. The group's insignificant role in primary productivity (with the exception of Ce) distinguishes the REY group from Ba (Luo and Byrne, 2004). Like Ba, the REY concentrations in sediments are greater in the freshwater zone than in the saline zone (Fig 5.12a) and they also exhibit similar estuarine desorption behaviour (Hoyle et al., 1984) to Ba/Ca and, therefore, may be applied in the same manner (e.g. Sinclair, 2005b). The elevated REY concentrations in the mid-Holocene coral records have been attributed to declining water quality conditions caused by sedimentation and turbidity (see section 8.2).

The REY in the 1812-1986 coral record systematically increased after European settlement in the Burdekin River catchment (Fig 6.34c; 8.16a). It appears that the increase in REY concentrations has occurred mainly from the baseline values rather than during flood events, unlike Ba. This interpretation is supported by the Y concentrations in the coral flood bands (Fig 8.16b) as well as by the sub-annual resolution records (Fig 6.26a-b) which were not significantly elevated above the background levels during floods events as opposed to Ba (Fig 8.12). Increased catchment erosion and possible coastal progradation probably influenced the increase in the coral REY concentrations. As more sediment accumulates in the tidal zone, the coastline expands seawards and the inshore environment becomes more turbid (Hopley, 1994).

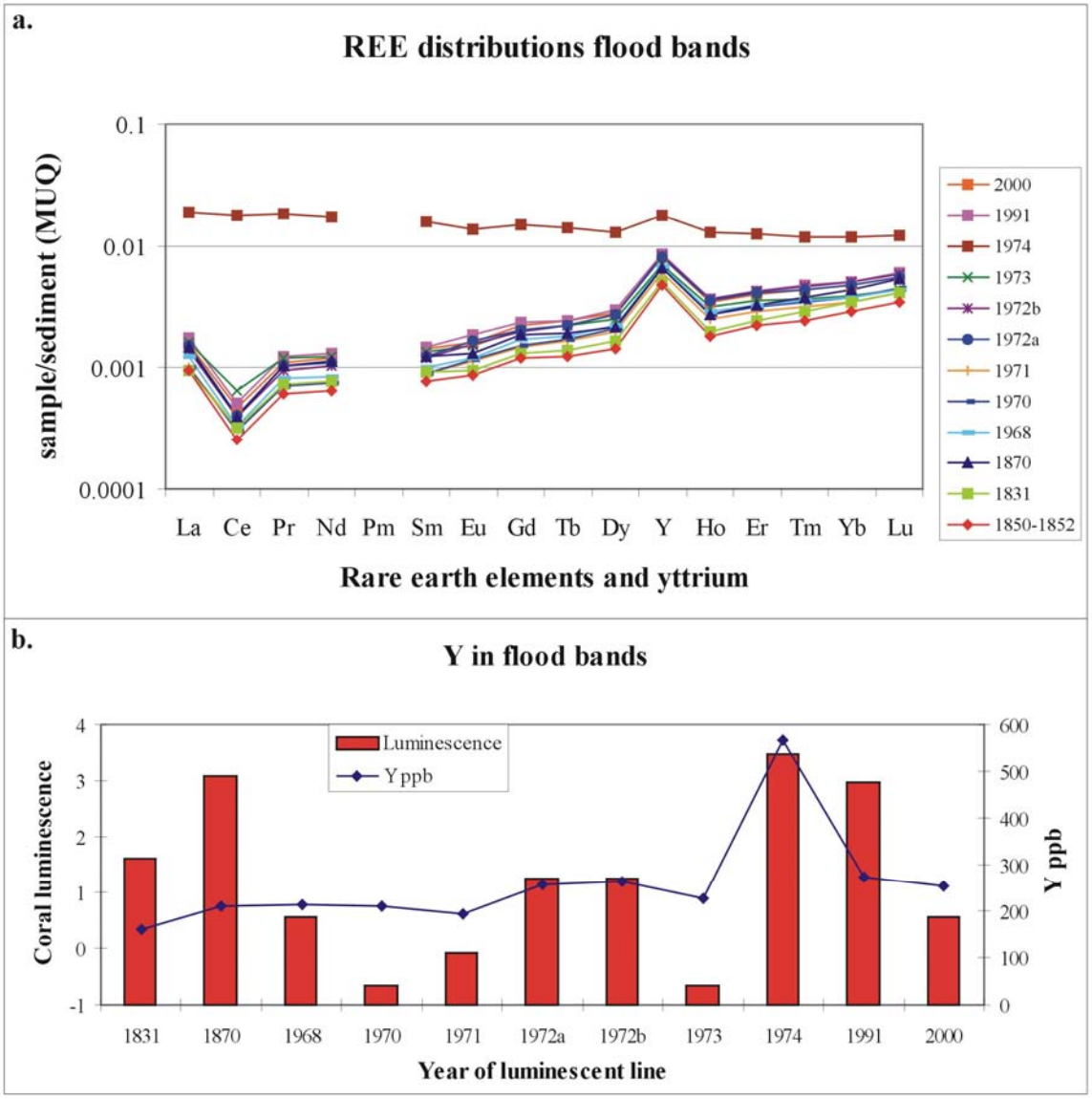

Figure 8.16 a-b. REY distributions (a) and Y concentrations (b) in coral luminescent lines. The REY distributions have systematically increased in flood bands since the arrival of Europeans (a), which matches a similar increase in the 2 yearly coral record (Fig 6.34). In addition, the Y concentrations (b) were not significantly elevated in coral flood bands after European settlement, when the increased baseline levels are taken into account (with the exception of the sediment-affected 1974 flood band). Therefore, the significant REY increase was related to baseline concentrations and suggests that the REY group may be gradually released from sediments.

The release of REY from sediments into seawater may have reverted back to a form of "steady state" equilibrium, as coral REY concentrations have not particularly increased in the 2000-2003 record (Fig 6.34b). While the coral/seawater REY concentrations are influenced by erosion of sediments from river catchments, the REY group may be gradually released from sediments into seawater. Sholkovitz (1993) found evidence for the addition of REE in seawater from benthic sediments or from a suspended particle source. This finding may explain the difference between the Ba and the REY concentrations in corals; Ba is quickly desorbed from sediment in the 10‰ zone, while REY are gradually released from sediments into seawater. The REY distributions may be a reliable proxy to assess the release of nutrients from particulate matter, and may have important implications for the study of particulate nitrogen and phosphorus to evaluate the release of these nutrient phases into seawater.

The significant positive correlation ($r= 0.86$, $p< 0.00$, $n=87$) between the Geoffrey Bay coral Y (Pr, Sm and Ho also correlated) concentrations and the Ba/Ca dataset from Havannah Island (McCulloch et al., 2003) indicates that both elements are affected by regional variations in sediment input. While the records parallel each other, Y concentrations show a higher correlation coefficient with total cattle numbers ($r= 0.64$; $p< 0.00$, $n= 52$) in the Burdekin River catchment than both the Ba/Ca records produced from Havannah ($r= 0.49$, $p< 0.00$, $n= 52$) and Magnetic Islands ($p> 0.05$: not significant), respectively (Table 8.1). As with the Ba/Ca ratio, coral Y concentrations did not respond immediately to the initial settlement in the Burdekin catchment and are inversely correlated with sheep numbers. The coral Y record appears to be responding to increased land-use and sediment runoff in the Burdekin River catchment from *cattle* rather than sheep grazing, in which case soil erosion and sediment runoff apparently only began to increase significantly during the late 1860s and early 1870s, as proposed by McCulloch et al. (2003) and may have continued to rise since then in proportion to fluctuating cattle numbers. Cattle numbers in the Bowen and Suttor sub-catchments increased mainly during the 1870s-1890s (Fig 3.12) and closely coincide with the increasing coral Ba/Ca ratios and Y concentrations (Figs 8.14; 8.9a). Therefore, the coral Ba/Ca ratios and Y concentrations after 1870 may be responding specifically to increased land-use in the Bowen River sub-

catchment. This finding is important for the management of soil erosion in the Burdekin River catchment and of sediment export to the GBR lagoon.

The residence time of REY in the ocean is disputed and extremely difficult to calculate, presumably because of the lack of measurements of REY supplied from rivers. Some researchers believe that the residence time of REY in the ocean is less than 20 years (Taylor and McLennan, 1985), while others have calculated residence times in excess of 1000 years (Nozaki, 2001). REY concentrations in freshwater systems behave in a complex manner (Lawrence et al., submitted), and the dissolved phase becomes significantly fractionated in favour of the heavy REE in the estuarine zone which, in turn, produces the distinctive REE seawater pattern (Sholkovitz et al., 1994). An understanding of the ocean biogeochemical cycling of the REY group would contribute to a better appreciation of the mechanisms that influence the incorporation of REY into corals. More research is required to understand the flux of REY from rivers so that the ocean residence time of the REY group can be calculated accurately.

8.6.3 The La anomaly

The La anomalies in the corals and sediments have been calculated from the La_N/Nd_N ratio (herein $_N$= normalised to MUQ sediment; Kamber et al., 2005). Seawater commonly contains a positive La anomaly, and La/Nd ratios range from 0.8 to 2 (de Baar et al., 1985a; b; Piepgras and Jacobsen, 1992; Shimizu et al., 1994). The La anomaly in the modern coral records are within this seawater range and average from 1.34 to 1.36, with the exception of the 1814-1816 coral sample (2.62; Fig 8.17 b,d,e). The cause for the one anomalous value is not clear; however, juvenile corals are known to produce inconsistent geochemical results (Marshall and McCulloch, 2002). Sediments measured in the local region also display positive La anomalies but their values (average 1.19) are lower than modern corals from Magnetic Island (Fig 8.17). Interestingly, the average La anomaly in the mid-Holocene corals is closer to the sediment values than to the modern corals (Fig 8.17 c,f). It appears that the La anomaly is unaffected by freshwater influx and is not particularly influenced by seasonal cycles (Fig 8.17g). These findings contradict the study of

Wyndham et al. (2004), who argued that the La anomaly in corals from the inshore GBR was strongly influenced by flood events.

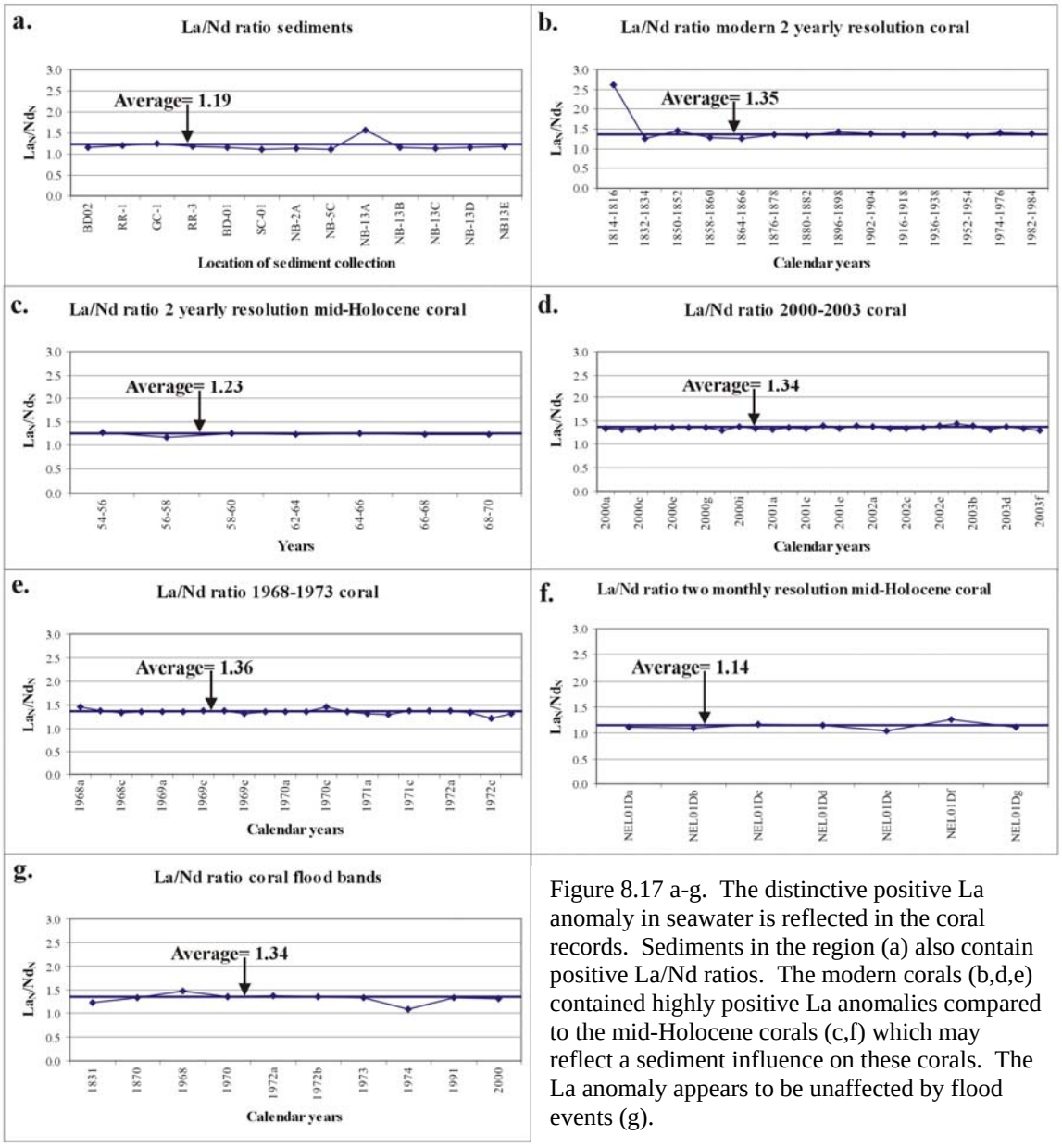

Figure 8.17 a-g. The distinctive positive La anomaly in seawater is reflected in the coral records. Sediments in the region (a) also contain positive La/Nd ratios. The modern corals (b,d,e) contained highly positive La anomalies compared to the mid-Holocene corals (c,f) which may reflect a sediment influence on these corals. The La anomaly appears to be unaffected by flood events (g).

8.6.4 The Ce anomaly

The strong negative Ce anomaly is a familiar component in seawater where Ce^{3+} is readily oxidised to the insoluble Ce^{4+} valence state (Sholkovitz et al., 1994). This negative anomaly is also a common feature in well-preserved seawater carbonates and phosphorites throughout the Phanerozoic Eon (e.g. Shields and Stille, 2001; Nothdurft et al., 2004). The only previous study to calculate the coral Ce/Ce* anomaly is Wyndham et al. (2004). Due to the absence of Pr, Wyndham et al. (2004) applied the $Ce/Ce^* = 3\times Ce_N/(2\times La_N+Nd_N)$ equation to calculate the Ce anomaly (Ce/Ce*= Ce anomaly). The presence of a positive La anomaly can influence this calculation and Bau and Dulski (1996a) proposed a new equation to evaluate the Ce anomaly by applying the normalised Pr value. A modified version of Bau and Dulski's (1996a) equation [$Pr/Pr^* = 2\times Pr_N/(Ce_N+Nd_N)$] has been employed in this study (Shields and Stille, 2001). The Ce anomalies were also calculated with Wyndham et al.'s (2004) equation, which produces results similar to the alternative Pr/Pr* calculation. This finding was not surprising as the La anomaly was remarkably consistent throughout the record and would not exert a large influence on the Ce anomaly. The modern corals displayed comparable negative Ce anomalies, with the averages ranging between 0.31-0.35 and 1.31-1.35 for Ce/Ce* and Pr/Pr*, respectively (Fig 8.18-8.19 b,d,e). Interestingly, the Ce anomalies and Pr/Pr* in the Magnetic Island corals did not appear to be influenced by flood events or seasonality, which contradicts the study of Wyndham et al. (2004) from Pandora Reef, Havannah Island and Davies Reef corals (Fig 8.18g-8.19g). The coral Ce anomaly is probably influenced by primary productivity from phytoplankton blooms following flood events.

Similarly to La, the coral Ce anomaly appears to be influenced by sediment trapped in the coral skeleton (that has no apparent anomaly; Fig 8.18-8.19 a) which was evident in the mid-Holocene coral records (Fig 7.31-7.32 c,f) and the 1974 flood (Figs 8.18g; 8.19 g). A summary of the data can be viewed using a Pr/Pr* v Ce/Ce* plot (Fig 8.20). The sediments (with the exception of NEL13a) sit within field I which is characterised by no Ce anomaly. However, the modern corals and the flood bands (except 1974) plot within the IIIb field and show a genuine negative Ce anomaly (Fig 8.20). The Ce anomaly in the 1974 flood

band sample was strongly influenced by sediment trapped within the coral lattice. The mid-Holocene corals displayed a transition between sediment and coral values, which suggests that the coral has been influenced by sediments.

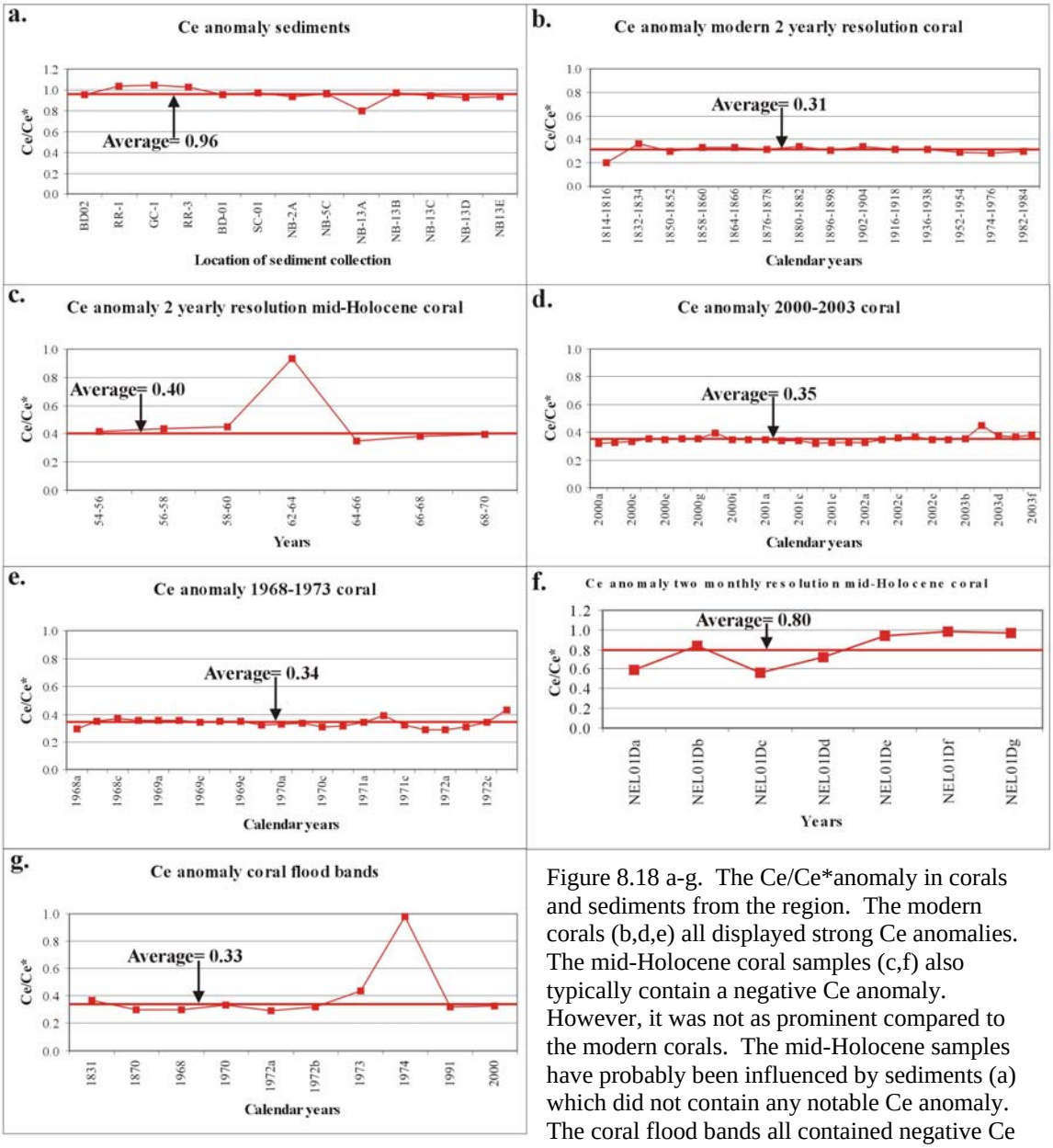

Figure 8.18 a-g. The Ce/Ce*anomaly in corals and sediments from the region. The modern corals (b,d,e) all displayed strong Ce anomalies. The mid-Holocene coral samples (c,f) also typically contain a negative Ce anomaly. However, it was not as prominent compared to the modern corals. The mid-Holocene samples have probably been influenced by sediments (a) which did not contain any notable Ce anomaly. The coral flood bands all contained negative Ce anomalies comparable to the modern corals, with the exception of the sediment-affected 1974 flood.

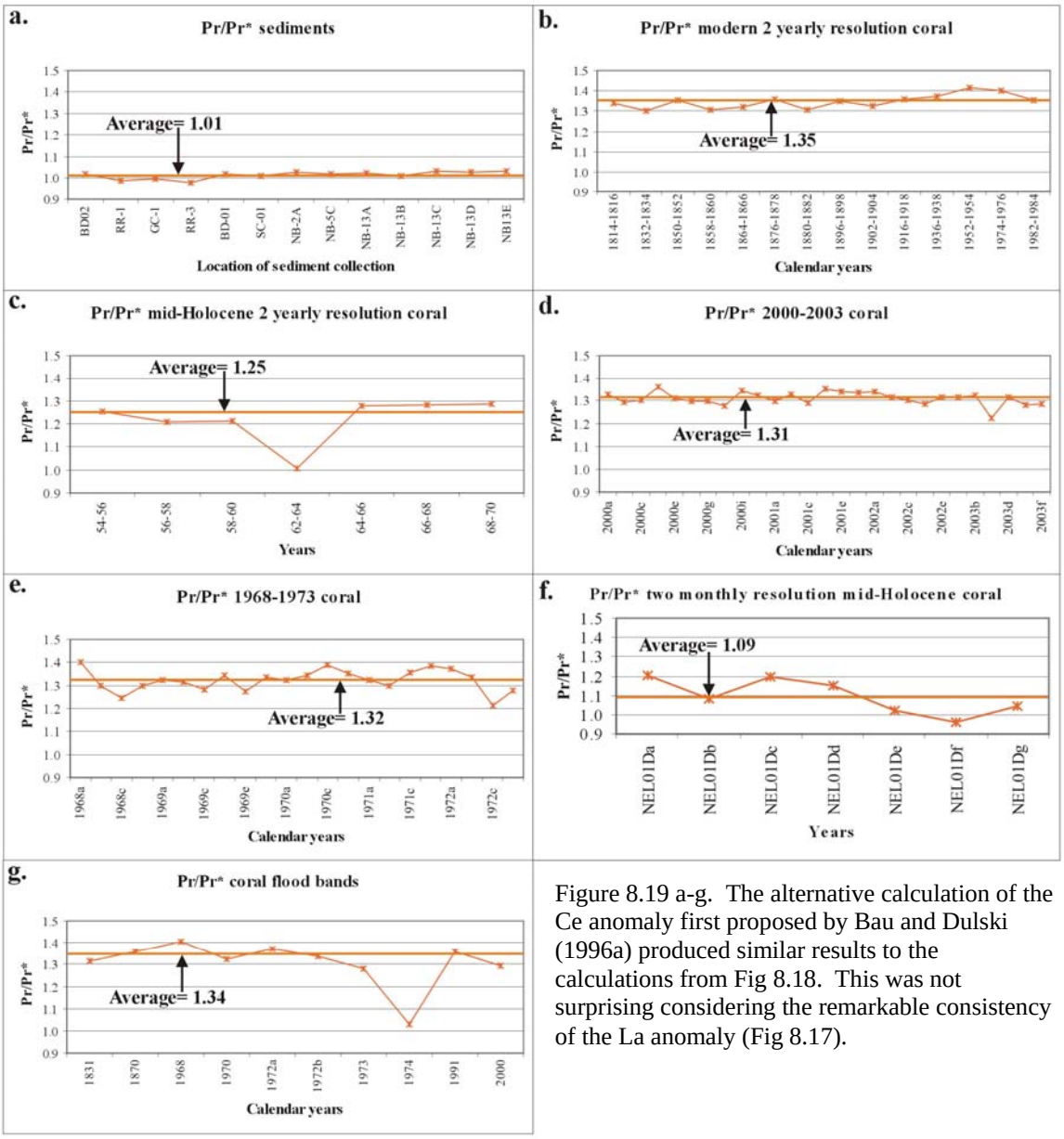

Figure 8.19 a-g. The alternative calculation of the Ce anomaly first proposed by Bau and Dulski (1996a) produced similar results to the calculations from Fig 8.18. This was not surprising considering the remarkable consistency of the La anomaly (Fig 8.17).

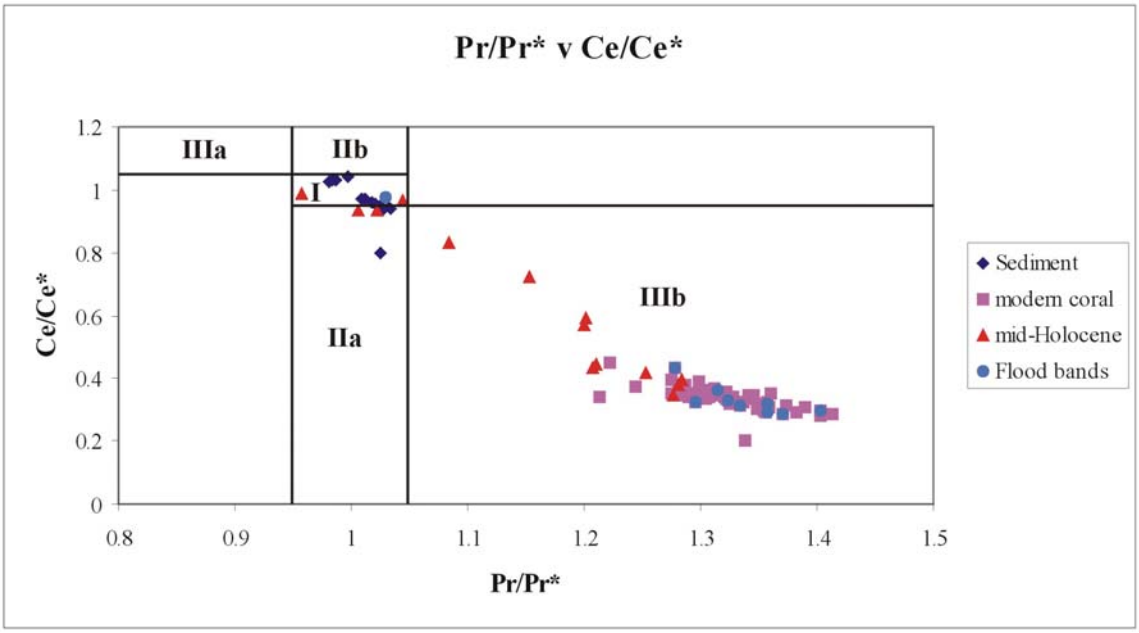

Figure 8.20. The Pr/Pr* v Ce/Ce* plot demonstrates that the negative Ce anomaly in the corals was a real feature. Samples in field IIIb indicate that there was a genuine negative Ce anomaly that could still be partially influenced by a positive La anomaly. Field IIa is characteristic of positive La anomaly results in an apparent Ce anomaly. Samples in Field IIb represents a negative La anomaly which causes an apparent positive Ce anomaly; Field I= no anomaly and field IIIa is a real, positive Ce anomaly. The sediments all contained no apparent Ce anomaly and the progressive sediment influence in the mid-Holocene corals produced a fractionation curve between the two fields. Interestingly, the Ce anomaly did not appear to be influenced by flood events, which contradicts Wyndham et al. (2004). The 1974 flood band displayed no real Ce anomaly as the sample contained sediment trapped within the coral skeleton.

8.6.5 Summary

Studies of REY distributions and the associated anomalies in coral skeletons are still at a preliminary stage, presumably due to the analytical difficulties in accurately measuring the entire REY group. However, recent technical advances in the analysis of REY have allowed this group to be measured with increased confidence. Preliminary studies have demonstrated the potential of REY in investigating environmental and anthropogenic impacts. The REY measured in *Porites* corals display a genuine seawater signature and suggest that they record oceanographic changes. This study has contributed to the understanding of the behaviour of the REY group and has developed new geochemical coral proxies to characterise terrestrial influences such as sediment provenance, sedimentation and the dominant source of freshwater runoff to coral reefs. Additional high-resolution coral studies accompanied by careful seawater and stream water analyses

are necessary to enhance knowledge of the mechanisms controlling the incorporation of the REY group in corals. The further development of the REY group is vital to better evaluate and address water quality on coral reefs.

8.7 Chapter summary

- The mid-Holocene corals died as a result of sedimentation. Coral Th concentrations, Y/Ho ratios and REY distributions are reliable proxies to determine if sediment is trapped within the coral lattice.
- The 1812-1986 modern coral records contained relatively low Th concentrations, and suggest that this coral has not been particularly affected by sedimentation. However, the REY distribution pattern indicated an increasing terrestrial influence on the coral which may be related to cattle grazing in the Burdekin River catchment. Coral Y/Ho ratios did not display any major deviations over the last 200 years, and may indicate that turbidity levels have remained constant throughout this period.
- The coral Ba/Ca ratio provided an excellent proxy to assess the export of fine-grained sediment from rivers. The Ba/Ca ratio in flood bands has significantly increased since the arrival of Europeans and was correlated with the study of McCulloch et al. (2003). The ratio may also be influenced by subtle, long-term salinity variations.
- Coral Mn concentrations track the rapid settlement of virgin land in the Burdekin River catchment. Elevated coral Mn coincided exactly with the first settlement and sheep run in the Belyando River sub-catchment. The concentrations of Mn in the 1812-1986 coral record rose and fell in accordance with the rise and fall in sheep and cattle numbers in the Burdekin catchment.
- Coral REY concentrations and the associated La and Ce anomalies displayed considerable promise as water quality proxies. As with the Ba/Ca ratio, the coral REY concentrations display a significant correlation with cattle numbers in the Burdekin River catchment and so they may be a reliable proxy of land-use and erosion. The REY distributions can be applied to determine the source of sediments trapped within the coral skeleton.

Chapter 9

Conclusions and scope for future study

9.1. Conclusions

The objective of this study was to investigate climate, water quality and the sedimentary evolution of Magnetic Island over the Holocene Epoch. The major aims and findings of this study are set out below:

Aim 1: To Investigate the Holocene evolution of the Nelly Bay fringing reef with a particular focus on the environmental setting for the mid-Holocene corals.

- Biological indicators suggest that sea level reached a height of + 1.0-1.5 m approximately 7,000 cal years BP and has oscillated up to four times since then. The sea level of eastern Australia has been stable for at least the last 1,250 cal years BP.
- The oldest C-14 age from the sediment cores suggest that Nelly Bay reef formed by at least 6,300 cal years BP. The age structure of these dates was consistent with a seawards prograding reef flat.

Aim 2: To Examine the cause of death of the mid-Holocene corals.

- Carbon-14 and U-Th dates from the outer growth layers of 3 fossil corals suggested that they died between 6,000-6,150 cal years BP. The NEL01 coral may have died around this time (growth hiatus) but regenerated and lived until 5,790 cal years BP.
- Stratigraphic evidence indicated that the mid-Holocene corals died because they were covered/buried by new coral recruits, coral fragments and fine-grained terrigenous sediments by a prograding reef flat.
- Sedimentation may have been the main contributor to the death of the mid-Holocene corals. Coral geochemical investigations from the final growth layers of the mid-Holocene corals revealed elevated Th concentrations (>20 ppb) and rare earth elements, significantly depleted Y/Ho ratios (<50) and relatively flat REY

distribution patterns. These proxies were all consistent with increasing sediments trapped within the coral skeleton.

Aim 3: To determine if the geochemical and physical coral proxies correlated with instrumental records of SST, rainfall, river discharge and turbidity.

- The coral Sr/Ca, Mg/Ca, U/Ca ratios and the O isotopes produced long-term SST estimates comparable to previous studies and instrumental data despite potential sampling, analytical and calibration errors. The long-term average for the geochemical and calcification thermometers also agreed well with each other and the instrumental record; however, large (1-3° C) variations in the SST proxies between individual samples for the 2 and 5 yearly resolution records could not all be attributed to SST. The Sr/Ca ratio was the most reliable coral SST proxy as it was the only geochemical proxy that was significantly correlated with instrumental SST and coral calcification; nevertheless, it should not be used exclusively to reconstruct SST.
- Fluctuations in the 1980-1984 two-monthly resolution coral $\Delta^{18}O$ record were linked with Burdekin River discharge data and the 1982 El Niño Southern Oscillation event. The 5 yearly salinity reconstruction displayed significant fluctuations between wetter and drier periods and coincides with the Pacific Decadal Oscillation but was not significantly correlated with coral luminescence records. The coral luminescence record was, however, significantly correlated with Burdekin River discharge and rainfall from the Burdekin River catchment. The lack of correlation between the coral $\Delta^{18}O$ record and the luminescence dataset indicates that these records were recording different environmental signals. The 5 yearly resolution coral $\Delta^{18}O$ record reveals subtle, long-term trends in salinity, whereas the luminescence dataset shows large short-term salinity variations from rainfall and river discharge events. The coral $\Delta^{18}O$ record suggests that relatively drier conditions persisted between 1830-1885 and 1935-1970, whereas wetter periods prevailed between 1885-1935 and post 1970.
- The coral Y/Ho ratio displays promise as a turbidity proxy but its full potential could not be ascertained.

Aim 4: To compare the climate and water quality conditions during the mid-Holocene with the modern coral records.

- The SST proxies suggest that seawater temperature 6,000 years ago was similar to the present.
- The long-term seawater salinity (coral $\Delta^{18}O$) average for the mid-Holocene coral was identical to the modern coral record. The two-monthly resolution NEL01D coral $\Delta^{18}O$ record showed that the mid-Holocene records may have experienced lower salinities during flood events because of the closer position of the Burdekin River at that time.
- The Ba/Ca ratios, Mn and Th concentrations, REY and heavy metals in the mid-Holocene corals were similar to the post 1850 averages measured in the modern Geoffrey Bay coral.

Aim 5: To investigate and quantify the magnitude of change in environmental characteristics using coral proxies after European settlement in the Burdekin River catchment (c. 1850).

- Sedimentation in the 1812-1986 modern coral record was negligible as apparent from the relatively low Th concentrations. However, the REY distributions indicate that there had been an increasing terrestrial influence on the coral since European settlement, and in particular, were linked to the establishment the cattle industry in the Burdekin River catchment. Coral Y/Ho ratios did not display any major deviations over this time and so turbidity levels may have remained constant throughout this period.
- The export of fine-grained sediments from rivers was examined from the coral Ba/Ca ratios. The Ba/Ca ratio in flood bands increased considerably by up to 4-5 fold since the arrival of Europeans, a finding supported by McCulloch et al. (2003). The ratio may also be influenced by long-term salinity variations. The average Ba/Ca ratio for the mid-Holocene corals was comparable to the post 1850 coral record. This suggested that the mid-Holocene coral heads may have been more influenced by either the Burdekin River or Gustav Creek than have the modern corals.

- Coral Mn concentrations appeared to track the rapid settlement of virgin land in the Burdekin River catchment. Elevated coral Mn coincided with the first settlement and sheep run in the Belyando and Suttor River sub-catchments. The concentrations of Mn in the 1812-1986 coral record rose and fell according to the rise and fall of sheep and cattle numbers in the Burdekin catchment. Relatively low coral Mn concentrations (~ < 1 ppm) were discovered in the mid-Holocene corals compared to the post 1850 coral record. This finding suggested that the enhanced coral Mn levels (> 4 ppm) in the waters surrounding Magnetic Island shortly after European settlement had not been recorded in the past and were anthropogenic impacts. More recently, coral Mn concentrations have returned to pre-1850 values.

9.2. Recommendations for further studies

Living and fossil massive corals contain a rich archive of past climate as well as environmental information essential to assess the impacts of past, present and future changes in coral reefs and adjacent catchments. While many of the coral proxies appeared to provide reliable estimations of environmental conditions, additional study is required to improve and develop coral proxies. This thesis recommends eight important topics for future research:

- Systematic study of SST calibrations of coral Sr/Ca, Mg/Ca and U/Ca proxies would significantly improve the reliability of future SST reconstructions. In particular, the study should investigate the SST calibrations for the same species of coral from one locality at varying water depths and wave exposure. Close examination of one location would provide valuable information about the minor influences on these proxies and could provide a basis for developing a strategy to correct the calibrations from possible environmental influences such as light and depth.
- Future low-resolution (~20-50 years) SST studies of *Porites* corals should use the calcification rate. This technique provides identical long-term SST estimates to the geochemical proxies, and is cheaper and less time consuming in comparison to the geochemical proxies.

- Future climatic reconstructions from coral records should use a suite of proxies ("multi-proxies") and also a number of coral records from each location to ensure accurate replication of records. The application of multi-proxy records improves the reliability of the SST reconstructions.
- The potential of the coral Y/Ho ratio as a proxy of turbidity needs to be further explored. Given that turbidity can be highly variable in the one embayment (see Appendix 12), the potential of this proxy may need to be assessed in the laboratory where turbidity and other environmental parameters can be controlled. The development of a coral turbidity proxy would be invaluable to examine long-term changes in water quality since European settlement and to assist in monitoring of reef water quality and improvements planned through the Reef Water Quality Protection Plan.
- The systematics of REE and Y in seawater should be carefully observed over a yearly period to discover how they are incorporated into the coral skeleton as well as to determine what causes REY fluctuations in corals. In addition, the release of REY from sediments into seawater in the estuarine and marine environments needs to be better understood. Seawater samples should be analysed monthly along a cross-shelf transect from the estuarine zone to the outer shelf. Measurements taken during the wet season, in particular, would furnish valuable data about the seawater mixing and the contribution of REY from rivers.
- The seasonal seawater chemistry of Ba also needs further investigation so that the various sources of Ba in seawater can be fully assessed and quantified. In particular, research would benefit from a thorough knowledge of how Ba is incorporated into the coral lattice. A cross-shelf seawater analysis, as was suggested for the REY composition, would provide insight into the behaviour of Ba in the marine environment. In addition, a thorough study of seawater chemistry during phytoplankton blooms and coral spawning events would determine their effects on coral geochemistry.
- Future historical water quality reconstructions on the GBR using coral proxies should be focused in the Cairns region where declining conditions have been

reported (e.g. Low Isles). This location would provide data to help develop potential coral water quality proxies.

- Hg, Cd and Cu concentrations should be measured in the Magnetic Island corals to examine the impact of heavy metals from mining in the Burdekin River catchment, as well as to assess any influences from the Townsville Port.

References

Abram, N.J. Gagan, M.K. McCulloch, M.T. Chappell, J. Hantoro, W.S. 2003. Coral reef death during the 1997 Indian Ocean dipole linked to Indonesian wildfires. *Science*, **301**: 952-955.

Adkins, J.F. Boyle, E.A. Curry, W.B. Lutringer, A. 2003. Stable isotopes in deep-sea corals and a new mechanism for "vital effects". *Geochimica et Cosmochimica Acta*, **67**: 1129-1143.

Akagi, T. Hashimoto, Y. Fu, F-F. Tsuno, H. Tao, H. Nakano, Y. 2004. Variation of the distribution coefficients of rare earth elements in modern coral lattices: Species and site dependencies. *Geochimica et Cosmochimica Acta*, **68**: 2265-2273.

Alibert, C. McCulloch, M.T. 1997. Strontium/calcium ratios in modern *Porites* corals from the Great Barrier Reef as a proxy for sea surface temperature: Calibration of the thermometer and monitoring of ENSO. *Paleoceanography*, **12**: 345-363.

Alibert, C. Kinsley, L. Fallon, S.J. McCulloch, M.T. Berkelmans, R. McAllister, F. 2003. Source of trace element variability in Great Barrier Reef corals affected by the Burdekin flood plumes. *Geochimica et Cosmochimica Acta*, **67**: 231-246.

Alibo, D.S. Nozaki, Y. 1999. Rare earth elements in seawater: Particle association, shale normalization, and Ce oxidation. *Geochimica et Cosmochimica Acta*, **63**: 363-372.

Allison, N. 1996. Geochemical anomalies in coral skeletons and their possible implications for palaeoenvironmental analyses. *Marine Chemistry*, **55**: 367-379.

Allison, N. Finch, A.A. Sutton, S.R. Newville, M. 2001. Strontium heterogeneity and speciation in coral aragonite: Implications for the strontium paleothermometer. *Geochimica et Cosmochimica Acta*, **65**: 2669-2676.

Allison, N. Finch, A.A. Newville, M. Sutton, S.R. 2005. Strontium in coral aragonite: 3. Sr coordination and geochemistry in relation to skeletal architecture. *Geochimica et Cosmochimica Acta*, **69**: 3801-3811.

Amos, K.J. Alexander, J. Horn, A. Pocock, G.D. Fielding, C.R. 2004. Supply limited sediment transport in a high-discharge event of the tropical Burdekin River, North Queensland, Australia. *Sedimentology*, **51**: 145-162.

Angulo, R.J. Giannini, P.C.F. Suguio, K. Pessenda, L.C.R. 1999. Relative sea-level changes in the last 5500 years in southern Brazil (Laguna-Imbituba region, Santa Catarina State) based on vermetid ^{14}C ages. *Marine Geology*, **159**: 323-339.

Baker, R.G.V. Haworth, R.J. 1997. Further evidence from relic shellcrust sequences for a late Holocene higher sea level for eastern Australia. *Marine Geology*, **141**: 1-9.

Baker, R.G.V. Haworth, R.J. 2000a. Smooth or oscillating late Holocene sea-level curve? Evidence from cross-regional statistical regressions of fixed biological

indicators. *Marine Geology*, **163**: 353-365.

Baker, R.G.V. Haworth, R.J. 2000b. Smooth or oscillating late Holocene sea-level curve? Evidence from the palaeo-zoology of fixed biological indicators in east Australia and beyond. *Marine Geology*, **163**: 367-386.

Baker, R.G.V. Haworth, R.J. Flood, P.G. 2001. Warmer or cooler late Holocene marine palaeoenvironments?: interpreting southeast Australian and Brazilian sea-level changes using fixed biological indicators and their $\delta^{18}O$ composition. *Palaeogeography, Palaeoclimatology, Palaeoecology*, **168**: 249-272.

Bard, E. Rostek, F. Ménot-Combes, G. 2004. A better radiocarbon clock. *Science*, **303**: 178-179.

Bar-Matthews, M. Wasserburg, G.J. Chen, J.H. 1993. Diagenesis of fossil coral skeletons: Correlation between trace elements, textures, and $^{234}U/^{238}U$. *Geochimica et Cosmochimica Acta*, **57**: 257-276.

Barnes, D.J. Lough, J.M. 1999. *Porites* growth characteristics in a changed environment: Misima Island, Papua New Guinea. *Coral Reefs*, **18**: 213-218.

Barnes, D.J. Taylor, R.B. 2001. On the nature and causes of luminescent lines and bands in coral skeletons. *Coral Reefs*, **19**: 221-230.

Barnes, D.J. Taylor, R.B. 2005. On the nature and causes of luminescent lines and bands in coral skeletons: II. Contribution of skeletal crystals. *Journal of Experimental Marine Biology and Ecology*, **322**: 135-142.

Barnes, D.J. Taylor, R.B. Lough, J.M. 2003. Measurement of luminescence in coral skeletons. *Journal of Experimental Marine Biology and Ecology*, **295**: 91-106.

Bau, M. 1996. Controls on the fractionation of isovalent trace elements in magmatic and aqueous systems: evidence from Y/Ho, Zr/Hf, and lanthanide tetrad effect. *Contributions Mineralogy and Petrology*, **123**: 323-333.

Bau, M. Dulski, P. 1996a. Distribution of yttrium and rare-earth elements in the Penge and Kuruman iron-formations, Transvaal Supergroup, South Africa, *Precambrian Res.*, **79**: 37-55.

Bau, M. Dulski, P. 1996b. Anthropogenic origin of positive gadolinium anomalies in river waters. *Earth and Planetary Science Letters*, **143**: 245-255.

Bau, M. Koschinsky, A. Dulski, P. Hein, J.R. 1996. Comparison of the partitioning behaviours of yttrium, rare earth elements, and titanium between hydrogenetic marine ferromanganese crusts and seawater. *Geochimica et Cosmochimica Acta*, **60**: 1709-1725.

Beale, E. 1970. *Kennedy workbook: a critical analysis of the route of E.B. Kennedy's 1848 exploration of Cape York Peninsula with a transcript of fragments of his journal*. Wollongong University College, Wollongong, 111 p.

Beaman, R. Larcombe, P. Carter, R.M. 1994. New evidence for the Holocene sea-level high from inner shelf central Great Barrier Reef, Australia. *Journal of Sedimentary Research,* **A64**: 881-885.

Beck, J.W. Lawrence Edwards, R. Ito, E. Taylor, F.W. Recy, J. Rougerie, F. Joannot, P. Henin, C. 1992. Sea-surface temperature from coral skeletal strontium/calcium ratios. *Science*, **257**: 644-647.

Beck, J.W., Recy, J., Taylor, F., Edwards, R.L. and Cabioch, G. 1997. Abrupt changes in early Holocene tropical sea surface temperature derived from coral records. *Nature*, **385**: 705-707.

Bell, P.R.F. 1992. Eutrophication and coral reefs- some examples in the Great Barrier Reef lagoon. *Water Research,* **26**: 553-568.

Bell, P.R.F. Gabric, A.J. 1991. Must GBR pollution become chronic before management reacts? *Search*, **22**: 117-119.

Bellwood, D.R. Hughes, T.P. Folke, C. Nystrom, M. 2004. Confronting the coral reef crises. *Nature,* **429:** 827-833.

Belperio, A.P. 1978. *An inner shelf sedimentation model for the Townsville region, Great Barrier Reef Province*. PhD Thesis- Dept of Geology, James Cook University, Townsville, Queensland.

Belperio, A.P. 1979. Negative evidence for a mid-Holocene high sea level along the coastal plain of the Great Barrier Reef province. *Marine Geology,* **32**: M1-M9.

Belperio, A.P. 1983. Terrigenous sedimentation in the central Great Barrier Reef lagoon: A model from the Burdekin Region. *BMR Journal of Geology and Geophysics*, **8**: 179-190.

Berkelmans, R. Oliver, J.K. 1999. Large-scale bleaching of corals on the Great Barrier Reef. *Coral Reefs,* **18**: 55-60.

Berkelmans, R. De'ath, G. Kininmonth, S. Skirving, W.J. 2004. A comparison of the 1998 and 2002 coral bleaching events on the Great Barrier Reef: spatial correlation, patterns, and predications. *Coral Reefs*, **23**: 74-83.

Bernstein, R.E. Byrne, R.H. 2004. Acantharians and marine barite. *Marine Chemistry,* **68**: 45-50.

Birkeland, C. 1982. Terrestrial runoff as a cause of outbreaks of *Acanthaster planci* (Echinodermata: Asteroidea). *Marine Biology,* **69**: 175-185.

Bishop, J.K. 1988. The barite-opal-organic carbon association in oceanic particulate matter. *Nature*, **332**: 341-343.

Blake, S.G., 1994. *Processes controlling sediment and nutrient concentrations in the Whitsunday Islands area: Implications for fringing reef communities.* PhD Thesis, Department of Geology, James Cook University, Townsville, Queensland.

Bode, A.M. 1984. *The pioneers went these ways*. A.M. Bode, Torrens Creek, QLD, 237 p.

Bolton, G.C. 1963. A thousand miles away: A history of north Queensland to 1920. *The Jacaranda Press*, Brisbane, 366 p.

BOM. 2004. Bureau of Meteorology- air temperatures Townsville. http://www.bom.gov.au/climate/averages/tables/cw_032040.shtml

Boto, K. and Isdale, P.J. 1985. Fluorescent bands in massive corals result from terrestrial fulvic acid inputs to nearshore zone. *Nature*, **315**: 396-397.

Bowman, D. 1998. Tansley review no. 101. The impact of Aboriginal landscape burning on the Australian biota. *New Phytol.*, **140**: 385-410.

Brodie, J.E. Mapstone, B.D. Mitchell, R.L. 1992. Magnetic Quay water quality and sediment baseline study. *Great Barrier Reef Marine Park Authority research publication no. 18*, Townsville, 103 p.

Brodie, J. McKergow, L.A. Prosser, I.P. Furnas, M. Hughes, A.O. Hunter, H. 2003. *Sources of sediment and nutrient exports to the Great Barrier Reef World Heritage Area*. ACTFR Report No. 03/11,Australian Centre for Tropical Freshwater Research, James Cook University, Townsville, 208 p. http://www.actfr.jcu.edu.au/Publications/PDFs/03%2711%20Sources%20of%20sediment%20and%20nutrient%20runoff%20to%20GBRWHA%201.pdf

Brodie. J. Fabricius, K. De'ath, G. Okaji, K. 2005a. Are increased nutrient inputs responsible for more outbreaks of crown-of-thorns starfish? An appraisal of the evidence. *Marine Pollution Bulletin*, **51**: 266-278.

Brodie, J., Duncan, I., Bainbridge, Z., Post, D., Furnas, M., 2005b. *Burdekin region water quality monitoring January 2005 event. Interim report to the Burdekin Dry Tropics Board, July 2005*. Available from: http://www.actfr.jcu.edu.au/PDFs/Burdekin%20region%20WQ%20monitoring%20Jan2005%20INTERIM%20REPORT.pdf

Brookins, D.G. 1989. Aqueous geochemistry of rare earth elements. In: Lipin, B.R. McKay, G.A. (Ed), Geochemistry and Mineralogy of Rare Earth Elements. *Min. Soc. Am., Rev. Mineral*, **21**: 221-225.

Brown, T.W. 1972. Silt pollution- the destruction of Magnetic Island's coral fringing reefs. *Theo W. Brown*, California, USA, 62 pp.

Bruno, J.F. Petes, L.E. Drew Havill, C. Hettinger, A. 2003. Nutrient enrichment can increase the severity of coral disease. *Ecology Letters*, **6**: 1056-1061.

Bryant, E.A. Young, R.W. Price, D.M. Short, S.A. 1992. Evidence for Pleistocene and Holocene raised marine deposits, Sandon Point, New South Wales. *Australian Journal of Earth Sciences*, **39**: 489-493.

Bryce, S. Larcombe, P. Ridd, P.V. 1998. The relative importance of landward-directed tidal sediment transport versus freshwater flood events in the Normanby River estuary, Cape York Peninsula, Australia. *Marine Geology*, **149**: 55-78.

Buddemeier, R.W. Kleypas, J.A. Aronson, R.B. 2004. Coral reefs and global climate change: Potential contributions of climate change to stresses on coral reef ecosystems. Pew Center on Global Climate Change report: www.pewclimate.org 44 pp.

Bunt, J.S. Williams, W.T. Bunt, E.D. 1985. Mangrove species distribution in relation to tide at the seafront and up rivers. *Australian Journal of Marine and Freshwater Research*, **36**: 481-492.

Byrne, R. Sholkovitz, E. 1996. Marine chemistry and geochemistry of lanthanides. In: Gschneider, K.A. Eyring, L. (ed). *Handbook on the Physics and Chemistry of the Rare Earths Vol 23*, Elsevier, Amsterdam, p 497-593.

Campbell, J. 1936. *The early settlement of Queensland*. The Bibliographical society of Queensland transactions second series no 1, Brisbane, 48 p.

Cardinal, D. Hamelin, B. Bard, E. Pätzold, J. 2001. Sr/Ca, U/Ca, and $\delta^{18}O$ records in recent massive corals from Bermuda: relationships with sea surface temperature. *Chemical Geology*, **176**: 213-233.

Carter, R.M. Carter, L. Johnson, D.P. 1986. Submergent shorelines in the SW Pacific: evidence for an episodic post-glacial transgression. *Sedimentology*, **33**: 629-649.

Carter, R.M. Johnson, D.P. 1986. Sea-level controls on the post-glacial development of the Great Barrier Reef, Queensland. *Marine Geology*, **71**: 137-164.

Carter, R.M. Johnson, D.P. 1987. *Post-glacial sediment distribution in Cleveland Bay, Townsville*. Marine Geoscience Group, Geology Department, James Cook University of North Queensland, Townsville.

Carter, R.M. Johnson, D.P. 1989. *Offshore seismic investigation, Nelly Bay Magnetic Island*. Report 7th August, 1989, James Cook University.

Carter, R.M. Johnson, D.P. Hooper, K.G. 1993. Episodic post-glacial sea-level rise and the sedimentary evolution of a tropical continental embayment (Cleveland Bay, Great Barrier Reef shelf, Australia. *Australian Journal of Earth Sciences*, **40**: 229-255.

Carter, R.M. Larcombe, P. 2002. Geological and sedimentary characteristics of Cleveland Bay. In: Cleveland Bay Status Report- 2002. www.clevelandbayconsortium.com

Chappell, J. Rhodes, E.G. Thom, B.G. Wallensky, E. 1982. Hydro-Isostasy and sea-level isobase of 5500 B.P. in North Queensland, Australia. *Marine Geology*, **49**: 81-90.

Chappell, J. 1983. Evidence for smoothly falling sea level relative to north Queensland, Australia, during the past 6,000 yr. *Nature*, **302**: 406-408.

Chappell, J. Chivas, A. Wallensky, E. Polach, H.A. Aharon, P. 1983. Holocene Palaeo-Environmental changes, central to north Barrier Reef inner zone. *Journal of Australian Geology and Geophysics*, **8**: 223-235.

Chirenje, T. Ma, L.Q. 2002. Impact of high-volume wood-fired boiler ash amendment on soil properties and nutrients. *Commun. Soil. Sci. Plant Anal.*, **33**: 1-17.

Cobb, K.M. Charles, C.D. Cheng, H. Kastner, M. Edwards, R.L. 2003. U/Th-dating living and young fossil corals from the central tropical Pacific. *Earth and Planetary Science Letters*, **210**: 91-103.

Coffey, M. Dehairs, F. Collette, O. Luther, G. Church, T. Jickells, T. 1997. The behaviour of dissolved barium in estuaries. *Estuarine, Coastal and Shelf Science*, **45**: 113-121.

Cohen, A.L. Layne, G.D. Hart, S.R. Lobel, P.S. 2001. Kinetic control of skeletal Sr/Ca in a symbiotic coral: Implications for the paleotemperature proxy. *Paleoceanography*, **16**: 20-26.

Cohen, A.L. Owens, K.E. Layne, G.D. Shimizu, N. 2002. The effect of algal symbionts on the accuracy of Sr/Ca paleotemperatures from coral. *Science*, **296**: 331-333.

Cohen, A.L. Sohn, R.A. 2004. Tidal modulation of Sr/Ca ratios in a Pacific reef coral. *Geophysical Research Letters*, **31**: L16310.

Colbert, D. McManus, J. 2005. Importance of seasonal variability and coastal processes on estuarine manganese and barium cycling in a Pacific Northwest estuary. *Continental Shelf Research*, **25**: 1395-1414.

Cole, J. 2003. Dishing the dirt on coral reefs. *Nature* **421**: 705-706.

Collins, J. 1987. Fringing reefs of Magnetic Island. In: Baldwin, C.L. (ed). *Fringing reef workshop: science, industry and management: proceedings of a workshop held at Arcadia Resort, Magnetic Island, Australia, October 23-25th 1986*. Great Barrier Reef Marine Park Authority, Townsville, p 44-49.

Cronin, T.M. 1999. *Principles of paleoclimatology*. Columbia University Press, New York, 560 p.

Crowley, T.J. Quinn, T.M. Hyde, W.T. 1999. Validation of coral temperature calibrations. *Paleoceanography*, **14**: 605-615.

Cunningham, M.W. 1895. *The pioneering of the River Burdekin*. Argus Office, Rockhampton, 6 p.

Dagg, M. Benner, R. Lohrenz, S. Lawrence, D. 2004. Transformation of dissolved and particulate materials on continental shelves influenced by rivers: plume processes. *Continental Shelf Research*, **24**: 833-858.

Davis, A.M. Aitchison, J.C. Flood, P.G. Morton, B.S. Baker, R.G.V. Haworth, R.J. 2000. Late Holocene higher sea-level indicators from the South China coast. *Marine Geology*, **171**: 1-5.

de Baar, H.J.W. Bacon, M.P. Brewer, P.G. 1985a. Rare earth elements in the Pacific and Atlantic Oceans. *Geochimica et Cosmochimica Acta*, **49**: 1943-1959.

de Baar, H.J.W. Bacon, M.P. Brewer, P.G. 1985b. Anomalies in rare earth distributions in seawater: Gd and Tb . *Geochimica et Cosmochimica Acta*, **49**: 1961-1969.

de Villiers, S. Shen, G.T. Nelson, B.K. 1994. The Sr/Ca-temperature relationship in coralline aragonite: Influence of variability in $(Sr/Ca)_{seawater}$ and skeletal growth parameters. *Geochimica et Cosmochimica Acta*, **58**: 197-208.

de Villiers, S. Nelson, B.K. Chivas, A.R. 1995. Biological controls on coral Sr/Ca and $d^{18}O$ reconstructions of sea surface temperatures. *Science*, **269**: 1247-1249.

de Vries, H. 1958. Variation in concentration of radiocarbon with time and location on Earth. *Proc. Koninkl. Akad. Wetenschappen*, **B61**: 1-9.

Devlin, M. Waterhouse, J. Taylor, J. Brodie, J. 2001. *Flood plumes in the Great Barrier Reef: Spatial and temporal patterns in composition and distribution*. GBRMPA Publication No. 68.

Devlin, M.J. Brodie, J. 2005. Terrestrial discharge into the Great Barrier Reef Lagoon: nutrient behaviour in coastal waters. *Marine Pollution Bulletin*, **51**: 9-22.

Dickenson, W.R. 2004. Impacts of eustasy and hydro-isostasy on the evolution and landforms of Pacific atolls. *Palaeogeography, Palaeoclimatology, Palaeoecology*, **213**: 251-269.

Doherty, G.B. Brunskill, G.J. Ridd, M.J. 2000. Natural and enhanced concentrations of trace metals in sediments of Cleveland Bay, Great Barrier Reef Lagoon, Australia. *Marine Pollution Bulletin*, **41**: 337-344.

Duke, N.C. Wolanski, E. 2001. Muddy coastal waters and depleted mangrove coastlines- depleted seagrass and coral reefs. In: Wolanski, E (ed). *Oceanographic processes of coral reefs- Physical and biological links in the Great Barrier Reef.* CRC Press, Boca Raton, p 77-91.

Dulski, P. 1994. Inferences of oxide, hydroxide and chloride analyte species in the determination of rare earth elements in geological samples by inductively coupled plasma-mass spectrometry. *Journal of Analytical Chemistry*, **350**: 194-203.

Dunbar, R.B. Wellington, G.M. Colgan, M.W. Glynn, P.W. 1994. Eastern Pacific sea surface temperature since 1600 A.D.: The δ18O record of climate variability in Galápagos corals. *Paleoceanography*, **9**: 291-315.

Eggins, S.M. Woodhead, J.D. Kinsley, L.P.J. Mortimer, G.E. Sylvester, P. McCulloch, M.T. Hergt, J.M. Handler, M.R. 1997. A simple method for the precise determination of > 40 trace elements in geological samples by ICPMS using enriched isotope internal standardisation. *Chemical Geology*, **134**: 311-326.

Endean, R. Kenny, R. Stephenson, W. 1956a. The ecology and distribution of intertidal organisms on the rocky shores of the Queensland mainland. *Marine and Freshwater Research*, **7**: 88-146.

Endean, R. Stephenson, W. Kenny, R. 1956b. The ecology and distribution of intertidal organisms on certain islands off the Queensland coast. *Marine and Freshwater Research*, **7**: 317-342.

Enmar, R. Stein, M. Bar-Matthews, M. Sass, E. Katz, A. Lazar, B. 2000. Diagenesis in live corals from the Gulf of Aqaba. I. The effect on paleo-oceanography tracers. *Geochimica et Cosmochimica Acta*, **64**: 3123-3132.

Epstein, S. Buchsbaum, R. Lowenstam, H.A. Urey, H.C. 1953. Revised carbonate-water isotopic temperature scale. *Bulletin of the Geological Society of America*, **64**: 1315-1326.

Esslemont, G. 2000. Heavy metals in seawater, marine sediments and corals from the Townsville section, Great Barrier Reef Marine Park, Queensland. *Marine Chemistry*, **71**: 215-231.

Esslemont, G. Russell, R.A. Maher, W.A. 2004. Coral record of harbour dredging: Townsville, Australia. *Journal of Marine Systems*, **52**: 51-64.

Evans, M.N. Kaplan, A. Cane, M.A. 2000. Intercomparison of coral oxygen isotope data and historical sea surface temperature (SST): Potential for coral-based SST field reconstructions. *Paleoceanography*, **15**: 551-563.

Fabricius, K.E. 2005. Effects of terrestrial runoff on the ecology of corals and coral reefs: review and synthesis. *Marine Pollution Bulletin*, **50**: 125-146.

Fabricius, K.E. Wolanski, E. 2000. Rapid smothering of coral reef organisms by muddy marine snow. *Estuarine, Coastal and Shelf Science*, **50**: 115-120.

Fabricius, K. De'ath, G. 2001a. Biodiversity on the Great Barrier Reef: Large-scale patterns and turbidity related local loss of soft coral taxa. In: Wolanski, E. (ed). *Oceanographic Processes on Coral Reefs*. CRC Press, Boca Raton, p 127-143.

Fabricius, K. De'ath, G. 2001b. Environmental factors associated with the spatial distribution of crustose coralline algae on the Great Barrier Reef. *Coral Reefs*, **19**: 303-309.

Fabricius, K. De'ath, G. McCook, L. Turak, E. Williams D. 2005. Changes in algal, coral and fish assemblages along water quality gradients on the inshore Great Barrier Reef. *Marine Pollution Bulletin*, **51**: 384-398.

Fallon, S.J. McCulloch, M.T. van Woesik, R. Sinclair, D.J. 1999. Corals at their latitudinal limits: laser ablation trace element systematics in *Porites* from Shirigai Bay, Japan. *Earth and Planetary Science Letters*, **172**: 221-238.

Fallon, S.J. White, J.C. McCulloch, M.T. 2002. *Porites* corals as recorders of mining and environmental impacts: Misima Island, Papua New Guinea. *Geochimica et Cosmochimica Acta*, **66**: 45-62.

Fallon, S.J. McCulloch, M.T. Alibert, C. 2003. Examining water temperature proxies in Porites corals from the Great Barrier Reef: a cross-shelf comparison. *Coral Reefs*, **22**: 389-404.

Faure, G. 1998. *Principles and applications of geochemistry: a comprehensive textbook for geology students* (2nd Ed). Prentice Hall, New Jersey.

Felis, T. Pätzold, J. Loya, Y. 2003. Mean oxygen-isotope signatures in *Porites* spp. corals: inter-colony variability and correction for extension-rate effects. *Coral Reefs*, **22**: 328-336.

Felis, T. Pätzold, J. 2003. Climate records from corals. **In**: Wefer, G. Lamy, F. Mantoura, F. (eds). *Marine Science Frontiers for Europe*, Springer-Verlag, Berlin, p 11-27.

Fensham, R.J. Fairfax, R.J. Butler, D.W. Bowman, D.M.J.S. Effects of fire and drought in a tropical eucalypt savanna colonized by rain forest. *Journal of Biogeography* **30**: 1405-1414.

Fielding, C.R. Trueman, J.D. Dickens, G.D. Page, M. 2003. Anatomy of the buried Burdekin River channel across the Great Barrier Reef shelf: how does a major river operate on a tropical mixed siliciclastic/carbonate margin during sea level lowstand? *Sedimentary Geology*, **157**: 291-301.

Fielding, C.R. Trueman, J.D. Dickens, G.D. Page, M. 2005a. Geomorphology and internal architecture of the ancestral Burdekin River across the Great Barrier Reef shelf, north-east Australia. *Special Publication International Association of Sedimentologists*, **35**: 321-347.

Fielding, C.R. Trueman, J. Alexander, J. 2005b. Sedimentology of the modern and Holocene Burdekin River delta of north Queensland, Australia- controlled by river output, not by waves and tides. **In:** Giosan, L. Bhattacharya, J (eds). *River deltas: Concepts, models and examples*, SEPM, special publication 83, p 467-496.

Fielding, C.R. Trueman, J.D. Alexander, J. 2006. Holocene depositional history of the Burdekin delta of northeastern Australia: A model for a low accommodation, highstand delta. *Journal of Sedimentary Research*, **76**: 411-428.

Fink, D. Hotchkis, Hua, Q. Jacobsen, G. Smith, A.M. Zoppi, U. Child, D. Mifsud, C. van der Gaast, H. Williams, A. Williams, M. 2004. The ANTARES AMS facility at ANSTO. *NIM B*, **223-224**: 109-115.

Flannery, T. 1994. *The future eaters: An ecological history of the Australasian lands and people*. Grove Press, New York 423 pp.

Flood, P.G. Frankel, E. 1989. Late Holocene higher sea level indicators from eastern Australia. *Marine Geology*, **90**: 193-195.

Furnas, M.J. 1989. Cyclonic disturbance and a phytoplankton bloom in a tropical shelf system. In: Okaichi, T. Anderson, D.M. Nemoto, T. (eds). *Red tides: Environmental science and toxicology*. Elsevier, Tokyo, p 273-276.

Furnas, M.J. 1991. Net in situ growth rates of phytoplankton in an oligotrophic, tropical shelf ecosystem. *Limnology and Oceanography*, **36**: 13-29.

Furnas, M. 2003. *Catchments and corals: Terrestrial runoff to the Great Barrier Reef.* Australian Institute of Marine Science, Townsville, 334 pp.

Furnas, M.J. Mitchell, A.W. Skuza, M. Brodie, J.E. 2005. The other 90 percent: phytoplankton responses to enhanced nutrient availability in the Great Barrier Reef lagoon. *Marine Pollution Bulletin*, **51**: 253-265.

Gagan, M.K. Chivas, A.R. Isdale, P.J. 1994. High-resolution isotopic records from corals using ocean temperature and mass spawning chronometers. *Earth and Planetary Science Letters*, **121**: 549-558.

Gagan, M.K. Ayliffe, L.K. Hopley, D. Cali, J.A. Mortimer, G.E. Chappell, J. McCulloch, M.T. Head, M.J. 1998. Temperature and surface-ocean water balance of the mid-Holocene tropical western Pacific. *Science*, **279**: 1014-1018.

Gagan, M.K. Ayliffe, L.K. Beck, J.W. Cole, J.E. Druffel, E.R.M. Dunbar, R.B. Schrag, D.P. 2000. New views of tropical paleoclimates from corals. *Quaternary Science Reviews*, **19**: 45-64.

GBRMPA. 2003. Sea surface temperature data Nelly and Geoffrey Bays. http://www.gbrmpa.gov.au/corp_site/info_services/science/seatemp/tsv.html

Gill, E.D. Hopley, D. 1972. Holocene sea levels in Eastern Australia- A discussion. *Marine Geology*, **12**: 223-242.

Gillespie, R. Polach, H.A. 1979. The suitability of marine shells for radiocarbon dating of Australian prehistory. In: Berger, R. Suess, H. (eds). *Proceedings of the Ninth International Conference on Radiocarbon Dating*, 404-421.

Golder Associates Pty Ltd. 2000. *Geotechnical investigation proposed revetments Nelly bay harbour development Magnetic Island, Queensland*. Report March 2000.

Griffiths, T. 2002. How many trees make a forest? Cultural debates about vegetation change in Australia. *Aust. J. Bot*. **50**: 375-389.

Hanna, R.G. Muir, G.L. 1990. Red Sea corals as biomonitors of trace metal pollution. *Environmental Monitoring and Assessment*, 14: 211-222.

Harris, P.T. Davies, P.J. Marshall, J.F. 1990. Late Quaternary sedimentation on the Great Barrier Reef continental shelf and slope east of Townsville, Australia. *Marine Geology*, **94**: 55-77.

Harris, P.T. 1999. Sequence architecture during the Holocene transgression: an example from the Great Barrier Reef shelf, Australia- Comment. *Sedimentary Geology*, **125**: 235-239.

Hayne, M. Chappell, J. 2001. Cyclone frequency during the last 5000 years at Curacoa Island, north Queensland, Australia. *Palaeogeography, Palaeoclimatology, Palaeoecology*, **168**: 207-219.

Haynes, D. Johnson, J.E. 2000. Organochlorine, Heavy Metal and Polyaromatic Hydrocarbon Pollutant Concentrations in the Great Barrier Reef (Australia) Environment: a Review. *Marine Pollution Bulletin*, **41**: 267-278.

Haynes, D. Michalek-Wagner, K. 2000. Water quality in the Great Barrier Reef World heritage Area: Past perspectives, current issues and new research directions. *Marine Pollution Bulletin*, **41**: 428-434.

Heiss, G.A. Camoin, G.F. Eisenhauer, A. Dullo, W.C. Hansen, B. 1997. Stable isotope and Sr/Ca-signals in corals from the Indian Ocean. *Proceedings from the 8th International Coral Reef Symposium, Panama*, **12**: 1713-1718.

Henderson, R.A. Walbran, P.D. 1992. Interpretation of the fossil record of *Ancanthaster planci* from the Great Barrier Reef: a reply to criticism. *Coral Reefs*, **11**: 95-101.

Hendy, E.J. 2003. *Coral reconstructions of decadal-to-centennial climate variability in the Great Barrier Reef since 1565 AD*. PhD Thesis, Australian National University, 317 pp.

Hendy, E.J. Gagan, M.K. Alibert, C.A. McCulloch, M.T. Lough, J.M. Isdale, P.J. 2002. Abrupt decrease in tropical Pacific sea surface salinity at end of little ice age. *Science*, **295**: 1511-1514.

Hendy, E.J. Lough, J.M. Gagan, M.K. 2003. Historical mortality in massive *Porites* from the central Great Barrier Reef, Australia: evidence for past environmental stress? *Coral Reefs*, **22**: 207-215.

Hendy, E.J. Gagan, M.K. Lough, J.M. Submitted. The origin of stable isotope variability in corals over multi-century timescales. *Geochimica et Cosmochimica Acta*,

Higley, M. 2000. *Fossil oyster beds of the mid-Holocene highstand of relative sea level: GBR shelf.* Honours Thesis, School of Earth Sciences, James Cook University, Townsville, 118 pp.

Hilliard, R.W. Raaymakers, S.C. 1996. Review of dredging operations at ports in the Great Barrier reef region. **In:** Larcombe, P. Woolfe, K. Purdon, R. (eds). *Great Barrier Reef: Terrigenous sediment flux and human impacts*. Marine Geophysical Laboratory, Earth Sciences Department, James Cook University, Second edition- November 1996.

Hoegh-Guldberg, O. 1999. Climate change, coral bleaching and the future of the world's coral reefs. *Marine Freshwater Research*, **50**: 839-866.

Hoegh-Guldberg, O. 2005. Coral reefs in 2050: life in a warm, acidic ocean. **In**: *Australian Coral Reef Society 81st Annual Conference: Managing and researching reefs in a changing world 19th-21st August 2005*, Heron Island Research Station Queensland.

Hopley, D. 1970a. *The geomorphology of the Burdekin delta north Queensland.* Department of Geography, James Cook University of North Queensland.

Hopley, D. 1970b. *Coastal geomorphology in the Townsville region: A study of the geomorphological evolution of the north Queensland coast between Cape Upstart and Hinchinbrook Island*. PhD Thesis, Department of Geography, James Cook University, Townsville.

Hopley, D. 1971. The origin and significance of north Queensland island spits. *Zeitschrift für Geomorphologie*, **15**: 371-389.

Hopley, D. 1973. Geomorphic evidence for climate change in the Late Quaternary of northeast Queensland, Australia. *Journal of Tropical Geography*, **36**: 20-30.

Hopley, D. 1974a. Coastal changes produced by Tropical Cyclone Althea in Queensland; December 1971. *The Australian Geographer*, **XII, 5**: 445-456.

Hopley, D. 1974b. The Cyclone Althea storm surge. *Australian Geographical Studies*, **12**: 90-106.

Hopley, D. 1975. Contrasting evidence for Holocene sea levels with special reference to the Bowen-Whitsunday area of Queensland. **In:** Douglas, I. Hobbs, J.E. Pigram, J.J. *Geographical essays in honour of Gilbert J. Butland*. Department of Geography, University of New England, Armidale, pp 51-84.

Hopley, D. 1978. *Geographical studies of the Townsville area*. Department of Geography monograph series no. 2. 143 p.

Hopley, D. 1980. Mid-Holocene high sea levels along the coastal plain of the Great Barrier Reef province: A discussion. *Marine Geology*, **35**: M1-M9.

Hopley, D. Slocombe, A.M. Grant, C. 1983. Nearshore fringing reefs in north Queensland. *Coral Reefs*, **1**: 151-160.

Hopley, D. 1983. Evidence of 15,000 years of sea level change in tropical Queensland. **In:** Hopley, D. (ed). *Australian sea levels in the last 15 000 years: A review*. Geography Department, Monograph Series Occasional Paper 3, James Cook University, Townsville, p 93-104.

Hopley, D. 1986. **In:** McIntyre and Associates Pty. Ltd. Magnetic Keys Development, Nelly Bay- Magnetic Island- impact assessment study volume 2- technical reports. Job no 5233, May 1986.

Hopley, D. 1994. Continental shelf systems. In: Carter, R.W.G. Woodroffe, C.D. (eds). *Coastal Evolution: Late Quaternary shoreline morphodynamics*. Cambridge University Press, p 303-340.

Hopley, D. Partain, B. 1987. The structure and development of fringing reefs off the Great Barrier Reef province. In: Baldwin, C.L. (ed). *Fringing reef workshop: science, industry and management: proceedings of a workshop held at Arcadia Resort, Magnetic Island, Australia, October 23-25th 1986*. Great Barrier Reef Marine Park Authority, Townsville, p 13-33.

Hopley, D. Yellowless, D. Cuff, C. 1991. Reef pollution in the 1980's. *Search*, **22**: 121.

Houghton, J.T. Ding, Y. Griggs, D.J. Noguer, M. *et al*. (eds). 2001. *Climate Change 2001: The scientific basis*. Cambridge University Press, New York.

Hoyle, J. Elderfield, H. Gledhill, A. Greaves, M. 1984. The behaviour of the rare earth elements during mixing of river and sea waters. *Geochimica et Cosmochimica Acta*, **48**: 143-149.

Hughen, K.A. Baillie, M.G.L. Bard, E. Bayliss, A. *et al*. 2004. Marine04 marine radiocarbon age calibration, 26-0 ka BP. *Radiocarbon*, **46**: 1059-1086.

Hughes, T.P. 1994. Catastrophes, phase shifts, and large-scale degradation of a Caribbean coral reef. *Science*, **265**: 1547-1551.

Hughes, T.P Baird, A.H. Bellwood, D.R. Card, M. Connolly, S.R. Folke, C. Grosberg, R. Hoegh-Guldberg, O. Jackson, J.B.C, Kleypas, J. Lough, J.M. Marshall, P. Nyström, M. Palumbi, S.R. Pandolfi, J.M. Rosen, B. Roughgarden, J. 2003. Climate change, human impacts, and the resilience of coral reefs. *Science*, **301**: 929-933.

Isdale, P. 1984. Fluorescent bands in massive corals record centuries of coastal rainfall. *Nature*, **310**: 578-579.

Isdale, P.J. Daniel, E. 1989. The design and deployment of a new lightweight submarine fixed drilling system for the acquisition and preparation on coral cores. *Marine Technology Society Journal*, **23**: 3-8.

Isdale, P.J. Stewart, B.J. Tickle, K.S. Lough, J.M. 1998. Palaeohydrological variation in a tropical river catchment: a reconstruction using fluorescent bands in corals of the Great Barrier Reef, Australia. *The Holocene*, **8**: 1-8.

Johnson, D.P. Searle, D.E. Hopley, D. 1982. Positive relief over buried post-glacial channels, Great Barrier Reef province, Australia. *Marine Geology*, **46**: 149-159.

Johnson, D.P. Searle, D.E. 1984. Post-glacial seismic stratigraphy, central Great Barrier Reef, Australia. *Sedimentology*, **31**: 335-352.

Johnson, D.P. Risk, M.J. 1987. Fringing reef growth on terrigenous mud foundation, Fantome Island, central Great Barrier Reef, Australia. *Sedimentology*, **34**: 275-287.

Jokiel, P.L. 2004. Temperature stress and coral bleaching. In: Rosenberg, E. Loya, Y. (eds). *Coral Heath and Disease*. Springer-Verlag, Berlin, p 401-425.

Jones, G.B. Mercurio, P. Olivier, F. 2000. Zinc in fish, crabs, oysters, and Mangrove Flora and Fauna from Cleveland Bay. *Marine Pollution Bulletin*, **41**: 345-352.

Jones, P.D. New, M. Parker, D.E. Martin, S. Rigor, I.G. 1999. Surface air temperature and its changes over the past 150 years. *Reviews of Geophysics*, **37**: 173-199.

Jones, R. 1969. Fire stick farming. *Australian Natural History, September issue*, **225**.

Jones, R.J. Berkelmans, R. Oliver, J.K. 1997. Recurrent bleaching of corals at Magnetic Island (Australia) relative to air and seawater temperature. *Marine Ecology Progress Series*, **158**: 289-292.

Kamber, B.S. Grieg, A. Collerson, K.D. 2005. A new estimate for the composition of weathered young upper continental crust from alluvial sediments, Queensland, Australia. *Geochimica et Cosmochimica Acta*, **69**: 1041-1058.

Kan, H. Nakashima, Y. Hopley, D. 1997. Coral communities during structural development of a fringing reef flat. Hayman Island, The Great Barrier Reef. *Proceedings 8th International Coral Reef Symposium* **1**: 465-470.

Keesing, J.K. Bradbury, R.H. De Vantier, L.M. Riddle, M.J. De'ath, G. 1992. Geological evidence for recurring outbreaks of the crown-of-thorns starfish: a reassessment from an ecological perspective. *Coral Reefs*, **11**: 79-85.

Kenny, R. 1974. Inshore surface sea temperatures at Townsville. *Australian Journal of Marine and Freshwater Research*, **25**: 1-5.

Kerr, J.D. 1994. *Black snow and liquid gold: A history of the Burdekin Shire*. Council of the Shire of Burdekin, Queensland.

Kershaw, A.P. 1970. A pollen diagram from Lake Euramoo, north-east Queensland, Australia. *New Phytol*, **69**: 785-805.

Kershaw, A.P. 1971. A late Pleistocene and Holocene pollen diagram from Lynch's Crater, north-eastern Queensland, Australia. *New Phytol*, **77**: 469-498.

Kershaw, A.P. 1974. A long continuous pollen sequence from north-eastern Australia. *Nature*, **251**: 222-223.

Kershaw, A.P. 1975a. A pollen diagram from Quincan Crater, north-eats Queensland, Australia. *New Phytol*, **70**: 669-681.

Kershaw, A.P. 1975b. Late Quaternary vegetation and climate in north-eastern Australia. In: Suggate, R.P. Cresswell, M.M. (Eds.). *Quaternary Studies*. The Royal Society of New Zealand, Wellington, pp.181-187

Kershaw, A.P. 1976. A late Pleistocene and Holocene pollen diagram from Lynch's Crater, north-eastern Queensland, Australia. *New Phytol*, **77**: 469-498.

King, B. McAllister, F. Wolanski, E. Done, T. Spagnol, S. 2001. River plume dynamics in the Central Great Barrier Reef. In: Wolanski, E. *Oceanographic Processes of Coral Reefs: Physical and biological links in the Great Barrier Reef*, CRC Press, Boca Raton, p 145-160.

Kinsey, D.W. 1988. Coral reef system response to some natural and anthropogenic stresses. *Galaxea,* **1**: 113-128.

Kinsey, D.W. 1991a. Can we resolve the nutrient issue for the reef? *Search*, **22**: 119-121.

Kinsley, D.W. 1991b. The coral reef: an owner-built, high-density, fully-serviced, self-sufficient housing estate in the desert- or is it? *Symbiosis*, **10**: 1-22.

Kinsman, D.J.J. 1964. Reef coral tolerance of high temperatures and salinities. *Nature,* **202**: 1280-1282.

Klein, R. Tudhope, A.W. Chilcott, C.P. Pätzold, J. Abdulkarim, Z. Fine, M. Fallick, A.E. Loya, Y. 1997. Evaluating southern Red Sea corals as a proxy record for the Asian monsoon. *Earth and Planetary Science Letters*, **148**: 381-394.

Kleypas, J.A. Buddemeier, R.W. Archer, D. Gattuso, J-P. Langdon, G. Opdyke, B.N. 1999. Geochemical consequences of increased atmospheric carbon dioxide on coral reefs. *Science*, **284**: 118-120.

Kleypas, J.A. Buddemeier, R.W. Eakin, C.M. Guttuso, J-P. Guinotte, J. Hoegh-Guldberg, O. Iglesias-Prieto, R. Jokiel, P.L. Langdon, C. Skirving, W. Strong, A.E. 2005. Comment on "Coral reef calcification and climate change: the effect of ocean warming". *Geophysical Research Letters*, **32**: L08601.

Knight, J.J. 1895. *In the early days: history and incident of pioneer Queensland.* Sapsford and Co., Brisbane, 390 p.

Knutson, R.A. Buddemeier, R.W. Smith, S.V. 1972. Coral chronometers: seasonal growth bands in coral reefs. *Science,* **177**: 270-272.

Koop, K. Booth, D. Broadbent, A. Brodie, J. *et al*. 2001. ENCORE: The effect of nutrient enrichment on coral reefs. Synthesis of results and conclusions. *Marine Pollution Bulletin,* **42**: 91-120.

Koskela, R. Lee, J. Venables, W. Fraser, A. Koskela, T. Fryar, R. Catchment modifications and temporal variation in water quality in Nelly Bay (Magnetic Island), Great Barrier Reef Marine Park. **In:** Haynes, D. Schaffelke, B. (March) 2004. *Catchment to reef: Water quality issues in the Great Barrier Reef Region.* CRC Reef Research Centre Technical Report no. **53**, p .

Lambeck, K. Nakada, M. 1990. Late Pleistocene and Holocene sea-level change along the Australian coast. *Palaeogeography, Palaeoclimatology, Palaeoecology,* **89**: 143-176.

Lambeck, K. Chappell, J. 2001. Sea level change through the last glacial cycle. *Science*, **292**: 679-686.

Lambeck, A. Woolfe, K.J. 2000. Composition and textual variability along the 10m isobath, Great Barrier Reef: evidence for pervasive northward sediment transport. *Australian Journal of Earth Sciences*, **47**: 327-335.

Larcombe, P. 2001. Holocene Great Barrier Reef: sedimentary controls and implications for environmental management. *Geological Society of Australia Special Publication*, **21**: 281-294.

Larcombe, P. Ridd, P.V. 1994. Data interpretation. **In:** Benson, L.J. Goldsworthy, P.M. Butler, I.R. Oliver, J. *Townsville Port Authority capital dredging works 1993: Environmental monitoring program.* Townsville Port Authority, Townsville 165-194.

Larcombe, P. Ridd, P.V. Prytz, A. Wilson, B. 1995a. Factors controlling suspended sediment on inner-shelf coral reefs, Townsville, Australia. *Coral Reefs*, **14**: 163-171.

Larcombe, P. Carter, R.M. Dye, J. Gagan, M.K. Johnson, D.P. 1995b. New evidence for episodic post-glacial sea-level rise, central Great Barrier Reef, Australia. *Marine Geology*, **127**: 1-44.

Larcombe, P. Carter, R.M. 1998. Sequence architecture during the Holocene transgression: an example from the Great Barrier Reef shelf, Australia. *Sedimentary Geology*, **117**: 97-121.

Larcombe, P. Woolfe, K.J. 1999a. Increased sediment supply to the Great Barrier Reef will not increase sediment accumulation at most coral reefs. *Coral Reefs*, **18**: 163-169.

Larcombe, P. Woolfe, K.J. 1999b. Terrigenous sediments as influences upon Holocene nearshore coral reefs, central Great Barrier Reef, Australia. *Australian Journal of Earth Sciences*, **46**: 141-154.

Larcombe, P. Costen, A. Woolfe, K.J. 2001. The hydrodynamic and sedimentary setting of nearshore coral reefs, central Great Barrier Reef shelf, Australia: Paluma shoals, a case study. *Sedimentology*, **48**: 811-835.

Lawrence, M.G. Grieg, A. Collerson, K.D. Kamber, B.S. Submitted. Rare earth elements and Yttrium variability in South East Queensland Waterways. *Aquatic Geochemistry*.

Lea, D.W. Shen, G.T. Boyle, E.A. 1989. Coralline barium records temporal variability in equatorial Pacific upwelling. *Nature*, **340**: 373-376.

Lee, J.H. Byrne, R.H. 1993. Complexation of trivalent rare earth elements (Ce, Eu, Gd, Tb, Yb) by carbonate ions. *Geochimica et Cosmochimica Acta*, **57**: 295-302.

Leichardt, L. 1847. *Journal of an overland expedition in Australia: from Moreton Bay to Port Essington, a distance of upwards of 3000 miles, during the years 1844-1845*. T. & W. Boone, London.

Li, Y-H. Chan, L-H. 1979. Desorption of Ba and ^{226}Ra from river-borne sediments in the Hudson Estuary. *Earth and Planetary Science Letters*, **43**: 343-350.

Linsley, B.K. Dunbar, R.B. Wellington, G.M. Mucciarone, D.A. 1994. A coral-based reconstruction if Intertropical Convergence Zone variability over Central America since 1707. *Journal of Geophysical Research*, **99 (C5)**: 9977-9994.

Lough, J.M. 1991. Rainfall variations in Queensland, Australia 1891-1986. *International Journal of Climatology*, **11**: 745-768.

Lough, J.M. 1994. Climate variation and El Niño-Southern Oscillation events on the Great Barrier Reef: 1958 to 1987. *Coral Reefs*, **13**: 181-195.

Lough, J.M. 1999. *Sea surface temperatures on the Great Barrier Reef: a contribution to the study of coral bleaching*. Great Barrier Reef Marine Park Authority, Research Publication No. 57.

Lough, J.M. 2000. 1997-1998 Unprecedented thermal stress to coral reefs? *Geophysical Research Letters*, **27**: 3901-3904.

Lough, J.M. 2001. Climate variability and change on the Great Barrier Reef. **In:** Wolanski, E. (ed). *Oceanographic processes of coral reefs- Physical and biological links in the Great Barrier Reef*. CRC Press, Boca Raton, p 269-300.

Lough, J.M. Barnes, D.J. 1997. Several centuries of variation in skeletal extension, density and calcification in massive Porites colonies from the Great Barrier Reef: A proxy for seawater temperature and a background of variability against which to identify unnatural change. *Journal of Experimental Marine Biology and Ecology*, **211**: 29-67.

Lough, J.M. Barnes, D.J. 2000. Environmental controls on growth of the massive coral *Porites*. *Journal of Experimental Marine Biology and Ecology*, **245**: 225-243.

Lough, J.M. Barnes, D.J. Devereux, M.J. Tobin, B.J. Tobin, S. 1999. *Variability in growth characteristics of massive Porites on the Great Barrier Reef*. Technical Report No. 28. CRC Reef Research Centre, Townsville, 95 pp.

Lough, J.M. Barnes, D.J. McAllister, F.A. 2002. Luminescent lines in corals from the Great Barrier Reef provide spatial and temporal records of reefs affected by runoff. *Coral Reefs*, **21**: 333-343.

Luo, Y-R. Byrne, R.H. 2004. Carbonate complexation of yttrium and rare earth elements in natural waters. *Geochimica et Cosmochimica Acta*, **68**: 691-699.

McConnaughey, T. 1989. ^{13}C and ^{18}O isotopic disequilibrium in biological carbonates: I. Patterns. *Geochimica et Cosmochimica Acta*, **53**: 151-162.

McConnaughey, T.A. 2003. Sub-equilibrium oxygen-18 and carbon-13 levels in biological carbonates: carbonate and kinetic models. *Coral Reefs*, **22**: 316-327.

McCormac, F.G. Hogg, A.G. Blackwell, P.G. Buck, C.E. Higham, T.F.G. Reimer, P.J. 2004. SHCal04 Southern Hemisphere calibration 0-1000 cal BP. *Radiocarbon*, **46**: 1087-1092.

McCrea, J. 1950. Isotopic chemistry of carbonates and paleotemperature scale. *J. Chem. Phys.*, **18**: 849-857.

McCulloch, M. 2003. Water quality in the inner Great Barrier Reef: What were the "natural" levels of turbidity and salinity prior to European settlement? **In:** *Australian Coral Reef Society 80th Annual Conference: Understanding and protecting coral reefs* 26th to 29th September 2003 Jupiters Hotel/Casino, Townsville, p 51.

McCulloch, M. 2004. Impact of European settlement on sediment and freshwater runoff into the Inner Great Barrier Reef. **In**: Haynes, D. Schaffelke, B. (eds). *Catchment to reef: Water quality issues in the Great Barrier Reef Region.* CRC Reef Research Centre Technical Report no. **53** p .

McCulloch, M.T. Gagan, M.K. Mortimer, G.E. Chivas, A.R. Isdale, P.J. 1994. A high resolution Sr/Ca and $\delta^{18}O$ coral record from the Great Barrier Reef, Australia, and the 1982-1983 El Niño. *Geochimica et Cosmochimica Acta*, **58**: 2747-2754.

McCulloch, M.T. Mortimer, G. Esat, T. Xianhua, L. Pillans, B. Chappell, J. 1996. High resolution windows into early Holocene climate: Sr/Ca coral records from Huon Peninsula. *Earth and Planetary Science Letters*, **138**: 169-178.

McCulloch, M.T. Alibert, C. Marshall, J. Mortimer, G. Burrows, D. 1998. The coral record of sea surface temperatures from the Great Barrier Reef. *Proceedings of the Australian Coral Reef Society 75th Anniversary Conference, Heron Island October 1997*. The University of Queensland, Brisbane, 167-176 pp.

McCulloch, M.T. Mortimer, G. Alibert, C. Marshall, J. 2000. El Niño and the coral record of sea surface temperatures from the Great Barrier Reef, Australia. In: Grove, R.H. Chappell, J. (eds). *El Niño- history and crisis*. The White Horse Press, pp 51-65.

McCulloch, M.T. Fallon, S. Wyndham, T. Hendy, E. Lough, J. Barnes, D. 2003. Coral record of increased sediment flux to the inner Great Barrier Reef since European settlement. *Nature*, **421**: 727-730.

McGregor, H.V. Gagan, M.K. 2003. Diagenesis and geochemistry of Porites corals from Papua New Guinea: Implications for paleoclimate reconstruction. *Geochimica et Cosmochimica Acta*, **67**: 2147-2156.

McIntyre and Associates Pty. Ltd. 1986. Magnetic Keys Development, Nelly Bay-Magnetic Island- impact assessment study, May 1986.

McIntyre and Associates Pty Ltd. 1989. Magnetic Quay Development Nelly Bay-Geotechnical investigation report job no 5565.

McLean, R.F. Stoddart, D.R. Hopley, D. Polach, H. 1978. Sea level change in the Holocene on the northern Great Barrier Reef. *Phil. Trans. R. Soc. Lond. A.* **291**: 167-186.

McNeil, B.I. Matear, R.J. Barnes, D.J. 2004. Coral reef calcification and climate change: The effect of ocean warming. *Geophysical Research Letters,* **31**: L22309.

McNeil, B.I. Matear, R.J. Barnes, D.J. 2005. Reply to comment by Kleypas et al. on "Coral reef calcification and climate change: The effect of ocean warming". *Geophysical Research Letters,* **32**: L08602.

Maitland, A.G. 1892. *The physical geology of Magnetic Island*. Geological Society of Queensland, Brisbane, 8 p.

Mania, J. Chauve, P. Remy, F. Verjus, P. 1989. Evolution of iron and manganese concentrations in presence of carbonates and clays in the alluvial groundwaters of the Ognon (Franche-Comté, France). *Geoderma*, **44**: 219-227.

Mann, M.E. Jones, P.D. 2003. Global surface temperatures over the past two millennia. *Geophysical Research Letters*, **30**: 1820, doi: 10.1029/2003GL017814.

Mantua, N.J. Hare, S.R. 2002. The Pacific Decadal Oscillation. *Journal of Oceanography*, **58**: 35-44.

Mapstone, B.D. Choat, J.H. Cumming, R.L. Oxley, W.G., 1992. *The fringing reefs of Magnetic Island: Benthic biota and sedimentation- A baseline study*. Research publication No. 13, Great Barrier Reef Marine Park Authority, Townsville, Queensland.

Maragos, J.E. Evans, C. Holthus, P. 1985. Reef corals in Kaneohe Bay six years before and after termination of sewage discharges. *Proceedings of the fifth international coral reef congress, Tahiti, 1985*, **4**: 189-194.

Marshall, J.F. 2000. *Decadal-scale, high resolution records of sea surface temperature in the eastern Indian and south western Pacific Oceans from proxy records of the strontium/calcium ratio of massive Porites corals*. PhD thesis, Research School of Earth Sciences, Australian National University.

Marshall, J.F. Burrows, D.P. McCulloch, M.T. 2000. Evidence of mid-Holocene cooling of the tropical Western Pacific from Sr/Ca ratios of corals from the central Great Barrier Reef, *Environmental Geochemistry and Geochronology Group, annual report for Research School of Earth Sciences*, 2000.

Marshall, J.F. McCulloch, M.T. 2001. Evidence of El Niño and the Indian Ocean Dipole from Sr/Ca derived SSTs for modern corals at Christmas Island, eastern Indian Ocean. *Geophysical Research Letters*, **28**: 3453-3456.

Marshall, J.F. and McCulloch, M.T., 2002. An assessment of the Sr/Ca ratio in shallow water hermatypic corals as a proxy for sea surface temperature. *Geochimica et Cosmochimica Acta*, **66**: 3263-3280.

Meibom, A. Stage, M. Wooden, J. Constantz, B.R. Dunbar, R.B. Owen, A. Grumet, N. Bacon, C.R. Chamberlain, C.P. 2003. Monthly strontium/calcium oscillations in a symbiotic coral aragonite: Biological effects limiting the precision of the paleotemperature proxy. *Geophysical Research Letters*, *30*: 71.

Meibom, A. Cuif, J-P. Hillion, F. Constantz, B.R. Juillet-Leclerc, A. Dauphin, Y. Watanabe, T. Dunbar, R.B. 2004. Distribution of magnesium in coral skeleton. *Geophysical Research Letters*, **31**: L23306.

Menghetti, D. 1992. Ravenswood: five heritage trails. Department of History and Politics, James Cook University, Townsville, 28 p.

Miller, I. Sweatman, H. 2004. Status of coral reefs in Australia and Papua New Guinea in 2004. **In:** Wilkinson, C. (ed). 2004. Status of coral reefs of the world: 2004. Australian Institute of Marine Science (www.aims.gov.au).

Millero, F.J. 1996. *Chemical Oceanography* (2nd Ed). CRC Press Boca Raton, 469 pp.

Min, G.R. Edwards, R.L. Taylor, F.W. Recy, J. Gallup, C.D. Beck, J.W. 1995. Annual cycles of U/Ca in coral skeletons and U/Ca thermometry. *Geochimica et Cosmochimica Acta*, **59**: 2025-2042.

Mitchell, T.L. 1848. *Journal of an expedition into the interior of tropical Australia : in search of a route from Sydney to the Gulf of Carpentaria*. Longman, Brown, Green and Longmans, London, 437 p.

Mitsuguchi, T. Matsumoto, E. Abe, O. Uchida, T. Isdale, P.J. 1996. Mg/Ca thermometry in coral skeletons. *Science*, **274**: 961-963.

Mitsuguchi, T. Uchida, T. Matsumoto, E. Isdale, P. Kawana, T. 2001. Variations in Mg/Ca, Na/Ca, and Sr/Ca ratios with chemical treatments: Implications for carbonate geochemistry. *Geochimica et Cosmochimica Acta*, **65**: 2865-2874.

Mitsuguchi, T. Matsumoto, E. Uchida, T. 2003. Mg/Ca and Sr/Ca ratios of *Porites* skeleton: Evaluation of the effect of skeletal growth rate. *Coral Reefs*, **22**: 381-388.

Morel, F.M.M. Price, N.M. 2003. The biogeochemical cycles of trace metals in the ocean. *Science*, **300**: 944-947.

Morrissey, J. 1980. Community structure and zonation of Macroalgae and Hermatypic corals on the fringing reef flat Magnetic Island (Queensland, Australia). *Aquatic Botany*, **8**: 91-139.

Moss, A.J. Rayment, G.E. Reilly, N. Best, E.K. 1992. *A preliminary assessment of sediment and nutrient exports form Queensland coastal catchments*. Department Of Primary Industries, Queensland.

Müller, A. Gagan, M.K. McCulloch, M.T. 2001. Early marine diagenesis in corals and geochemical consequences for paleoceanographic reconstructions. *Geophysical Research Letters,* **28**: 4471-4474.

Müller, A. Gagan, M.K. Lough, J.M. 2004. Effect of early marine diagenesis on coral reconstructions of surface-ocean $^{13}C/^{12}C$ and carbonate saturation state. *Global Biogeochemical Cycles,* **18**: GB1033.

Muslim, I. 1995. *Nutrient variation and sediment flux at a fringing coral reef in Nelly Bay, Townsville-Australia*. Department Molecular Sciences of James Cook University, Townsville.

Muslim, I. Jones, G. 2003. The seasonal variation of dissolved nutrients, chlorophyll *a* and suspended sediments at Nelly Bay, Magnetic Island. Estuarine*, Coastal and Shelf Science,* **57**: 445-455.

Neil, D.T. Orpin, A.R. Ridd, P.V. Yu, B. 2002. Sediment yield and impacts from the river catchments to the Great Barrier Reef lagoon. *Marine Freshwater Research*, **53**: 733-752.

Nothdurft, L.D. Webb, G.E. Kamber, B.S. 2004. Rare earth element geochemistry of Late Devonian reefal carbonates, Canning Basin, Western Australia: Confirmation of a seawater REE proxy in ancient limestones. *Geochimica et Cosmochimica Acta,* **68:** 263-283.

Nott, J. 1996. Late Pleistocene and Holocene sea-level highstands in northern Australia. *Journal of Coastal Research,* **12** (4): 907-910

Nott, J. Price, D. 1994. Plunge pools and paleoprecipitation. *Geology*, **22**: 1047-1050.

Nott, J. Hayne, M. 2001. High frequency of 'super-cyclones' along the Great Barrier Reef over the past 5,000 years. *Nature,* **413**: 508-511.

Nott, J. Bryant, E. Price, D. 1999. Early-Holocene aridity in tropical northern Australia. *The Holocene,* **9**: 231-236.

Nozaki, Y. 2001. Rare earth elements and their isotopes. In: Steele, J. Thorpe, S. Turekian, K.K. (eds). *Encyclopaedia of ocean sciences, Vol. 4,* Academic Press, London, pp 2354-2366.

O'Donnell, D. 1989. *A history of Clermont and district: Belyando Shire*. Belyando Shire Council, Clermont, Queensland.

Okai, T. Suzuki, A. Kawahata, H. Terashima, S. Imai, N. 2002. Preparation of a New Geological Survey of Japan Geochemical Reference Material: Coral JCp-1. *Geostandards Newsletter,* **26**: 95-100.

Orme, G.R. Webb, J.D. Kelland, N.C. Sargent, G.E.G. 1978. Aspects of the geological history and structure of the northern Great Barrier Reef. *Phil. Trans. R. Soc. Lond., Ser A.* **291**: 23-35.

Orpin, A.R. Ridd, P.V. Stewart, L.K. 1999. Assessment of the relative importance of major sediment transport mechanisms in the central Great Barrier Reef lagoon. *Australian Journal of Earth Sciences*, **46**: 883-896.

Orpin, A.R. Brunskill, G.J. Zagorskis, I. Woolfe, K.J. 2004. Patterns of mixed siliciclastic-carbonate sedimentation adjacent to a large dry-tropics river on the central Great Barrier reef shelf, Australia. *Australian Journal of Earth Sciences*, **51**: 665-683.

Pandolfi, J.M. 1992. A palaeobiological examination of the geological evidence for recurring outbreaks of the crown-of-thorns starfish, *Acanthaster planci* (L.). *Coral Reefs*, **11**: 87-93.

Pandolfi, J.M. Bradbury, R.H. Sala, E. Hughes, T.P. *et al*. 2003. Global trajectories of the long-term decline of coral reef ecosystems. *Science*, **301**: 955-958.

Pandolfi, J.M. Jackson, J.B.C. Baron, N. Bradbury, R.H. *et al*. 2005. Are U.S. coral reefs on the slippery slope to slime? *Science*, **307**: 1725-1726.

Pelejero, C. Calvo, E. McCulloch, M.T. Marshall, J.F. Gagan, M.K. Lough, J.M. Opdyke, B.N. 2005. Preindustrial to modern interdecadal variability in coral reef pH. *Science*, **309**: 2204-2207.

Piepras, D.J. Jacobsen, S.B. 1992. The behaviour of rare earth elements in seawater: precise determination of variations in the North Pacific water column. *Geochimica et Cosmochimica Acta*, **56**: 1851-1862.

Porter, J.G. 1983. *Discovering Magnetic Island*. Kullari Publications, Tully, QLD, 114 pp.

Post, J.E. 1999. Manganese oxide minerals: Crystal structures and economic and environmental significance. *Proceedings National Academy of Science*, **96**: 3447-3454.

Pringle, A.W. 1989. *The history of dredging in Cleveland Bay, Queensland and its effects on sediment movement and on the growth of mangroves, corals and seagrass*. Great Barrier Reef Marine Park Authority, Townsville, 177 p.

Pringle, A. W. 1996. History, Geomorphological problems and effects of dredging in Cleveland Bay, Queensland. *Australian Geographical Studies*, **34**: 58-80.

Prosser, I. P. Rutherfurd, I.D. Olley, J.M. Young, W.J. Wallbrink, P.J. Moran, C.J. 2001. Large-scale patterns of erosion and sediment transport in river networks, with examples from Australia. *Marine Freshwater Research*, **52**: 81-99.

Rasmussen, C.E. 1988a. Effects of nutrients carried by mainland runoff on reefs of the Cairns area: A research plan and preliminary results. **In:** Baldwin, C.L. Nutrients in the

Great Barrier Reef region, workshop series no. 10. *Great Barrier Reef Marine Park Authority,* Townsville.

Rasmussen, C.E. 1988b. The use of strontium as an indicator of anthropogenically altered environmental parameters. *Proceedings of the 6th International Coral Reef Symposium, Australia,* 2: 325-330.

Rasmussen, C.E. 1994. *Anthropogenic disturbance of environmental signals retained in massive corals*. PhD Thesis, Sir George Fisher Centre for Tropical Marine Studies, James Cook University, Townsville.

Reichelt, A.J. 1993. *The characterisation and fate of suspended sediments associated with dredging and dumping activities in Cleveland Bay, Australia*. Masters Thesis, Department of Molecular Sciences, James Cook University.

Reichelt, A.J. Jones, G.B. 1994. Trace metals as tracers of dredging activity in Cleveland Bay- Field and laboratory studies. *Australian Journal of Marine and Freshwater Research,* **45**: 1237-1257.

Reichelt-Brushett, A.J. McOrist, G. 2003. Trace metals in the living and nonliving components of scleractinian corals. *Marine Pollution Bulletin*, **46**: 1573-1582.

Reynaud, S. Ferrier-Pagès, C. Boisson, F. Allemand, D. Fairbanks, R.G. 2004. Effect of light and temperature on calcification and strontium uptake in the scleractinian coral *Acropora verweyi*. *Marine Ecology Progress Series*, **279**: 105-112.

Ridd, P.V. Larcombe, P. 1994. Biofouling control for optical backscatter turbidity sensors. *Marine Geology*, **16**: 255-258.

Rosenfeld, M. Yam, R. Shemesh, A. Loya, Y. 2003. Implication of water depth on stable isotope composition and skeletal density banding patterns in a *Porites lutea* colony: results from a long-term translocation experiment. *Coral Reefs,* **22**: 337-345.

Runnalls, L.A. Coleman, M.L. 2003. Record of natural and anthropogenic changes in reef environments (Barbados West Indies) using laser ablation ICP-MS and sclerochronology on coral cores. *Coral Reefs,* **22**: 416-426.

Scoffin, T.P. Tudhope, A.W. Brown, B.E. 1989. Fluorescent and skeletal density banding in *Porites lutea* from Papua New Guinea and Indonesia. *Coral Reefs*, **7**: 169-178.

Scoffin, T.P. Stoddart, D.R. 1978. The nature and significance of microatolls. Phil. *Trans. R. Soc. Lond. B.* **284**: 99-122.

Schrag, D.P. 1999. Rapid analysis of high-precision Sr/Ca ratios in corals and other marine carbonates. *Paleoceanography*, **14**: 97-102.

Schrag, D.P. Linsley, B.K. 2002. Corals, chemistry, and climate. *Science*, **296**: 277-278.

Shen, G.T. Boyle, E.A. 1987. Lead in corals: reconstruction of historical fluxes to the surface ocean. *Earth and Planetary Science Letters*, **82**: 289-304.

Shen, G.T. Boyle, E.A. 1988. Determination of lead, cadmium and other trace metals in annually-banded corals. *Chemical Geology*, **67**: 47-62.

Shen, G.T. Sanford, C.L. 1990. Trace element indicators of climate variability in reef-building corals. In: Glynn, P.W. (ed). *Global ecological consequences of the 1982-83 El Niño Southern Oscillation*. Elsevier Oceanography Series, **52**: 255-283.

Shen, G.T. Campbell, T.M. Dunbar, R.B. Wellington, G.M. Colgan, M.W. Glynn, P.W. 1991. Paleochemistry of manganese in corals from the Galapagos Islands. *Coral Reefs*, **10**: 91-100.

Shen, G.T. Cole, J.E. Lea, D.W. Linn, L.J. McConnaughey, T.A. Fairbanks, R.G. 1992a. Surface ocean variability at Galapagos from 1936-1982: Calibration of geochemical tracers in corals. *Paleoceanography*, **7**: 563-588.

Shen, G.T. Linn, L.J. Campbell, T.M. 1992b. A chemical indicator of trade wind reversal in corals from the Western Tropical Pacific. *Journal of Geophysical Research*, **97**: 12689-12697.

Shen, G.T. Dunbar, R.B. 1995. Environmental controls on uranium in reef corals. *Geochimica et Cosmochimica Acta*, **59**: 2009-2024.

Shields, G. Stille, P. 2001. Diagenetic constraints on the use of cerium anomalies as palaeoseawater redox proxies: an isotopic and REE study of Cambrian phosphorites. *Chemical Geology*, **175**: 29-48.

Shimizu, H. Tachikawa, K. Masuda, A. Nozaki, Y. 1994. Cerium and neodymium isotope ratios and REE patterns in seawater from the north Pacific Ocean. *Geochimica et Cosmochimica Acta*, **58**: 323-333.

Sholkovitz, E.R. 1993. The geochemistry of rare earth elements in the Amazon River estuary. *Geochimica et Cosmochimica Acta*, **57**: 2181-2190.

Sholkovitz, E. Landing, W.M. Lewis, B.L. 1994. Ocean particle chemistry: the fractionation of the rare earth elements between suspended particles and seawater. *Geochimica et Cosmochimica Acta*, **58**: 1567-1580.

Sholkovitz, E. Shen, G.T. 1995. The incorporation of rare earth elements in modern coral. *Geochimica Cosmochimica Acta*, **59**: 2749-2756.

Shulmeister, J. 1996. Holocene climate change in Queensland: implications for sea-level change and coastal sedimentation. **In:** Larcombe, P. Woolfe, K. Purdon, R. (eds). *Great Barrier Reef: Terrigenous sediment flux and human impacts*. Marine Geophysical Laboratory, Earth Sciences Department, James Cook University, Second edition- November 1996

Sinclair, D.J. 2005a. Correlated trace element "vital effects" in tropical corals: A new geochemical tool for probing biomineralization. *Geochimica et Cosmochimica Acta*, **69**: 3265-3284.

Sinclair, D.J. 2005b. Non-river flood barium signals in the skeletons of corals from coastal Queensland, Australia. *Earth and Planetary Science Letters*, **237**: 354-369.

Sinclair, D.J. Kinsley, L.P.J. McCulloch, M.T. 1998. High resolution analysis of trace elements in corals by laser ablation ICP-MS. *Geochimica et Cosmochimica Acta*, **62**: 1889-1901.

Sinclair, D.J. McCulloch, M.T. 2004. Coral record low mobile barium concentrations in the Burdekin River during the 1974 flood: evidence for limited Ba supply to rivers? *Palaeogeography, Palaeoclimatology, Palaeoecology*, **214**: 155-174.

Sinclair Knight Merz. 1998. *Nelly bay Supplement: Nelly bay Harbour- supplementary environmental impact study* (Appendix D- Seismic Survey), October 1998.

Smith, A.S. 1974. *Classification and distribution of sediments on some north Queensland fringing reefs*. Masters thesis, Department of Geography, James Cook University.

Smith, A. 1978. Case study: Magnetic Island and its fringing reefs. In: Hopley, D. (ed). *Geographical Studies of the Townsville area*. Department of Geography monograph series no. 2, James Cook University, Townsville, p 59-65.

Smith, S.V. Buddemeier, R.W. Redalje, R.C. Houck, J.E. 1979. Strontium-calcium thermometry in coral skeletons. *Science*, **204**: 404-407.

Smithers, S. Larcombe, P. 2003. Late Holocene initiation and growth of a nearshore turbid-zone coral reef: Paluma Shoals, central Great Barrier Reef, Australia. *Coral Reefs*, **22**: 499-505.

Solow, A.R. Huppert, A. 2004. A potential bias in coral reconstruction of sea surface temperature. *Geophysical Research Letters*, **31**: L06308 1-4.

Spenceley, A.P. 1980. *The geomorphological and zonational development of mangrove swamps in the Townsville area, north Queensland*. PhD thesis, Department of Geography, James Cook University.

Statistics of the colony of Queensland/Statistics of the state of Queensland. Bureau of Census and Statistics, Queensland Office, Brisbane.

Stoll, H.M. Schrag, D.P. 1998. Effects of Quaternary sea level cycles on strontium in seawater. *Geochimica et Cosmochimica Acta*, **62**: 1107-1118.

Stroobants, N. Dehairs, F. Goeyens, L. Vanderheijden, N. Van Grieken, R. 1991. Barite formation in the Southern Ocean water column. *Marine Chemistry*, **35**: 411-421.

Stuiver, M. Reimer, P.J. Reimer, R.W. 2005. CALIB 5.0. www.calib.org

Swart, P.K. White, K.S. Enfield, D. Dodge, R.E. Milne, P. 1998. Stable isotope composition of corals from the Gulf of Guinea as indicators of periods of extreme precipitation conditions in the sub-Sahara. *Journal of Geophysical Research,* **103 (C12)**: 27,885-27,891.

Sweatman, H. Delean, S. 2005. Decadal decline of coral cover on the Great Barrier Reef. **In**: *Australian Coral Reef Society 81st Annual Conference: Managing and researching reefs in a changing world 19th-21st August 2005, Heron Island Research Station Queensland*.

Taylor, R.B. Barnes, D.J. Lough, J.M. 1995. On the inclusion of trace materials into massive coral skeletons. 1. Materials occurring in the environment in short pulses. Journal of *Experimental Marine Biology and Ecology,* **185**: 255-278.

Taylor, S.R. McLennan, S.M. 1985. *The continental crust: Its composition and evolution*. Blackwell Scientific Publ., Oxford, England, 312 pp.

Taylor, J. 1995. Sediment input to the Great Barrier Reef lagoon via river discharge: the Barron River. **In:** Larcombe, P. Woolfe, K. (eds). *Great Barrier Reef: Terrigenous sediment flux and human impacts*. CRC Reef Research Centre, Research symposium proceedings, Townsville, p 92-94.

The Royal Society. 2005. *Ocean acidification due to increasing atmospheric carbon dioxide*. The Clyvedon Press Ltd, Cardiff, 60 pp. http://www.royalsoc.ac.uk

Thorpe, B. 1996. *Colonial Queensland: perspectives on a frontier society*. University of Queensland Press, Brisbane, 287 p.

Trezise, D.L. Stephenson, P.J. 1990. *Rocks and landscapes of the Townsville district*. Department of Resource Industries, Brisbane, *QLD*, 60 pp.

Tucker, G.B. 1975. Climate: is Australia changing? *Search*, **6**: 323-328.

Tudhope, A.W. Shimmield, G.B. Chilcott, C.P. Jebb, M. Fallick, A.E. Dalgleish, A.N. 1995. Recent changes in climate in the far western equatorial Pacific and their relationship to the Southern Oscillation: oxygen isotope records from massive corals, Papua New Guinea. *Earth and Planetary Science Letters*, **136**: 575-590.

Tudhope, A.W. Lea, D.W. Shimmield, G.B. Chilcott, C.P. Head, S. 1996. Monsoon climate and Arabian Sea coastal upwelling recorded in massive corals from Southern Omen. *Palaios*, **11**: 347-361.

Turekian, K.K. Wedepohl, K.H. 1961. Distribution of the elements in some major units of the Earth's crust. *Geological Society of America Bulletin*, **72**: 175-192.

van Woesik, R. Tomascik, T. Blake, S. 1999. Coral assemblages and physico-chemical characteristics of the Whitsunday Islands: evidence of recent community changes. *Marine and freshwater research*, **50**: 427-440.

Walbran, P.D. Henderson, R.A. Jull, A.J.T. Head, M.J. 1989. Evidence from sediments of long-term *Acanthaster planci* predation on corals of the Great Barrier Reef. *Science*, **245**: 847-850.

Walker, T.A. 1981a. Dependence of phytoplankton chlorophyll on bottom resuspension in Cleveland Bay, northern Queensland. *Australian Journal of Marine and Freshwater Research*, **32**: 981-986.

Walker, T. 1981b. Annual temperature cycle in Cleveland Bay, Great Barrier Reef province. *Australian Journal of Marine and Freshwater Research*, **32**: 987-991.

Walker, T.A. 1991. Is the reef really suffering from chronic pollution? *Search*, **22**: 115-117.

Walker, T.A. O'Donnell, G. 1981. Observations on Nitrate, Phosphate and Silicate in Cleveland Bay, Northern Queensland. *Australian Journal of Marine Freshwater Research*, **32**: 877-887.

Ward, I.A.K. Larcombe, P. Cuff, C. 1995. Stratigraphic control of the geochemistry of Holocene inner-shelf facies, Great Barrier Reef. *Marine Geology*, **129**: 47-62.

Watanabe, T. Minagawa, M. Oba, T. Winter, A. 2001. Pretreatment of coral aragonite for Mg and Sr analysis: Implications for coral thermometers. *Geochemical Journal*, **35**: 265-269.

Webb, G.E. and Kamber, B.S. 2000. Rare earth elements in Holocene reefal microbialites: A new shallow water proxy. *Geochimica et Cosmochimica Acta*, **64**: 1557-1565.

Weber, J.N. Woodhead, P.M.J. 1972. Temperature dependence of oxygen-18 concentration in reef coral carbonates. *Journal of Geophysical Research*, **77**: 463-473.

Wei, G. Sun, M. Li, X. Nie, B. 2000. Mg/Ca, Sr/Ca, and U/Ca ratios of a Porites from Sanya Bay, Hainan Island, South China Sea and their relationships to sea surface temperature. *Palaeoceanography, Palaeoclimatology, Palaeoecology*, **162**: 59-74.

Wellington, G.M. Dunbar, R.B. 1995. Stable isotope of El Niño Southern Oscillation events in eastern tropical Pacific reef corals. *Coral Reefs*, **14**: 5-25.

Wild, F.J. Jones, A.C. Tudhope, A.W. 2000. Investigation of luminescent banding in solid coral: the contribution of phosphorescence. *Coral Reefs*, **19**: 132-140.

Wilkinson, C. (ed). 1998. *Status of coral reefs of the world: 1998*. Australian Institute of Marine Science (www.aims.gov.au).

Wilkinson, C. (ed). 2004. *Status of coral reefs of the world: 2004*. Australian Institute of Marine Science (www.aims.gov.au).

Willis, B.L. 1987. *Morphological variation in the reef corals Turbinaria mesenterina and Pavona cactus: Synthesis of transplant, histocompatibility, electrophoresis, growth,*

and reproduction studies. PhD Thesis, Department of Marine Biology, James Cook University, Townsville.

Wolanski, E. Gibbs, R. Ridd, P. King, B. Hwang, K.Y. Mehta, A. 1991. *Fate of dredge spoil, Cleveland Bay, Townsville*. Coastal Engineering- Climate for change, 10th Australasian Conference on Coastal and Ocean Engineering, Auckland.

Wolanski, E. Gibbs, R. Ridd, P. Mehta, A. 1992. Settling of ocean-dumped dredged material, Townsville, Australia. *Estuarine, Coastal and Shelf Science*, **35**: 473-489.

Wolanski, E. Spagnol, S. 2000. Pollution by mud of Great Barrier Reef coastal waters. *Journal of Coastal Research*, **16**: 1151-1156.

Woodroffe, C.D. 2003. *Coasts: Form process and evolution.* Cambridge University Press, Cambridge, 623 p.

Woodroffe, C.D. Kennedy, D.M. Hopley, D. Rasmussen, C.E. Smithers, S.G. 2000. Holocene reef growth in Torres Strait. *Marine Geology*, **170**: 331-346.

Wooldridge, S. Done, T. Berkelmans, R. Jones, R. Marshall, P. 2005. Precursors for resilience in coral communities in a warming climate: a belief network approach. *Marine Ecology Progress Series*, **295**: 157-169.

Woolfe, K.J. Larcombe, P. 1998. Terrigenous sediment accumulation as a regional control on the distribution of reef carbonates. *Special Publication International Association of Sedimentologists*, **25**: 295-310.

Woolfe, K.J. Larcombe, P. 1999. Terrigenous sedimentation and coral reef growth: a conceptual framework. *Marine Geology*, **155**: 331-345.

Wyndham, T. McCulloch, M. Fallon, S. Alibert, C. 2004. High-resolution coral records of rare earth elements in coastal seawater: Biogeochemical cycling and a new environmental proxy. *Geochimica et Cosmochimica Acta*, **68**: 2067-2080.

Young, A. 2000. *Environmental change in Australia since 1788* (2nd Ed). Oxford University Press, Melbourne, 243 p.

Zhao, J. Yu, K. 2002. Timing of Holocene sea-level highstands by mass spectrometric U-series ages of a coral reef from Leizhou Peninsula, South China Sea. *Chinese Pollution Bulletin*, **47**: 348-352.